DETECTION, STABILITY AND FACTORS INFLUENCING THE FORMATION OF PROMUTAGENIC ENDOGENOUS DNA DAMAGE

Thesis submitted for the degree of
Doctor of Philosophy
at the University of Leicester

by

Elke Gottschalg née Griech
BMI Section at the MRC Toxicology Unit
University of Leicester

January 2002

ProQuest LLC
789 East Eisenhower Parkway
P.O. Box 1346
Ann Arbor, MI 48106-1346

Abstract

DETECTION, STABILITY AND FACTORS INFLUENCING THE FORMATION OF PROMUTAGENIC ENDOGENOUS DNA DAMAGE

Elke Gottschalg née Griech

Genotoxic agents derived from diet may contribute to the total human burden of potentially carcinogenic DNA damage. The major malondialdehyde (MDA) DNA adduct, malondialdehyde-2'-deoxyguanosine (M_1-dG) and two adducts formed by nitrosated glycine derivatives, O^6-carboxymethyl-2'-deoxyguanosine (O^6-CMdG) and O^6-methyl-2'-deoxyguanosine (O^6-MedG), were studied.

The long-term stability of M_1-dG in calf thymus DNA (CT-DNA) was assessed. MDA-treated CT-DNA standards were found to be relatively stable at room temperature (RT), 4°C, -20°C and -80°C. Degradation at RT was detectable after 3 weeks of storage. CT-DNA standards were more stable in water when compared to phosphate buffer. Levels of M_1-dG in highly modified CT-DNA could be reduced substantially using primary amines. M_1-dG stability in human DNA was assessed using an immunoslot blot (ISB) assay incorporating a propidium iodide staining procedure for the correction of differences in DNA binding to the ISB filter. Studies on the stability of low levels of M_1-dG in human DNA were not fully conclusive, although changes in adduct levels were temperature independent.

The ratio of the two O^6-alkylguanine adducts induced by potassium diazoacetate (KDA) treatment of DNA could be modulated using different buffer systems. These findings provided a unique opportunity to investigate the contribution of O^6-CMdG and O^6-MedG to the p53 mutational spectrum using a yeast-based p53 functional assay. Although adduct levels differed considerably, the two spectra obtained for KDA treatments in Tris-EDTA and phosphate buffer were statistically indistinguishable. The KDA-induced mutation spectra were, however, significantly different from that induced by N-methyl-N-nitrosourea, indicating that the key features of KDA-induced p53 spectra were caused mainly by O^6-CMdG. Studies on MDA-induced mutational spectra were less conclusive due to a much smaller number of mutations detectable following sequencing.

The results presented in this thesis highlight some key aspects of methodology as well as the significance of DNA damage measurements in studies of diet-related cancer risk.

Abbreviations

2'-dA	2'-deoxyadenosine
2'-dC	2'-deoxycytidine
2'-dG	2'-deoxyguanosine
^{32}pNpg	phosphoglycolate species
^{32}pNpT^{g}	thymine glycol-containing dinucleotide
AGT	O^{6}-alkylguanine-DNA alkyltransferase
APNG	N-(N'-acetyl-L-prolyl)-N-nitrosoglycine
AS	azaserine
ATP	adenosine-5'-triphosphate
BDS	base deactivated silica
BW buffer	binding and washing buffer
cDNA	complementary DNA
CCNU	chloroethyl-cyclohexyl-nitroso-urea
CSPDE	calf spleen phosphodiesterase
CT-DNA	calf thymus DNA
dAp	2'-deoxyadenosine-3'-monophosphate
dCp	2'-deoxycytidine-3'-monophosphate
dGp	2'-deoxyguanosine-3'-monophosphate
DMSO	dimethyl sulphoxide
dN	2'-deoxynucleoside
DMS	dimethyl sulphate
DNA	deoxyribonucleic acid
DNase I	deoxyribonuclease I
dNp	2'-deoxynucleoside-3'-monophosphate; 2'-deoxynucleotide
dNTP	2'-deoxynucleoside 5'-triphosphate
ds DNA	double-stranded DNA
dTp	thymidine-3'-monophosphate
E. coli	*Escherichia coli*
EDTA	ethylenediaminetetra-acetic acid (disodium salt)
ENU	N-ethyl-N-nitrosourea
EPIC	European Prospective Investigation into Cancer and Nutrition
EtBr	ethidium bromide
EtOH	ethanol
FA	formic acid
FORA	food risk assessment
Fs/In/Del	frameshift/insertion/deletion
GI	gastrointestinal
HCC	hepatocellular carcinoma
HCl	hydrochloric acid

HFBA	heptafluorobutyric acid
H_2O_2	hydrogen peroxide
HOCl	hypochlorous acid
HPLC	high performance liquid chromatography
H. pylori	*Helicobacter pylori*
IAC(s)	immunoaffinity column(s)
IARC	International Agency for Research on Cancer
IDB	immunodot blot
IgG	immunoglobulin G
ISB	immunoslot blot
KDA	potassium diazoacetate
KOH	potassium hydroxide
KP	K_2HPO_4, di-potassium hydrogen orthophosphate
LiAc	lithium acetate
M_1-dG	malondialdehyde-2'-deoxyguanosine
M_1-dGp	malondialdehyde-2'-deoxyguanosine-3'-monophosphate
M_1-G	malondialdehyde-guanine
MDA	malondialdehyde
MeOH	methanol
MMR	mismatch repair
MMS	methyl methanesulphonate
MN	micrococcal nuclease
MNNG	N-methyl-N'-nitro-N-nitrosoguanidine
MNU	N-methyl-N-nitrosourea
MOPS	3-[N-morpholino]propanesulfonic acid
MPO	myeloperoxidase
mtDNA	mitochondrial DNA
$M_{compound\ x}$	molecular weight of compound x in [g/mol]
M_n	average fragment length
M_w	average molecular weight
N_2	nitrogen
NaAc	sodium acetate
NaMDA	sodium malondialdehyde
NaOH	sodium hydroxide
NC	nitrocellulose
NER	nucleotide excision repair
NH_4Ac	ammonium acetate
NMSC	non-melanoma skin cancer
NO	nitric oxide
NOC	N-nitroso compounds
NOGC	N-nitrosoglycocholic acid
NP1	nuclease P1
O.D.	optical density
$O.D._{ISB}$	optical density obtained for ISB assay

$O.D._{PI}$	optical density obtained for PI assay
O^6-CMdG	O^6-carboxymethyl-2'-deoxyguanosine
O^6-CMG	O^6-carboxymethylguanine
O^6-MedG	O^6-methyl-2'-deoxyguanosine
O^6-MeG	O^6-methylguanine
o/n	overnight
P	probability
PBS	phosphate buffered saline
PBS-T	PBS-Tween 20
PCR	polymerase chain reaction
PEG	polyethylene glycol 4000
PI	propidium iodide
R^2	correlation coefficient
RNA	ribonucleic acid
RNase A	ribonuclease A
RNase T_1	ribonuclease T_1
RP-HPLC	reverse phase HPLC
RT	room temperature
S. cerevisiae	*Saccharomyces cerevisiae*
SAP	shrimp alkaline phosphatase
SSC	sodium chloride/trisodium citrate buffer
SSCC	sodium succinate/calcium chloride buffer
ss DNA	single-stranded DNA
SVPD	snake venom phosphodiesterase
T4PNK	T4 polynucleotide kinase
TAE	Tris-acetate EDTA buffer
TBA-MDA	malondialdehyde tetrabutylammonium salt
TBE	Tris-borate EDTA buffer
TE	Tris-EDTA
TEA	triethylammonium acetate
TFA	trifluoroacetic acid
TMP	tetramethoxypropane
Tris	tris[hydroxymethyl]aminomethane
Triton X-100	t-octylphenoxypolyethoxyethanol
Tween 20	polyoxyethylenesorbitan monolaurate
U	unit(s)
UV	ultraviolet
WBC	white blood cells

Acknowledgements

I would like to thank Dr. Chiara Leuratti and Professor David Shuker for their guidance, supervision and assistance throughout this project. Furthermore, I am grateful for support and constructive comments I received from my committee, Dr. Liz Martin and Dr. Don Jones, and members of the Biomonitoring and Molecular Interactions section, especially Dr. Raj Singh, Dr. Belinda Cupid and Rebekah Jukes. Thank you to everybody in BMI, past and present members, who made the last years so enjoyable.

I would like to extend my gratitude to Lynda Langford and Dr. Don Jones at the Centre for Mechanisms of Human Toxicity for help and performance of SVPD-^{32}P-postlabelling experiments and glyoxal gels.

I am most grateful to Dr. Phil Burns and Dr. Gina Scott for the great and fruitful collaboration, kindness and fabulous time I had in Leeds while analysing MDA mutants. I not only learned a lot but also felt most welcome.

To my husband Ralph, thank you for endless support and belief in me.

Table of Contents

1 Introduction

1.1 Biomarkers as Indicators of Exposure

DNA adducts are thought to be important in many cases of chemical carcinogenesis and can be formed by exogenous and endogenous genotoxic compounds. Many carcinogens and mutagens, that are presently known to induce DNA adducts, act directly while others need metabolic activation to reactive intermediates. Initiation of chemical carcinogenesis is, in many cases, believed to result from covalent modification of DNA. If not repaired, such modifications can then be converted into mutations during replication. Mutations that occur at critical DNA sequences can lead to the activation of oncogenes and inactivation of tumour suppressor genes which can ultimately lead to initiation and progression of cancer. One of the most frequently mutated genes in human malignancies is the tumour suppressor gene p53. Exposure assessment can be carried out at different stages in the process that can lead to the development of tumours as illustrated in Figure 1.1.

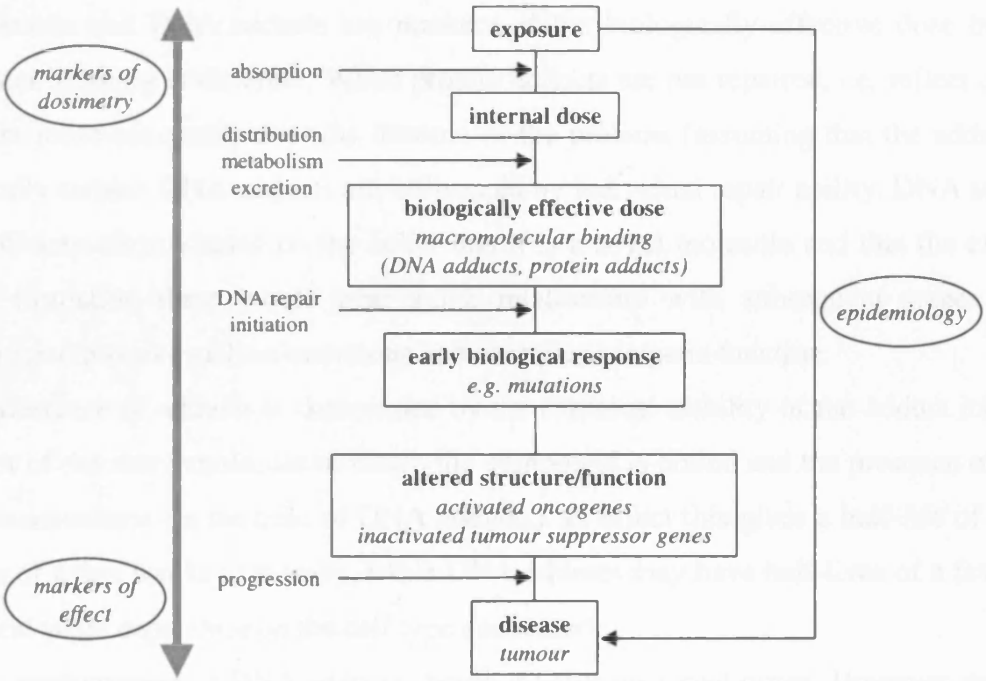

Figure 1.1: *Biomonitoring exposure to genotoxic compounds.* The formation and prevalence of DNA adducts is dependent on a multitude of events such as absorption of the genotoxic compound, its distribution to different tissues, and if necessary its metabolic activation to reactive intermediates. In general, DNA adducts reflect on individual susceptibility as well as differences in DNA repair.

As outlined by several authors [e.g. Beach (1992), Decaprio (1997), Farmer (1994), La (1996), Ward (1996), Wild (1998)] the analysis of biomarkers is increasingly being incorporated into epidemiological studies to gain greater knowledge of the risk factors and mechanisms responsible for the induction of cancer. This approach has the advantage of being directly relevant to human risk, unlike animal or other experimental models that require extrapolation to humans. Furthermore, carcinogen adducts provide a relevant measure of exposure at the target molecule.

In principle, adducts present a more objective measure of exposure to carcinogens in humans than can be obtained by environmental measurements or questionnaires. Adducts provide a measure of the biologically effective dose as they represent exposure, absorption, distribution to different tissues, metabolism (activation and detoxification), DNA repair and cell turnover. Carcinogen adducts are also potentially highly specific for the exposure of interest making them particularly suitable when specific carcinogens are investigated. The development of analytical methods, such as ^{32}P-postlabelling, has enabled highly sensitive detection of these biomarkers and thus helped to avoid misclassification of individuals with regard to their exposure status.

Both protein and DNA adducts are markers of the biologically effective dose but their biological meaning is different. While protein adducts are not repaired, i.e. reflect external exposure more accurately over the lifetime of the proteins (assuming that the adducts are chemically stable), DNA adducts are influenced by individual repair ability. DNA seems to be an obvious choice based on the belief that it is a target molecule and that the extent of adduct formation there would bear some relationship with subsequent stages in the carcinogenic process such as mutations and alterations in gene function.

The persistence of adducts is determined by the chemical stability of the adduct itself, the turnover of the macromolecule to which the compound is bound and the presence of active repair mechanisms (in the case of DNA adducts). In effect this gives a half-life of protein adducts of a few weeks to months, while DNA adducts may have half-lives of a few hours to several years depending on the cell type concerned.

Ideally, measurement of DNA adducts should involve the target organ. However, sampling of human target organs is usually not feasible. DNA adducts of carcinogens are measured instead in more accessible surrogate tissues, such as peripheral blood. Adducts at non-target sites must correlate quantitatively with those at target sites in order to serve as a valid indicator of risk.

Interindividual variation is another factor which has to be taken into account when correlating a given external exposure and adduct levels. Variations can be based on differences in metabolism or DNA repair with both being dependent on the genetic background of each individual.

The interpretation of adduct data made in target and/or non-target tissue requires the understanding of several factors. These include (i) the specificity and sensitivity of the measurement, (ii) the temporal relationship between exposure, adduct level and disease and (iii) the mechanistic role of the adduct of interest in the carcinogenic process. This knowledge as well as careful study design are essential prior to application of biomarkers such as DNA and protein adducts to epidemiological studies.

DNA adducts formed by potent alkylating agents originating from the endogenous nitrosation of amino acids and peptides, O^6-carboxymethyl-2'-deoxyguanosine (O^6-CMdG) and O^6-methyl-2'-deoxyguanosine (O^6-MedG), and their contribution to mutations of the tumour suppressor gene p53 will constitute a substantial part of this work. O^6-CMdG is a DNA adduct formed specifically by nitrosated glycine derivatives and thus may reflect on diet and endogenous processes within the body. In contrast, O^6-MedG is not only formed by nitrosated glycine derivatives but also by a multitude of (environmental and endogenously formed) methylating agents and is therefore a less specific and indicative measure.

Further focus of this project will be directed at the main DNA adduct formed via reaction of malondialdehyde, a metabolite of lipid peroxidation and arachidonic acid metabolism, with DNA, namely malondialdehyde-2'-deoxyguanosine (M_1-dG). M_1-dG can also be formed through direct oxidation of DNA bases. This particular adduct can be related to oxidative stress but has also been shown to depend on dietary constituents thus reflecting exposure to a broader spectrum (as opposed to the carcinogen-specific formation of e.g. aflatoxin-DNA adducts). In particular the stability of M_1-dG upon long-term storage and its involvement in p53 mutations will be explored as part of this thesis.

Background information on O^6-alkylguanine and M_1-dG adducts as well as the tumour suppressor gene p53 will thus be given in Sections 1.2, 1.3 and 1.4 respectively. As a final point the aims of this project will be briefly summarised in Section 1.5.

1.2 Endogenous Nitrosation and Formation of DNA Adducts

The human diet contains a multitude of precursors that can be nitrosated in the gastrointestinal (GI) tract, particularly in the stomach, to form N-nitroso compounds (NOC). Among others, precursors belong to the classes of alkylamines, aromatic amines, amino acids, amides and peptides, ureas, bile acids and guanidines. These precursors differ markedly with regard to daily intake, rate of nitrosation and carcinogenicity of the nitroso compound [Shephard (1989)]. As the main focus of this work is directed at the carboxymethyl adduct of guanine, a potential marker of exposure to nitrosation products of amino acids and peptides, other dietary precursors will not be considered in the following. In subsequent sections, DNA damage by alkylating agents in general will be described in more detail. Particular attention will be paid to the endogenous nitrosation of amino acids and peptides and the formation of resulting biomarkers.

1.2.1 DNA Damage by Alkylating Agents

Alkylation of DNA is considered to be a key step in the induction of cancer by many different compounds [Miller (1978)]. N-nitroso compounds are very potent alkylating agents. Dependent on the structure of the N-substituent NOC decompose spontaneously to generate alkyl or aromatic diazonium ions. The diazonium ion is a reactive electrophile and can react with nucleophilic sites in the cell such as proteins or nucleic acids. Reaction with the latter results in the formation of DNA adducts. The formation of DNA adducts has been studied extensively as a potential mechanism by which NOC exert biological effects.

1.2.1.1 Reaction of Alkylating Agents with DNA

Alkylating agents react with the nucleophilic nitrogen and oxygen centres in DNA and at the oxygen atoms of the phosphate internucleotide linkages. There are at least 15 sites in DNA that can be targeted by alkylating agents (Figure 1.2). The specificity of reactions at different centres is dependent on factors such as the nucleophilicity of the DNA site, reactivity of the electrophilic species as well as steric effects i.e. accessibility. Ring nitrogens such as N3 and N7 of adenine and guanine are the most nucleophilic sites in DNA whereas the exocyclic base oxygens are less nucleophilic centres [Singer (1985), Saffhill (1985), Beranek (1990)].

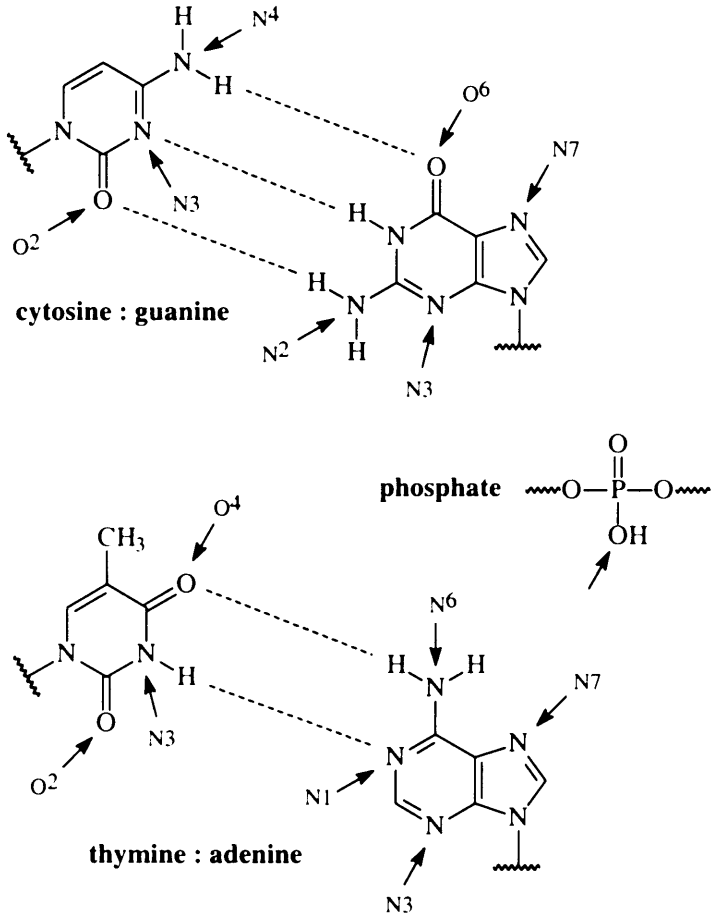

Figure 1.2: *Different sites of modification by alkylating agents in DNA.*

Each alkylating agent produces a different spectrum of adducts and can react via either S_N1 or S_N2 mechanisms (Figure 1.3).

S_N1 mechanism *e.g. methyldiazonium ion*

$$1^{st}\text{ step} \quad RY \xrightarrow{slow} R^+ + Y^-$$

$$2^{nd}\text{ step} \quad R^+ + X^- \xrightarrow{fast} RX$$

S_N2 mechanism *e.g. MMS*

$$X^- + RY \rightleftharpoons [X\cdots R\cdots Y]^- \longrightarrow XR + Y^-$$

Figure 1.3: *S_N1 and S_N2 types of nucleophilic substitution.* RY alkylating agent/electrophile (R alkyl group, Y leaving group), R^+ (electrophilic) carbocation, X nucleophilic site in DNA, RX alkylated product, MMS methyl methanesulphonate.

Nucleophilic substitution involving the S_N2 pathway is a bimolecular reaction which is highly dependent on steric accessibility. During this type of substitution a transition complex is formed which results from the attack of the electrophile on the nucleophilic centre of DNA. An alkylated product is formed upon release of the leaving group [Ehrenberg (1980)].

In contrast, S_N1 reactions are unimolecular and follow in general first order kinetics. The rate of the reaction is dependent on the formation of a reactive electrophilic intermediate, the so called carbocation. The carbocation subsequently reacts with the nucleophilic site in DNA thereby forming a covalently bound DNA adduct [Beranek (1990)].

Less reactive, weak electrophiles such as methyl methanesulphonate (MMS) usually react via S_N2 mechanisms resulting predominantly in alkylation of DNA sites with high relative nucleophilicity. Consequently, adducts are mainly formed with nitrogen centres with very little reaction at oxygen sites. In contrast, highly reactive electrophiles such as the methyldiazonium ion tend to react via the S_N1 mechanism. These electrophiles show less discrimination to the nucleophilicity of DNA sites thereby generating a broader spectrum of DNA adducts with alkylation occurring at nitrogen and oxygen sites (Table 1.1).

	Percentage of Total Alkylation by				
Adduct	MNU	ENU	MNNG	MMS	DMS
N1-alkyladenine	0.7-1.3	0.2-0.3	1.0	1.9-3.8	1.0-3.0
N3-alkyladenine	8.0-9.0	2.8-5.6	12.0	10.4-11.3	15.0-18.0
N7-alkyladenine	0.8-2.0	0.3-0.6	-	1.8	2.0
N3-alkylguanine	0.6-1.9	0.6-1.6	-	0.6	1.1-1.3
N7-alkylguanine	65.0-70.0	11.0-11.5	67.0	81.0-83.0	71.0-76.0
O^6-alkylguanine	5.9-8.2	7.8-9.5	7.0	0.3	0.2-0.3
N3-alkylcytosine	0.06-0.6	0.2-0.6	2.0	< 0.1	< 2.2
O^2-alkylcytosine	0.1	2.7-2.8	-	n.d.	n.d.
N3-alkylthymine	0.1-0.3	0.8	-	0.1	-
O^2-alkylthymine	0.1-0.3	7.4-7.8	-	n.d.	-
O^4-alkylthymine	0.1-0.7	1.0-2.5	-	n.d.	-
phosphotriesters	12.0-17.0	55.0-57.0	-	0.8	-

Table 1.1: *In vitro alkylation patterns of DNA expressed as percentage of total alkylation* [Beranek (1990)]. MNU N-methyl-N-nitrosourea, ENU N-ethyl-N-nitrosourea, MNNG N-methyl-N'-nitro-N-nitrosoguanidine, MMS methyl methanesulphonate, DMS dimethyl sulphate, n.d. not detected or below limit of detection, dash indicates data not reported.

Alkylating agents such as N-methyl-N-nitrosourea (MNU), N-ethyl-N-nitrosourea (ENU) and N-methyl-N'-nitro-N-nitrosoguanidine (MNNG) follow the S_N1 mechanism whereas MMS and DMS (dimethyl sulphate) follow the S_N2 reaction pathway [Beranek (1990)].
These reactions can also be explained by the Swain-Scott substrate constant describing the reactivity of the alkylating agent with nucleophiles [Swain (1953)]. Reagents with a low Swain-Scott constant tend to react more extensively with less nucleophilic centres (e.g. O^6 position of guanine). In contrast, alkylating agents such as MMS with a higher constant tend to react with the more nucleophilic nitrogen centres (e.g. N7 of guanine) [Vogel (1994)].
In essence, S_N1 and S_N2 mechanisms represent extremes for DNA alkylating agents. There is evidence that the methyldiazonium ion $CH_3N_2^+$ reacts via the S_N2 (and not S_N1) pathway. This ion is, however, so reactive that it shows little discrimination between the nitrogen and oxygen centres in DNA [Loechler (1994)].
The degree to which DNA is alkylated and the relative quantities of various adducts depend on the type of alkylating agents and the nature of the alkyl group. The potential to react with oxygen atoms enhances the relative mutagenicity and carcinogenicity of various simple alkylating agents [Saffhill (1985)], thus explaining the increased mutagenicity reported for N-nitroso compounds compared to alkyl methanesulphonates and N-nitroso-N-ethylurea compared to its methyl analogue.

1.2.1.2 Relevance of Certain Alkyl DNA Adducts to Mutation Induction

It is highly unlikely that DNA adducts formed at different sites in DNA contribute equally to mutation induction. One has to distinguish between sites that are generally more susceptible to alkylation and those that are biologically more significant. In general, DNA adducts at sites involved in hydrogen base pairing (such as exocyclic oxygen sites) are more likely to be promutagenic and to result in misincorporation during DNA replication than those centres which are not involved, such as N3 and N7 of guanine and adenine.
Although N7-alkylguanine is predominantly formed by alkylating agents the mutagenic, carcinogenic and cytotoxic potential of the DNA adduct has been considered to be of little biological significance compared to other DNA lesions [Pieper (1998)]. Nevertheless, N3- and N7-alkypurines become easily depurinated at neutral pH due the lability of their glycosidic bond thereby resulting in the formation of biologically significant apurinic sites [Pieper (1998), Saffhill (1985)]. Depurination of N3-methyladenine, N3- and N7-

methylguanine may be further facilitated by DNA glycosylases [Loeb (1986)]. Apurinic sites lead to the preferential misincorporation of adenine residues opposite to these lesions during DNA replication resulting in GC→TA and AT→TA transversions in the case of N7-methylguanine and N3-methyladenine respectively [Loeb (1986)].

Reactions at oxygen sites such as O^6 of guanine, O^2 and O^4 of thymine and O^2 of cytosine are generally more likely to be promutagenic lesions than DNA damage resulting from reactions at nitrogen centres [Saffhill (1985), Singer (1986), Singer (1991)].

O^4-methylthymine, along with O^6-methylguanine is considered to be a major promutagenic lesion formed by alkylating agents. O^4-methylthymine adducts have been shown *in vitro* and *in vivo* to mispair with guanine during DNA replication (Figure 1.4). This stable mispair results in the formation of AT→GC transitions [Preston (1986)]. This class of mutation is consistent with the mutagenic and carcinogenic potential of alkylating agents that form O^4-methylthymine adducts. Although O^4-alkylthymine is formed to a lesser extent than O^6-alkylguanine, the contribution of this adduct to the mutagenic effect of alkylating agents may be significant due to its persistence [Singer (1986)].

The potential relevance of O^6-alkylguanine adducts to the mutagenicity and carcinogenicity of alkylating agents was first investigated by Loveless [Loveless (1969)]. These lesions have been the focus of many studies as their presence and persistence was correlated with alkylation-induced mutagenesis in cells and carcinogenesis in animals [Swann (1968), Loveless (1969), Goth (1974), Samson (1977), Frei (1978), Richardson (1987)]. The mispairing of O^6-methylguanine with thymine (Figure 1.4) during DNA replication results exclusively in GC→AT transitions [Loechler (1984)].

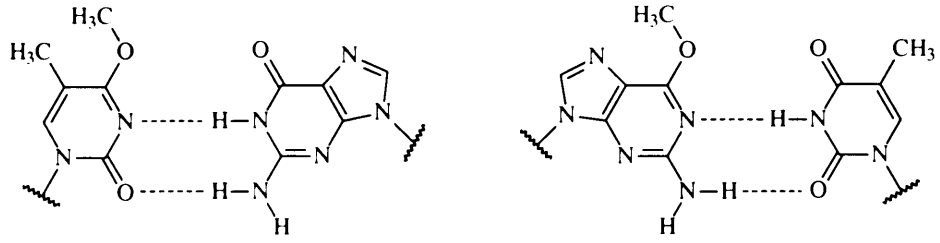

O^4-methylthymine : guanine **O^6-methylguanine : thymine**

Figure 1.4: *O^4-methylthymine and O^6-methylguanine form stable mispairs with guanine and thymine respectively.*

The biological importance of O^6-methylguanine and resulting GC→AT mutations became apparent when it was demonstrated that *ras* oncogenes, which are present in mammary tumours induced by single exposure to MNU in rats, can be activated by GC→AT transitions. Each of the MNU-induced *ras* oncogenes carried the same activating G^{35}→A mutation i.e. transition of the second guanine in codon 12 [Zarbl (1985)]. This type of mutation is common in human colorectal cancer cases expressing *ras* mutations [Bos (1989)].

1.2.1.3 Sequence Specificity and DNA Repair of O-Alkylated Bases

DNA adduct formation is not only influenced by the class of alkylating agent but can also be affected by sequence context, as the reaction of electrophiles with nucleophilic sites in DNA can be affected by bases neighbouring the target base [Richardson (1990)]. A strong preference has been observed in *Escherichia coli* for GC→AT transitions induced by S_N1 agents that act via an alkyldiazonium ion at sites preceded 5' by a purine base (5'-PuG-3'). This preference could not be shown for S_N2 alkylating agents such as alkylsulphates and alkyl alkanesulphonates [Glickman (1987)]. Furthermore GC→AT transitions were nine and five times more likely to occur at guanine residues preceded 5' by guanine or adenine respectively than those preceded by a pyrimidine base (5'-PyG-3') [Burns (1987)]. This sequence preference was explained by an influence of flanking base pairs on the molecular electrostatic potential of the O^6 position in guanine. This observed preference for 5'-PuG-3' over 5'-PyG-3' sites corresponds well with alterations mentioned earlier in the H-*ras* oncogene following MNU treatment [Zarbl (1985)]. The influence of the sequence context also extends to AT→GC transitions. Mutations induced by ENU primarily occurred at 5'-PuT-3' sites, suggesting that the distribution of mutations directed by O^4-alkylthymine lesions is influenced by the same base context effect which appears to control the distribution of O^6-alkylguanine directed mutations [Burns (1988), Dolan (1988)]. Studies have also shown that O^6-alkylguanine and O^4-alkylthymine lesions which are flanked on both sites by GC base pairs are removed less efficiently by excision repair mechanisms. Excision repair appears to preferentially reduce the presence of these ethylation-induced transitions at sites flanked by AT base pairs [Horsfall (1990), Burns (1988)].

DNA repair generally varies with species, cell type and organ explaining in part the sensitivity of certain cells and organs to tumourigenesis. There are two main repair

processes for adducts generated by alkylating agents: (i) direct reversal of the modification by removal of only the altered group and (ii) base/nucleotide excision repair [Singer (1997)].

Lesions at the O^6 position of guanine are repaired predominantly from DNA by the action of an alkyltransferase protein, namely O^6-alkylguanine-DNA alkyltransferase (AGT). The repair enzyme catalyses the transfer of the alkyl group to a cysteine residue within the protein itself. The DNA sequence is thereby restored in a single step. The cysteine acceptor site of the repair enzyme is not regenerated in this process [Pegg (2000), Lindahl (1982), Kyrtopoulos (1998)]. Consequently, the capacity of rapid repair is limited to the number of molecules of O^6-alkylguanine-DNA alkyltransferase present. The amount of enzyme present is specific for species and organs, subsequently more tumours are formed in tissues with less alkyltransferase activity [Pegg (1984), Karran (1985)]. The alkylated form of the repair enzyme is unstable in mammalian cells and degrades rapidly [Pegg (1992)].

Presently there is no evidence of repair enzymes from eukaryotic sources that are able to repair or remove O-alkylpyrimidines i.e. O^2- and O^4-alkylthymine and O^2-alkylcytosine efficiently [Singer (1986)]. However, the *E. coli* AGT protein has been reported to repair O^4-methylthymine very efficiently using the same acceptor site as for the repair of O^6-methylguanine, whereas the human AGT enzyme appears to be very poor in its function [Pegg (2000)].

1.2.2 Biomarkers of Exposure to Nitrosation Products of Amino Acids and Peptides

1.2.2.1 Main Pathways of Endogenous Nitrosation

Numerous authors have proposed that endogenous nitrosation and subsequent formation of N-nitroso compounds plays an important role in human carcinogenesis, in particular in the development of gastric cancer [Mirvish (1995), Correa (1992), Correa (1988), Bartsch (1992)]. Further support for this hypothesis has come from studies reporting elevated levels of NOC in the gastric juice of patients with various pathological gastric conditions [Xu (1993)] and from reports that O^6-methylguanine levels are increased in humans at elevated risk of gastrointestinal tumours [The EUROGAST Study Group (1994), Hall (1991), Kyrtopoulos (1984), Jackson (1996)]. Ohshima and Bartsch [Ohshima (1981)] reported that proline can be substrate to endogenous nitrosation in humans leading to the

formation of stable, non-carcinogenic N-nitrosoproline (NPRO). This observation suggested that endogenous formation of NOC could indeed occur *in vivo*.

Two main pathways have been identified for endogenous N-nitrosation: (i) acid-catalysed reaction and (ii) bacterially-mediated reaction. The fact that the pH optimum of the acid-catalysed reaction is about 2 limits the occurrence of N-nitrosation to the acid stomach. The optimal pH of nitrosation varies for individual, nitrosatable precursors. The main factors influencing the rate of NOC formation in the acidic environment of the stomach are (i) pH, (ii) nitrite concentration, (iii) nitrosatable nitrogen concentration, (iv) presence/absence of catalysts/inhibitors and (v) incubation time [Hill (1996a)]. pH of the normal resting stomach is between 1.0 and 2.0, but can rise to higher values (pH ~ 5) following intake of meals [Kyrtopoulos (1989)]. In acidic aqueous systems, various active intermediates arising from nitrite ions can be formed as illustrated in Figure 1.5.

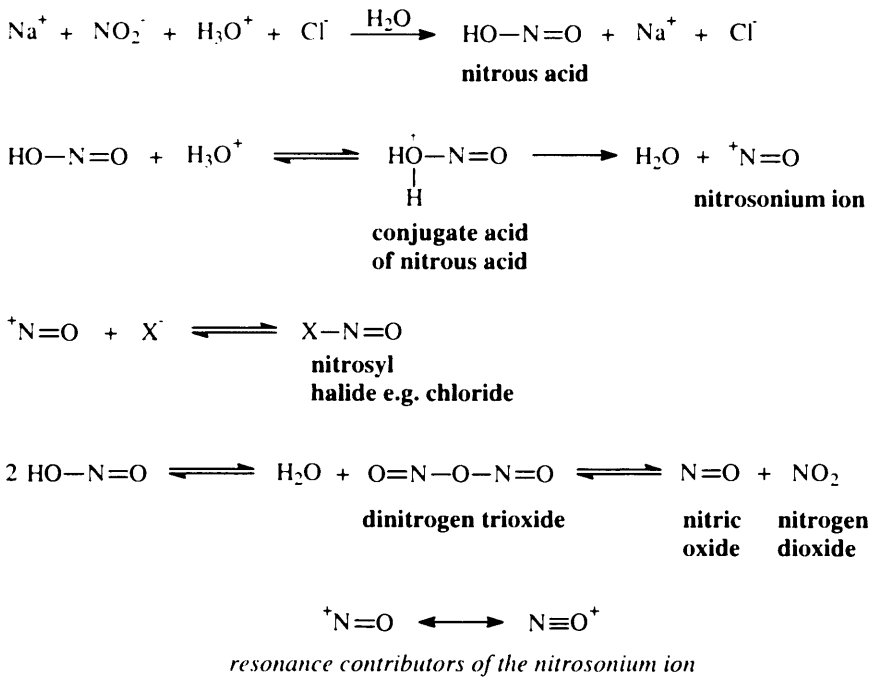

Figure 1.5: *Nitrosating species arising from aqueous acidic nitrite.* Nitrous acid, formed in the presence of nitrite in aqueous acidic environments, is unstable and therefore exists in equilibrium with numerous other species making the definite identification of the reacting species difficult. Nitrous acid is in equilibrium with its anhydride, dinitrogen trioxide. The latter coexists with nitric oxide and nitrogen dioxide. In strongly acidic solutions, nitrous acid is protonated. Its conjugate acid then loses water to give rise to the nitrosonium ion. In the presence of halide ions nitrosyl halides can also be formed. All of these species are potentially sources of the electrophilic nitrosonium ion, a potent nitrosating agent [Leaf (1989)].

Dietary nitrite levels are minimal, thus the main source of nitrite in the stomach is of salivary origin. The level of salivary nitrite is dependent on salivary nitrate and consequently based on dietary intake of nitrate. Salivary nitrate is reduced by bacteria to nitrite and swallowed in the saliva with food [Bartholomew (1984)]. About 10% of nitrate is reduced to nitrite by oral bacteria and enters the stomach as salivary nitrite [Bartholomew (1984)] thus contributing predominantly (~ 80%) to intragastric nitrite found in the normal acidic stomach [Kyrtopoulos (1989), Xu (1993)].

Endogenous nitrosation, usually requiring highly acidic conditions in the absence of bacteria, can also proceed at neutral pH through bacterial enzymes. Bacterially-mediated nitrosation can occur anywhere in the body where bacteria, nitrate or nitrite and nitrosatable nitrogen coexist. The mouth, stomach, large bowel, urinary bladder and vagina are all possible sites for bacterial N-nitrosation [Hill (1996b), Hill (1996)]. In the stomach, reduction of nitrate can only occur in conditions of impaired gastric acid secretion, when a gastric pH consistently > 4 allows extensive colonisation with nitrate-reducing bacteria [Hill (1996a)]. As proposed by Correa [Correa (1988), Correa (1992)] chronic atrophic gastritis and other pathological conditions lead to reduced acid secretion in the stomach. In chronic atrophic gastritis, pH of the gastric juice can increase to pH 3-6, thus permitting the colonisation by bacteria including nitrate-reducing micro-organisms. Intragastric nitrite concentrations increase substantially via this pathway, contributing over 90% of total gastric nitrite in the hypochlorhydric stomach [Kyrtopoulos (1989)], not only because nitrite is formed *in situ* but also because it is more stable at neutral pH [Xu (1993)].

However, endogenous nitrosation is not only influenced by pH and levels of nitrite but is also dependent on the presence or absence of catalysts and inhibitors. Thiocyanate and halides such as chloride which are known to be present in some physiological fluids such as saliva and gastric juice, act as catalysts when present in the reaction system due to the formation of nitrosating species such as nitrosyl halides [Kyrtopoulos (1989), Hill (1996a)]. The average concentration of thiocyanate has been reported to be increased up to six times in the saliva of smokers [Tenovuo (1986)]. In contrast, ascorbic acid, α-tocopherol and polyphenols amongst others act efficiently as inhibitors of endogenous nitrosation. The nitrosating species is scavenged by especially ascorbic acid and converted to innocuous products [Mirvish (1996), Kyrtopoulos (1989), Leaf (1989)].

Another pathway likely to contribute to endogenous nitrosation is the elevated formation of nitric oxide (NO) by macrophages and neutrophils during inflammation. The more reactive higher oxides of nitrogen (NO_2, N_2O_3 and N_2O_4) are produced via reaction of NO with

dissolved oxygen and can react in aqueous systems at neutral pH to form nitrite and nitrate. Chronic viral, bacterial and parasite infections and resulting inflammation have long been recognised as risk factors in a variety of human cancers. Gastric cancer and *Helicobacter pylori*, hepatocellular carcinoma and hepatitis B virus as well as ulcerative colitis and increased risk of colon cancer are just some of many examples [Liu (1995), Mirvish (1995), Ohshima (1994)].

Unlike most other bacteria *H. pylori* can tolerate the low pH of gastric juice and will thus survive. Its urease enzyme can neutralise gastric acidity and induce inflammation [Stadtländer (1999)]. A loss of gastric acid would raise the pH thereby permitting colonisation with nitrate-reducing bacteria. Another consequence associated with this particular type of infection is reduced vitamin C concentration in gastric juice [Mirvish (1995)]. Ascorbic acid is normally a protective factor against the formation of NOC [Mirvish (1996)]. *Helicobacter pylori* was recently classed as a Class 1 carcinogen by the IARC and WHO, suggesting that there is sufficient evidence in humans for the carcinogenicity of infection with *H. pylori*.

1.2.2.2 Nitrosation of Amino Acids and Peptides

Peptides and amino acids belong to a multitude of dietary precursors that can become nitrosated [Shephard (1989)]. The nitrosation of amino acids, peptides and proteins has attracted interest due to their high gastric concentrations. Peptides represent the most abundant source of nitrosatable substrates in human gastric juice. Free amino acids are derived from gastric proteolysis of proteins and peptides. Two general pathways have been identified for the nitrosation of peptides which are irrespective of individual constituents. The first reaction involves the terminal primary amino group and results in the formation of diazopeptides (Figure 1.6), alternatively the peptide N-atom can be nitrosated to form N-nitrosopeptides [Challis (1989)].

It was demonstrated using simple dipeptides as model substrates that formation of diazopetides rather than N-nitrospeptides is the major pathway for the nitrosation of small proteins and peptides under gastric conditions [Challis (1987)]. Diazopeptides are rapidly formed at neutral pH via reaction of peptides with gaseous nitrogen oxides and are relatively stable under conditions similar to those found in blood, saliva and the achlorohydric stomach. Under normal gastric conditions (pH < 4, 37°C) several nitrosating agents such as N_2O_3 and NOCl can react with the neutral peptide. Diazopeptides are

generated via an N-nitrosoammonium ion intermediate, formation of the latter being the rate-limiting step. However, diazopeptides decompose rapidly under acidic conditions. In contrast, N-nitrosopeptides are more stable than diazopeptides at both neutral and acidic pH. N-nitrosopeptides decompose to either diazotic acid or diazopeptide (longer chain N-nitrosopeptides), both decomposition products are alkylating agents [Challis (1989)].

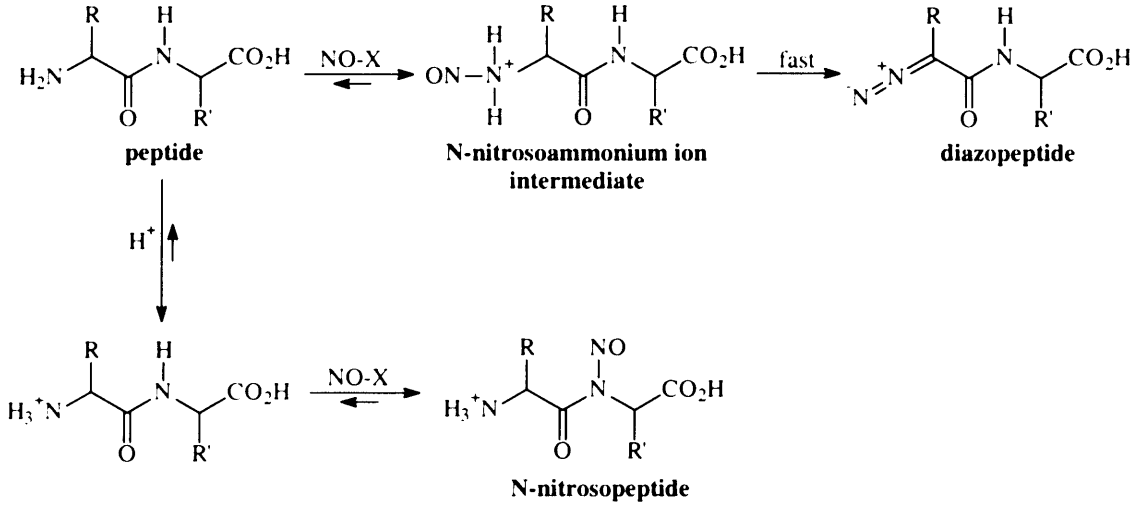

Figure 1.6: *Formation of N-nitrosopeptides and diazopeptides.*

N-nitrosopeptides such as N-(N'-acetyl-L-prolyl)-N-nitrosoglycine (APNG, Figure 1.7) have been shown to be mutagenic [Challis (1989)] and carcinogenic [Anderson (1994)]. These biological properties could originate from the decomposition products of N-nitrosopeptides, diazotic acid or diazopeptides. Although the exact mechanism of genotoxicity has still not been identified, N-nitrosopeptides are likely to exert their effects via DNA alkylation products.

As reviewed by Challis [Challis (1989)] diazopeptides are directly acting mutagens and exhibit cytotoxic properties. Two N-(diazoacetyl)-glycine peptides have also been reported to be tumourigenic, primarily pulmonary adenomas and leukaemia were induced in Swiss mice following intraperitoneal administration [Brambilla (1972)]. Again, it appears likely that cytotoxic and mutagenic properties of diazopeptides relate to their potential to alkylate DNA.

1.2.2.3 Nitrosated Glycine Derivatives: Features and Reaction with DNA

Several compounds known to be mutagenic and carcinogenic share the common feature of being derived from the simplest α amino acid (Figure 1.7). *In vitro* studies with a number of nitrosated glycine derivatives led to the concomitant formation of two O^6-alkylguanine DNA adducts, O^6-CMdG and O^6-MedG [Harrison (1999), Shuker (1997)].

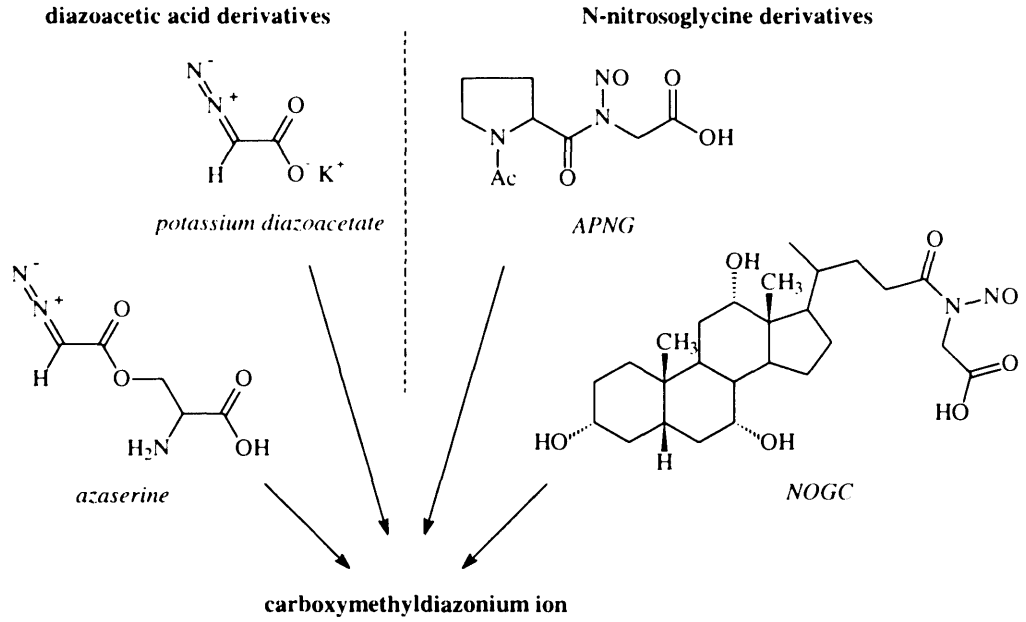

Figure 1.7: *Several diazoacetic acid and N-nitrosoglycine derivatives.* Both diazoacetic acid and N-nitrosoglycine derivatives give rise to a common reactive, potent alkylating intermediate, the carboxymethyldiazonium ion. APNG N-(N'-acetyl-L-prolyl)-N-nitrosoglycine, NOGC N-nitrosoglycocholic acid. NOGC is a carcinogenic and mutagenic derivative of the naturally occurring bile acid conjugate glycocholic acid [Shuker (1981), Puju (1982), Busby (1985)].

CT-DNA was treated with a range of concentrations *in vitro* using the N-nitrosoglycine derivative N-(N'-acetyl-L-prolyl)-N-nitrosoglycine (APNG, 0-50mM) and two different diazoacetic acid derivatives, namely potassium diazoacetate (KDA, 0-5mM) and azaserine (AS, 0-10mM). Samples were analysed using immunoaffinity purification followed by HPLC fluorescence. The limits of detection of this assay were 0.1 pmol and 0.05 pmol per injection for O^6-CMdG and O^6-MedG respectively [Harrison (1999)]. In all cases, dose-dependent increases in O^6-CMdG and O^6-MedG levels were observed. Interestingly, relative proportions of both DNA adducts differed markedly with generally more O^6-CMdG being formed. The ratio of carboxymethyl to methyl adduct ranged from 10:1,

16:1 to 39:1 for APNG, KDA and AS respectively. Furthermore the capacity of these nitrosated glycine derivatives also differed quite dramatically with regard to DNA carboxymethylation. Relative levels of O^6-CMdG were 1:11:134 following 5mM treatments using AS, APNG and KDA respectively [Harrison (1999)], indicating that potassium diazoacetate was the most potent carboxymethylating agent.

Similarly, the nitrosated bile acid conjugate N-nitrosoglycocholic acid (NOGC), which is also a N-nitrosoglycine derivative, gives rise *in vitro* to a number of carboxymethylated DNA adducts including N7-carboxymethylguanine (N7-CMG), N3-carboxymethyladenine and O^6-CMdG. Additionally, DNA is methylated forming O^6-MedG and N7-methyl-guanine [Shuker (1997)].

Although KDA was synthesised and described first in 1908 [Müller (1908)], its genotoxic effects have been investigated only recently by Anderson et al. [Anderson (1999)] using the single cell gel electrophoresis (Comet) assay, which measures DNA strand breakage. Treatment with KDA induced DNA damage in three different cell types, namely human adenocarcinoma colon Caco-2 cells, freshly isolated rat primary colon cells and human peripheral lymphocytes. This study confirmed that KDA is genotoxic in a range of mammalian cells.

Azaserine (O-diazoacetyl-L-serine), a pancreatic carcinogen [Longnecker (1975)], has also been shown to carboxymethylate DNA at the N7 position of guanine, and N7-CMG was detected in DNA extracted from pancreatic acinar cells treated with [^{14}C]azaserine [Zurlo (1982)].

Recently, O'Driscoll et al. investigated DNA repair pathways and the contribution of DNA lesions to AS-induced cytotoxicity in human cells [O'Driscoll (1999)]. DNA repair pathways were: (i) AGT which directly reverses potentially cytotoxic O^6-MedG to guanine, (ii) mismatch repair (MMR) which converts unrepaired O^6-MedG into lethal DNA damage and (iii) nucleotide excision repair (NER) which selectively excises lesions that significantly distort DNA structure. O'Driscoll's experiments demonstrated that AGT-deficient cells were not significantly more sensitive than repair-proficient cell lines. Furthermore, absence of an active MMR pathway did not alter cellular sensitivity to the azaserine. Similar results were also obtained for KDA. In contrast, NER-deficient cell lines were significantly more sensitive to the diazoacetic derivative AS than NER-proficient cells. Thus, it was concluded that the main contributors to the cytotoxicity of nitrosated glycine derivatives are the more bulky carboxymethyl adducts and that these lesions are

repaired by nucleotide excision repair. In contrast O^6-MedG was considered to play only a minor role in AS lethality in human cells.

1.2.2.4 Mechanism and Support for the Nitrosation of Glycine

Since glycine is one of the most common and structurally simplest dietary amino acids, it would appear likely that its nitrosation products would constitute a major source of alkylating agents. Nitrosation of glycine to form diazoacetate is more likely to occur than nitrosation of peptides to give N-nitroso compounds such as APNG [Challis (1989)]. It would therefore seem likely that nitrosation products of glycine (and other amino acids) would constitute a major source of alkylating agents. The proposed mechanism for the nitrosation of glycine is illustrated in Figure 1.8.

Diazoacetic acid is formed as an intermediate that can generate both carboxymethyldiazonium and methyldiazonium ions, the latter reactive species being formed via decarboxylation of diazoacetate. Both diazonium ions are highly reactive electrophiles and potent alkylating agents. Carboxymethyldiazonium and methyldiazonium ions can react with nucleophilic sites in DNA to form O^6-CMdG and O^6-MedG adducts respectively.

Recent *in vitro* studies lend further support to the hypothesis that nitrosated glycine derivatives are formed via reaction of dietary amino acids with nitrosating agents. Cupid et al. [Cupid (2001)] demonstrated that glycine can be nitrosated under physiological conditions using NO in the presence of oxygen. Formation of the transitory intermediate diazoacetate was found to be linear with glycine and nitrosating agent concentration (measured as nitrite). Furthermore, the product from nitrosation of glycine was found to react with 2'-deoxyguanosine and CT-DNA at conditions likely to be present in the GI tract *in vivo* and to form O^6-CMdG adducts.

Further evidence of the likely exposure to nitrosated peptides and amino acids is based on the fact that O^6-CMdG is indeed detectable in human gastric biopsies using a sensitive ISB assay [Singh (2000)]. The limit of detection of this assay used in our laboratory is 15 O^6-CMdG adducts per 10^8 normal nucleotides using 1 μg of DNA. Gastric biopsies analysed by the ISB assay had been collected from patients recruited into a *H. pylori* eradication clinical trial. O^6-CMdG was present in about half of the gastric biopsies at levels ranging up to 68 adducts per 10^8 normal nucleotides. The presence in some cases

and absence in others might indicate valuable information about individual risk and exposure from dietary nitrosated amino acids.

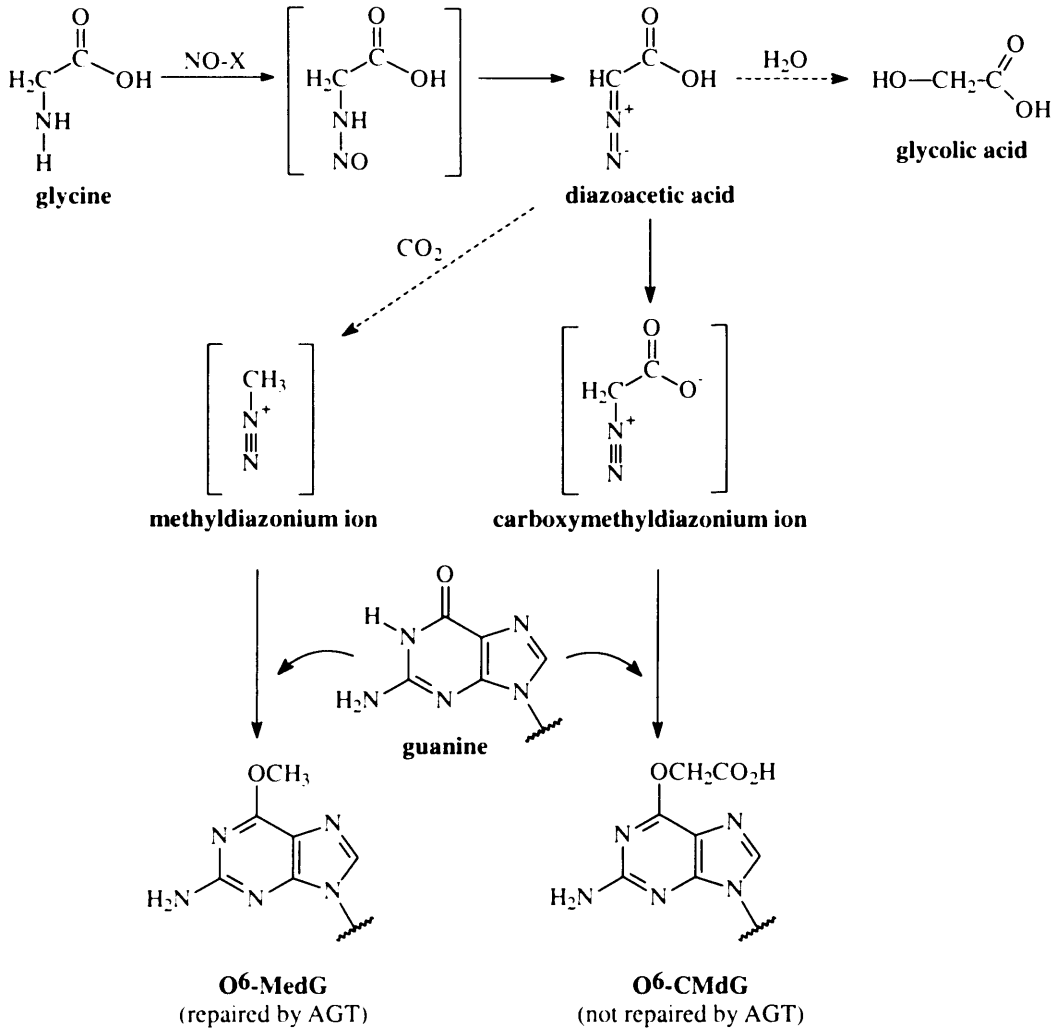

Figure 1.8: *Mechanism for the nitrosation of glycine and subsequent formation of O^6-MedG and O^6-CMdG.* Nitrosation of glycine gives rise to alkylating agents which carboxymethylate and methylate DNA. Diazoacetic acid is formed as a common intermediate.

The finding that the major O^6 guanine adduct of nitrosated glycine derivatives, O^6-CMdG, is not repaired by bacterial and mammalian O^6-alkylguanine-DNA alkyltransferases [Shuker (1997)] suggests that this adduct is likely to accumulate in the DNA of gastrointestinal tract tissues and possibly be a promutagenic lesion. Although it has been shown recently that carboxymethylated bases are repaired by NER [O'Driscoll (1999)], they appear to be an important contributor to lethal damage in human cells. Formation of the carboxymethyldiazonium ion and resulting DNA adducts are a common feature of

nitrosated glycine derivatives, thus carboxymethylated DNA bases in particular O^6-CMdG appear to be group-specific markers of exposure to diet-related nitrosation pathways.

1.3 Malondialdehyde DNA Adducts as Biomarkers of Lipid Peroxidation

Malondialdehyde (MDA) is a carbonyl compound produced during arachidonic acid metabolism for the synthesis of prostaglandins [Marnett (1994a)] and by lipid peroxidation [Janero (1990)]. The structures of malondialdehyde and its tautomer β-hydroxyacrolein are shown in Figure 1.9. Several pathways leading to the endogenous generation of MDA, products generated via its reaction with DNA as well as properties such as repair and mutagenicity of the main DNA adduct M_1-dG are explained further in subsequent sections of the introduction.

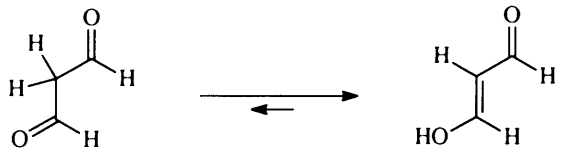

Figure 1.9: *Structures of malondialdehyde and its tautomer β-hydroxyacrolein.*

1.3.1 Generation of MDA by Lipid Peroxidation

Lipid peroxidation is a chain reaction that involves the participation of free radical species. The reaction sequence is characterised by 3 different steps known as (i) initiation, (ii) propagation and (iii) termination (Table 1.2).

The initiation step results from the attack of a free radical on methylene ($-CH_2-$) groups between or adjacent to *cis* double bonds of polyunsaturated fatty acids, and is followed by a chain of reactions known as propagation. This second step yields several types of secondary free radicals such as primary lipid radicals ($L^\bullet$), alkoxyl radicals ($LO^\bullet$) and peroxyl radicals ($LO_2^\bullet$). In the final step of lipid peroxidation, also referred to as termination, a substantial number of non-radical products, mainly alkanes and carbonyl compounds (ketones and aldehydes) are formed [Vaca (1988)].

Initiation	$LH + X^{\bullet} \rightarrow L^{\bullet} + XH$
Propagation	$L^{\bullet} + O_2 \rightarrow LO_2^{\bullet}$ $LO_2^{\bullet} + LH \rightarrow LOOH + L^{\bullet}$ $LO^{\bullet} + LH \rightarrow LOH + L^{\bullet}$
	$LOOH \rightarrow LO^{\bullet} + HO^{\bullet}$ $2\ LOOH \rightarrow LO_2^{\bullet} + LO^{\bullet} + H_2O$
Termination	$2\ L^{\bullet} \rightarrow$ stable products $L^{\bullet} + LO_2^{\bullet} \rightarrow$ stable products $2\ LO_2^{\bullet} \rightarrow$ stable products

Table 1.2: *Key steps of lipid peroxidation.* LH polyunsaturated fatty acid, $X^{\bullet}$ free radical, $L^{\bullet}$ lipid radical, $LO_2^{\bullet}$ peroxyl radical, $LO^{\bullet}$ alkoxyl radical, LOOH hydroperoxide.

Some of the fundamental mechanisms of lipid peroxidation are illustrated in more detail in Figure 1.10. Polyunsaturated fatty acids contain one or more methylene groups located between *cis* double bonds. On attack of free radicals, one hydrogen atom of the methylene group is abstracted and thereby a carbon-centred radical formed. Peroxyl radicals are then formed upon reaction of carbon-centred radicals with oxygen.

If the peroxyl radical is located at the end of the double bond system, it is reduced to a hydroperoxide via reaction with another polyunsaturated fatty acid, thus generating another carbon-centred radical. In the absence of metals, fatty acid hydroperoxides are simple, reasonably stable products of lipid peroxidation. Due to the profusion of metals in the human body though, e.g. in metal complexes or metalloproteins, hydroperoxides are rapidly reduced to alkoxyl radicals (mechanism not shown).

Alternatively if the peroxyl radical is located at an internal position of the double bond system a cyclic peroxide next to a carbon-centred radical can be formed via cyclisation to a neighbouring double bond. The radical position of the cyclic peroxide can then react with oxygen to form a peroxyl radical which is subsequently reduced to a hydroperoxide (mechanism not shown). Alternatively the radical can undergo a second cyclisation to form a bicyclic peroxide. After coupling to oxygen and reduction (e.g. through another fatty acid) a structural analogue to the prostaglandin endoperoxide, PGG_2, is formed. In the final step shown in Figure 1.10 malondialdehyde is generated via chemical conversion of the bicyclic peroxide group [Janero (1990), Marnett (1999)].

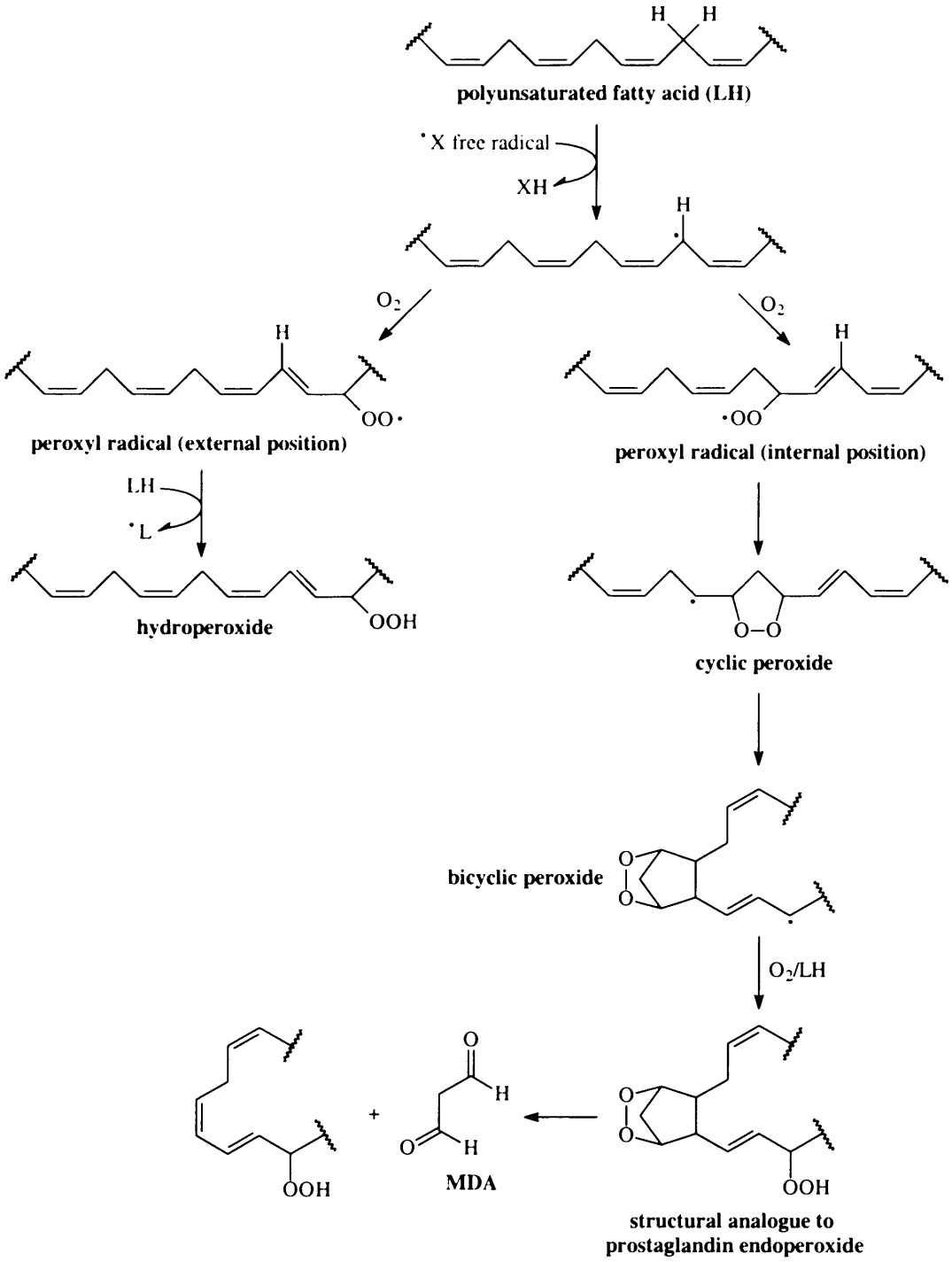

Figure 1.10: *Mechanism of lipid peroxidation and formation of MDA.*

1.3.2 Generation of MDA During Arachidonic Acid Metabolism

MDA can also be generated via the cyclooxygenase pathway of arachidonic acid metabolism (Figure 1.11). Phospholipase A_2 catalyses the conversion of phospholipids (e.g. in cellular membranes) to arachidonic acid. Cyclooxygenase (COX) then converts arachidonic acid to the prostaglandin endoperoxide PGG_2. PGH_2 is formed via reduction of

PGG_2 by the peroxidase activity of the COX enzyme. MDA can be generated via enzymatic and non-enzymatic breakdown of the prostaglandin endoperoxide PGH_2 (Figure 1.12). Several enzymes of the cytochrome P450 family such as thromboxane synthase and prostacycline synthase convert PGH_2 to MDA and other by-products [Plastaras (2000a)]. For example interaction of PGH_2 with thromboxane synthase results in the formation of MDA, 12-hydroxyheptadecatrienoic acid and thromboxane A_2 in a 1:1:1 ratio.

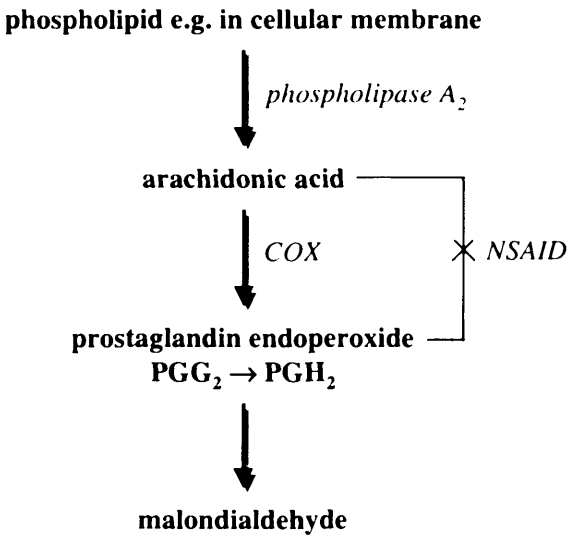

Figure 1.11: *Generation of MDA during arachidonic acid metabolism.* COX cyclooxygenase, NSAID non-steroidal anti inflammatory drugs.

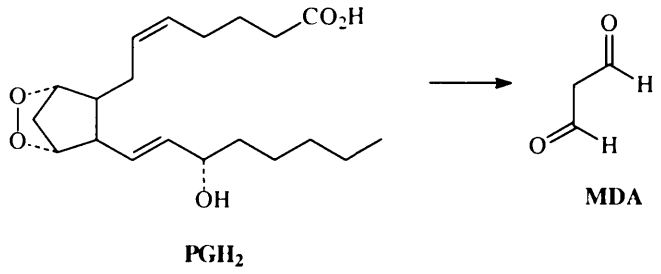

PGH_2

Figure 1.12: *Production of MDA via breakdown of prostaglandin PGH_2.* MDA can be generated via enzymatic and non-enzymatic pathways. The breakdown of the prostaglandin endoperoxide PGH_2 can be catalysed by ferrous ion, heme or enzymes of the cytochrome P450 superfamily.

The biosynthesis of prostaglandins and thus the generation of MDA can be inhibited using non-steroidal anti-inflammatory drugs (NSAID). Specifically, NSAID such as aspirin inhibit the cyclooxygenase activity of this enzyme by acetylating the terminal amino

group. Prostaglandins enhance inflammatory effects whereas aspirin diminishes them. In contrast to that, generation of MDA via the lipid peroxidation pathway is not inhibited by NSAID [Marnett (1994a)].

1.3.3 Alternative Pathway Resulting in the Generation of Reactive Aldehydes

A third pathway has been described recently for the formation of reactive aldehydes. This mechanism, independent of lipid peroxidation and arachidonic acid metabolism, might be important for the generation of genotoxic compounds. Hazen et al. [Hazen (1998)] have shown that activated phagocytes (e.g. neutrophils) utilize the myeloperoxidase-H_2O_2-chloride system to oxidise almost all α-amino acids to a variety of reactive aldehydes. The heme protein myeloperoxidase has been reported to generate hypochlorous acid (HOCl), a potent oxidant, in the presence of chloride ions [Hazen (1996)]. HOCl then oxidises α-amino acids to chloramines which lose chloride and carbon dioxide to form imines. In a final step the imines are hydrolysed to reactive aldehydes (Figure 1.13).

In the case of threonine for example, the hydroxyaldehyde intermediate undergoes dehydration to form acrolein, thus possibly representing an important source of endogenous, DNA damaging acrolein in humans (Figure 1.13, bottom mechanism).

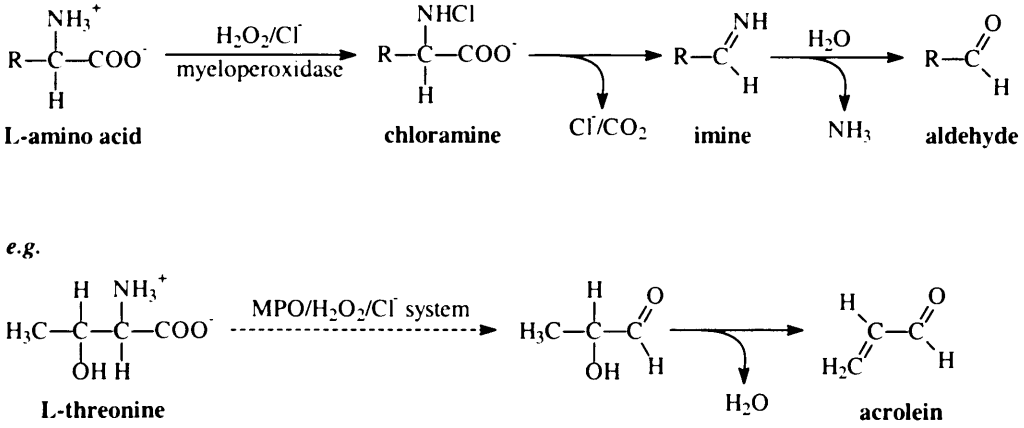

Figure 1.13: *Proposed mechanism for the generation of aldehydes via the myeloperoxidase pathway.* The top pathway illustrates the general transformation of common amino acids to reactive aldehydes via the myeloperoxidase (MPO)-H_2O_2-chloride pathway. The bottom mechanisms gives an explicit example for the generation of acrolein via this pathway originating from L-threonine.

Oxidation of common amino acids via the myeloperoxidase system of neutrophils and subsequent formation of reactive aldehydes may represent an important oxidative pathway utilised by phagocytes at sites of inflammation.

1.3.4 Characteristics of MDA Including Formation and Detection of DNA Adducts

MDA is carcinogenic to rats [Spalding (1988)] and mutagenic to bacteria and mammalian cells [Mukai (1976), Basu (1983), Yau (1979)].

The carbonyl compound reacts with DNA at neutral pH to form multiple adducts. MDA forms a pyrimidopurinone adduct M_1-dG (Figure 1.14) by reaction with N1 and N^2 of 2'-deoxyguanosine with concurrent loss of two molecules of water [Seto (1983), Marnett (1986)]. MDA also forms adducts with deoxyadenosine [Stone (1990a)] and deoxycytidine [Stone (1990b)] as well as interstrand DNA cross-links [Basu (1984)]. Structures of N^6-(3-oxo-propenyl)deoxyadenosine (M_1-dA) and N^4-(3-oxo-propenyl)deoxycytidine (M_1-dC) are shown in Figure 1.15. Comparison of relative amounts of MDA DNA adducts reveals that the pyrimido[1,2-α]purin-10(3H)-one (M_1-dG) is the major adduct. The amount of M_1-dG is approximately five times that of M_1-dA. M_1-dC is formed in only trace amounts.

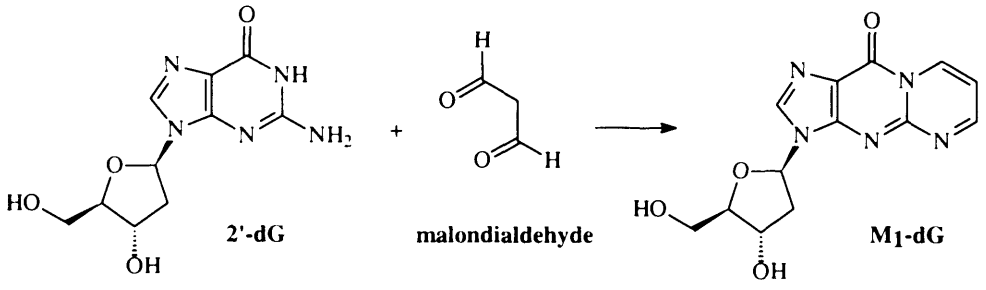

Figure 1.14: *Reaction of malondialdehyde with 2'-deoxyguanosine.* Malondialdehyde forms a pyrimidopurinone adduct M_1-dG by reaction with N1 and N^2 of 2'-deoxyguanosine (2'-dG) and elimination of two molecules of water. Aromatisation provides the driving force for the dehydrations.

The main DNA adduct, a highly fluorescent cyclic pyrimidopurinone (Figure 1.14) has been detected in human white blood cell, breast tissue and gastric DNA using ^{32}P-post-labelling techniques [Vaca (1995), Wang (1996), Leuratti (1998), Yi (1998)]. M_1-dG levels reported ranged for example from 1 to 5 adducts per 10^7 nucleotides in white blood cells

and were on average 3.0 ± 1.3 M_1-dG adducts per 10^7 normal nucleotides in normal breast tissue [Vaca (1995)].

Levels of M_1-dG adducts in leukocytes have also been shown to depend on dietary fatty acid composition using ^{32}P-postlabelling [Fang (1996)]. A substantial increase in M_1-dG levels was detected in subjects on a diet high in polyunsaturated fatty acids (e.g. sunflower oil) when compared to a group which was fed a high rapeseed oil diet (i.e. rich in monounsaturated fatty acids). Higher levels of M_1-dG in leukocytes were consistent with elevated concentrations of polyunsaturated fatty acids detected in plasma triglycerides.

Apart from ^{32}P-postlabelling another method has been employed for the detection of M_1-dG using gas chromatography/mass spectrometry with electron capture negative chemical ionisation detection (GC/EC NCI/MS). Application of GC/EC NCI/MS to disease-free human liver and leukocyte DNA showed that M_1-dG is present at levels of approximately 9 in 10^7 and 6 in 10^8 normal nucleotides respectively [Chaudhary (1994), Rouzer (1997)].

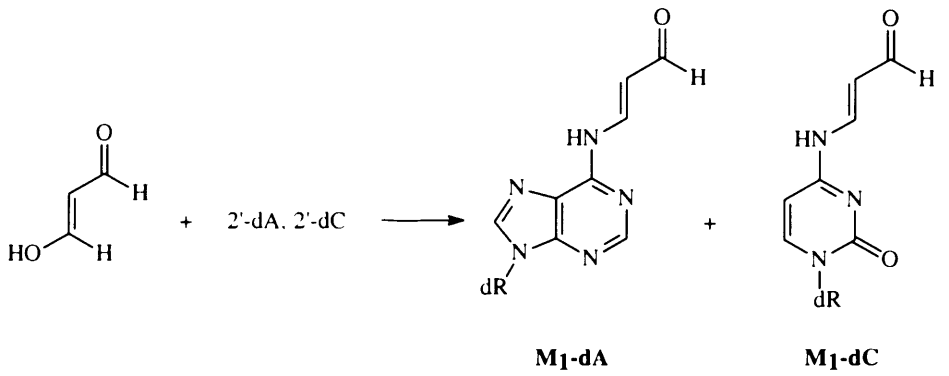

Figure 1.15: *Monomeric adducts formed by reaction of malondialdehyde with deoxyadenosine and deoxycytidine.* Malondialdehyde also forms adducts, M_1-dA and M_1-dC, with deoxyadenosine (2'-dA) and deoxycytidine (2'-dC). Products with 2'-dA and 2'-dC arise by addition of one of the carbonyl equivalents of MDA to the exocyclic amino groups to form an oxopropenyl derivative, followed by elimination of water.

Recently, an immunoslot blot assay (ISB) has been developed for the detection of M_1-dG in intact DNA [Leuratti (1998)]. The limit of detection for M_1-dG in the ISB assay is approximately 5 adducts per 10^8 nucleosides [Leuratti (1999)]. The basic principle of this assay as well as a detailed description are given later in this report (see Chapter 3). The monoclonal antibody D10A1 used in this assay for the detection of M_1-dG has been developed and characterised previously by Sevilla et al. [Sevilla (1997)]. Since its

development, the ISB assay has been applied in our laboratory for the detection of the endogenously formed M_1-dG adduct in various different human tissues such as gastric [Everett (2001)] and colon biopsies [Leuratti (2002)], whole blood as well as animal tissues [Singh (2001)]. M_1-dG levels analysed by ISB assay ranged from undetectable to approximately 12 adducts per 10^7 normal nucleotides in human colorectal tissue [Leuratti (2002)]. Compared to other methods, this assay only requires small amounts of DNA (< 5 μg). Each sample is usually analysed in triplicate on the same filter with only 1 μg of DNA per well needed. Other advantages are that the ISB assay is less laborious and time consuming, thus permitting a high throughput of samples in relatively short time.

1.3.5 Alternative Pathways Leading to the Formation of M_1-dG

Recently, Dedon et al. [Dedon (1998)] have shown that M_1-dG can be formed via direct oxidation of DNA (Figure 1.16), a mechanism independent of lipid peroxidation and arachidonic acid metabolism.

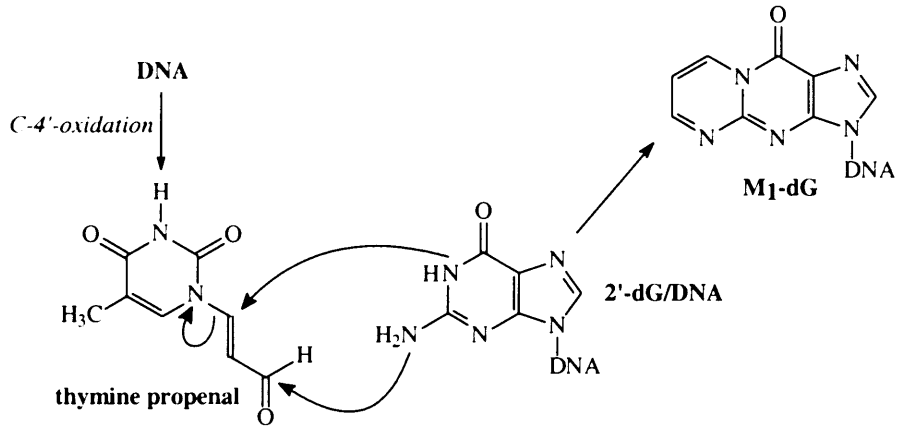

Figure 1.16: *Reaction of thymine propenal with DNA to form M_1-dG.* Direct oxidation of DNA by agents that abstract the 4'-hydrogen atom of the sugar backbone initiates multiple reactions that lead to the formation of base propenals. Thymine propenal, given as an example of base propenals in above scheme, transfers its oxopropenyl group to 2'-dG to form M_1-dG.

The pyrimidopurinone adduct of deoxyguanosine was formed in complete absence of lipids following treatment of DNA with bleomycin or calicheamicin, agents both known to produce base propenals. Base propenals form M_1-dG 30-150 times more efficiently than MDA and have also been reported to be 30-60 times more mutagenic than the product of

lipid peroxidation in the *Salmonella typhimurium* strain *hisD3052* [Plastaras (2000b), Dedon (1998)].

Base propenals can be formed among other products via radical-mediated abstraction of the 4'-hydrogen atom of deoxyribose. A series of reactions leading to the formation of base propenals can be initiated by hydroxyl radicals and agents known to abstract the 4'-hydrogen atom of the sugar backbone such as bleomycin and calicheamicin.

Base propenals are oxopropenyl base derivatives, thus structural analogues to the enol tautomer of malondialdehyde, β-hydroxyacrolein. These derivatives are substituted at the β position with moderate to good leaving groups. The oxopropenyl group of these compounds is transferred to 2'-dG to form M_1-dG (Figure 1.16) thereby providing another pathway linking oxidative stress to the formation of M_1-dG in DNA. Since DNA is directly involved in this pathway this mechanism might represent an important source of M_1-dG. Other DNA damaging agents such as MDA need to diffuse first from the site of generation i.e. lipid membranes prior to interaction with DNA.

1.3.6 Structural Peculiarities and Stability of M_1-dG

M_1-dG is stable at neutral pH and 37°C but unstable to strong bases and when stored in the presence of Tris buffers at -20°C [Niedernhofer (1997)]. The Tris-M_1-dG conjugate is formed exclusively in frozen solutions and is unstable at ambient temperatures but remains stable in organic solvents at room temperature. The reaction might be driven by the Tris buffer becoming more alkaline upon freezing. Alkaline pH ring-opens the M_1-dG adduct to its acyclic form, N^2-(3-oxo-1-propenyl)deoxyguanosine (Figure 1.17). The ring-opened form of M_1-dG possesses a free aldehyde group that could react with primary amines such as Tris.

Another structural peculiarity of M_1-dG was described only recently by Mao et al. [Mao (1999)]. Mao and co-workers reported that M_1-dG undergoes rapid and quantitative ring-opening to N^2-(3-oxopropenyl)-deoxyguanosine at neutral pH when present in duplex DNA opposite to cytosine (Figure 1.17). Ring-opening was shown to be reversible when the duplex was heat-denatured. No ring-opening was detectable when thymine was placed opposite to the exocyclic adduct in duplexes. Furthermore ring-opening did not occur in single-stranded oligonucleotides. The transformation of one adduct into the other with duplex DNA catalysing the reaction might have serious implications for mutagenesis and repair.

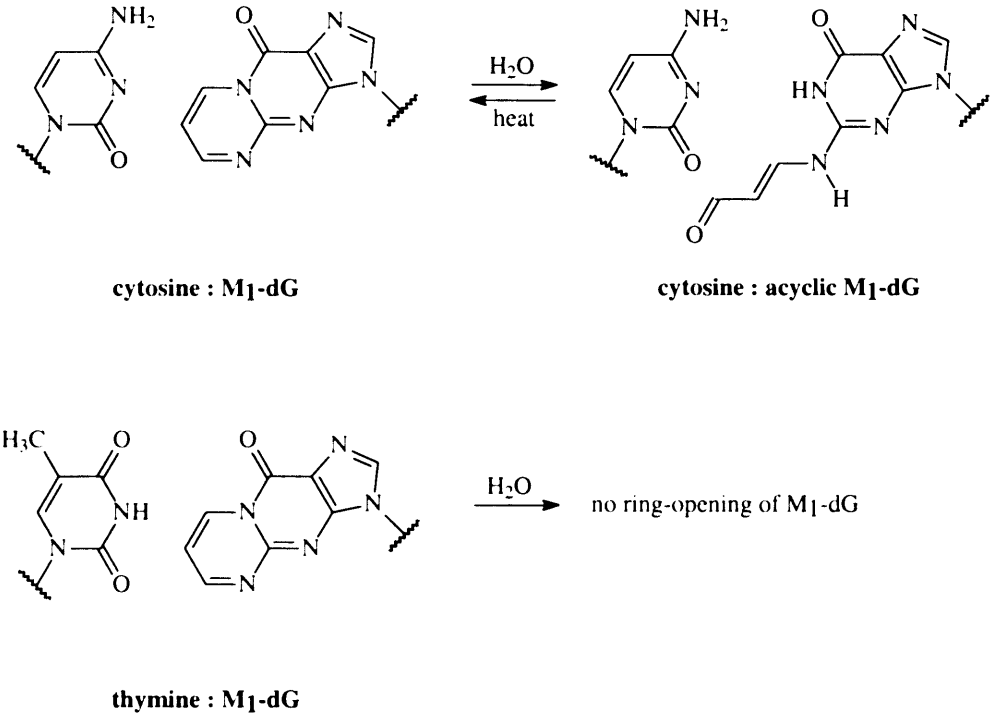

Figure 1.17: *Transformation of M_1-dG in DNA to its acyclic form, N^2-(3-oxopropenyl)-deoxy-guanosine.*

1.3.7 Mutagenic Potential and Repair of M_1-dG

Benamira et al. evaluated the mutagenicity of MDA in the *lacZ*$_\alpha$ forward mutation assay using a recombinant M13 bacteriophage, M13MB102 [Benamira (1995)]. The single-stranded M13 vector was reacted with MDA at neutral pH and the modified DNA was transformed into strains of *Escherichia coli*. The most common mutations induced by MDA were base pair substitutions (76%). 43% of all substitutions were transversions, most of which were accounted for by G→T mutations (83%). Transitions represented 57% of the base pair substitutions and were comprised exclusively of A→G (44%) and C→T (56%) mutations. Frameshift mutations were identified in 16% of the induced mutants (14/89) and involved mainly single base additions occurring in a run of two or more of the same base (11/14). Neither of the two deletions observed occurred in a sequence of reiterated base pairs. Based on the assumption that mutations are targeted to sites of adduction, the capability of MDA to cause base pair substitutions at guanine, adenine and cytosine but not thymine residues corresponded to the generation of M_1-dG, M_1-dA and M_1-dC adducts by MDA.

M_1-dG is believed to be a non-informative lesion based on the fact that the base pairing region of the exocyclic adduct is obstructed, thus explaining the occurrence of G→T transversions [Benamira (1995), Strauss (1991)]. On the other hand, the predominant occurrence of transitions at adenine (A→G) and cytosine (C→T) residues suggested that M_1-dA and M_1-dC are mispairing lesions [Benamira (1995)].

The mutagenic potential of M_1-dG was investigated in a site-specific mutagenesis study [Fink (1997)]. M_1-dG was placed at a defined site in a double-stranded M13 vector and replicated in *Escherichia coli*. M_1-dG placed opposite to cytosine induced equal numbers of M_1-dG→A transitions and M_1-dG→T transversions but only few M_1-dG→C mutations in repair-proficient bacteria. The mutation frequency induced by M_1-dG was approximately 500 greater than the spontaneous one. Results reported by Fink et al. using modified genomes containing thymine opposite to M_1-dG suggested that the exocyclic adduct was a strong block to replication [Fink (1997)].

In general, repair of the exocyclic DNA adduct was assessed by transformation of M_1-dG containing genomes into *E. coli* strains deficient in certain DNA repair genes. Interpretation of findings was based on the assumption that inactivation of a repair gene would increase the half-life of M_1-dG and increase its mutagenicity in site-specific experiments.

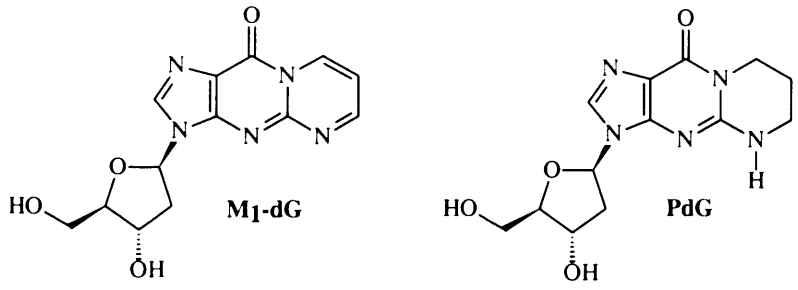

Figure 1.18: *Structures of pyrimido[1,2-α]purin-10(3H)-one (M_1-dG) and its structural analogue 1,N^2-propano-2'-deoxyguanosine (PdG).*

It was reported in the literature that M_1-dG and a structural analogue, propanodeoxyguanosine (PdG), are removed in *E. coli* by nucleotide excision repair [Fink (1997), Johnson (1997)]. PdG is frequently used as a model for the chemically unstable M_1-dG adduct and is excised by both *E. coli* and the mammalian nucleotide excision repair complexes *in vitro*. PdG was shown to be a relatively poor substrate for repair by *E. coli*

nucleotide excinuclease *in vitro* but an excellent one for the removal by the mammalian enzyme complex. The structural analogue to M_1-dG was not a substrate for glycosylases though, whereas certain cyclic adducts such as 1,N^6-ethenodeoxyadenosine and N^2,3-ethenodeoxyguanosine are substrates for bacterial and mammalian 3-methyladenine glycosylases [Johnson (1997)]. Consistent with these findings and by analogy to PdG, M_1-dG has also been reported to be not repaired by 3-methyladenine glycosylase or formamidopyrimidine glycosylase [Fink (1997), Marnett (1999)].

A recent study conducted by Johnson et al. [Johnson (1999)] provides *in vitro* and *in vivo* evidence that repair systems such as nucleotide excision and mismatch repair can overlap and compete when the removal of small DNA adducts, in this particular case M_1-dG and PdG, is concerned. Both adducts were recognised by MutS and repaired by methyl-directed mismatch repair when the genome was not methylated. Binding of MutS to small lesions such as M_1-dG and PdG, even in the absence of subsequent repair, was shown to block the repair of these lesions by nucleotide excision repair. It was also suggested by the authors that the reduced ability of MutS to bind to M_1-dG:C duplexes *in vitro* when compared to M_1-dG:T complexes may result from the formation of the ring-opened form of M_1-dG when the latter is placed opposite to cytosine [Mao (1999), Johnson (1999)].

In conclusion, the evidence presented above indicates that M_1-dG is a highly mutagenic DNA adduct which has also been detected in humans. There are several pathways leading to the formation of M_1-dG, e.g. reaction of MDA with guanine residues in DNA or transferral of an oxopropenyl group from base propenals. The endogenous formation of malondialdehyde in humans and data on its mutagenicity and genotoxictity suggest its potential role in carcinogenesis. Correlation between increase in M_1-dG levels and unsaturated fatty acids in diet, as well as epidemiological association of high fat intake with certain types of cancer [Bartsch (1999), Woutersen (1999)] might indicate an important role of MDA and the M_1-dG adduct in the induction of mutations and ultimately malignant and other human genetic diseases.

1.4 The Role of Tumour Suppressor Gene p53 in Carcinogenesis

Carcinogenesis is a multistage process and involves the activation of oncogenes and inactivation of tumour suppressor genes. Of the many genes associated with the development of cancer the p53 tumour suppressor gene is probably the most striking

example as it is currently known to be the most commonly altered gene in human malignancies. p53 is either lost or contains mutations that inactivate the gene in about half of almost all types of cancer arising from a broad range of tissues. Frequently mutated genes, such as p53, are suitable candidates for the assessment of genetic consequences of carcinogen-DNA adducts and oxyradical induced DNA damage. The majority of cancer types does not show a strong etiological link to one single agent, as multiple carcinogens probably contribute to most tumour types including those of the GI tract.

As part of this project, p53 mutations were induced *in vitro* using malondialdehyde and potassium diazoacetate, both known to induce M_1-dG and O^6-CMdG DNA adducts respectively. Thereby induced mutational spectra were compared to a large p53 database held at the International Agency for Research on Cancer (IARC) in Lyon, France. In the following sections the key facts about p53 and its function are briefly described, in addition the most frequent p53 mutations and characteristic 'mutagen fingerprints' are elucidated.

1.4.1 p53 - Structure and Function

The p53 gene is a tumour suppressor gene which is located on the short arm of the human chromosome 17 (17p13.1). The p53 gene is approximately 20 kb in length and contains 11 exons, the first one non-coding. Exons 2 to 11 of human p53 code for a 53 kDa nuclear phosphoprotein (hence p53) which contains 393 amino acids and is organised in five structural and functional regions. These zones include (i) a transcriptional activation domain in the acidic N terminus (amino acid 1-44), (ii) a proline-rich regulatory domain (amino acid 62-94), (iii) a sequence-specific DNA binding domain (amino acid 102-292), (iv) an oligomerisation domain (amino acid 323-358) responsible for the formation of p53 tetramers and (v) a multifunctional basic C terminus involved in the regulation of DNA binding (amino acid 363-393) [Cho (1994), Hainaut (2000), Hainaut (1995)].

In normal cells the active form of the p53 protein protects DNA from a multitude of physical or chemical DNA damaging agents such ionising (X and γ rays) or UV irradiation, cytotoxic drugs, oxidising agents and carcinogens. Consequently the protein has been often described as the 'guardian of the genome' against genotoxic and non-genotoxic stress. The p53 protein is a multifunctional transcription factor that controls and regulates the expression of various genes involved in a multitude of cellular pathways. It has been implicated in the control of the cell cycle, DNA replication and repair, cell differentiation,

apoptosis and maintenance of genomic stability (Figure 1.19). To date, the role of p53 is best understood as a nuclear transcription factor that binds as a tetramer to specific DNA response elements. p53 can also undergo protein-protein interactions by engaging in numerous complex formations with other cellular and viral proteins [Moll (1998)].

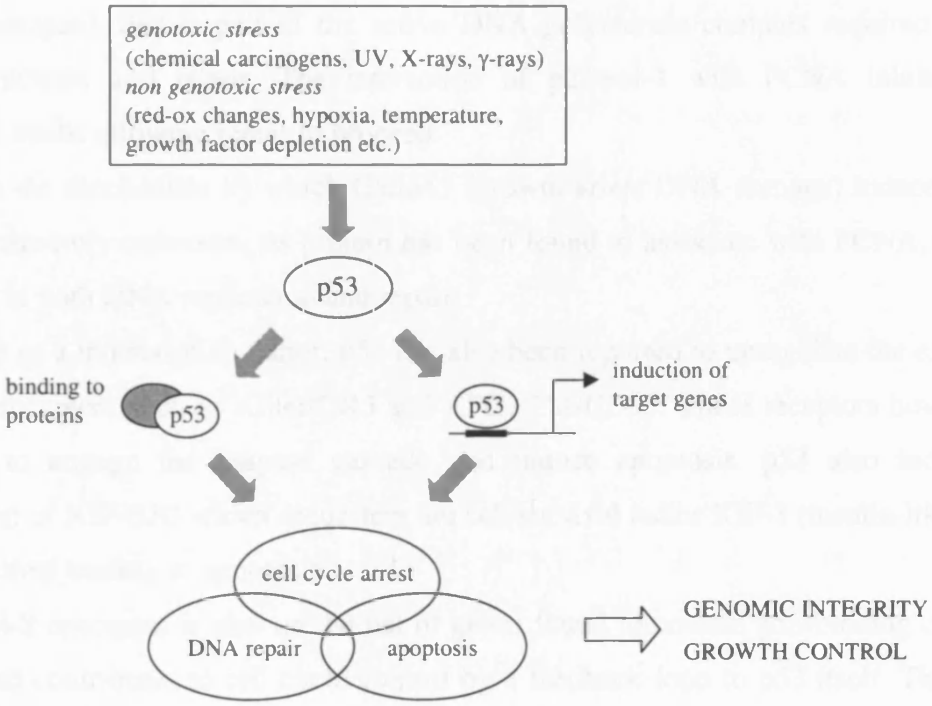

Figure 1.19: *p53 acts on several pathways that control cell life and death.*

To date numerous genes have been identified that contain regulatory sequences capable of binding p53 and whose activity is altered by that interaction. Both stimulatory and inhibitory effects have been documented depending on the gene involved [reviewed by e.g. Sidransky (1996), Moll (1998), May (1999) and Hainaut (2000)]. The three cellular responses influenced mainly by these genes are (i) cell proliferation, (ii) apoptosis and (iii) DNA repair.

In normal cells, transient expression of p53 enables it to fulfil multiple functions primarily, but not exclusively, through its role as a transcription factor. It increases for example transcription of genes involved in the inhibition of DNA replication (p21waf-1, Gadd45) but has opposing effects on the two genes, Bax and Bcl-2, that help regulate apoptosis. Expression of Bax is increased whereas that of Bcl-2 is inhibited. This alteration in Bax to Bcl-2 ratio relieves a block in the apoptosis pathway. Bcl-2 inhibits apoptosis and so a p53-mediated block of Bcl-2 transcription permits this form of cell death. Bax is necessary

for apoptosis; its increased synthesis also results in cell death. The net outcome of above events is blocked proliferation that enables repair to proceed and increased apoptosis that eliminates cells with damaged DNA.

The p21waf-1 protein is an inhibitor of the cyclin-dependent kinases that are essential for the progression through the cell cycle. It also binds to a protein, PCNA (proliferating cell nuclear antigen), that is part of the active DNA polymerase complex required for both DNA synthesis and repair. The interaction of p21waf-1 with PCNA inhibits DNA synthesis whilst allowing repair to proceed.

Although the mechanism by which Gadd45 (growth arrest DNA damage) induces growth arrest is currently unknown, its protein has been found to associate with PCNA, a protein involved in both DNA replication and repair.

In its role as a transcription factor, p53 has also been reported to upregulate the expression of death receptors such as Killer/DR5 and APO1/Fas/CD95. These receptors bind adaptor proteins to engage the caspase cascade and induce apoptosis. p53 also induces the expression of IGF-BP3 which sequesters the cell survival factor IGF-1 (insulin-like growth factor-1) thus leading to apoptosis.

The mdm-2 oncogene is also on the list of genes found to contain p53-binding consensus motifs and contributes to cell cycle control by a feedback loop to p53 itself. The mdm-2 protein binds to the transcription-promoting domain in the N terminus of p53, inhibiting this activity.

The tumour suppressor cannot only exert its effect via acting as a transcription factor but also through protein-protein interaction. p53 interacts with several components of the transcription, replication and repair machineries to either suppress or promote their activities. For example p53 prevents transcription by binding to TBP (TATA box-binding protein) and TBP-associated factors. The p53 protein is also involved in directly inhibiting DNA replication through its association with the single-stranded DNA binding protein complex RPA (replication protein A) that is required for DNA unwinding during replication. p53 also facilitates repair by interacting with two of the xeroderma pigmentosum proteins (XPD/ERCC2 and XPB/ERCC3). Furthermore, the p53 protein stimulates the activity topoisomerase-I through protein binding thereby controlling transcription and DNA repair.

1.4.2 Inactivation of p53 and the Most Frequent Mutations

Inactivation of p53 function occurs by several mechanisms. The p53 protein is inactivated in most human cancers as a result of mutations in the p53 gene or through binding to viral proteins. Some of the DNA tumour virus genes, including the E6 gene of the human papilloma virus, encode proteins that bind to p53 preventing normal binding and thus preventing transcriptional activation. The occurrence of missense mutations, deletions, or nonsense mutations of the gene prevents the protein from oligomerising and forming tetrameric complexes that can bind specific DNA sequences [Hussain (1998)]. p53 somatic mutations are found in most types of sporadic human cancers, the frequency varies from 20% to 60% among tumour types and can be over 80% in some histological subtypes [Greenblatt (1994)]. Mutations of the tumour suppressor gene may also be inherited in families with a predisposition to multiple cancers, as in the Li-Fraumeni syndrome [Malkin (1994)].

In contrast to other tumour suppressor genes about 87% of somatic p53 mutations are missense mutations that lead to amino acid substitutions in proteins thus altering protein conformation. Approximately 13% are complex mutations and short insertions or deletions. More than 90% of all mutations identified to date have been observed in the DNA binding domain and mainly affect amino acids in highly conserved regions. Residues most commonly mutated (codons 175, 245, 248, 249, 273 and 282) represent about 30% of all somatic mutations (Figure 1.20) [Hainaut (2000)]. With the exception of codon 245, five of the six most frequently mutated codons encode arginine residues. These codons play distinct roles in protein-DNA interactions either via directly contacting DNA (residues 248 and 273) or via contributions to the stability of the DNA binding surface (residues 175, 249 and 282) [Cho (1994)].

Hotspots at codon 175, 248 and 273 account for approximately 21% of all mutations. This high rate can be explained in part by the presence of a CpG dinucleotide in these residues. CpG dinucleotides are known to be frequently methylated in the vertebrate genome increasing the probability of mutations at such sites. The high frequency of C→T transitions found at CpG dinucleotides in general is believed to result from spontaneous deamination of 5-methylcytosine. Thymidine is formed via deamination of 5-methyl-cytosine thus resulting in a G:T mismatch which, if not repaired, creates a C→T transition [Ehrlich (1981), Hussain (1998)].

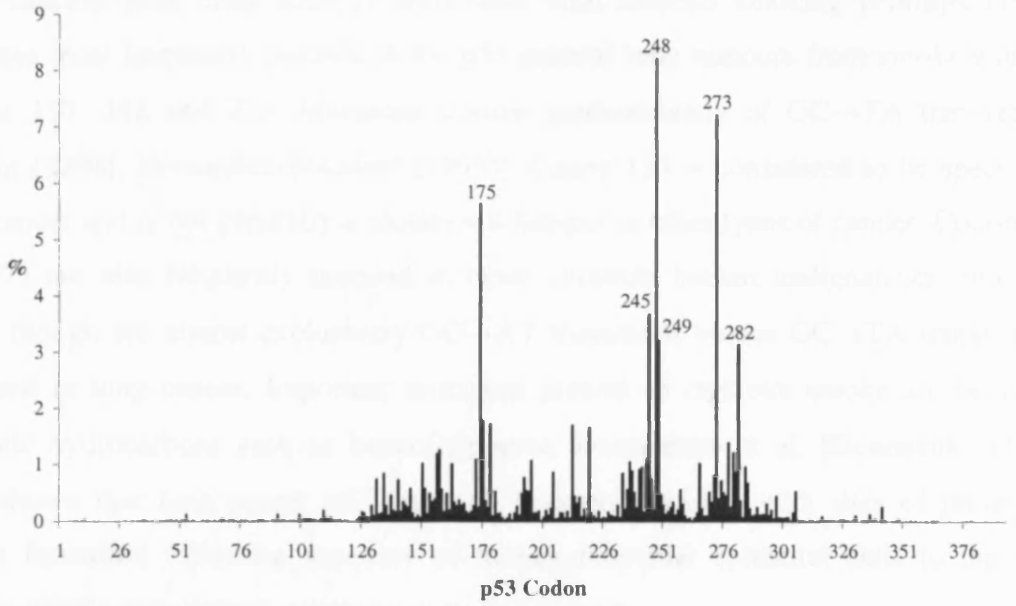

Figure 1.20: *Codon distribution of somatic p53 mutations according to version R5 of the IARC p53 mutation database* [Hernandez-Boussard (1999)].

On average these mutations account for approximately 25% of tumour mutations in all human malignancies. The prevalence of GC→AT transitions at CpG sites is higher in cancers such as colorectal cancer (~ 50%), whereas in patients with head and neck cancer, mutations at CpG sites are relatively uncommon [Sidransky (1996), Moll (1998)].

1.4.3 p53 Mutations as 'Carcinogen Fingerprints'

In several cancers the nature of p53 mutations and their distribution along the coding sequence have allowed the identification of tumour-specific mutation spectra, revealing clues on the mechanism that might have caused the mutation. Some of these 'mutagen fingerprints' are well characterised and mutations have been linked to specific exposure and tumour sites using epidemiological and experimental evidence. Well characterised and extensively documented [Greenblatt (1994), Hollstein (1998), Hussain (1999), Hainaut (2000)] examples are (i) the association of GC→TA transversions in lung cancer with tobacco smoke, (ii) the link between dietary exposure to aflatoxin B_1 and GC→TA transversions at codon 249 (Arg→Ser) in hepatocellular carcinomas (HCC) and (iii) the strong correlation between CC→TT tandem dipyrimidine transitions in skin cancer and exposure to sunlight.

Lung cancers have been strongly associated with tobacco smoking [Phillips (1996)]. Residues most frequently mutated in the p53 gene of lung tumours from smokers include codons 157, 248 and 273. Mutations consist predominantly of GC→TA transversions [Pfeifer (1998), Hernandez-Boussard (1998)]. Codon 157 is considered to be specific for lung cancer and is not generally a mutational hotspot in other types of cancer. Codons 248 and 273 are also frequently mutated in other common human malignancies, mutations found though are almost exclusively GC→AT transitions versus GC→TA transversions observed in lung cancer. Important mutagens present in cigarette smoke are polycyclic aromatic hydrocarbons such as benzo[α]pyrene. Denissenko et al. [Denissenko (1996)] have shown that lung cancer p53 mutation hotspots correlate with sites of preferential adduct formation following exposure of human bronchial epithelial cells to the major tobacco smoke metabolite benzo[α]pyrene diol epoxide.

The high prevalence of G→T transversions affecting the third nucleotide of codon 249 in HCC (Arg→Ser) has been distinctively associated with aflatoxin B_1 exposure [Hsu (1991), Bressac (1991)]. p53 mutational spectra in HCC from different regions of the world have been reported to vary greatly [Montesano (1997)]. In areas of high aflatoxin B_1 exposure, such as Qidong (China) and Mozambique, the frequency of GC→TA mutations in particular at codon 249 clearly dominates the spectrum (~ 90%). In contrast HCC from countries with low or no exposure to the mycotoxin, for instance Europe or the USA, exhibit a distinctly different p53 spectrum with low prevalence of GC→TA transversions (< 10%).

Another strong association has been established using experimental and epidemiological data between UV irradiation and the development of human skin cancer. Mutations of the p53 gene have been found in non-melanoma skin cancers (NMSC) to a large extent. NMSC exhibit a high frequency of C→T transitions including tandem CC→TT mutations, according to the IARC p53 database [Hernandez-Boussard (1999)] these mutations account for 56% and 11% of all mutations. Both types of mutations correlate well with the mutagenic effects of UV light *in vitro*. UV light produces characteristic photoproducts such as cyclobutane pyrimidine dimers. These pyrimidine dimers, if not repaired, result in tandem mutations most characteristically in CC→TT transitions, a distinctive mutation very uncommon in other types of malignancies [Brash (1996), Greenblatt (1994)].

Above examples are the few types of human cancer for which the causative agent is known. Most human malignancies show a more multifaceted and heterogenous p53

mutational pattern though, suggesting a more complex exposure and aetiology. Essential contributors to cancers at other sites in the human body including stomach and colon have yet to be identified and links established.

1.5 Aims of the Thesis

A largely unexplored area of research is the stability of DNA adducts under conditions of long-term storage, and relevant studies are reviewed in the introduction of Chapter 4. This knowledge is important to acquire prior to application of biomarkers to prospective studies such as the European Prospective Investigation into Cancer and Nutrition (EPIC) though. Therefore, not only were existing methods for the detection of two endogenous DNA adducts, M_1-dG and O^6-CMdG, evaluated and further improved, but a major focus of this work directed at the stability of M_1-dG upon storage in CT-DNA standards and human samples.

Mutations at critical DNA sequences can lead to the activation of oncogenes and/or inactivation of tumour suppressor genes. One of the most frequently mutated genes in human cancers is the tumour suppressor gene p53. As part of a collaborative project the yeast expression vector pLS76 harbouring wild-type p53 cDNA was treated *in vitro* using MDA and KDA, thereby induced p53 mutations were analysed and compared to the IARC p53 database. Adduct levels generated by these treatments were also determined.

A brief summary of the aims of this project is given below:

- Further development of the existing ISB assay for the detection of M_1-dG
- Development of the propidium iodide staining for the correction of ISB results
- Reduction and modulation of M_1-dG levels in CT-DNA
- Assessment of M_1-dG stability upon storage in highly modified CT-DNA by HPLC
- Evaluation of M_1-dG stability in long-term stored human samples by ISB assay
- Modulation of O^6-alkylguanine adduct formation using different buffer systems
- Treatment of plasmid pLS76 using diazoacetate, detection of thereby induced mutations and comparison of results to the IARC p53 database
- Detection of O^6-MedG and O^6-CMdG adducts in KDA-treated plasmid
- Treatment of plasmid pLS76 using malondialdehyde, detection of thereby induced mutations and comparison of results to the IARC p53 database
- Detection of M_1-dG adducts in MDA-treated plasmid

2 Materials and Methods

2.1 Materials

Tetramethoxypropane, guanine, calf thymus DNA (type I, sodium salt; D-1501), 2'-deoxyadenosine, 2'-deoxyadenosine-3'-monophosphate, genomic ultrapure CT-DNA (D-4764), propidium iodide, methoxyamine, hydroxylamine, O^6-methyl-2'-deoxy-guanosine (M-8025), reduced glutathione, desferrioxamine, histidine, micrococcal nuclease, nuclease P1, proteinase K, ribonuclease A from bovine pancreas and ribonuclease T_1 from *Aspergillus oryzae* as well as heptafluorobutyric acid (HFBA) and trifluoroacetic acid (TFA) were obtained from Sigma Chemical Co. Ltd. (Dorset, UK). Generally, reagents of highest analytical grade were purchased.

Calf spleen phosphodiesterase, Eco RI, Sau 3A and human genomic DNA (1691112) were purchased from Boehringer Mannheim (Lewes, East Sussex, UK).

Phosphate buffered saline (PBS) tablets (Dulbecco A) were purchased from Oxoid Ltd. (Basingstoke, Hampshire, England). Synthetic M_1-dG and a murine monoclonal antibody (D10A1) for the detection of M_1-dG were kindly provided by Professor L.J. Marnett, Nashville, USA. The Minifold II, 72-well slot blot microfiltration apparatus and the nitrocellulose (NC) filters BA79 (0.1 μm) and BA85 (0.45 μm) were purchased from Schleicher & Schuell (Dassel, Germany). Goat anti-mouse IgG horseradish peroxidase conjugate (P0447) was obtained from Dako (Glostrup, Denmark). Hyperfilm-ECL was purchased from Amersham Life Sciences (Buckinghamshire, UK). Immunoaffinity column kits (polystyrene columns and polyethylene frits), dimethylpimelimidate dihydrochloride and SuperSignal Ultra were obtained from Pierce (Chester, UK). 96-well dot blot apparatus, buffer salts and methanol for HPLC analysis for fluorescence application purchased from Fisher. All other reagents and solvents of analytical grade or HPLC grade were obtained from Fisher Scientific Ltd. (Loughborough, UK) or Sigma, unless otherwise stated.

The National Blood Service Centre, Sheffield supplied whole blood (supplemented with citrate phosphate dextrose anticoagulant) used for the storage experiments.

2.1.1 Antibodies

The murine monoclonal antibody D10A1 specific for the M_1-dG adduct has been prepared and characterised by Sevilla et al. [Sevilla (1997)]. In a direct enzyme-linked immunosorbent assay (ELISA), the antibody has been shown to bind to RNA or DNA that have been reacted with MDA, but not to unmodified proteins, RNA or DNA. In a competitive ELISA, the antibody showed an affinity for M_1-G ribonucleoside that was 2-fold higher than its affinity for the deoxyribonucleoside and 10-fold higher than its affinity for the M_1-G base. Competitive inhibition studies also showed much lower specificity (100- to > 10000-fold) of D10A1 binding to other related exocyclic adducts e.g. etheno-dG and glyoxal-dG [Sevilla (1997)].

The O^6-CMdG rabbit polyclonal antiserum was prepared by D.E.G. Shuker in December 1989 and later characterised by Harrison et al. [Harrison (1997)]. Good recognition of O^6-CMdG was obtained compared to normal deoxynucleosides and carboxymethylated DNA bases using a competitive ELISA. The O^6-CMG ribonucleoside was 30 times less efficient as an inhibitor than O^6-CMdG illustrating the selectivity of the antiserum. O^6-alkylated deoxyguanosine (O^6-MedG and O^6-EtdG), N7-carboxymethylguanine, N3-carboxy-methyladenine and unmodified deoxynucleosides were at least 5000 times less efficient as inhibitors when compared to O^6-CMdG [Harrison (1997)].

O^6-MedG monoclonal antibody kindly provided by G. Margison, Manchester (supplied as cell supernatant) has been prepared and characterised originally by Wild et al. [Wild (1983)]. The specificity of the antibody was established by comparing relative amounts of normal and modified nucleosides needed to yield 50% inhibition of [^{3}H]O^6-MedG binding in radioimmunoassay. The monoclonal antibody was reported to recognise primarily adducts at the O^6 position of guanine. Inhibition by deoxynucleosides modified at this site decreased as the size of the alkyl group increased. Deoxynucleosides modified at other sites as well as five naturally occurring deoxynucleosides (dA, dC, dG, dT and 5-MedG) yielded very little inhibition [Wild (1983)].

The monoclonal antibody EM-2-3 specific for the O^6-MedG adduct was kindly supplied by M. Rajewsky, Essen, Germany. The antibody had been concentrated from hybridoma culture supernatant by ammonium sulphate precipitation and purified using fast performance liquid chromatography (FPLC) prior to receipt [personal communication with P. Lorenz].

2.2 Methods Applied to M_1-dG Work

2.2.1 Synthesis of MDA and Treatment of DNA Using MDA

MDA is a mutagen and carcinogen and should be handled with extreme care.

Malondialdehyde (MDA, 106mM) was prepared by hydrolysis of 14.76 µl 1,1,3,3-tetramethoxypropane stock solution (TMP, 6.97M) with 416 µl of 0.1M HCl at 40°C for 40 min. After this time, 416 µl of 0.1M KOH were added to the mixture in order to stop the reaction.

Calf thymus DNA (CT-DNA) was dissolved in 0.1M potassium dihydrogen orthophosphate solution (KH_2PO_4, pH 4.5) and then treated with MDA (usually at a final concentration of 2mM). The mixture was then incubated at 37°C for 4 days in a gently shaking water bath.

DNA was precipitated by addition of 0.8 volumes of isopropanol. The contents were mixed by inversion and then centrifuged at 4°C for 20 min at 4000 rpm. After the supernatant was discarded the DNA pellet was washed using 70% ethanol. The DNA was recovered by centrifugation for 15 min at 14000 rpm at RT. The supernatant was removed, the DNA pellet was air-dried and then resuspended in HPLC grade H_2O.

2.2.2 Synthesis of Sodium Malondialdehyde

NaMDA is a mutagen and carcinogen and should be handled with extreme care.

Sodium malondialdehyde (NaMDA) was prepared by acid resin catalysed hydrolysis of 1,1,3,3-tetramethoxypropane (TMP) followed by neutralisation according to Gómez-Sánchez et al. [Gómez-Sánchez (1993)]. Dowex 50WX8-100 ion exchange resin (8 g, Aldrich) was placed in a roundbottomed flask with 8 ml water. TMP (16 ml) was added and the mixture was stirred vigorously at RT for 40 min. The reaction is complete when no separation between water and TMP is visible. The ion exchange resin was filtered off using a fine glass frit funnel under vacuum. The resin was discarded and the pH of the filtrate adjusted to pH 7.0 using 10M NaOH. The neutralised solution was extracted three times using 20 ml ethylacetate. The organic phase was discarded and the aqueous phase kept. The aqueous solution (cold) was added dropwise to approximately 300 ml ice-cold acetone. The NaMDA crystals were found to form immediately if the acetone is kept cold. The crystals were filtered under vacuum and stored immediately at -20°C under N_2 gas.

Purity was checked by UV absorbance [λ_{max} (pH > 7) 267 nm, ε 31800] using a Beckman DU 7500 spectrophotometer.

2.2.3 Immunoslot Blot Assay for the Detection of M_1-dG

Modified CT-DNA was diluted with unmodified DNA to obtain decreasing amounts of M_1-dG adduct and used for generating standard curves in the immunoslot blot assay (ISB). Immunoslot blots were carried out essentially as described by Leuratti et al. [Leuratti (1998)] unless otherwise stated. Briefly, 3.5 μg DNA were dissolved in a total volume of 35 μl of 10mM dipotassium hydrogen orthophosphate (K_2HPO_4, KP buffer, pH 7), 115 μl of PBS were then added. The origin of samples analysed by ISB was either CT-DNA containing various amounts of M_1-dG, control CT-DNA, internal standards, human or cellular DNA. All DNA samples were sonicated for 15 min in an ultrasonic bath (Decon FS100b) to obtain fragmented DNA. The DNA was then heat-denatured for 10 min in a boiling water bath, immediately cooled with ice for at least 10 min, and mixed with an equal volume of 2M ammonium acetate (NH_4Ac, 150 μl). The resulting single-stranded DNA (86 μl containing 1 μg DNA per sample, in triplicate) was immobilised on nitrocellulose filters (NC, BA79, pore size 0.1 μm) using a Minifold II, 72-well slot blot microfiltration or 96-well dot blot apparatus applying a moderate vacuum. The slots were rinsed (after allowing them to run dry) with 200 μl 1M NH_4Ac (150μl for dot blots) and left under vacuum for a further 20 min. The filters were subsequently removed from the support and baked at 80°C for 90 min. The filters were bathed for 1 h in 100 ml PBS-Tween 20 (PBS-T, 0.1%) containing 5% fat-free milk powder (Marvel, Premier Brands, UK) in order to block non-specific binding and washed twice for 5 min with PBS-T (50 ml) prior to incubation with anti-M_1-dG monoclonal antibody. The blots were incubated at RT for 2 h then at 4°C overnight with the primary antibody, diluted 1:48,000 (dilutions varied slightly between different M_1-dG antibody batches) in 40 ml PBS-T containing 0.5% fat-free milk powder. The filters were washed after incubation with the primary antibody with 50 ml PBS-T for 1 min followed by three 5 min washes also using PBS-T. The NC filters were then incubated with goat anti-mouse IgG horseradish peroxidase conjugate, diluted 1:4000 in 32 ml PBS-T containing 0.5% fat-free milk powder for 2 h at RT. After incubation with the secondary antibody the filters were washed with 50 ml PBS-T for 15 min followed by three 5 min washes. Finally the membranes were incubated for 5 min with the chemiluminescent reagent consisting of 4 ml

luminol/enhancer solution plus 4 ml stable peroxide buffer (SuperSignal West Dura extended duration substrate; Pierce, Rockford, IL). Filters were exposed to ECL-hyperfilm (chemiluminescent sensitive hyperfilm) prior to the signal being captured using a Biorad Fluor-S^{TM} MultiImager. The chemiluminescent signal was captured using a Tamron 20-40 mm zoom lens and the following conditions: (a) filter 'chemiluminescence' (no emission filter), (b) manual integration for 10-20 min (depending on signal intensity), (c) light source 'chemi no light' and (d) high sensitivity. The signal intensity for each band was determined using the MultiAnalyst software. Results obtained via volume analysis were given as 'adjusted volume' and corrected for local background. Calibration lines were generated using modified CT-DNA (optical density signal versus amount of M_1-dG in fmol/μg). Adduct levels in samples were quantified by referring to the standard curve.

At a later stage during the work the ISB was carried out with some minor modifications [Leuratti (2002)]. Standard CT-DNA and (human) sample DNA (3.5 μg) were dissolved in 10mM K_2HPO_4 (pH 7.0, 100 μl total volume) and PBS (150 μl). DNA samples were sonicated for 20 min in a water bath sonicator, heat-denatured in a boiling water bath for 5 min, then cooled on ice for at least 10 min before mixing with an equal volume of 2M NH_4Ac. The samples and standards were then loaded onto the NC membrane (143 μl containing 1 μg DNA per sample). Final dilution of primary antibody was 1:48,000 of the 0.3 mg/ml D10A1 stock solution. Concentration of secondary antibody remained also the same (1:4000). The number of 5 min washes following primary and secondary antibody incubations was reduced from three to two washes.

2.2.4 DNA Quantitation After the ISB Assay - Propidium Iodide Stain

The NC filters were bathed after the ISB procedure in PBS overnight. They were then incubated for 3 h at RT in 50 ml of PBS containing 250 μg propidium iodide (PI, 5 μg/ml). The filters were washed for 1 h in PBS followed by two further washes for 15 min in PBS (50 ml). The box containing the filter was protected from light for the duration of the staining and washes. The fluorescent signal was captured using the Biorad Fluor-S^{TM} MultiImager equipped with a Tamron 20-40 mm zoom lens and the following conditions: (a) filter '520 nm long pass', (b) automatic integration (stop integrating when more than 0.1% of pixels are greater than 49.0% of full range), (c) light source 'Epi-UV' and (d) high resolution. The level of DNA bound to the filter was determined by integrating the intensity of each band on the filter using the image analysis software. Results obtained via

volume analysis using the MultiAnalyst software were given as 'adjusted volume' and corrected for local background.

An average fluorescent signal was calculated, dividing the total intensity of all bands representing the calibration line by the number of bands (usually 24 or 27 slots/dots). The intensity of individual samples was subsequently divided by this value resulting in a ratio specific for each band. This ratio was then used to correct the chemiluminescent signal and consequently M_1-dG adduct level acquired via ISB assay, thus correcting for individual differences in DNA binding to the NC filter.

2.2.5 DNA Extraction from Whole Blood and Cells

2.2.5.1 Separation of Nuclei

One volume of ice-cold cell lysis buffer C1 (320mM saccharose, 5mM $MgCl_2$, 10mM Tris/HCl, 1% Triton X-100, pH 7.5) and 3 volumes of ice-cold ultrapure H_2O were added to one volume of whole blood. The contents of the tube were mixed by inversion until the suspension became translucent (note: when processing blood samples that are two months old or older, the suspension does not become translucent). The samples were then incubated on ice for 10 min, after which the lysed blood was centrifuged at 1300g for 15 min at 4°C. The supernatant was discarded after centrifugation. The pelleted nuclei were then resuspended by vortexing in ice-cold buffer C1 (1 volume) and ultrapure H_2O (3 volumes) and once again centrifuged as described previously.

In case of nuclei separation from cells, cells growing in suspension were recovered by centrifugation at 1500g for 10 min at 4°C. The cells were washed twice with PBS, and resuspended in PBS to a final concentration of 10^7 cells/ml. Generally 10^7 cells were used for DNA extraction using a Qiagen genomic tip 100/G. The separation of nuclei from cells was carried out as described above for blood samples.

The pelleted nuclei from cells or whole blood could be frozen at this stage at -20°C if necessary.

2.2.5.2 Extraction of Genomic DNA Using Qiagen Genomic-Tips

The nuclei pellet was defrosted and then resuspended by vortexing for at least 30 s in general lysis buffer G2 (800mM GuHCl, 30mM EDTA, 30mM Tris/HCl, 5% Tween-20, 0.5% Triton X-100, pH 8.0). Proteinase K (160 U), RNase A (400 U) and RNase T_1

(400 U) were added in order to digest proteins and RNA. The samples were incubated at 50°C for 60 min. Afterwards the samples were vortexed for 10 s and applied to an equilibrated 100/G Qiagen Genomic-tip (equilibration was carried out using 4 ml buffer QBT containing 750mM NaCl, 50mM MOPS, 15% ethanol, 0.15% Triton X-100, pH 7.0) and allowed to enter the resin by gravity flow. The Qiagen genomic-tip was subsequently washed with 5x 5 ml of a wash buffer QC (1M NaCl, 50mM MOPS, 15% ethanol, pH 7.0). The genomic DNA was finally eluted with 5 ml of elution buffer QF (1.25M NaCl, 50mM Tris/HCl, 15% EtOH, pH 8.5) which was warmed to 50°C to increase the DNA yield. To precipitate the DNA, isopropanol (0.7 volumes, 3.5 ml) was added and the tube stored overnight at -20°C to aid precipitation. The DNA was pelleted (4000 rpm, 4°C, 25 min) and the supernatant discarded. The DNA was transferred to an Eppendorf tube in 1 ml 70% EtOH, re-centrifuged (14000 rpm, 6 min, RT) and air-dried after discarding the supernatant. The pellet was then dissolved in ultrapure water on a shaker overnight at 4°C.

2.2.5.3 Extraction of DNA Using the Qiagen QIAamp Blood Maxi Kit

Buffers used in this section were part of the extraction kit and thus supplied by the company. No details on their specific contents were given in the instructions for use. Blood samples (10 ml) or separated nuclei (pellet taken up in 10 ml PBS) were dissolved in 12 ml lysis buffer AL. Proteinase K (320 U), RNase A (400 U) and RNase T_1 (400 U) were added. The suspension was mixed thoroughly by vortexing. The homogeneous solution was incubated at 50°C for 1 h (originally 10 min at 70°C). Absolute ethanol (10 ml) was added to the sample and mixed again by vortexing. The solution was then carefully applied onto a QIAamp maxi column placed in a 50 ml centrifuge tube and centrifuged at 1850g for 3 min at RT. The column was then removed, the filtrate discarded and the column placed back into the centrifugation tube. Buffer AW1 (5 ml) was then added to the column, and the tube centrifuged at 4500g for 1 min at RT. Buffer AW2 (5 ml) was applied to the column and the tube centrifuged at 4500g for 15 min at RT. The centrifugation tube containing the filtrate was then discarded and the QIAamp column placed in a clean 50 ml centrifuge tube. 1 ml of HPLC grade H_2O was pipetted directly onto the membrane of the column. After incubation at RT for 5 min the tubes were centrifuged at 4500g for 5 min. To obtain highly concentrated DNA and a good yield, the eluate containing the DNA was reloaded onto the membrane along with a further 250 μl of H_2O. The column was then left

for another incubation at RT for 5 min before it was centrifuged again at 4500g for 5 min.

2.2.6 DNA Quantitation and Enzymatic Digestion

2.2.6.1 Analysis Using a UV Spectrophotometer

The DNA concentration was determined by measuring the UV absorbance at 260 nm and 280 nm, assuming that if $A_{260} = 1$, the content equals 50 μg/ml of double-stranded DNA. The purity was assessed by the ratio A_{260}/A_{280} (and by RP-HPLC after digestion to nucleotides). This ratio should be ideally 1.8 for DNA. A GeneQuant II RNA/DNA calculator (Pharmacia Biotech) was used for the UV determinations. The equation used for the calculation of the DNA concentration in [μg/μl] was as follows:

$$[\text{DNA}] = \frac{A_{260} \times DF \times 50}{1000} = \frac{A_{260} \times DF}{20}$$

where DF is the dilution factor of the sample and A_{260} the UV absorbance at 260 nm.

2.2.6.2 Enzymatic Digestion to Nucleotides and Nucleosides

Enzymatic digestion, illustrated in Figure 2.1, was performed with minor modifications according to the procedure described earlier by Leuratti et al. [Leuratti (1998)] and Podmore et al. [Podmore (1997)].

DNA (4 μg) was digested to 2'-deoxynucleotides (dNp) using 0.35 U micrococcal nuclease (MN) and 6 mU calf spleen phosphodiesterase (CSPDE, needs to be dialysed prior to use). SSCC buffer (2 μl of 100mM sodium succinate, 50mM $CaCl_2$, pH 6) was added and the final volume adjusted with ultrapure water to 12.5 μl. The samples were mixed by vortexing, centrifuged and then incubated at 37°C (water bath) for 2 hours. Afterwards, they were dried down in a DNA speed vac, ultrapure H_2O was added (40 μl, solution A) and 20 μl (equivalent to 2 μg of DNA) were taken out from solution A for further digestion to 2'-deoxynucleosides (dN).

10 μl of the remaining solution A (20 μl) were injected onto the HPLC (1 μg/injection) for dNp analysis and DNA quantitation (HPLC system described in Section 2.2.6.3). DNA

was quantitated using a 2'-deoxyadenosine-3'-monophosphate calibration line (dAp, 100 to 1000 pmol).

The following treatment was carried out in order to digest M_1-dGp to M_1-dG. For the digestion to dNs, nuclease P1 (NP1) was added to the aliquot taken out from solution A (20 µl i.e. 2 µg). The samples were digested using 10 µl NP1 (dissolved in 0.28M sodium acetate pH 5.0, 0.5mM $ZnCl_2$ at a final concentration of 2 µg/µl or 0.4 U/µl). The samples were incubated overnight (17 h) in a 37°C water bath. The samples were dried down after incubation and taken up in 20 µl ultrapure water (solution B). 10 µl of solution B (equivalent to 1 µg/injection) were then injected onto the HPLC using the system described in Section 2.2.6.3 and compared to a M_1-dG calibration line (2.5 to 30 pmol) for determination of the adduct.

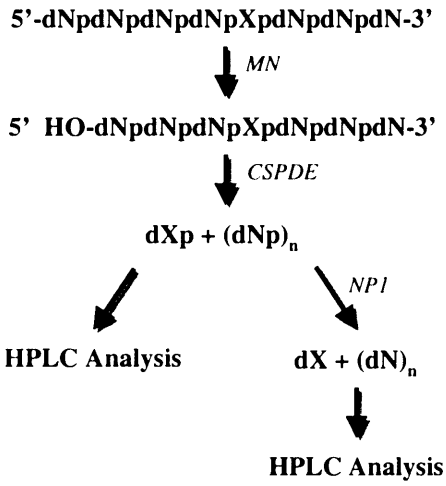

Figure 2.1: *Scheme of DNA digestion using MN, CSPDE and NP1.* DNA is hydrolysed using a cocktail of two enzymes, MN and CSPDE, in the first step of the digestion. MN mediates the endonucleolytic cleavage of DNA yielding strand breaks possessing 5'-HO ends. CSPDE mediates the 5'→3' exonucleolytic digestion of DNA from 5'-HO termini to give nucleoside-3'-monophosphates. Both unmodified (dNp) and modified bases (dXp) are recovered in this fashion and can be analysed by HPLC. In the second step, the 3'-phosphates are removed using NP1 yielding both modified (dX) and normal (dN) 2'-deoxynucleosides. These products of enzymatic hydrolysis can be analysed by HPLC.

2.2.6.3 HPLC Instrumentation for dNp and dN Analysis

All HPLC separations for normal and MDA-modified nucleotides and nucleosides were performed using a Waters 2690 Separations Module (Alliance Autosampler) equipped with a Waters 484 UV (exchanged later for a Waters 2487 dual λ absorbance UV detector) and

Waters 470 fluorescence detector, a narrow bore Hypersil BDS C18 column (100 x 2.1 mm; including a prefilter) and isocratic conditions with 0.1M triethylammonium acetate (TEA, pH 5.0) containing 4% methanol as the eluent. The flow rate was 0.2 ml/min. Peaks for M_1-dGp and M_1-dG were detected by fluorescence (excitation wavelength λ_{Ex} 360 nm, emission wavelength λ_{Em} 500 nm). UV detection at 260 nm was performed in order to analyse and separate the unmodified dNps and dNs.

Enzymatic digestion to dNp followed by HPLC using above system and UV detection was also frequently used to check DNA quality as well as to confirm UV spectroscopic data on a regular basis.

2.2.7 Acid Hydrolysis and HPLC Analysis of DNA Bases

2.2.7.1 Original Acid Hydrolysis Procedure Using 0.1M Formic Acid

For quantitation of the M_1-dG adduct in standard CT-DNA to be used for immunoslot blot, MDA-modified CT-DNA was hydrolysed to the modified and unmodified bases using 0.1M formic acid. This method was described originally by De Groot et al. [De Groot (1994)].

A volume equivalent to 4 μg of DNA was transferred into an Eppendorf tube. The solution was evaporated to dryness using a DNA speed vac (DNA 120, Savant; low temperature). The DNA was dissolved in 0.1M formic acid (100 μl), vortexed, centrifuged at 14000 rpm for 30 s and incubated at 70°C for 1 h. The solution centrifuged again, evaporated to dryness and redissolved in 40 μl of 1mM formic acid. The hydrolysed DNA was vortexed, centrifuged at 14000 rpm for 10 min and injected in triplicate (10 μl/sample) onto the HPLC.

The RP-HPLC separations were performed essentially as described in Section 2.2.6.3, mobile phase was 0.1M TEA (pH 5.0) containing 1% methanol. The peak for the modified base, i.e. M_1-G, was detected by fluorescence (λ_{Ex} 360 nm, λ_{Em} 500 nm). UV detection at 260 nm was performed in order to analyse and separate the purine bases guanine and adenine.

2.2.7.2 Modifications of Above Method

The following acid hydrolysis conditions were tried in order to improve DNA quantitation using this approach. Each method was performed in triplicate and all samples were injected

in triplicate onto the HPLC (system described in 2.2.7.1). 4 μg of MDA-treated CT-DNA were dried down and subjected to the conditions summarised in Table 2.1.

No.	Type of Acid (Amount)	Conditions	Reference
1	1M formic acid (100 μl)	70°C for 1 h	
2	0.1M HCl (100 μl)	70°C for 1 h	
3	1M HCl (100 μl)	70°C for 1 h	
4	0.1M formic acid (100 μl)	100°C for 1 h	
5	0.01N HCl (40 μl)	100°C for 1 h	[Goda (1991)]
6	0.1N HCl (40 μl)	100°C for 1 h	[Goda (1991)]
7	6N HCl (40 μl)	100°C for 1 h	[Goda (1991)]

Table 2.1: *Different acid hydrolysis conditions.* Incubations at 70°C were carried out in a heating block, those at 100°C in a water bath. HCl abbreviates hydrochloric acid.

The original method described in Section 2.2.7.1 was also carried out for comparison. Samples obtained for (1)-(4) were redissolved using 1mM formic acid (40 μl) containing 9-ethylguanine (9-EtG) as an internal standard (concentration of 9-EtG was 0.0046 μg/μl), whereas samples (5)-(7) were taken up in 1mM HCl (40 μl) prior to HPLC injection.

2.2.8 Various Methods for DNA Fragmentation

2.2.8.1 Comparison of Different Sonication Methods

(1) Volumes equivalent to 1 μg of DNA [human genomic DNA (Boehringer Mannheim), MDA-treated and untreated CT-DNA, ultrapure genomic CT-DNA (Sigma) and human samples] were sonicated in 2 different ultrasonic baths for 15 min (Decon FS100b and Kerry KS200), heat-denatured in a boiling water bath for 10 min and put on ice for a further 10 min.

(2) Untreated CT-DNA and human genomic DNA were treated as follows: (a) no sonication, (b) the samples were heat-denatured first for 10 min, put on ice for 10 min and then treated in an ultrasonic bath (Decon FS100b) for 15 min, (c) same treatment as described in part (1) using the Decon ultrasonic bath and (d) the samples were sonicated using the Branson Sonifier 250 sonicator (timer: hold, duty cycle: 10%, output control: 2, time: 5 s), then heat-denatured and put on ice and (e) samples were heat-denatured and put on ice (10 min each).

(3) Different conditions were investigated using the Branson Sonifier 250 sonicator and human genomic DNA. (a) output control: 2, time of sonication: 5, 10, 15 or 20 seconds and (b) output control: 3, same duration as in part (a). Human genomic DNA was compared to CT-DNA, which was only heat-denatured.

The fragmentation of all samples was monitored using agarose gel electrophoresis as described in Section 2.2.8.3.

2.2.8.2 Utilisation of Restriction Enzymes Eco RI and Sau 3A

Restriction endonucleases Eco RI and Sau 3A were used to digest DNA samples replacing the sonication step. Sau 3A recognises the sequence 5'-↓GATC-3' whereas Eco RI recognises the sequence 5'-G↓AATTC-3'. The fragmentation of human genomic DNA and CT-DNA was monitored by gel electrophoresis (Section 2.2.8.3).

3 U, 6 U or 9 U of Sau 3A or Eco RI were used to digest 3.5 μg of DNA (either CT or human genomic DNA). 4 μl of the appropriate buffer (10x concentrated, see below) were added to the samples and the final volume adjusted to 40 μl with ultrapure water.

The 1x concentration of the buffer supplied by Boehringer Mannheim for the incubation with the restriction enzymes was as follows: (a) for Eco RI: 50mM Tris-HCl, 10mM $MgCl_2$, 100mM NaCl, 1mM dithioerythritol, $pH_{37°C}$ 7.5 and (b) for Sau 3A: 33mM Tris-acetate, 10mM Mg-acetate, 66mM potassium acetate, 0.5mM dithiothreitol, $pH_{37°C}$ 7.9. The samples were incubated at 37°C for 30, 60, 90 or 120 min. 10 μl were taken out (0.875 μg DNA) at each time-point and the enzymatic reaction stopped by addition of 0.2 μl 0.5M EDTA, pH 8.0. Final concentration of the chelating agent EDTA was 10mM i.e. equivalent to the concentration of Mg^{2+} contained in the digestion buffer. EDTA was added as Mg^{2+} ions might inhibit DNA binding to NC filters [Kube (1997)]. The samples were heat-denatured for 10 min, then put on ice for a further 10 min prior to analysis using agarose gel electrophoresis (Section 2.2.8.3).

2.2.8.3 Neutral Agarose Gel Electrophoresis

The samples, which were either fragmented by sonication or restriction endonucleases, were separated by electrophoresis using a 2% agarose gel. Each 100 ml agarose gel contained 2 μl ethidium bromide (EtBr, 10 mg/ml) and was run in 1x Tris-borate EDTA

(TBE) buffer [working solution: 0.09M Tris-borate, 0.002M EDTA; preparation of one litre 5x TBE: 54 g Tris base, 27.5 g boric acid, 20 ml 0.5M EDTA (pH 8.0) made up to 1 litre using ultrapure water]. The samples were separated by electrophoresis at 120 V for 1.75 h. A 100 bp DNA ladder (Life Technologies, No. 15628-019, 0.25 μg/μl) was used as a marker (fragment sizes: 2072, 1500, 1400, ..., 200, 100 bp) to determine the fragment range of the different samples. A volume equivalent to 1 μg DNA or 1 μl of marker was mixed with 2 μl of gel loading solution (type 1, 6x concentrate, Sigma G-7654). The final volume was adjusted with ultrapure water to 10 μl, and the entire sample loaded on the gel. An image of the gel was captured using a Dual-Intensity UV Transilluminator (UVP) and a Polaroid MP-4 Land Camera. At later stages a digital image of the gel was acquired using the Biorad Fluor-S^{TM} MultiImager equipped with a Tamron 20-40 mm zoom lens and the following conditions: (a) filter '520 nm long pass', (b) automatic integration (stop integrating when more than 0.1% of pixels are greater than 49.0% of full range), (c) light source 'scan: UV 302(#1)' and (d) high resolution, the scan width being 80 mm.

2.2.8.4 Fragmentation of DNA Using Eco RI and Sau 3A Prior to ISB Analysis

Restriction endonucleases Eco RI and Sau 3A were used to digest DNA samples prior to analysis by ISB assay, replacing the sonication step in order to fragment human and CT-DNA to the same size.

3.5 μg DNA of various origins were dissolved in a total volume of 35 μl of water. 3 U of Sau 3A or Eco RI were used to digest the DNA. 5 μl of a master mix containing 3 U Eco RI or Sau 3A, 10x concentrated digestion buffer (4 μl) and water were added to each sample. The samples were incubated at 37°C for 30 min. The enzymatic reaction was stopped by addition of 110 μl PBS containing 0.5M EDTA, pH 8.0 (EDTA at a final concentration of 10mM). The fragmented DNA was then heat-denatured for 10 min in a boiling water bath, immediately cooled with ice for 10 min, and mixed with an equal volume, i.e. 150 μl of 2M NH_4Ac. The samples were then processed and blotted as described in Sections 2.2.3 and 2.2.4 and compared to sonicated samples on the same immunodot blot.

2.2.9 Potential Improvement of DNA Binding to NC Filters

The following conditions were examined in order to try and improve DNA binding to NC filters and assessed by ISB (Section 2.2.3) and PI assay (Section 2.2.4).

(1) Comparison of two different NC filters, BA79 (0.1 μm) and BA85 (0.45 μm).

(2) As described by Nehls et al. [Nehls (1984)] the filters were baked in a vacuum oven at 80°C for 1.5 h.

(3) NC filters were bathed for 5 min in SSC buffer (0.75M NaCl, 0.075M trisodium citrate, pH 7.0) and then baked for 1.5 h at 80°C in an oven [Nehls (1984)].

2.2.10 Reduction of M_1-dG Levels in CT-DNA Using Methoxyamine

2.2.10.1 pH Study

Three aliquots of 2mM MDA-treated CT-DNA containing approximately 50 μg of DNA were dried down and taken up in 250 μl 10mM K_2HPO_4 buffer (pH 8.0, 8.5 and 9.0). An equivalent of 5mM of a methoxyamine stock was added to each DNA solution. The samples were stored overnight at -20°C and incubated the next day at 37°C. Samples equivalent to 4 μg were taken in duplicate after 0, 0.5, 1, 6 and 24 h incubation and digested to nucleotides using MN and CSPDE following the procedure described in Section 2.2.6.2. The samples were dried down after digestion and taken up in 40 μl water and analysed using the HPLC system described in Section 2.2.6.3. M_1-dGp area obtained by HPLC fluorescence for methoxyamine-treated samples was compared to the area detected in appropriate controls. Final results were expressed as a percentage of the original area.

2.2.10.2 Use of Different Methoxyamine Concentrations

50 μg aliquots of MDA-treated CT-DNA were dried down and taken up in an appropriate volume of 10mM K_2HPO_4, pH 8.0 or water (negative control) to give a final DNA concentration of 0.2 μg/μl. The samples taken up in phosphate buffer were treated with volumes of a 100x stock equivalent to 5, 20 and 50mM methoxyamine treatment. All samples were stored for 66 h at -20°C and then incubated at 37°C. Aliquots containing 4 μg of DNA were taken out after 0, 1, 6, 24, 48 and 72 h incubation and processed as described above (see Section 2.2.10.1).

2.2.10.3 Treatment of Control CT-DNA Prior to ISB

Approximately 350 μg untreated control CT-DNA routinely used for ISB assay were dried down, then taken up in 10mM K_2HPO_4, pH 8.0 to give a final DNA concentration of 0.2 μg/μl. The solutions were treated as summarised in Table 2.2.

Sample	Methoxyamine	Incubation I	Incubation II
A	2.5mM	18 h at -20°C	24 h at 37°C
B	5mM	18 h at -20°C	24 h at 37°C
C	0mM	18 h at -20°C	24 h at 37°C
D	5mM	70 h at -20°C	24 h at 37°C
E	5mM	94 h at -20°C	none

Table 2.2: *Summary of methoxyamine treatments carried out using control CT-DNA.* Incubation I was followed by Incubation II. Samples were analysed by ISB following above incubations and DNA precipitation.

DNA was precipitated using isopropanol, and then 70% EtOH used to wash the DNA pellet. Pellets were dissolved in water and the DNA concentration determined using a UV spectrophotometer (Section 2.2.6.1). All samples were then analysed using the ISB assay described in Section 2.2.3 followed by the PI staining to correct for differences in binding (Section 2.2.4).

2.2.10.4 Follow-up Experiments Using Methoxyamine and Hydroxylamine

Exp. No.	Buffer System	pH	Reagent	Time of Incubation
I	50mM K_2HPO_4	7.4 + 8.0	methoxyamine	0 + 3 h
	50mM K_2HPO_4	7.4 + 8.0	hydroxylamine	0 + 3 h
	50mM MOPS	7.4 + 8.0	methoxyamine	0 + 3 h
	50mM MOPS	7.4 + 8.0	hydroxylamine	0 + 3 h
II	10mM K_2HPO_4	7.4 + 8.0	methoxyamine	0, 1.5, 3, 24, 48 + 120 h
	10mM K_2HPO_4	7.4 + 8.0	hydroxylamine	0, 1.5, 3, 24, 48 + 120 h
	10mM MOPS	7.4 + 8.0	methoxyamine	0, 1.5, 3, 24, 48 + 120 h
	10mM MOPS	7.4 + 8.0	hydroxylamine	0, 1.5, 3, 24, 48 + 120 h

Table 2.3: *Conditions for treatments of MDA-modified CT-DNA using methoxyamine and hydroxylamine.* Final concentration used for all treatments was 5mM methoxyamine or hydroxylamine. Appropriate controls were used in each case, i.e. incubation with buffer system or water only.

Aliquots containing 50 μg of 1mM MDA-treated CT-DNA were dried down and taken up in either MOPS or K_2HPO_4 buffer at a final DNA concentration of 0.2 μg/μl. An equivalent of 5mM of a methoxyamine or hydroxylamine stock was added to each DNA solution. Appropriate controls were used in each case, i.e. incubation with buffer system or water only. All samples were then incubated at 37°C. Details of the different treatment schemes are summarised in Table 2.3. Samples equivalent to 4 μg were taken in duplicate and digested to nucleotides followed by HPLC analysis as described earlier (Section 2.2.6.2).

2.2.10.5 Methoxyamine Treatment of Control CT-DNA

Control CT-DNA was treated using 5mM methoxyamine in 10mM K_2HPO_4 (pH 7.4) prior to analysis by ISB. Untreated CT-DNA was taken up in the buffer system to give a final concentration of 0.2 μg/μl and treated with methoxyamine for 48 h at 37°C. Appropriate controls were incorporated such as incubation with buffer system only (48 h at 37°C) and dissolving the DNA in water. CT-DNA was precipitated following treatments using isopropanol, pellets were washed in 70% EtOH and dissolved in water. DNA concentrations were measured using a UV spectrophotometer (Section 2.2.6.1) and then confirmed by HPLC (Section 2.2.6.2 and 2.2.6.3). Calibration lines using MDA-treated CT-DNA and controls were prepared and analysed by ISB and PI assay (Section 2.2.3 and 2.2.4).

In order to monitor the reaction, 1mM MDA-treated CT-DNA was treated simultaneously (in duplicate) using identical conditions described above for control CT-DNA. Again appropriate controls were included. Samples were taken after 0, 3, 24 and 48 h incubation at 37°C in duplicate and analysed by HPLC (Section 2.2.6.3) following enzymatic digestion to dNp (Section 2.2.6.2).

2.2.11 Methods for the Detection of DNA Damage Caused by Long-Term Storage in CT-DNA Standards and Human DNA

MDA-treated CT-DNA standards as well as human DNA extracted from leukocytes were analysed further in order to determine the type of DNA damage caused by long-term storage. DNA samples were analysed using alkaline and glyoxal gel electrophoresis and SVPD-^{32}P-postlabelling, thus enabling the detection of single-strand breaks and certain

DNA lesions (thymine glycols, phosphoglycolates and abasic sites), respectively. DNA samples had been stored for approximately 2 years prior to analysis.

2.2.11.1 Alkaline Gel Electrophoresis

Alkaline gel electrophoresis was essentially carried out as described by Drouin et al. [Drouin (1996a)]. An agarose gel (1.0%) was prepared in a solution of 50mM NaCl, 4mM EDTA. After the gel was set, it was soaked overnight at RT in 500 ml of alkaline running buffer (30mM NaOH, 2mM EDTA). 3.5 μl of denaturing gel loading buffer (1M NaOH, 50% glycerol, 0.05% bromocresol green) were added to 2 μg (ca. 4 μl) of DNA sample and 1 μl H_2O and left at RT for 20 min prior to loading. For comparison, a mixture (2 μg each) of the following markers was used: λ DNA/*Hind* III fragments (23130, 9416, 6557, 4361, 2322, 2027, 564 and 125 bp; Life Technologies) and ΦX174 RF DNA/*Hae* III fragments (1353, 1078, 872, 603, 310, 271/281, 234, 194, 118 and 72 bp; Life Technologies). The entire sample was loaded onto the gel which was then run at 40 V for about 4.5 h in a large gel apparatus to dissipate the heat. After running the gel it was neutralised in 500 ml of 500mM Tris-HCl (pH 8.0) for at least 30 min at RT. The gel was stained for 30 min in H_2O containing ethidium bromide at a final concentration of 1μg/ml. Afterwards, the gel was destained for about 40 min in 500 ml H_2O. An image of the gel was acquired using the Biorad Fluor-S^{TM} MultiImager. The appropriate settings were described earlier for neutral agarose gels (Section 2.2.8.3).

In such a gel mobility analysis, the average molecular weight (M_w) approximately coincides with the peak density of mass distribution (M_r). The average fragment length M_n is equal to $M_w/2$, provided fragment lengths are normally distributed. The inverse of the average fragment length ($1/M_n$) is the average frequency of DNA strand breaks (lesion density per kb). This figure is multiplied by factor 10 in order to determine the number of strand-breaks per 10^4 bp [Drouin (1996b)].

2.2.11.2 Glyoxal Gel Electrophoresis

Glyoxal agarose gel electrophoresis of single-stranded DNA at neutral pH size fractionates DNA as in an alkali-agarose gel but while retaining alkali-labile sites intact. This type of gel electrophoresis enables a more realistic measure of single-strand breaks, as alkali-labile

lesions do not contribute to the total number of breaks detected. Glyoxal gel electrophoresis was essentially carried out as described by Drouin et al. [Drouin (1996a)]. An agarose gel (1.2%) was prepared in a solution of 10mM sodium phosphate (Na_3PO_4; pH 7.0) using agarose (type I, low EEO; Sigma A-6013). DNA pellets (3 μg) were dissolved in the following mix: 4.5 μl distilled water, 2 μl 0.1M Na_3PO_4 (pH 7.0), 3.5 μl of 6M glyoxal (1M final concentration) and 10 μl DMSO (50% final concentration). Reference markers (3 μg each, λ DNA/*Hind* III and ΦX174 RF DNA/*Hae* III fragments) were mixed with 6.4 μl 0.1M Na_3PO_4, 11 μl glyoxal and 32 μl DMSO (for two lanes). Samples and marker mix were incubated overnight at 4°C, then heated at 50°C for 1 h. The loading buffer was added to each sample (3.8 μl to samples, 12.4 μl to marker) prior to loading. Usually clear loading dye (10mM Na_3PO_4 pH 7.0, 50% glycerol) was used for all samples whereas a blue one [clear dye plus 0.25% bromophenol blue (Sigma B-5525), 0.25% xylene cyanole FF (Sigma X-4126)] was loaded into the outer wells. The entire volume was loaded onto the gel, which was then run submerged in 10mM phosphate buffer (Na_3PO_4, pH 7.0) at 90 V with constant recirculation of the buffer. This is required to maintain the pH at 7.0 and is critical because glyoxal readily dissociates from DNA at pH 8.0 or higher. Electrophoresis was stopped when the bromophenol blue had migrated 65 to 75% of the length of the gel (xylene cyanole FF will have migrated between 30 to 40% at this stage). The gel was stained with SYBR Green II (40 μl in 200 ml 1x TBE; Molecular Probes) at RT for 45 min. An image of the gel was acquired using the Biorad Fluor-S^{TM} MultiImager. The appropriate settings were described earlier for neutral agarose gels in Section 2.2.8.3. The number of strand breaks per 10^4 bp is calculated as described previously in Section 2.2.11.1 for alkaline agarose gels.

2.2.11.3 Snake Venom Phosphodiesterase-Based ^{32}P-Postlabelling Assay

2.2.11.3.1 Basic Principle

In snake venom phosphodiesterase-based ^{32}P-postlabelling (SVPD-^{32}P-postlabelling), digestion yields certain lesions (thymine glycols, phosphoglycolates and abasic sites) as damage containing dimer species, which are ready substrates for labelling. The method, illustrated in Figure 2.2, was carried out as described by Weinfeld et al. [Weinfeld (1996)]. The assay utilises a cocktail of three enzymes in the digestion step. Deoxyribonuclease I (DNase I) mediates the endonucleolytic cleavage of DNA to yield strand breaks possessing

3'-OH ends. Snake venom phosphodiesterase (SVPD) mediates the 3'→5' exonucleolytic digestion of DNA from 3'-HO termini to produce nucleoside-5'-monophosphates (pdN). However, particular lesions inhibit SVPD-mediated hydrolysis of the phosphodiester bond immediately 5' to the lesion. Having arrested at this position the SVPD cleaves the next phosphodiester bond releasing the damage as dimer species (pdNpX). Finally, the 5'-phosphates of both the damage-containing dimers and the 5'-mononucleotides are removed by shrimp alkaline phosphatase (SAP) to yield the corresponding damage-containing 'dinucleoside'-monophosphate species (dNpX) and nucleosides (dN).

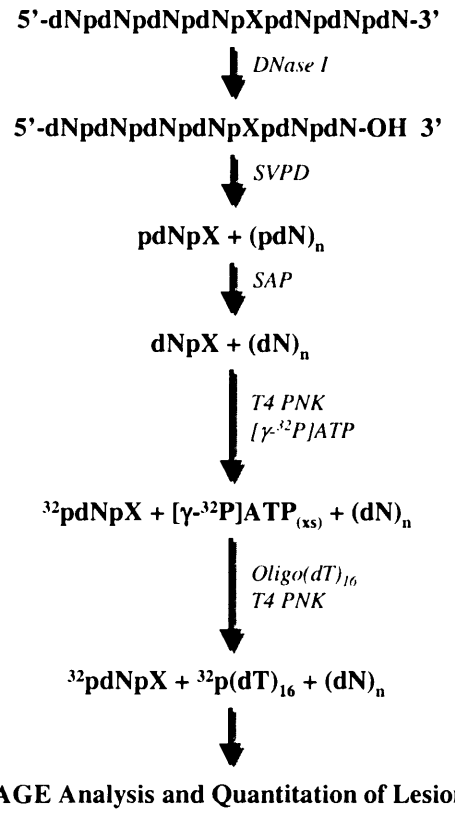

Figure 2.2: *Scheme of SVPD-^{32}P-postlabelling, a technique utilised for the detection of oxidative damage.*

Damage-containing dNpX species possess an unmodified 5'-HO-bearing nucleoside-3'-monophosphate moiety which are ready substrates for 5' ^{32}P-end-labelling by incubation with T4 polynucleotide kinase (T4PNK) plus [γ-^{32}P]ATP. Recovered mononucleosides, representing mainly undamaged DNA, are not substrates for the kinase and remain thus unlabelled.

2.2.11.3.2 Detailed Protocol

DNA samples (10 μg) were digested to mononucleosides and damaged-containing 'dinucleoside'-monophosphate species (dNpX) by an overnight incubation at 37°C using 0.4 U of DNase I (Type II from bovine pancreas), 0.044 U of SVPD (Type IV from *Crotalus atrox*) and 0.4 U of SAP in 30 μl DNA digestion buffer (10mM Tris, 1mM EDTA, 4mM $MgCl_2$, pH 7.5). After digestion the enzymes were precipitated by addition of 3 volumes of ice-cold EtOH and storage at -20°C for 1 h. Precipitates were removed by centrifugation (21000g, 15 min, 4°C) in a microcentrifuge. Aliquots were transferred to Eppendorf tubes, evaporated to dryness and the resulting residues dissolved in distilled water (0.1 μg digested DNA/μl). The samples were heated at 100°C for 15 min to inactivate residual nuclease and phosphatase activity. The samples could then be stored at -20°C.

To phosphorylate the damage-containing 'dinucleoside'-monophosphates in 5 μl of digested DNA, 1 μl of 10x T4PNK buffer [0.5M Tris-HCl (pH 7.6), 100mM $MgCl_2$, 100mM 2-mercaptoethanol], 0.5 μl (3 kCi/mM, 1.65 pmol) [γ-^{32}P]-ATP, 7.5 U of T4PNK, and distilled water to a total volume of 10 μl were added. The samples were then incubated for 1 h at 37°C. To consume the excess ATP, 1 μl of oligo$(dT)_{16}$ (5 A_{260} U/ml) and 3.75 U of T4PNK were added to each sample and incubated for a further 30 min at 37°C. In general with regard to above described incubations, a mastermix (n + 2) was prepared for n samples and an appropriate volume added to each individual sample.

An equal volume of gel loading buffer (90% formamide, 0.02% bromophenol blue, 0.02% xylene cyanole FF in 1x TBE) was added to each sample. Half of the reaction mixture was then loaded onto a 0.8 mm thick 20% polyacrylamide/7M urea gel and run at 1200 V using a Gibco Life Technologies S2 vertical gel system until the lead dye (bromophenol blue) had run 11-12 cm from the bottom of the sample wells (3-4 h). The rest of the reaction mixture could be stored at -20°C. After electrophoresis the radiolabelled products were visualised by autoradiography on Kodak X-Omat AR film (40 x 30 cm) or by PhosphorImager analysis (Model 425E, Molecular Dynamics, Sunnyvale, CA; using ImageQuant software version 3.2).

The level of damage (^{32}pdNpX) expressed as fmol damage per μg of DNA was obtained for each sample as follows. If all radioactivity had been retained on the gel, the molar quantity of radiolabel in a particular number of bands could be quantified by determining

the percentage of the lane's total radioactivity present in those bands, and multiplying this by the molar quantity of [γ-^{32}P]-ATP used in the reaction.

2.3 Methods Applied to Work on O^6-Alkylguanine Adducts

Reagents generating carboxymethyldiazonium ions are alkylating agents and should be handled with extreme caution (probable, potent carcinogens). Unused solutions of potassium diazoacetate (KDA) should be decomposed by overnight treatment using 1M aqueous acetic acid.

2.3.1 HPLC Analysis of O^6-Alkylguanine Adducts

HPLC analysis of O^6-alkylguanine standards as well as KDA-treated, digested DNA samples (CT-DNA and plasmid pLS76) was carried out as part of this project using one of the HPLC systems described in subsequent sections.

2.3.1.1 HPLC System 1

The RP-HPLC separations were performed using a Waters 2690 system equipped with a Waters 470 fluorescence detector (excitation wavelength λ_{Ex} 286 nm, emission wavelength λ_{Em} 378 nm) and a Waters 2487 dual λ absorbance UV detector (260 nm) using a Shandon, Hypersil BDS C18 (5 μ, 4.6 mm x 25 cm) column connected to a Hypersil BDS C18 guard cartridge. Analysis was performed using a flow rate of 1.0 ml/min and the gradient given in Table 2.4 [Singh (2000)].

Time [min]	Flow [ml/min]	% A	% B	Curve
0	1.0	98	2	
20	1.0	65	35	6
25	1.0	98	2	6

Table 2.4: *Gradient conditions used for HPLC analysis of O^6-alkylguanine adducts.* Solvent A is 0.1% Heptafluorobutyric acid (HFBA)/water and solvent B is 0.1% HFBA/MeOH. Curve number 6 indicates a linear increase in solvent percentage.

2.3.1.2 HPLC Systems 2, 3 and 4

HPLC System No.	HPLC Column	Flow Rate	Mobile Phase
2	BDS C18 column (3μ, 100 x 2.1 mm)	0.2 ml/min isocratic	0.1% HFBA 10% MeOH
3	BDS C18 column (3μ, 100 x 2.1 mm)	0.2 ml/min isocratic	0.1% HFBA 12.5% MeOH
4	BDS C18 column (3μ, 100 x 2.1 mm)	0.2 ml/min isocratic	0.1% HFBA 15% MeOH

Table 2.5: *HPLC optimisation for the detection of O^6-alkylguanine adducts.* HPLC system 2 using 0.1% HFBA and 10% MeOH was originally developed and described by Harrison et al. [Harrison (1999)].

The RP-HPLC separations were performed using a Waters 2690 system equipped with a Waters 470 fluorescence detector (excitation wavelength λ_{Ex} 286 nm, emission wavelength λ_{Em} 378 nm) and a Waters 2487 dual λ absorbance UV detector (260 nm) using narrow bore Hypersil BDS C18 column (3μ, 100 x 2.1 mm) including a prefilter. As summarised in Table 2.5 the flow rate was 0.2 ml/min for all three systems. The methanol contents of the mobile phase varied though.

2.3.2 Synthesis of O^6-Carboxymethyldeoxyguanosine

The synthesis of O^6-CMdG was carried out by Rebekah Jukes, her help and input are most gratefully acknowledged. 2'-deoxyguanosine was protected at the 3' and 5' position by reaction with isobutyric anhydride for the synthesis of O^6-CMdG. The O^6 position was then reacted with mesitylene sulphonyl chloride, replaced with quinuclidine, and finally reacted with methylglycolate giving rise to the protected O^6-CMdG-methylester. The O^6-CMdG-methylester was then deprotected with NaOH yielding the product, O^6-CMdG.

2.3.3 Depurination of O^6-CMdG to O^6-CMG

O^6-CMG was needed as HPLC standard for quantitation of samples and therefore prepared by depurination of O^6-CMdG using several different conditions. According to Harrison et al. [Harrison (1999)] complete hydrolysis of O^6-CMdG to O^6-CMG was achieved by heating the samples in 1M TFA at 50°C for 60 minutes. Above conditions were compared with incubations of O^6-CMdG (2 pmol/μl) using 0.1M TFA at RT and 1M acetic acid at

50°C for 3 h. Samples were taken at defined time points and 10 µl directly injected onto the HPLC (Section 2.3.1.2, system 2) for simultaneous detection of O^6-CMdG and O^6-CMG.

2.3.4 Depurination of O^6-MedG to O^6-MeG

A time-course was undertaken in order to confirm hydrolysis conditions for O^6-MedG previously described by Harrison et al. [Harrison (1999)]. O^6-MedG (approximately 2.74 pmol/µl) was incubated in 0.1M HCl at 50°C. Aliquots (20 µl) were taken out at interval time-points and 10 µl injected immediately onto HPLC (Section 2.3.1.2, system 4).

2.3.5 Preparation of O^6-Alkylguanine Stock Solutions

(1) O^6-MeG (molecular weight M_{O6MeG} = 165.15 g/mol) was available from previous work and dissolved in 0.1M HCl (0.95 mg in 100 µl), which was then taken up in 900 µl PBS. Several sub-dilutions were prepared from this stock solution (5752 pmol/µl) which were then used for the preparation of HPLC standards ranging from 0.5 pmol to 100 pmol per injection.

(2) A standard stock solution was made for O^6-MedG (M_{O6MedG} = 281.3 g/mol), 0.77 mg (Sigma) were weighed out and dissolved in 1 ml ultrapure water yielding a stock solution of 2737 pmol/µl. Several dilutions were prepared from this stock solution using H_2O and used in subsequent experiments.

(3) O^6-CMdG had been synthesised as described in Section 2.3.2. A stock solution of O^6-CMdG was also prepared for comparison by dissolving 1.05 mg O^6-CMdG in 1 ml water and thus yielding a concentration of 3228 pmol/µl (M_{O6CMdG} = 325.28 g/mol). Appropriate dilutions were prepared accordingly.

(4) Samples were also compared to an appropriate calibration line ranging from 0.5 to 120 pmol O^6-CMG per injection. The initial stock solution was prepared by dissolving 2.20 mg O^6-CMG in 2 ml 10mM Na_2CO_3 which is equivalent to 5259 pmol/µl (M_{O6CMG} = 209.16 g/mol). All subsequent dilutions were carried out using ultrapure water.

The standards described above and their appropriate dilutions were either used for the generation of HPLC calibration lines or to determine the recovery of immunoaffinity

columns (IACs). Appropriate standards were prepared taking the volume of injection (40 μl or 10 μl) for each individual HPLC system (Sections 2.3.1.1 and 2.3.1.2) into account.

2.3.6 Preparation of Immunoaffinity Columns for O^6-CMdG Analysis

Immunoaffinity columns were used during this work in order to enrich O^6-alkylguanine adducts, in this case O^6-CMdG, from DNA samples/digests prior to HPLC analysis. Immunoaffinity columns were prepared by covalently linking the ammonium sulphate-precipitated IgG fraction of sera to protein A-Sepharose 4 Fast Flow (Pharmacia Biotech) and using the resultant gel to prepare small (1 ml) columns as described by Friesen et al. [Friesen (1991)].

2.3.6.1 Preparation of IgG from Serum

O^6-CMdG rabbit antiserum (5 ml) was placed in a small beaker to which cold saturated ammonium sulphate was added to a final concentration of 40% and the solution was stirred for 5 minutes. The solution was then transferred to a plastic centrifuge tube and centrifuged at 3000g for 15 minutes, after which the supernatant was discarded and the precipitate washed twice with cold 50% saturated ammonium sulphate. The pellet was then resuspended in 5 ml PBS and dialysed overnight in a cold room against 3 litre PBS with one change. A Pierce Slide-A-Lyzer 10K dialysis cassette was used for this purpose. The dialysate was centrifuged at 3000g to remove suspended matter and supernatant was used directly in the next step (pellet was discarded).

2.3.6.2 Preparation of IgG-Protein A Sepharose

Protein A-Sepharose 4 Fast Flow (5 ml) was washed twice with 20 ml Tris buffer (0.1M, pH 7.4) and suspended in the same buffer to a total volume of 10 ml. The IgG fraction (5 ml) was added and the mixture stirred end over end for 30 min at room temperature. The gel was washed several times with Tris buffer in order to remove excess, unbound IgG. The gel was then washed twice with 20 ml of triethanolamine solution (0.2M, pH 8.2) and resuspended in 40 ml dimethylpimelimidate solution (Pierce, 20mM freshly made up in triethanolamine buffer), and finally made up to 100 ml with the same solution in a polypropylene screw-cap centrifuge tube. This solution was then stirred end over end for a

further 45 min at room temperature. The gel was recovered by low-speed centrifugation and treated with 100 ml aqueous buffered ethanolamine solution (20mM in triethanolamine buffer) for 5 minutes to block unreacted cross-linking agents. The gel was then recovered and washed several times with PBS/azide (0.02%). The gel was poured into polystyrene minicolumns in 1 ml aliquots and maintained in place by use of hydrophobic plastic frits, both below and on top of the gel. Prior to use the IACs were washed extensively with PBS/azide (0.02%) and stored at 4°C.

2.3.7 Preparation of IACs for O^6-MedG Analysis

Similarly to O^6-CMdG, O^6-MedG adducts were also purified from DNA digests using immunoaffinity purification prior to HPLC analysis.

Several monoclonal antibodies against O^6-MedG were tried in order to make IACs for O^6-MedG purification. An O^6-MedG monoclonal antibody was provided by Dr. Geoff Margison, Manchester which had been used previously to make IACs in our laboratory [Harrison (1999)]. Alternatively, the O^6-MedG monoclonal antibody EM-2-3 (1 mg) was purchased from Prof. Manfred Rajewsky's research group in Essen, Germany. Especially the help and support of Dr. Petra Lorenz from Prof. Rajewsky's laboratory is most gratefully acknowledged.

Columns were prepared according to protocols described earlier for the preparation of IACs for O^6-CMdG (Section 2.3.6.1 and 2.3.6.2). Separation of IgG from serum appeared unnecessary (no precipitate was formed when using 40% ammonium sulphate solution), and thus was omitted in subsequent attempts.

2.3.8 Enzymatic Digestion to Nucleosides Prior to IAC Purification

Enzymatic digestion was performed according to Section 2.2.6.2 with minor modifications. DNA (usually 24 μg in triplicate) was digested to dNp using 1.75 U MN and 30 mU CSPDE. 10 μl SSCC buffer were added and the final volume adjusted with ultrapure water to 62.5 μl. The samples were mixed by vortexing, centrifuged and incubated at 37°C for 2 hours. They were then dried down in a DNA speed vac. For the digestion to dN, 50 μl NP1 (2 μg/μl, approximately 20 U) were added and the mixture incubated overnight (17 h) at 37°C.

2.3.9 Immunoaffinity Purification of O^6-CMdG and O^6-MedG

KDA-treated DNA (24 μg) was digested as detailed in Section 2.3.8. Afterwards the samples were processed with minor changes as described previously by Harrison et al. [Harrison (1999)]. The digest was taken up in 2 ml PBS/azide (0.02%) passed through the first immunoaffinity column (O^6-CMdG) which eluted directly on the second immunoaffinity column (O^6-MedG) and washed with 3 ml PBS/azide. The columns were then separated for an independent wash using water (10 ml) and elution with either 5 ml 1M TFA (O^6-CMdG) or 4 ml 80% MeOH (O^6-MedG). The immunoaffinity columns were then washed with PBS/azide (20 ml) and stored at 4°C for further use.

All eluates were dried down in a DNA speed vac overnight. Prior to HPLC analysis, the eluates from the O^6-MedG columns were heated at 50°C for 30 min to complete the hydrolysis of O^6-MedG to O^6-MeG using 100 μl 0.1M HCl. The solution was then neutralized using 0.1M NaOH (100 μl) and dried down again. It was shown earlier that depurination of O^6-CMdG to O^6-CMG takes place instantaneously in 1M TFA i.e. no further treatment of the eluates from the O^6-CMdG columns was needed.

Samples were redissolved for injection in 16 μl 0.1% HFBA. The RP-HPLC separations were performed as described in Section 2.3.1.2 using 0.1% HFBA with 15% MeOH (system 4). 10 μl of each sample, i.e. an equivalent of 15 μg of DNA, were injected onto the HPLC.

2.3.10 Comparison of Various Methods for O^6-Alkylguanine Detection

CT-DNA (approximately 1 mg/ml) was dissolved in PBS and treated overnight at 37°C using 8mM KDA. DNA was precipitated using isopropanol, the pellet was washed with 70% EtOH and finally taken up in water. 20 μg of treated CT-DNA (determined by UV) were dried down and digested/hydrolysed in triplicate comparing the following methods.

(1) acid hydrolysis using 0.1M formic acid at 70°C for 1 h [Singh (2000), De Groot (1994)]
(2) acid hydrolysis using 0.1M HCl at 100°C for 30 min, samples were neutralised with 0.1M NaOH prior to drying down
(3) enzymatic digestion according to Section 2.3.8
(4) enzymatic digestion followed by IAC clean-up (Section 2.3.8 and 2.3.9)

All samples were dried down after digestion/hydrolysis and taken up in 0.1% HFBA (50 μl), except for samples derived from method (3), which were taken up in water and analysed using the HPLC system described in Section 2.3.1.1. 40 μl of each sample, i.e. an equivalent of 16 μg of DNA, were injected onto the HPLC.

2.3.11 Treatment of CT-DNA in Various Buffer Systems Using KDA

Treatments of CT-DNA using potassium diazoacetate were originally performed in PBS [Harrison (1997)]. In order to modulate carboxymethylation and methylation, CT-DNA (ca. 1 mg/ml) was treated in duplicate using 8mM KDA overnight at 37°C in various buffer systems (Table 2.6).

Treatment No.	Buffer System
(I)	PBS 1x TE
(II)	0.5x TE 1x TE 2x TE
(III)	0.05x TE 0.1x TE 0.5x TE
(IV)	0.1x PBS PBS

Table 2.6: *Buffer systems used during 8mM KDA treatments of CT-DNA.* KDA (M_{KDA} = 124.1 g/mol) used in these DNA treatments had been quantitated and synthesised by B. Cupid via alkaline hydrolysis of ethyl diazoacetate (Aldrich). TE Tris-EDTA buffer (pH 7.5), PBS phosphate buffered saline (pH 7.3), 0.05x TE (0.5mM Tris, 0.05mM EDTA), 0.1x (1mM Tris, 0.1mM EDTA), 0.5x TE (5mM Tris, 0.5mM EDTA), 1x TE (10mM Tris, 1mM EDTA), 2x TE (20mM Tris, 2mM EDTA).

pH of the buffer system was measured prior to treatment and if necessary adjusted to pH 7.5 (pH_{PBS} 7.3). DNA was precipitated using isopropanol, the pellet was washed with 70% EtOH and finally taken up in water. DNA concentration was measured using the GeneQuant II RNA/DNA calculator. Usually a smaller aliquot of DNA (4 μg) was digested to dNp and analysed by HPLC using methods described in Section 2.2.6.2 and 2.2.6.3 in order to confirm the DNA concentration determined by UV.

DNA samples (24 μg in triplicate) were digested to nucleosides according to the protocol detailed in Section 2.3.8, purified and analysed using the procedure and HPLC system described in Section 2.3.9.

2.4 Methods Applied to the Detection of p53 Mutations

2.4.1 KDA Treatment of Plasmid pLS76

Plasmid pLS76 was either treated *in vitro* in PBS using 0, 4, 6, 8 and 10mM KDA, or in 1x TE using 0, 8 and 10mM KDA overnight at 37°C. The KDA stock solution was prepared and quantitated by B. Cupid. 8mM KDA treatments were performed multiple times in parallel in order to obtain enough mutants for the p53 analysis. Some aliquots were kept for O^6-CMG and O^6-MeG adduct analysis. Samples were digested and immunopurified as described in Section 2.3.8 and 2.3.9 for the determination of O^6-CMdG and O^6-MedG by HPLC (Section 2.3.1.2, system 4).

Glycogen (usually 1 μl), 3M NaAc (pH 6.0, 1/10 of final reaction volume), isopropanol (1 volume) or 100% EtOH (2 volumes) were added and the samples used for the analysis of KDA-induced p53 mutations sent on dry ice to Leeds. Mutation analysis was performed by Dr. Gina Scott and Dr. Phil Burns as part of the collaboration between Leicester and Leeds.

2.4.2 MDA Treatment of Plasmid pLS76

Plasmid pLS76 was treated *in vitro* in 0.1M KH_2PO_4 (pH 4.5) for 1 h at 37°C using MDA. 200mM MDA stock solution was effectively prepared as described in Section 2.2.1 and diluted using 0.1M KH_2PO_4 (pH 4.5) to give rise to a 100mM MDA solution. Plasmid was treated at final concentrations of 0, 1, 5, 10 and 15mM MDA. As 10mM MDA was found to be the most appropriate concentration, treatments were repeated multiple times and several aliquots were kept for adduct analysis.

After incubation isopropanol (approximately equal volume) and glycogen (1 μl) were added and samples sent to Leeds on dry ice. MDA-induced p53 mutations were analysed by myself during a visit in Leeds.

For the determination of M_1-dG samples were effectively digested as described earlier in Section 2.2.6.2. Briefly, 6 μg of DNA were digested to dNp using MN and CSPDE, dried

down and taken up in 60 μl water. Samples were then split in 20 μl which were used for dNp analysis by HPLC (injection of 10 μl i.e. 1 μg) and 40 μl which were digested further to dN using 16 μl NP1 (2 μg/μl). Samples for M_1-dG analysis were dried down after digestion and taken up in 16 μl of water prior to HPLC injection of 10 μl (2.5 μg). HPLC analysis was carried out as detailed in Section 2.2.6.3.

2.4.3 Various Media Needed in Subsequent Sections

2.4.3.1 Minimal Medium

Minimal medium supplemented with 5 mg/l adenine (MM+ade5) was used to test p53 status and contained 1.7 g yeast nitrogen base (w/o amino acids or ammonium sulphate) and 5 g ammonium sulphate (for plates 25 g agar were added to 1 litre of medium). After autoclaving the medium was supplemented with adenine (5 mg/l), tryptophan (50 mg/l), histidine (50 mg/l), 20 g/l dextrose and 10 ml amino acid stock solution. Supplementation using 10 ml of amino acid stock solution resulted in 20 mg arginine, 20 mg methionine, 30 mg isoleucine, 50 mg phenylalanine, 100 mg glutamic acid, 100 mg aspartic acid, 150 mg valine, 200 mg threonine and 400 mg serine per litre medium.
Minimal medium containing 200 mg adenine per litre (MM+ade200) was used to grow ade- clones prior to preparation of plasmid from yeast (Section 2.4.5).

2.4.3.2 Complete Medium

Complete medium (CM+ade200) was used for routine cultures and contained 10 g yeast extract (Difco 0127-17-9), 20 g peptone (Difco 0118-17-0) and 20 g dextrose, for preparation of plates 25 g agar were added to 1 litre of medium. After autoclaving adenine was added to a final concentration of 200 mg per litre of medium.

2.4.4 Yeast Transformation

Complete medium containing excess adenine (10 ml of CM+ade200) was inoculated with a single colony of yeast strain yIG397 and grown overnight at 30°C in a shaking incubator. 5 ml of the overnight culture were diluted into 50 ml prewarmed CM+ade200 and grown at 30°C for 4 to 5 h until the culture reached an OD_{600nm} of 0.8-1.0 (4 h is enough to ensure that the culture is in mid-log phase). The culture was centrifuged in a 50 ml tube (bench

top centrifuge, 1000 rpm, RT, 5 min). The pellet was then washed at RT with 50 ml sterile water, followed by 10 ml sterile water, and finally using 5 ml LiAc/TE (0.1M lithium acetate pH 7.5, 10mM Tris-HCl pH 7.5, 1mM EDTA). After each step the centrifugation described above was repeated and the supernatant discarded. The pellet was resuspended in 250 μl LiAc/TE and transferred to a sterile Eppendorf tube, then spun in a microfuge (full speed, approximately 10 s) and resuspended again in 250 μl LiAc/TE. Approximately 200 ng of treated plasmid were transformed into yIG397 by a lithium acetate procedure [Guthrie (1991)]. For each transformation reaction a sterile Eppendorf tube containing 10 μl carrier DNA (single-stranded herring sperm DNA 5 mg/ml) and 150-200 ng of treated pLS76 plasmid was prepared. The total volume should not be more than 20 μl. 50 μl yeast in LiAc/TE and 300 μl LiAc/TE/PEG (LiAc/TE solution containing 40% polyethylene glycol 4000) were added, briefly vortexed to mix and incubated at 30°C for 30 min in a shaking incubator. The transformations were heat-shocked at 42°C for 15 min (any agitation of the samples was avoided at this stage). The samples were spun briefly in a microfuge (approximately 10 s) and the pellet resuspended in 500 μl sterile water. 50 μl of the suspension were spread as uniformly as possible on each plate of minimal medium containing limiting concentrations of adenine (MM+ade5). The plates were then incubated at 35°C for 3-5 days. Total number of colonies and the number of red colonies were counted. Mutational frequency was calculated by dividing the number of reds by the total number of transformants. Mutant red colonies were picked from the primary transformation plates and sub-cultured on MM+ade5 plates to confirm their mutant phenotype. All plates were then stored at 4°C.

2.4.5 Preparation of Plasmid from Yeast

Single colonies of yIG397 (containing pLS76) were picked from above plates and grown overnight in 10 ml minimal medium containing excess adenine (MM+ade200) at 30°C in a shaking incubator. Plasmid was rescued from these cultures using a phenol/chloroform based DNA extraction procedure [Guthrie (1991)]. The overnight culture was centrifuged in a 15 ml centrifuge tube in a bench top centrifuge for 5 min at 1000 rpm at RT. The supernatant was discarded and the pellet resuspended in 200 μl breaking buffer (2% Triton X-100, 1% sodium dodecyl sulphate (SDS), 100mM NaCl, 10mM Tris-HCl pH 8.0, 1mM EDTA). The cell suspension was transferred to a screw top Eppendorf tube containing 0.3 g glass beads (0.5 mm diameter) and 200 μl phenol/chloroform, vortexed for 2 min and

then centrifuged in a microfuge (13000 rpm for 5 min at RT). The aqueous (top) phase was transferred to a new tube. The nucleic acid was precipitated by adding 20 μl 3M NaAc (pH 6.0) and 400 μl EtOH, contents were mixed by vortexing. The supernatant was discarded and the pellet washed in 70% EtOH. The pellet was then resuspended in 50 μl water. RNase mix (1μl), containing RNase A at 10 mg/ml (Sigma) and 100 U/ml RNase T_1 (Boehringer Mannheim), was added to the tube and incubated at 37°C for approximately 30 min. The template DNA was then stored at 4°C.

2.4.6 Polymerase Chain Reaction PCR

An appropriate volume of DNA template (1 μl) was mixed with 5 μl of 10x magnesium free buffer (reaction buffer IV; ABgene AB-0289), 2 μl 25mM magnesium solution (ABgene), 8 μl 1.25mM dNTP (2'-deoxynucleoside 5'-triphosphate) mix (1.25mM stock used at 200μM final concentration), 1 μl primer BB5 (5'-Biotin-CCAGGTCCAG ATGAAGCTCC-3', 20 pmol/μl), 1 μl primer NBE3 (5'-GGAGAGGAGCTGGT GTTGTT-3', 20 pmol/ml), 0.25 μl Thermoprime Plus DNA Polymerase (5 U/μl; ABgene AB-0301) and water to 50 μl total volume.

The DNA was amplified according to given PCR conditions [94°C/5 min, (94°C/30 s, 58°C/30 s, 72°C/2 min) x 30-35 cycles, 72°C/7min, hold 4°C] in the Perkin Elmer GeneAmp System 2400 (or 9700) PCR machine.

After amplification, the PCR products were separated by electrophoresis in a 1.0% agarose gel. The PCR product (5 μl) was mixed with 1 μl gel loading solution type II [0.25% bromophenol blue, 0.25% xylene cyanole and 25% Ficoll (type 400 in water)]. Each 100 ml agarose gel contained ethidium bromide and was run in 1x TAE buffer (Tris-acetate EDTA buffer; working solution: 0.04M Tris-acetate, 0.001M EDTA). The PCR products were separated by electrophoresis at 100 V for approximately 20 min.

2.4.7 Dynabeads Protocol for the Separation of Single-Stranded DNA

Dynabeads M-280 Streptavidin (Dynal) suspension (10 μl) was used for each PCR reaction. The required volume of Dynabeads was transferred in a 1.5 ml Eppendorf tube and the latter placed in a magnet. The supernatant was discarded and the beads washed using 1x binding and washing buffer (BW buffer). The washes were repeated three times. The Dynabeads were then resuspended in 2x BW buffer (10mM Tris-HCl pH 7.5, 1mM

EDTA, 2M NaCl). 45 μl of this Dynabead suspension were aliquoted into Eppendorf tubes and 45 μl of PCR product added. The mixture was incubated at RT for at least 15 min, and the Dynabeads kept in suspension by periodically shaking the tubes. The supernatant was discarded and the beads which now had the PCR product attached were washed with water. Again the supernatant was discarded and the Dynabeads+DNA resuspended in 40 μl 0.1M freshly prepared NaOH, and incubated at RT for 10 min. The supernatant was discarded and the Dynabeads+DNA washed with water. This approach gave rise to single-stranded DNA. The Dynabeads+DNA were finally resuspended in 20 μl water (10 μl for each sequencing reaction) after discarding the supernatant.

2.4.8 Sequencing Reaction and Analysis

Codons 90 to 290 of the PCR products were sequenced on solid phase (Dynabeads) using an ABI Prism dRhodamine dye terminator cycle sequencing kit and an ABI Prism 377 DNA sequencer. An appropriate volume of single-stranded DNA (10 μl) was mixed with 1 μl primer [NF3 (5'-TGGGCAGTGCTCGCTTAGTG-3') or NF9 (5'-CCATGCAGG AACTGTTACAC-3'), 3 pmol/μl] and 8 μl ready reaction mix (dRhodamine Terminator Cycle Sequencing Ready Reaction Kit with AmpliTaq DNA Polymerase; ABI Prism PE Biosystems, Warrington, England). The DNA was sequenced according to given conditions [(96°C/10 s, 50°C/5 s, 60°C/4 min) x 25 cycles, hold 4°C] in the Perkin Elmer GeneAmp 2400 PCR machine.

In order to precipitate the single-stranded sequencing products 1.5 ml Eppendorf tubes containing 2 μl 3M sodium acetate (pH 6.0) and 50 μl EtOH were prepared for each reaction. The entire sequencing reaction was added to the ethanol/sodium acetate mix, vortexed briefly and centrifuged for approximately 25 min (13000 rpm at RT). While discarding the supernatant, care was taken not to disturb the pellet at that stage. 100 μl 70% EtOH were added slowly. The supernatant was discarded and the pellet allowed to air dry for 5-10 min. The pellet was then dissolved in 4 μl formamide/dextran blue (5:1 ratio).

An acrylamide stock (4.25%) was prepared using 10.6 ml acrylamide 40%, 36 g urea, 1 g amberlite and adjusted to 90 ml with water. 10 ml of 10x TBE [Tris-borate EDTA buffer; working solution: 0.09M Tris-borate, 0.002M EDTA] were added after filtering the mixture under vacuum. In order to prepare a 4.25% acrylamide gel, 30 ml acrylamide solution were mixed with 21 μl TEMED (N,N,N',N'-tetramethylethylene-diamine) and 150 μl freshly prepared 10% ammonium persulphate. The gel was left to set for 2 h.

The samples were heat-denatured at 95°C for 2 min prior to loading onto the gel. 2 μl per sample were loaded into each well. The gel was run in 1x TBE buffer using an Applied Biosystems Inc. 377 DNA Automated Sequencer (Perkin-Elmer).

The resulting sequences were analysed using an ABI Prism Sequence Navigator software. The mutations that were identified were then compared to the IARC p53 mutation database (http://www-p53.iarc.fr/p53DataBase.htm; version R5 June 2001) available on the internet [Hernandez-Boussard (1999)].

3 Further Development of the ISB Assay

3.1 Introduction

The immunoslot blot technique (ISB) was originally developed by Nehls et al. [Nehls (1984)] for the detection of O^6-ethyldeoxyguanosine in intact DNA. Its basic principle is shown in Figure 3.1.

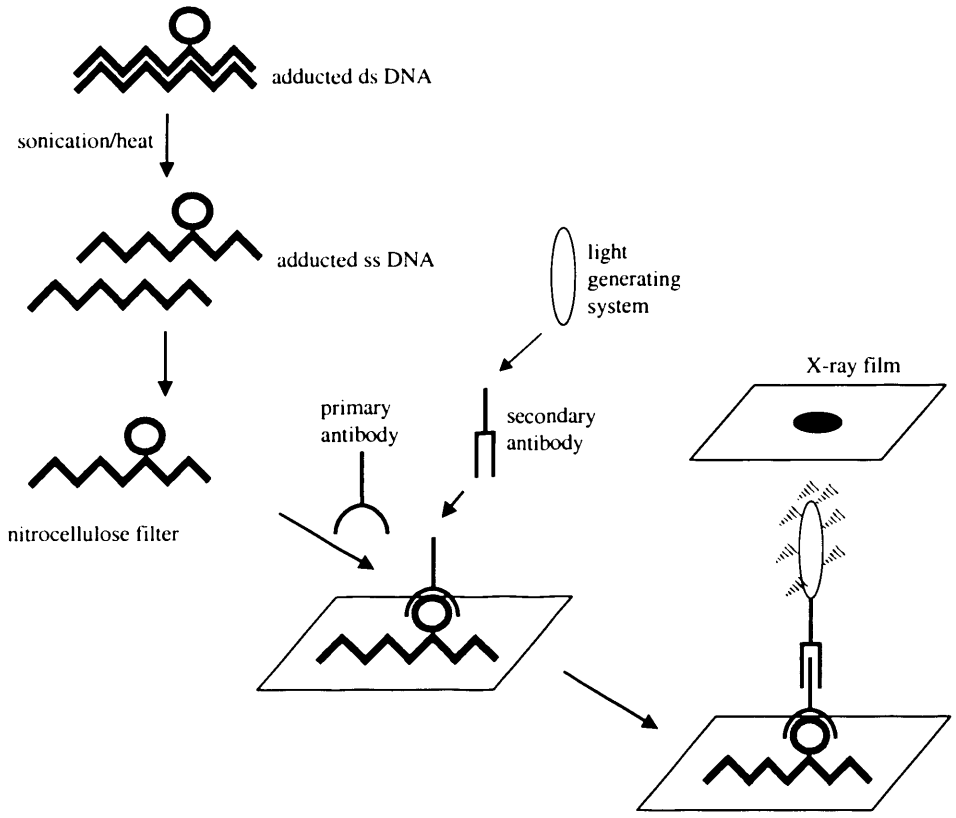

Figure 3.1: *Principle of the immunoslot blot assay.* Modified, double-stranded DNA (ds DNA) is sonicated and heat-denatured to yield fragmented, single-stranded DNA (ss DNA), which is afterwards immobilised on nitrocellulose filters. The membrane is baked in an 80°C oven, the immobilised DNA is then reacted with the primary antibody, which is specifically directed against the adduct of interest e.g. M_1-dG, and afterwards with the secondary antibody directed against the primary one. The secondary antibody is linked to an enzyme complex, for example horseradish peroxidase, which is capable of eliciting a colour reaction with a suitable substrate which enables its detection. Visualisation of the specifically bound secondary antibody is achieved by the incubation of the membrane with chemiluminescence reagents. Those reagents allow the enzymatic activity associated with the conjugated antibody to generate a luminescent signal that can be detected by exposure of the filter to an X-ray film or directly captured using the Biorad Fluor-S™ MultiImager.

Since its initial development the ISB assay has been used and adapted for the detection of various different DNA adducts such as O^6-(2-hydroxyethyl)-2'-deoxyguanosine [Ludeke (1988)], 8-hydroxy-2'-deoxyguanosine [Musarrat (1994)], N7-ethylguanine [Mientjes (1996)] and N7-(2-hydroxyethyl)guanosine [Van Delft (1994)].

Recently, Leuratti et al. [Leuratti (1998)] developed an ISB assay for the detection of M_1-dG, the main DNA adduct formed via reaction of MDA with DNA. The major advantage of the ISB assay compared to many other techniques of measuring DNA damage is that it only requires a small amount of DNA, while still being very sensitive. In the case of M_1-dG the limit of detection is approximately 5 adducts per 10^8 normal nucleotides [Leuratti (1999)]. Furthermore, this assay is much less laborious and time consuming than other assays, thus allowing routine analyses of a large number of samples in relatively short time.

As part of this project it had been proposed to investigate the long-term stability of M_1-dG in stored human samples using the ISB assay. It is important before starting any long-term experiment that the methods of choice are reliable and accurate. This not only includes the technique used for adduct determination, but also aspects such as DNA extraction from whole blood, quantitation of adduct levels in standards and quantitation of DNA in general. Therefore, a considerable amount of time was spent on the evaluation and the development of existing as well as novel techniques prior to starting the storage experiments.

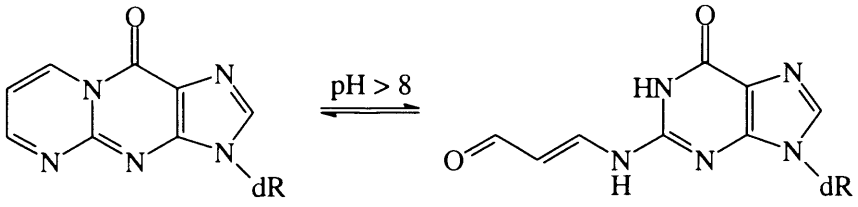

(1) (2)

Figure 3.2: *Scheme of the ring-opening reaction of M_1-dG.* M_1-dG is ring-opened to N^2-(3-oxo-propenyl)deoxyguanosine in the presence of base (pH > 8). (1) M_1-dG or pyrimido[1,2-α]purin-10(3H)-one; (2) ring-opened form of M_1-dG or N^2-(3-oxo-1-propenyl)deoxy-guanosine.

One potential problem of the ISB assay (or any highly sensitive assay measuring DNA adducts) which was of particular concern, was the existence of background levels of M_1-dG in untreated, control CT-DNA. With regard to the ISB assay, a strategy to address this problem was to modify the adduct in a way that it was no longer recognised by the

primary antibody. According to Niedernhofer et al. [Niedernhofer (1997)] M_1-dG can be ring-opened to N^2-(3-oxo-propenyl)deoxyguanosine in the presence of base (Figure 3.2). The intention was thus to ring-open the adduct and to stabilise the new structure. Reoccurrence of ring formation was inhibited by reaction of the aldehyde group present in N^2-(3-oxo-propenyl)deoxyguanosine with primary amines.

In summary, the following aims were addressed as part of this chapter prior to starting the long-term storage of DNA samples:

- DNA quantitation prior to ISB assay i.e. comparison of UV spectroscopic data, acid hydrolysis and enzymatic digestion
- development of the novel propidium iodide assay for the quantitation of DNA binding to NC filters
- fragmentation of human and CT-DNA and pattern of DNA binding to NC membranes
- comparison of different methods used for DNA extraction from whole blood
- reduction of M_1-dG levels using primary amines (methoxyamine and hydroxylamine)

3.2 Results

3.2.1 DNA Quantitation Prior to ISB Assay

A GeneQuant II RNA/DNA calculator, determining A_{260} and A_{280}, was used for routine DNA quantitation as it was less time consuming than other techniques and fairly reliable. This method was particularly useful for human samples as it was quick and only small amounts of DNA were needed. Values obtained also compared well with DNA quantitation by HPLC analysis following enzymatic digestion using CSPDE and MN (results shown later).

However, a method was required to quantify the level of M_1-dG modification in MDA-treated CT-DNA used as a standard in the ISB assay. Furthermore, a technique was needed to evaluate M_1-dG stability in long-term stored highly modified CT-DNA standards. Acid hydrolysis was one way to hydrolyse DNA, it is rapid and routinely used in many laboratories. Another possibility for M_1-dG determination was enzymatic digestion. In general, acid hydrolysis of MDA-treated CT-DNA yields DNA bases in this case M_1-G,

whereas enzymatic digestion to deoxynucleotides and deoxynucleosides results in M_1-dGp and M_1-dG, respectively. As synthetic M_1-dG was available as a HPLC standard, enzymatic digestion to deoxynucleosides appeared to be the method of choice. In general, the technique was more time consuming than acid hydrolysis.

3.2.1.1 DNA Quantitation Prior to ISB Assay – Acid Hydrolysis

Results obtained in initial experiments for acid hydrolysis using 0.1M formic acid at 70°C for 1 h (Section 2.2.7.1) did not correspond well with UV data and were generally lower (data not shown). One potential problem for this discrepancy could have been insufficient solubility and homogeneity of DNA. Therefore, sonication of DNA was introduced prior to analysis in order to disrupt the structure and to make it more soluble. An internal standard, 9-ethylguanine (9-EtG, 0.0046 $\mu g/\mu l$), was also introduced to exclude and correct for variations in HPLC injection. No major differences between single injections using the Waters 2690 Alliance autosampler were observed, as peaks for 9-EtG remained within appropriate standard deviations. It was also discovered that sonication did not alter the outcome (data not shown). Results obtained were basically identical to non-sonicated samples.

The primary HPLC standard used for DNA quantitation was another possible explanation for the inconsistency observed between UV and acid hydrolysis data. It could have been that the primary guanine standard used for HPLC analysis was not weighed out correctly or no longer fully dissolved due to storage at -80°C. Acid hydrolysis results were based on a calibration line (y_A, Figure 3.3) made from a guanine stock solution which had been prepared during previous work. In order to address this potential problem a new guanine stock solution was made. The already existing guanine stock (0.125 $\mu g/\mu l$, dissolved in 50mM formic acid, solution A) was used as comparison to check for the accuracy of the new standard. A similar concentration was wanted, but the standard did not dissolve completely upon sonication, hence more formic acid (50mM) was added giving a final 0.0625 $\mu g/\mu l$ concentration of guanine (solution B).

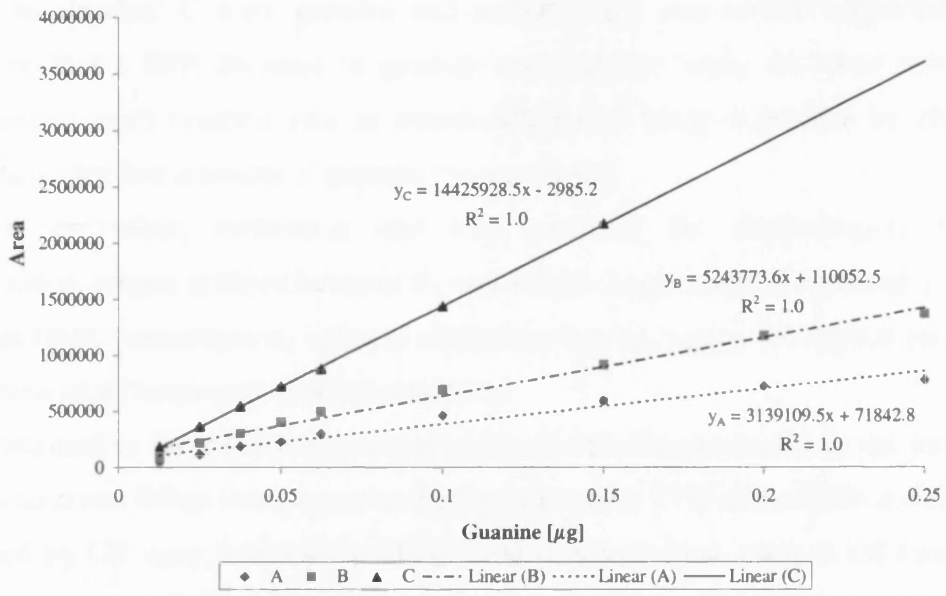

Figure 3.3: *Comparison of three different guanine standards using HPLC.* Guanine was dissolved in 50mM formic acid and diluted with ultrapure water prior to injection onto HPLC. Mobile phase was 0.1M TEA (pH 5) containing 1% MeOH, HPLC system used for the analysis is described in more detail in Section 2.2.7.1. Retention time observed for guanine was about 2.9 min. Solution A contained 0.125 µg/µl and solution B 0.0625 µg/µl. Concentrations ranging from 0.0125 to 0.25 µg guanine were injected at least 5 times. For the third calibration line, guanine was dissolved in 1M HCl (1 µg/µl, solution C). The two highest concentrations were not injected for solution C to avoid overloading the HPLC column. Results shown are average ± standard deviation.

Major differences in area were observed for guanine solutions A and B when compared by HPLC (Figure 3.3). The integrated area obtained for any particular guanine concentration was approximately 1.7 times higher for solution B. It seemed most likely that poor solubility of guanine was the cause of this phenomenon as stock solutions were milky in appearance. Therefore, a new guanine stock was prepared (solution C). Guanine (1 µg/µl) was dissolved in 1M HCl and sonicated for 1 h in an ultrasonic bath (Kerry KS200) to achieve complete solubilisation. The stock solution was diluted with ultrapure water prior to HPLC analysis. In comparison to solution A, roughly 3.5 times more guanine was dissolved in solution C and therefore a corresponding larger area detectable by HPLC.

As accuracy of the primary standard, in this case guanine, was vital for precise determination of DNA concentration and adduct level in ISB standards, the experiment was repeated by a colleague. Identical results were found, confirming findings shown in Figure 3.3. It can therefore be assumed that DNA concentrations and adduct levels based

on guanine standard C were genuine and correct. This was further supported by the observation that a 50% decrease in guanine concentration using the same solvent (i.e. 50mM formic acid) resulted also in major differences being detectable by HPLC for theoretically identical amounts of guanine (y_B versus y_A).

Dependent on which calibration line was used for the determination of DNA concentrations, results differed between 2- and 4-fold. Application of equation y_C yielded the lowest DNA concentration, whereas calibration line (y_A) gave the highest results as a consequence of differences in guanine solubility.

Results obtained so far for acid hydrolysis indicated that the approach was not suitable for DNA quantitation. When using equation y_C, approximately 27% of the DNA concentration determined by UV were detected by HPLC following hydrolysis using 0.1M formic acid. In order to improve DNA quantitation and yield several conditions for acid hydrolysis were examined and compared with each other. Details of all methods are given in Section 2.2.7.2. Techniques were compared to incubation of DNA with 0.1M formic acid for 1 h at 70°C. The DNA concentration was calculated in [$\mu g/\mu l$] using guanine calibration line y_C and compared to the UV value determined by GeneQuant II RNA/DNA calculator (Table 3.1).

Type of Analysis	DNA Concentration [$\mu g/\mu l$]	% of UV Value
UV spectrophotometer	0.444 ± 0.013	
0.1M formic acid, 70°C, 1 h	0.120 ± 0.001	27.0
1M formic acid, 70°C, 1 h	0.130 ± 0.015	29.3
0.1M HCl, 70°C, 1 h	0.136 ± 0.006	30.6
1M HCl, 70°C, 1 h	0.156 ± 0.002	35.1
0.1M formic acid, 100°C, 1 h	0.109 ± 0.022	24.5

Table 3.1: *Comparison of UV spectroscopic data with data obtained using various acid hydrolysis conditions.* Each method was performed in triplicate for the same MDA-treated CT-DNA and samples were injected in triplicate onto HPLC. Results are given as DNA concentration [$\mu g/\mu l$] ± standard deviation. DNA concentration was calculated using guanine calibration line $y_C = 14425928.5x - 2985.2$ ($R^2 = 1.0$).

As evident from Table 3.1, large differences were observed between UV data and results obtained using different types of acid hydrolysis. DNA concentrations calculated for acid hydrolysis ranged between 24.5% and 35.1% of the UV value suggesting that acid

hydrolysis did not go to completion and was not fully efficient. The highest value was acquired using 1M HCl at a temperature of 70°C.

Figure 3.4 illustrates the corresponding variations in guanine and M_1-G measured by HPLC UV and fluorescence detection, respectively. Results shown for guanine and M_1-G were compared to 0.1M formic acid (70°C, 1h) and are expressed as a percentage of that result. In order to correlate with UV data, approximately a 4-fold increase in guanine and thus DNA concentration would need to be observed. For M_1-G a steady decrease was noticed, lowest results were obtained using 0.1M formic acid at 100°C, maximum area was detected for originally described hydrolysis conditions (0.1M formic acid, 70°C). Less adduct was detectable as a consequence of an increase in acidity (hydrochloric versus formic acid). An increase in temperature by 30°C also resulted in less M_1-dG being measurable by HPLC fluorescence. However, with regard to the unmodified bases an increase in acidity yielded an increase in guanine being detectable. Highest guanine result was achieved using 1M HCl (70°C, 1h), which was roughly 31% higher than in the reference sample. However, higher guanine results did not coincide with more M_1-G being detectable, because the more vigorous hydrolysis conditions resulted in some degradation of the adduct.

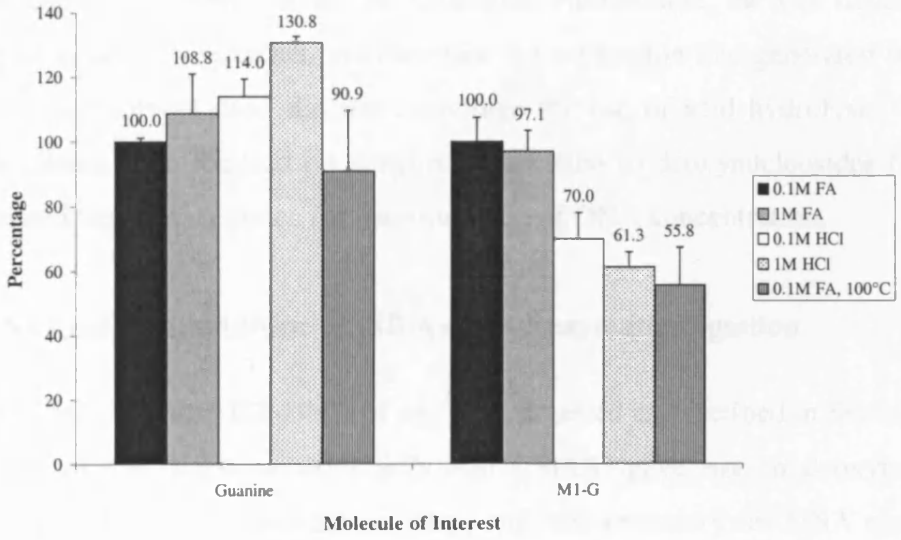

Figure 3.4: *Percentage of guanine and M_1-G.* Results shown for guanine and M_1-G were compared to 0.1M formic acid (70°C, 1 h) and are normalised to that result (black bar). All samples were hydrolysed at 70°C for 1 h unless mentioned otherwise. FA formic acid; HCl hydrochloric acid.

Conditions described earlier by Goda and Marnett [Goda (1991)] were also applied to the same batch of MDA-treated DNA. CT-DNA was incubated with 0.01N HCl, 0.1N HCl or 6N HCl at 100°C for 1 h (Section 2.2.7.2). Even when 6N HCl was used DNA yield was very poor, approximately 40% of the UV value were detectable (using equation y_C for the calculation of results). Purine as well as pyrimidine bases were released under these extreme conditions. As expected incubation with 0.01N and 0.1N HCl resulted in even lower DNA concentrations (31.5% and 35.6% of the UV value respectively). Since milder acidic conditions and temperatures already resulted in a loss of M_1-G, the adduct was completely destroyed following treatment with 6N HCl. M_1-G was only detectable for incubation of DNA with 0.01N HCl. However, the adduct peak was very small. Only approximately 13% of the level observed for 0.1M formic acid (70°C) were measurable. As mentioned earlier, differences in DNA yield and adduct level were also quite apparent if the temperature was raised by 30°C. The DNA concentration increased by approximately 5% accompanied by complete destruction of the adduct when CT-DNA was incubated for example using 0.1M HCl at 100°C instead of 70°C. These results suggested that with increasing acidity and temperature, more guanine was released with a corresponding loss of M_1-G.

None of these methods appeared to be promising with respect to concomitant DNA quantitation and determination of the M_1-G adduct. Furthermore, the vast dependency of the primary standard, i.e. guanine, and therefore the calibration line generated from it, on concentration and solvent used did not encourage the use of acid hydrolysis. Therefore future experiments were focused on enzymatic digestion to deoxynucleosides for M_1-dG quantitation and deoxynucleotides for determination of DNA concentration.

3.2.1.2 DNA Quantitation Prior to ISB Assay – Enzymatic Digestion

Untreated and MDA-treated CT-DNA (4 μg) were digested as described in Section 2.2.6.2. The first step of the digestion using MN and CSPDE gave rise to deoxynucleotides (2'-deoxynucleoside-3'-monophosphates, dNp) and was necessary for DNA quantitation. The DNA concentration was based on the comparison of the sample peak area with a 2'-deoxyadenosine-3'monophosphate (dAp) calibration line (Figure 3.5).

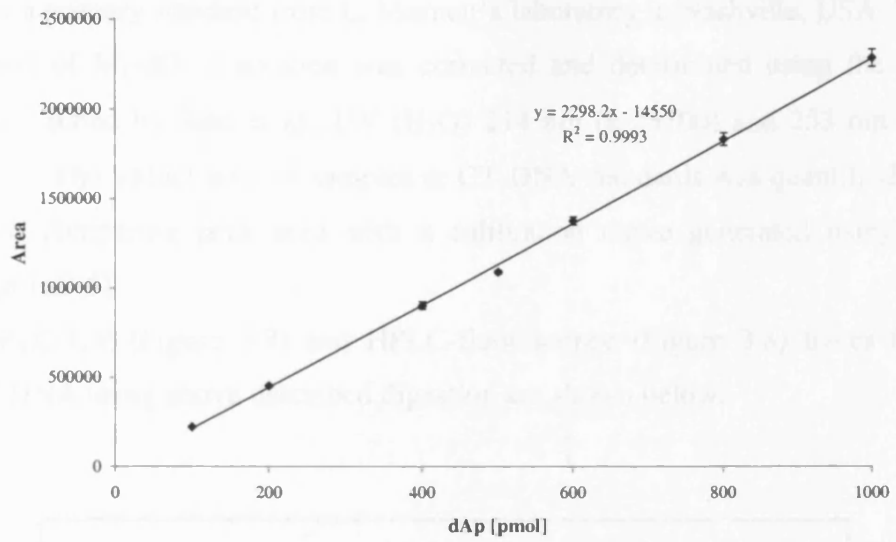

Figure 3.5: *Calibration line for dAp.* RP-HPLC analysis was performed as described in Section 2.2.6.3 with 0.1M TEA (pH 5.0) containing 4% methanol as the eluent. The flow rate was 0.2 ml/min. Detection was via UV, 260 nm. Between 100 and 1000 pmol dAp were injected six times each.

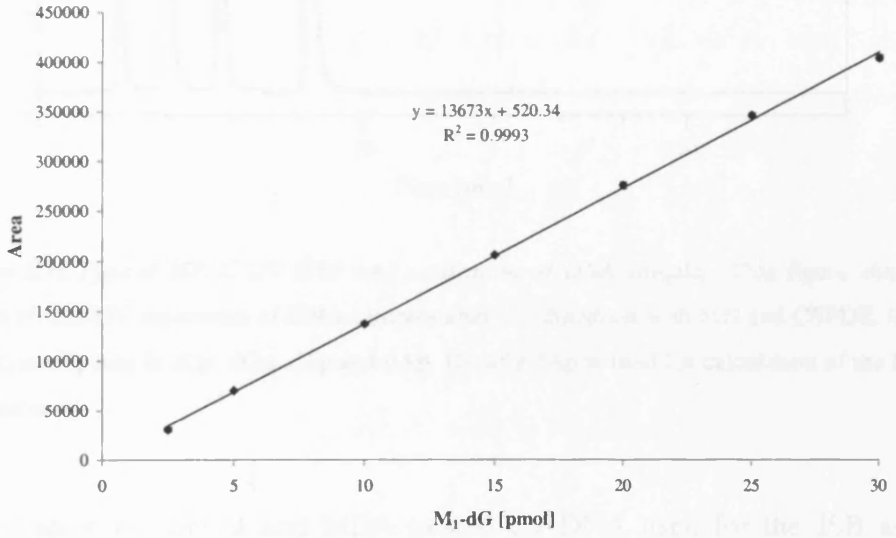

Figure 3.6: *Calibration line for M_1-dG.* RP-HPLC analysis was performed as described in Section 2.2.6.3 using 0.1M TEA (pH 5.0) containing 4% methanol as the eluent. Detection was via fluorescence (excitation 360 nm, emission 500 nm). Amounts ranging from 2.5 to 30 pmol M_1-dG were injected (6x each). Results shown are average ± standard deviation.

In the second step, nucleotides were digested further to 2'-deoxynucleosides using NP1 to determine the M_1-dG adduct level in MDA-treated CT-DNA. Synthetic M_1-dG was

available as a primary standard from L. Marnett's laboratory in Nashville, USA. The actual concentration of M_1-dG in solution was corrected and determined using the extinction coefficient(s) stated by Seto et al., UV (H_2O) 214 nm (ε 23700) and 253 nm (ε 16400) [Seto (1983)]. The adduct level in samples or CT-DNA standards was quantified by HPLC fluorescence comparing peak area with a calibration curve generated using synthetic M_1-dG (Figure 3.6).

Typical HPLC-UV (Figure 3.7) and HPLC-fluorescence (Figure 3.8) traces for MDA-treated CT-DNA using above described digestion are shown below.

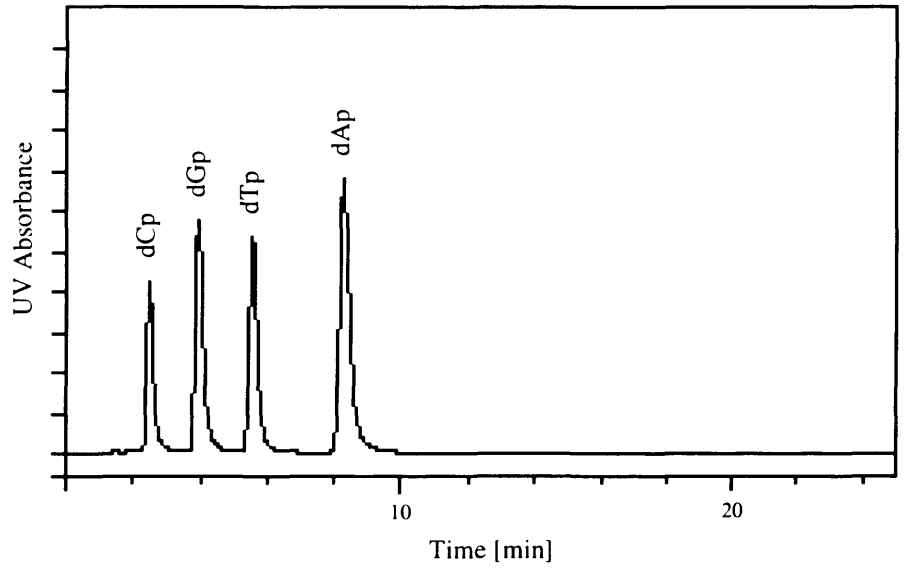

Figure 3.7: *Typical HPLC-UV (260 nm) separation of DNA samples.* This figure shows a typical HPLC-UV separation of DNA samples after 2 h digestion with MN and CSPDE. Order of elution of peaks is dCp, dGp, dTp and dAp. Usually dAp is used for calculation of the DNA concentration.

The concentration of control and MDA-treated CT-DNA used for the ISB assay were determined according to this method to be 0.714 μg/μl (control) and 0.312 μg/μl (treated) which correlated well with the UV data. DNA concentrations measured with the GeneQuant II RNA/DNA calculator were 0.747 μg/μl for control CT-DNA and 0.308 μg/μl for MDA-treated CT-DNA. The M_1-dG adduct level was determined to be 18.0 ± 0.6 pmol/μg and also confirmed by J. Plastaras, Nashville, USA who established the level of adduct to be 17 pmol/μg by LC-MS.

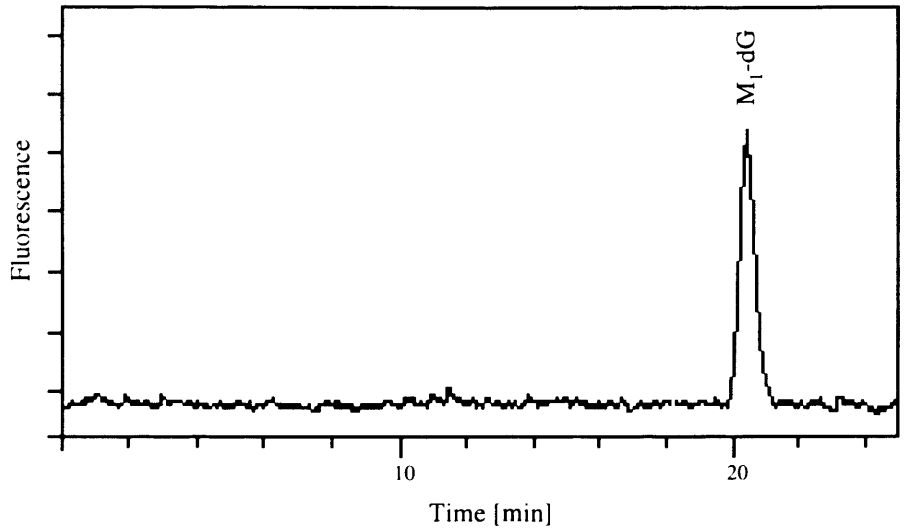

Figure 3.8: *Typical HPLC-fluorescence separation of DNA samples.* This figure shows a typical HPLC-fluorescence separation of DNA samples for the determination of M_1-dG adduct levels following enzymatic digestion using MN/CSPDE (2 h) and NP1 (o/n). RP-HPLC analysis and detection were performed as described in Section 2.2.6.3.

G:C and A:T ratios were determined for the two step digestion by comparison of sample peak areas to calibration lines for all four nucleotides. Calibration lines (Figure 3.9), ranging from 100 to 1000 pmol, were generated for 2'-deoxyguanosine-3'-monophosphate (dGp), 2'-deoxycytidine-3'-monophosphate (dCp) and thymidine-3'-monophosphate (dTp) and analysed as described earlier for dAp. The calibration line for dAp shown in Figure 3.5 was used for subsequent calculations.

Results obtained for MDA-treated CT-DNA were 662.7 ± 7.1 pmol dCp, 644.9 ± 9.7 pmol dGp, 813.6 ± 10.8 pmol dTp and 884.2 ± 12.4 pmol dAp. Consequently G:C and A:T ratios were determined to 0.97 ± 0.006 and 1.09 ± 0.005 respectively. Results obtained for control CT-DNA were similar.

One minor disadvantage of the method described above was that it was fairly time-consuming. It was therefore tried to digest DNA using all three enzymes at the same time. Units used for individual enzymes remained the same. It was discovered that the digestion of M_1-dGp was incomplete, consequently both M_1-dGp and M_1-dG were detectable by HPLC fluorescence (data not shown). Therefore, DNA had to be digested to dNp first using MN and CSPDE before using NP1 for further digestion to dN.

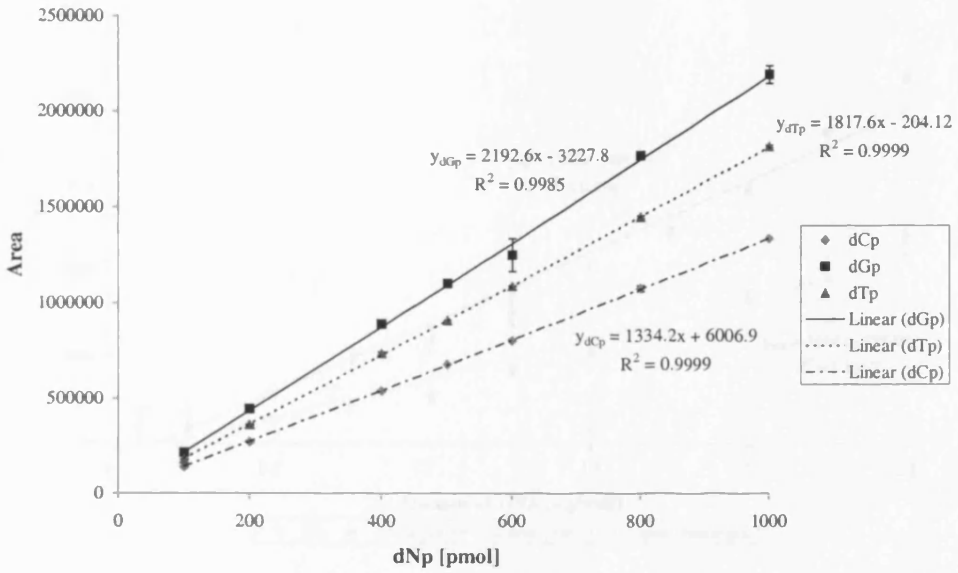

Figure 3.9: *Calibration lines for dCp, dGp and dTp ranging from 100 to 1000 pmol.* Retention times observed for deoxynucleotides were approximately 2.6 min for dCp, 4.2 min for dGp, 6.1 min for dTp and 9.3 min for dAp (calibration line shown in Figure 3.5). Calibration lines were generated using the HPLC system described in Section 2.2.6.3 by UV detection at 260 nm.

3.2.2 Development of the Propidium Iodide Assay

The aim of the propidium iodide assay was to be able to quantify the actual amount of DNA binding to NC membranes and to correct results obtained for the ISB assay. Consequently one would be able to correct for inaccuracies in pipetting, mistakes in DNA quantitation before the ISB assay and differences in DNA binding to NC filters. The fluorescent dye propidium iodide (PI) is a phenanthridinium intercalator. It binds with little or no sequence preference at a stoichiometry of one dye per 4 to 5 base pairs of DNA. PI also binds to RNA. The samples therefore need to be treated with RNases, a step which is routinely carried out during DNA extraction.

Various amounts of MDA-treated CT-DNA (0.1, 0.25, 0.5, ..., 2.5 μg/well) were spotted on the NC filter without considering the level of M_1-dG. The filter was washed twice for 10 min in 50 ml PBS after baking it for 1.5 h at 80°C. The filter was then split in half and incubated either overnight or for 3 h in 50 ml PBS containing 250 μg PI to investigate which length of exposure would be more suitable. After incubation with PI, the filters were washed twice for 15 min and for a further hour in 50 ml PBS. The fluorescent signal was captured using the Biorad Fluor-S^{TM} MultiImager (conditions see Section 2.2.4).

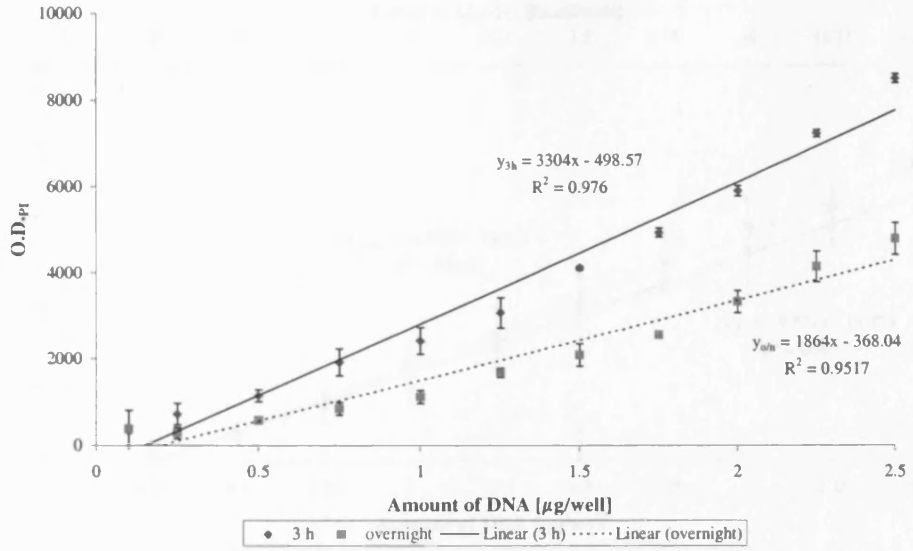

Figure 3.10: *Propidium iodide stain for different amounts of CT-DNA after 3 h and overnight exposure.* Various amounts of CT- DNA (0.1, 0.25, 0.5, ..., 2.5 µg/well) were spotted on a NC filter (BA79) and exposed after baking the membrane to propidium iodide [250 µg/50 ml PBS] for 3 h and overnight.

It appeared that there were no major differences and advantages between staining the NC filter overnight or only for 3 hours with PI (Figure 3.10). Nevertheless, the signal seemed to be slightly higher after 3 h exposure and more accurate (R^2 = 0.976). Differences in signal intensity could have also been caused by the fact that the images could not be taken at the same time using the Biorad Fluor-S™ MultiImager. Nevertheless, exposure for 3 h to PI was chosen for future experiments as longer incubation did not improve the results, and the procedure was less time-consuming.

In order to investigate the effect of antibodies and other reagents used in the ISB assay on PI staining, various amounts of DNA, containing different amounts of M_1-dG, were spotted in duplicate on a NC filter. Firstly, the standard procedure for the ISB assay was performed and the chemiluminescent signal captured using the Biorad (Figure 3.11, ISB 1 and ISB 2). The filter was then cut in half, one part was washed twice for 10 min in PBS and then exposed for 3 h to PI ('instant'). The other part of the filter was left washing in PBS overnight ('o/n wash') and stained with PI the following day according to Section 2.2.4 (Figure 3.12).

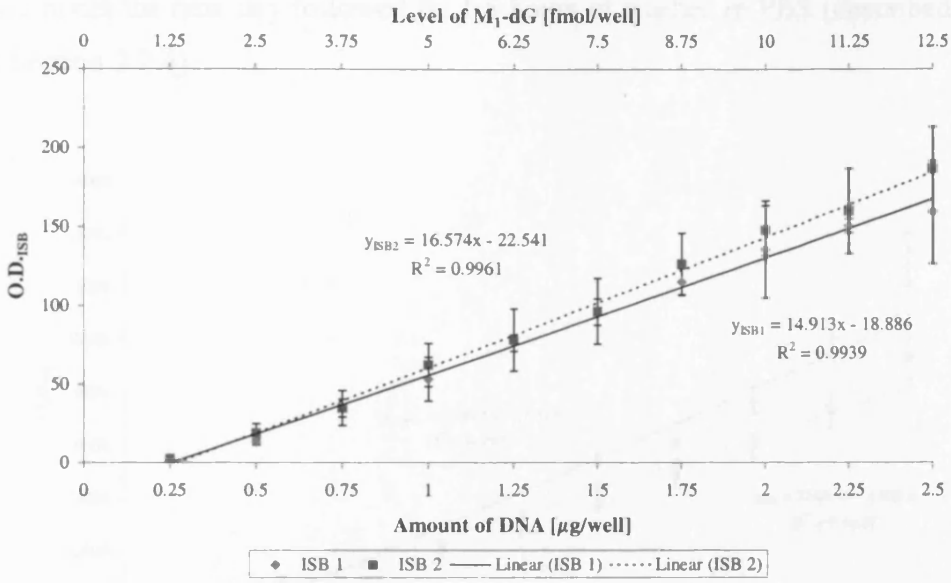

Figure 3.11: *M_1-dG calibration line generated by ISB assay for CT-DNA containing different amounts of DNA and different levels of M_1-dG.* Samples containing various amounts of DNA and M_1-dG [0.5 fmol in 0.1 µg DNA (not detectable), 1.25 fmol in 0.25 µg, 2.5 fmol in 0.5 µg, ..., 12.5 fmol in 2.5 µg] were spotted in duplicate (ISB 1 and ISB 2) on a NC filter. Chemiluminescent signal was detected using the Biorad Fluor-S™ MultiImager.

Figure 3.11 clearly shows the linear relationship between levels of M_1-dG (1.25-12.5 fmol/well, top X-axis) and the corresponding chemiluminescent signal ($O.D._{ISB}$). The adduct level, and thereby the chemiluminescent signal, was also proportional to the amount of DNA binding to the NC filter (0.25-2.5 µg/well, bottom X-axis). No chemiluminescent signal was detectable for 0.5 fmol M_1-dG, i.e. 0.1 µg CT-DNA. Both blots (ISB 1 and ISB 2) corresponded well with each other, values obtained for one blot were well within the standard deviation of the other blot.

It had no apparent effect on the fluorescent signal ($O.D._{PI}$) whether the blot was washed overnight or bathed for only 20 min in PBS prior to PI staining (Figure 3.12). Differences that were found could probably be due to the fact that the images were not taken at the same time using the Biorad Fluor-S™ MultiImager, thereby causing differences in signal intensity. However, the correlation between amount of DNA binding and fluorescent signal appeared to be more linear after an overnight wash in PBS. The line obtained for the filter exposed instantaneously to PI appeared to be more curved and less linear. Therefore, in future experiments the NC filter was washed overnight in PBS after ISB assay and exposed

to PI for 3 hours the next day followed by 1.5 hours of washes in PBS (described in more detail in Section 2.2.4).

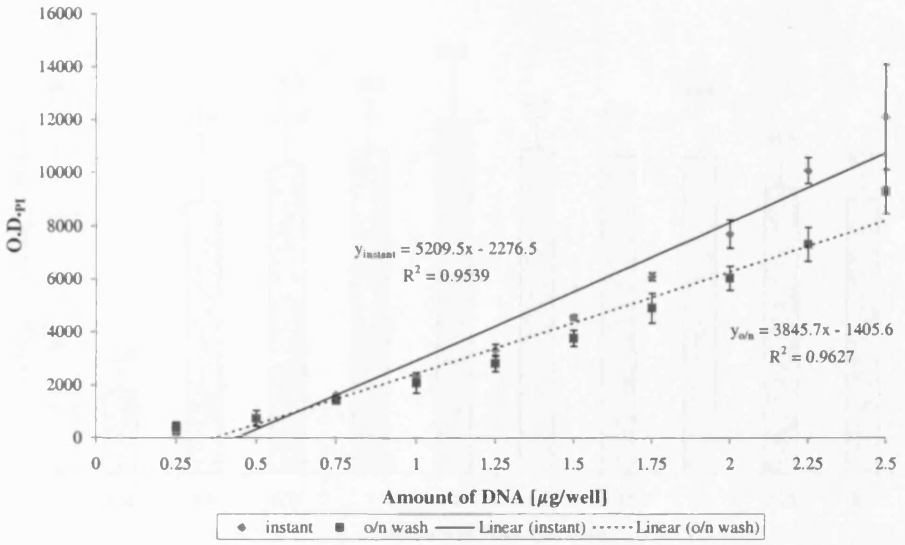

Figure 3.12: *Results of the PI staining for samples containing different amounts of CT-DNA and different levels of M_1-dG.* Samples containing various amounts of DNA and M_1-dG adduct [0.5 fmol in 0.1 μg DNA, 1.25 fmol in 0.25 μg, 2.5 fmol in 0.5 μg, ..., 12.5 fmol in 2.5 μg] were spotted in duplicate on one NC filter. 'instant' indicates that the filter was stained with PI straight after ISB assay. 'o/n wash' abbreviates that the ISB filter was washed overnight in PBS prior to PI exposure. Fluorescent signal was detected using the Biorad Fluor-S™ MultiImager.

In the following, data shown earlier were combined in order to see whether results obtained by ISB assay (Figure 3.11) could be corrected for DNA binding (Figure 3.12). An average fluorescent signal was calculated for CT-DNA standards representing 1 μg of DNA. The intensity of individual samples was subsequently divided by this value resulting in a ratio specific for each band. This ratio was then used to correct the chemiluminescent signal acquired by ISB assay.

In this particular example, the correction should result theoretically in a uniform signal over the whole range of DNA concentrations blotted i.e. all of them being corrected to a signal intensity expected for 1 μg of DNA. It can be clearly seen in Figure 3.13 that most results corrected well. Signals obtained after correction between 0.5 μg and 2.5 μg CT-DNA were within the same range, with an overall average of 48.02 ± 7.6. Only for the lowest amount of DNA binding, 0.25 μg, the correction using the PI ratio did not

correspond. $O.D._{ISB}$ after PI correction was 12.8 ± 3.3, which was about four times lower than would be expected for 1 μg.

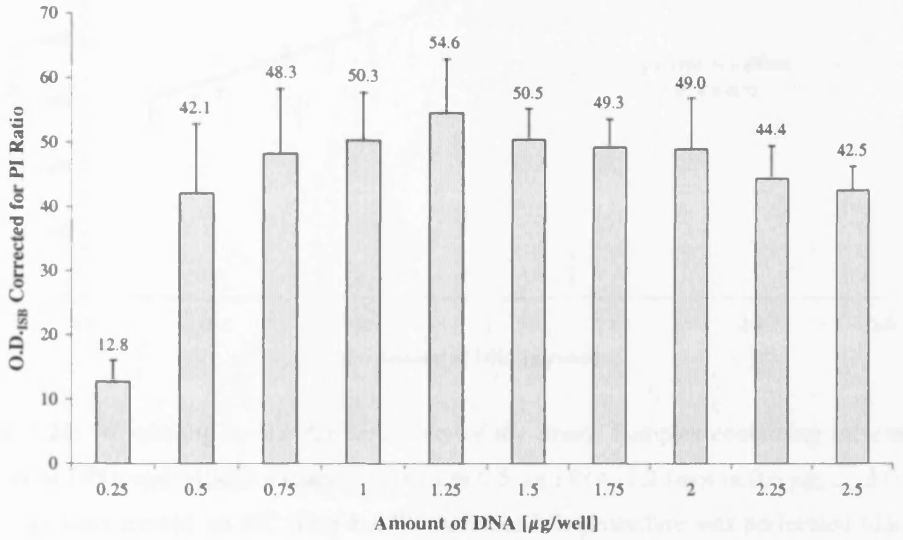

Figure 3.13: *ISB results corrected for PI ratio.* Results obtained earlier for ISB (Figure 3.11) and PI (Figure 3.12) were combined in this figure. The chemiluminescent signal obtained using the ISB assay was corrected with the PI ratio thereby correcting for the amount of DNA binding.

In another experiment, in order to investigate the sensitivity of the PI assay incremental amounts of DNA (steps of 0.1 μg) containing various amounts of M_1-dG (1.0 fmol M_1-dG in 0.5 μg DNA, 1.2 fmol in 0.6 μg, ..., 3.0 fmol in 1.5 μg of DNA) were spotted onto a NC filter. Standard ISB procedure (data not shown) and PI staining (Section 2.2.4) were performed and the final fluorescent signal was detected using the Biorad MultiImager (Figure 3.14).

The correlation between fluorescent signal ($O.D._{PI}$) and amounts of DNA differing by 0.1 μg was quite good ($R^2 = 0.9675$) and the standard deviations quite small. However, the assay might impose some difficulties to actually differentiate between 0.95 and 1.0 μg of DNA. It also appeared quite difficult to distinguish between 1.4 and 1.6 μg of DNA as the signal intensity observed for the upper region did not differ greatly. However, this was not the case in earlier experiments were a broader spectrum of DNA concentrations had been blotted.

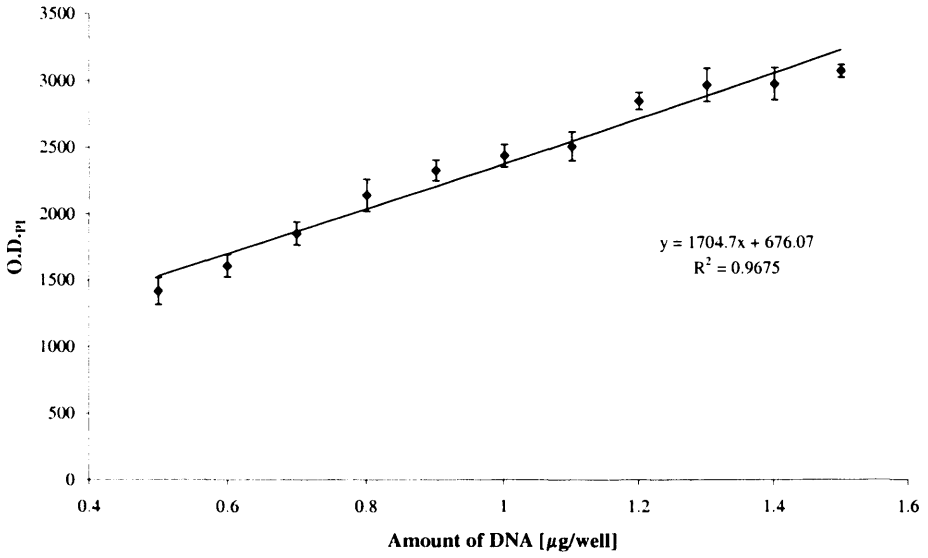

Figure 3.14: *PI staining to test for sensitivity of the assay.* Samples containing incremental amounts of DNA and M_1-dG adduct (1.0 fmol in 0.5 µg DNA, 1.2 fmol in 0.6 µg, ..., 3.0 fmol in 1.5 µg) were spotted on NC filter BA79. Standard ISB procedure was performed (data not shown), the filter was then washed overnight in PBS, stained for 3 h using 250 µg PI in 50 ml PBS and finally washed in PBS for 1.5 h in total. Fluorescent signal was detected using the Biorad Fluor-S™ MultiImager. Results ($O.D._{PI}$) were corrected for local background.

Nevertheless, it was decided to use the PI staining in future studies to correct M_1-dG results obtained by ISB assay, thus rectifying for differences in DNA binding as well as errors in pipetting. This correction ensures that high results in M_1-dG are genuine and not due to more DNA being bound to the filter.

Figure 3.15-A shows a typical image of an immunoslot blot filter with the calibration line on the left and DNA samples on the right. In this case the calibration line ranged from 0 to 10 fmol M_1-dG per µg of DNA. Figure 3.15-B shows a typical image obtained using the Biorad MultiImager following staining with propidium iodide as described in Section 2.2.4. As explained earlier the calculated level of adduct in each sample was corrected for the amount of DNA bound to the filter as determined by propidium iodide staining. It can be clearly seen from the given example that the PI staining for CT-DNA standards was very uniform, indicating that virtually identical amounts of DNA were bound to the NC filter. This amount of DNA was assumed to be 1 µg per well for standards. Comparison of DNA samples and standards clearly demonstrated that the signal intensity differed greatly indicating that differences in DNA binding between samples definitely existed.

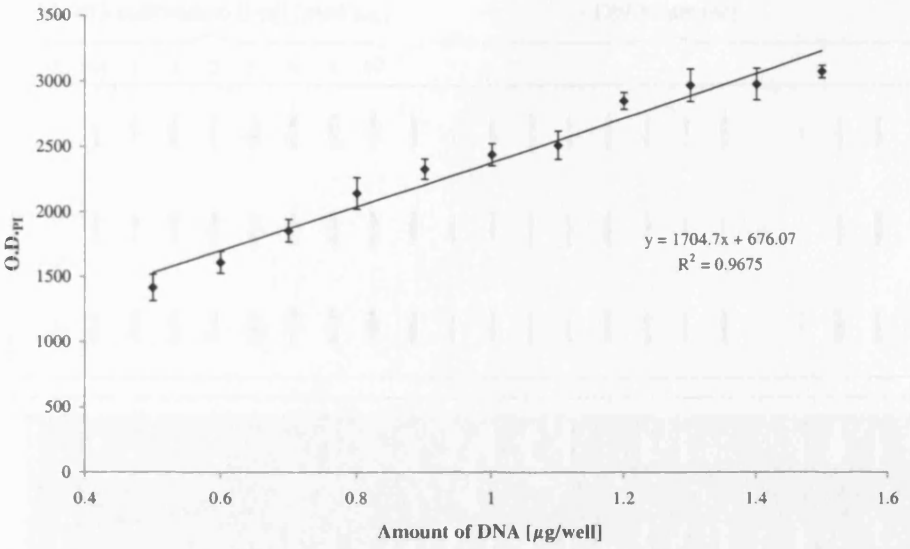

Figure 3.14: *PI staining to test for sensitivity of the assay.* Samples containing incremental amounts of DNA and M_1-dG adduct (1.0 fmol in 0.5 μg DNA, 1.2 fmol in 0.6 μg, ..., 3.0 fmol in 1.5 μg) were spotted on NC filter BA79. Standard ISB procedure was performed (data not shown), the filter was then washed overnight in PBS, stained for 3 h using 250 μg PI in 50 ml PBS and finally washed in PBS for 1.5 h in total. Fluorescent signal was detected using the Biorad Fluor-S^{TM} MultiImager. Results ($O.D._{PI}$) were corrected for local background.

Nevertheless, it was decided to use the PI staining in future studies to correct M_1-dG results obtained by ISB assay, thus rectifying for differences in DNA binding as well as errors in pipetting. This correction ensures that high results in M_1-dG are genuine and not due to more DNA being bound to the filter.

Figure 3.15-A shows a typical image of an immunoslot blot filter with the calibration line on the left and DNA samples on the right. In this case the calibration line ranged from 0 to 10 fmol M_1-dG per μg of DNA. Figure 3.15-B shows a typical image obtained using the Biorad MultiImager following staining with propidium iodide as described in Section 2.2.4. As explained earlier the calculated level of adduct in each sample was corrected for the amount of DNA bound to the filter as determined by propidium iodide staining. It can be clearly seen from the given example that the PI staining for CT-DNA standards was very uniform, indicating that virtually identical amounts of DNA were bound to the NC filter. This amount of DNA was assumed to be 1 μg per well for standards. Comparison of DNA samples and standards clearly demonstrated that the signal intensity differed greatly indicating that differences in DNA binding between samples definitely existed.

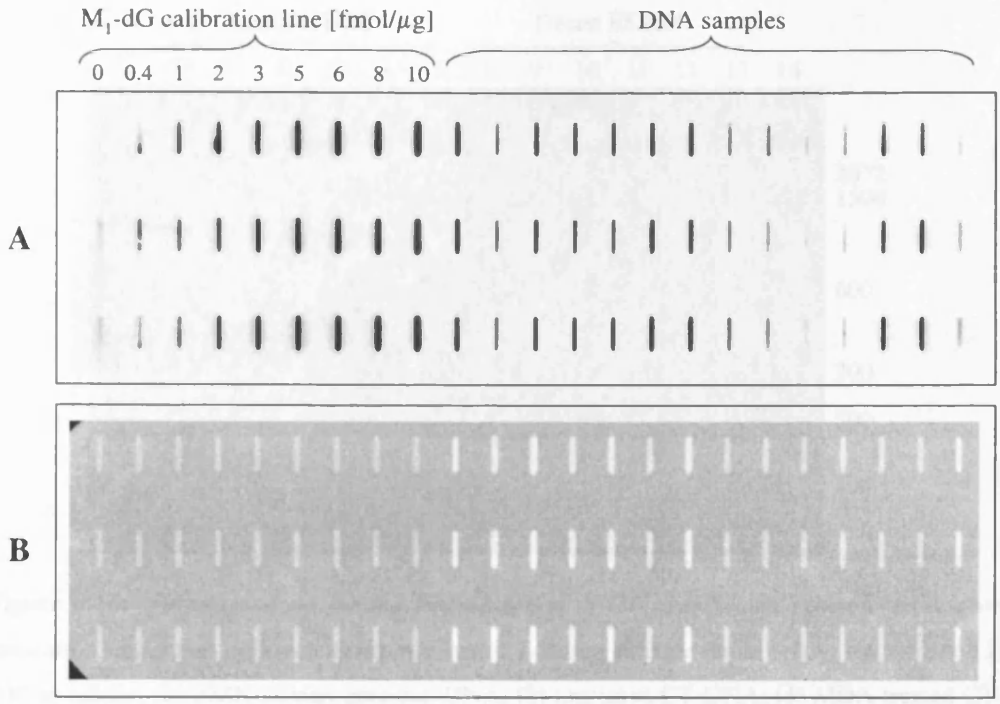

Figure 3.15: *Typical images obtained for the immunoslot blot filter using the Biorad Fluor-S™ MultiImager following incubation with (A) chemiluminescent reagent and (B) propidium iodide.* Each DNA sample and CT-DNA standard (1 μg per slot) was blotted onto the filter in triplicate.

3.2.3 Fragmentation and DNA Binding to NC Membranes

In general, the PI assay was found to be beneficial for the correction of ISB results, especially as it revealed major differences in binding between human and CT-DNA to NC membranes. Usually between 1.5 and 2.5 times more human WBC DNA was binding to the NC filter compared to CT-DNA standards. As the method used for DNA quantitation was the same and reasonably reliable for samples and standards the underlying cause for higher or stronger binding of human samples had to be found within the sample preparation during the ISB assay. One possible explanation was that there might be differences in fragmentation of human WBC and CT-DNA following sonication.

As described in Section 2.2.8.1 part (1), fragmentation of human genomic DNA and CT-DNA was investigated following 15 min sonication in two different ultrasonic baths. Samples were heat-denatured and put on ice for 10 min each, and then loaded onto an agarose gel (Section 2.2.8.3). The comparison of the two different ultrasonic baths is shown in Figure 3.16.

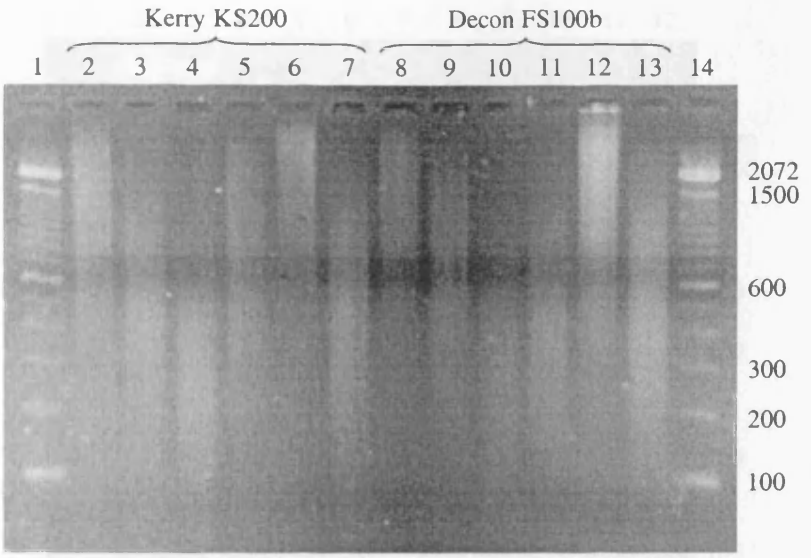

Figure 3.16: *2% agarose gel for the fragmentation of CT- and human genomic DNA upon sonication using two different ultrasonic baths.* Loading scheme (from left to right): lane (1) 100 bp ladder; (2) BMH human genomic DNA; (3) untreated CT-DNA; (4) MDA-treated CT-DNA I; (5) human sample; (6) Sigma ultrapure CT-DNA; (7) MDA-treated CT-DNA II; (8) BMH human genomic DNA; (9) untreated CT-DNA; (10) MDA-treated CT-DNA I; (11) human sample; (12) Sigma ultrapure CT-DNA; (13) MDA-treated CT-DNA II; (14) 100 bp ladder. Samples loaded in lane (2)-(7) were sonicated in the Kerry KS200 and samples loaded in lane (8)-(13) were sonicated in the Decon FS100b ultrasonic bath, which is used routinely for the ISB assay.

Differences in fragmentation between CT-DNA and human WBC DNA (Boehringer Mannheim and DNA from human blood samples) were quite apparent. Generally CT-DNA fragmented to lower molecular weight fragments ranging from 100 to 600 bp. In contrast sonication of human genomic DNA yielded fragments of higher molecular weight, > 600 bp. Fragment size of either DNA type was independent of the sonicator used. Ultrapure CT-DNA (Sigma) did not follow the general pattern for CT-DNA, but fragmented upon sonication similarly to human genomic DNA yielding fragments greater than 600 bp.

In order to obtain the same fragment size for both types of DNA, which might solve the problem of DNA binding, samples were fragmented using different conditions. In the following experiment untreated CT-DNA and human genomic DNA (Boehringer Mannheim) were used and treated as described in Section 2.2.8.1, part (2). Some of the samples were heat-denatured prior to sonication in order to investigate whether sonicating single-stranded DNA would be beneficial.

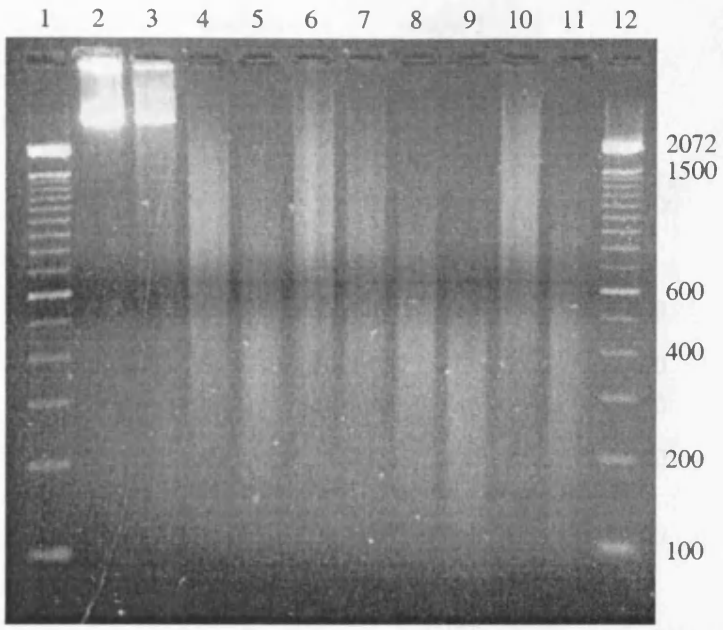

Figure 3.17: *2% agarose gel for human genomic and CT-DNA using various different methods in order to fragment DNA to the same size.* Loading scheme (from left to right): lane (1) 100 bp ladder; (2) unsonicated human genomic DNA (BMH); (3) unsonicated, untreated CT-DNA; (4) human DNA (BMH), 10 min at 100°C, 10 min on ice, 15 min sonication in ultrasonic bath; (5) CT-DNA, same treatment as (4); (6) human DNA (BMH), 15 min sonicaton in ultrasonic bath, 10 min at 100°C, 10 min on ice; (7) CT-DNA, same treatment as (6); (8) human DNA (BMH), 'Sonifier sonicator' (timer: hold, duty cycle: 10%, output control: 2, time: 5 s), 10 min at 100°C, ice 10 min; (9) CT-DNA, same as (8); (10) human DNA (BMH), 10 min at 100°C, 10 min on ice; (11) CT-DNA, same as (10); (12) 100 bp ladder.

Figure 3.17 confirms results obtained earlier, again CT-DNA fragmented to smaller fragments compared to human genomic DNA. This was observed for all different types of treatment. However, the Branson Sonifier 250 probe sonicator seemed to fragment human genomic DNA to smaller fragments than the ultrasonic bath. It was therefore decided to increase time (5-20 seconds) and output level (difference between level 2 and 3) of this specific sonicator in order to fragment human genomic DNA to sizes ranging from 100 to 600 bp [Section 2.2.8.1, part (3)]. Denaturing CT-DNA at 100°C (10 min; lane 11) resulted in similarly sized fragments as the ones obtained during routine ISB procedure (ultrasonic bath, followed by heat-denaturing the DNA; lane 7) or seemed to even decrease them. Therefore, human genomic DNA was compared in the next experiment to boiled CT-DNA (Figure 3.18).

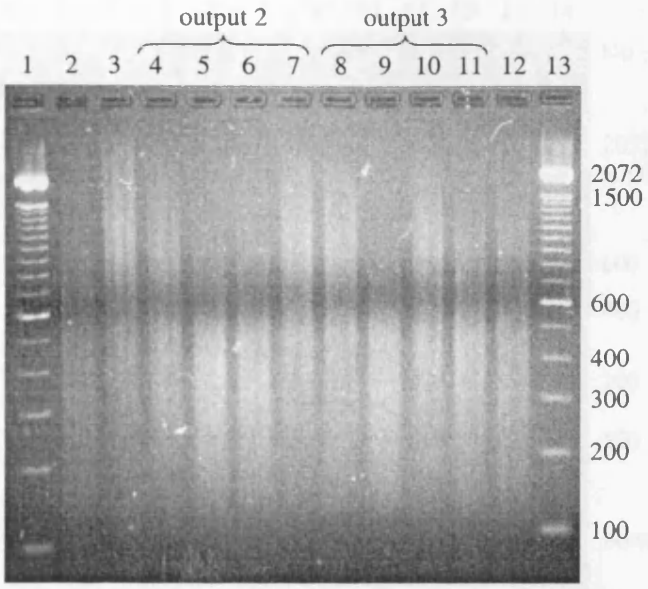

Figure 3.18: *2% agarose gel for the fragmentation of human genomic DNA generated using the Branson Sonifier sonicator.* Loading scheme (from left to right): lane (1) 100 bp ladder; (2) heat-denatured CT-DNA; (3) heat-denatured human genomic DNA. Lanes (4)-(11) represent human genomic DNA (BMH) using the following conditions for the Branson Sonifier sonicator. Lanes (4)-(7): output control 2 and varying time with (4) 5 s; (5) 10 s; (6) 15 s; (7) 20 s; Lanes (8)-(11): output control 3, time increased again with (8) 5 s; (9) 10 s; (10) 15 s; (11) 20 s; (12) heat-denatured CT-DNA; (13) 100 bp ladder.

It appeared that fragmentation of human genomic DNA using the Branson Sonifier sonicator (lane 11; output level 3, 20 s) was generating equivalent fragment sizes as heat-denatured CT-DNA (lanes 2 and 12). However, fragmentation using this particular type of sonicator seemed somewhat random and not fully reproducible. All results seemed to be unreliable and not following one pattern, i.e. the higher the output level and the longer the time the smaller the fragments.

Although it appeared feasible to generate similar fragment sizes for CT-DNA standards and human DNA samples by using different procedures, this approach was abandoned. It was important to treat samples and standards in the same way in order to avoid any unnecessary variations. It was thus essential to find a technique that would fragment both types of DNA to the same size in order to probably avoid the necessity of PI correction. Use of restriction endonucleases appeared to be one possibility and was therefore investigated in the following experiments.

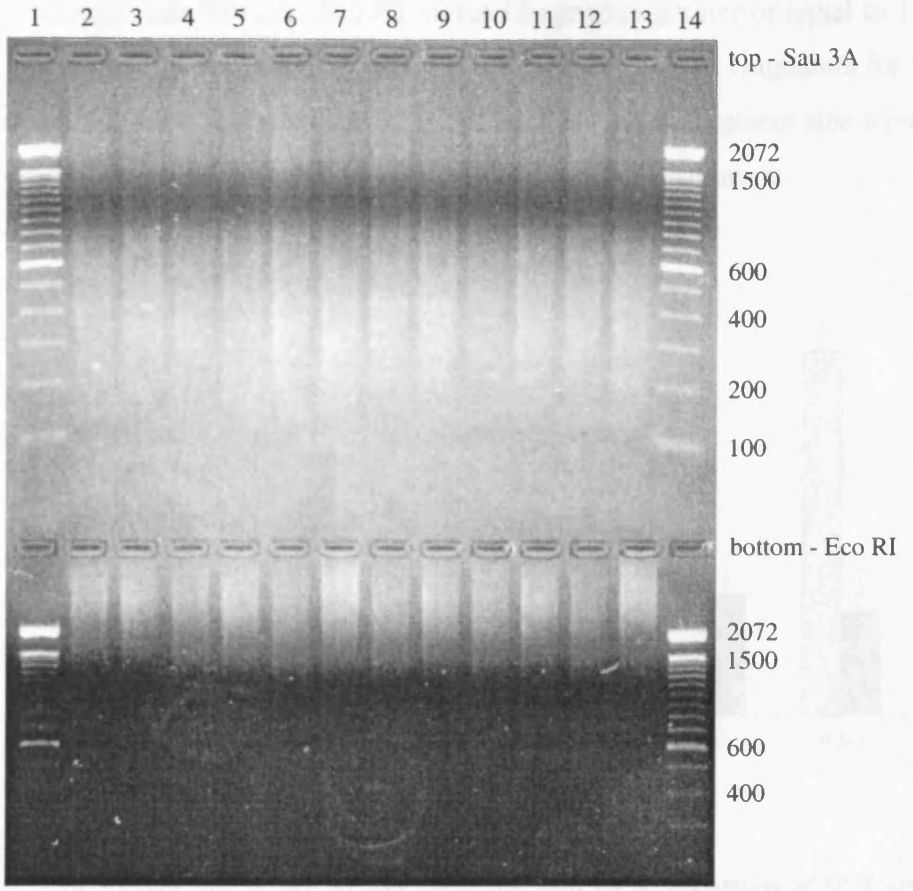

Figure 3.19: *2% agarose gel for the fragmentation of human genomic and CT-DNA generated by restriction endonucleases Sau 3A (top) and Eco RI (bottom).* Loading scheme (from left to right) TOP: lane (1) 100 bp ladder; (2) CT-DNA, 3 U Sau 3A; (3) human genomic DNA, 3 U Sau 3A; (4) CT-DNA, 6 U Sau 3A; (5) human genomic DNA, 6 U Sau 3A; (6) CT-DNA, 9 U Sau 3A; (7) human genomic DNA, 9 U Sau 3A; (8) CT-DNA, 3 U Sau 3A; (9) human genomic DNA, 3 U Sau 3A; (10) CT-DNA, 6 U Sau 3A; (11) human genomic DNA, 6 U Sau 3A; (12) CT-DNA, 9 U Sau 3A; (13) human genomic DNA, 9 U Sau 3A; (14) 100 bp ladder. Lanes (2)-(7): 30 min incubation time, lanes (8)-(13): 60 min incubation time. BOTTOM: samples were loaded in the same order as in the top part of the gel, instead of Sau 3A Eco RI was used. Units and incubation times at 37°C were as described above.

CT-DNA and human genomic DNA samples were digested using restriction endonucleases Eco RI and Sau 3A as described in Section 2.2.8.2. Results following 30 and 60 min incubation with Sau 3A and Eco RI respectively are shown in Figure 3.19. Results obtained for 90 and 120 min incubation with the enzymes is not shown, as the pattern was basically identical to the one shown in Figure 3.19. CT-DNA and human genomic DNA showed the same pattern of fragmentation. High molecular weight fragments were generated using Eco RI, whereas a wide range of smaller fragments was produced using

restriction endonuclease Sau 3A. Eco RI yielded fragments greater or equal to 1500 bp for both CT- and human genomic DNA. Sau 3A in contrast yielded fragments for both types of DNA between 100 bp and roughly 2072 bp. No changes in fragment size were observed due to increasing amounts of enzymes or prolonged time of incubation.

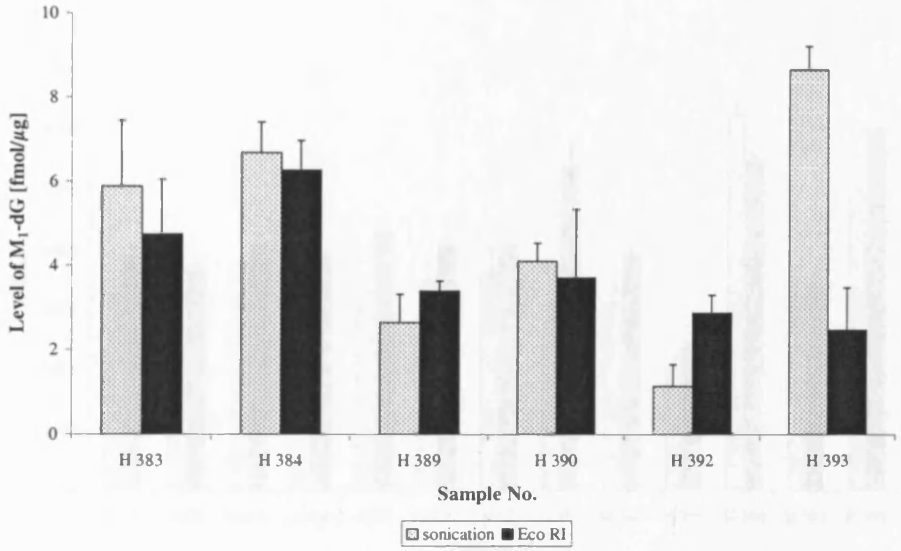

Figure 3.20: *Comparison of Eco RI and sonication used for fragmentation of DNA prior to ISB analysis.* This figure shows PI corrected chemiluminescent data (average ± standard deviation) obtained by IDB assay. Results were also corrected for M_1-dG levels detected in control CT-DNA. DNA used in this experiment originated from *H. pylori* gastric biopsies.

This method appeared to be the most promising way of uniform DNA fragmentation but still needed to be tested using the ISB assay. In this case a dot blot was used as more samples could be analysed in parallel on the same blot. Calibration lines and samples were digested using one of the restriction endonucleases (3 U, 30 min at 37°C) and compared to sonicated samples and standards on the same blot. The approach is described in more detail in Section 2.2.8.4.

Figure 3.20 shows the results obtained by immunodot blot (IDB) assay for six human gastric biopsy samples. Samples were either sonicated or digested using Eco RI (black bars). Levels of M_1-dG detected for most samples corresponded well with each other, with the exception of sample H392 and H393.

However when looking at DNA binding reflected in PI values ($O.D._{PI}$), use of Eco RI did not result in an improvement (Figure 3.21). Variations in binding between CT-DNA

standards and human DNA samples were still detectable and could only be corrected by PI staining.

An increase in DNA binding to the NC membrane by approximately 18% was noticeable for standards that were digested using Eco RI in comparison to sonicated ones. Average $O.D._{PI}$ of sonicated CT-DNA standards was 3388 versus 4007 for Eco RI digested samples.

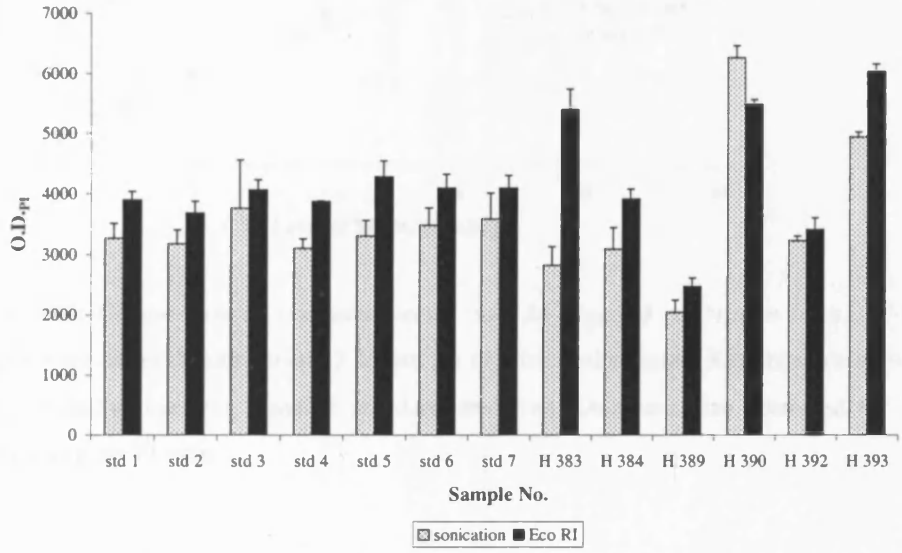

Figure 3.21: *Comparison of $O.D._{PI}$ values of sonicated and Eco RI digested DNA samples.* Std 1 to std 7 were CT-DNA calibration samples, M_1-dG values ranging from 0 to 10 fmol/μg. Samples H383 to H393 were identical *H. pylori* samples shown before in Figure 3.20. Values shown are average PI signal ± standard deviation.

This result was to be expected as Eco RI yielded much higher molecular weight fragments than sonication. More binding was also observed for most human samples which were digested with the endonuclease, but no general trend was observable. Although Eco RI appeared to standardise fragment size of various types of DNA (Figure 3.19), it did not have the same advantageous effect on DNA binding to NC filters.

The above experiment was repeated with Eco RI being replaced by Sau 3A. Again 3 units of the enzyme were used for 30 min at 37°C to digest DNA and compared to sonicated samples. The calibration line generated using Sau 3A digested standards cut the y-axis at a lower intercept (Figure 3.22). This was to be expected since less DNA was binding for those samples (Figure 3.23). Apart from that, calibration lines obtained for sonicated and Sau 3A digested standards were very similar.

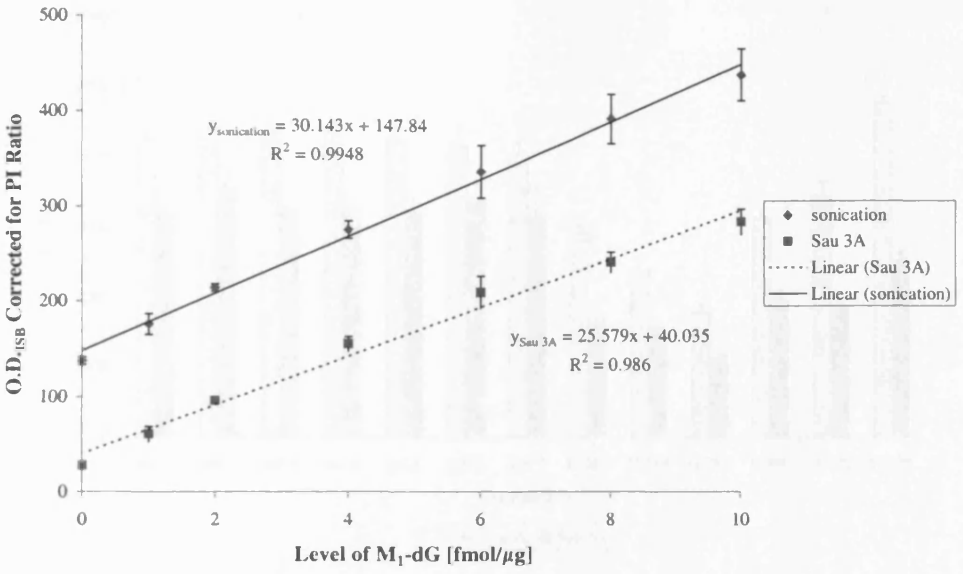

Figure 3.22: *Comparison of sonicated versus Sau 3A digested calibration lines.* CT-DNA standads were either digested using 3 U Sau 3A or sonicated as usual. Results show above are average chemiluminescent signal ± standard deviation. Data was also corrected for DNA binding using the PI ratio.

Approximately 23% less DNA binding occurred when samples were digested using Sau 3A (Figure 3.23). Average $O.D._{PI}$ of sonicated CT-DNA standards was 8484 versus 6564 for Sau 3A digested samples. Less binding also occurred for most human samples which were digested with the endonucleases. No general percentage was observable though. Similar to Eco RI, use of Sau 3A appeared to standardise DNA fragmentation, however it did not have any influence on standardising DNA binding. Additionally it also had an unexplainable and unwanted adverse effect on the chemiluminescent detection of samples. Although the PI assay showed that human DNA was binding to the membrane, and a chemiluminescent signal was detectable for CT-DNA standards, no signal was detectable for DNA extracted from human gastric biopsies. A repeat of the experiment yielded identical results. Somehow, use of Sau 3A appeared to interfere with the chemiluminescent signal of human samples but not of CT-DNA.

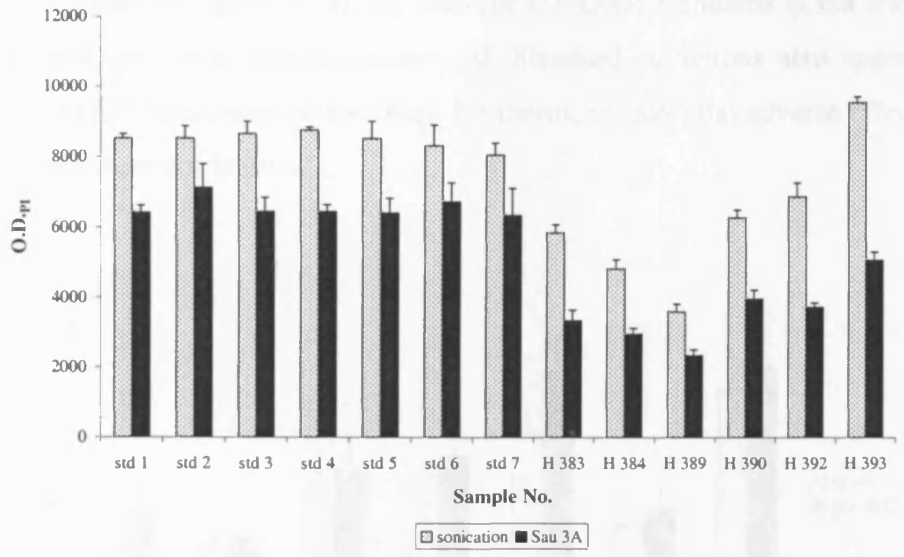

Figure 3.23: *Comparison of O.D.$_{PI}$ values of sonicated and Sau 3A digested DNA samples.* Std 1 to std 7 were CT-DNA calibration samples, M_1-dG values ranging from 0 to 10 fmol/μg. Samples H383 to H393 were *H. pylori* samples which had been used before. Values shown are average PI signal ± standard deviation.

Since its development in 1984 [Nehls (1984)], several modifications of the ISB assay have been published. Some of the variations that differ from our standard ISB protocol and their effect on DNA binding were investigated in the following (detailed in Section 2.2.9). The most common modifications were use of different membranes e.g. [Musarrat (1994)], vacuum oven [Musarrat (1994), Van Delft (1994)] and bathing the membrane in SSC buffer (0.75M NaCl, 0.075M trisodium citrate) prior to baking [Ludeke (1988), Nehls (1984)].

Binding of DNA to two different NC membranes was studied using the PI assay. As expected, more DNA was found to bind to filter BA79, which is routinely used in the ISB assay in our laboratory and has a pore size of 0.1 μm. Only about 40% bound to filter BA85 (pore size 0.45 μm) when comparing DNA binding to both membranes (O.D.$_{PI,\ BA79}$ 3388.0 versus O.D.$_{PI,\ BA85}$ 1368.3).

Both, use of vacuum oven and SSC buffer were found to be beneficial for binding of DNA to NC filters when used separately. An increase in DNA binding by approximately 80% was observed for the filter, which had been washed for 5 min in SSC buffer prior to baking (O.D.$_{PI,\ plus\ SSC}$ 2089.9 versus O.D.$_{PI,\ no\ SSC}$ 1157.9). However, when PI ratios of individual samples were compared to values generated by standard ISB procedure it appeared that treatment with SSC buffer enhanced slightly the differences in binding between human

genomic and CT-DNA (Figure 3.24). PI ratio for CT-DNA standards is not shown in the following figures, as it was approximately 1.0. Standard deviations also appeared to be higher following SSC treatment of the filter. Furthermore, potential adverse effects of SSC buffer on M_1-dG were not known.

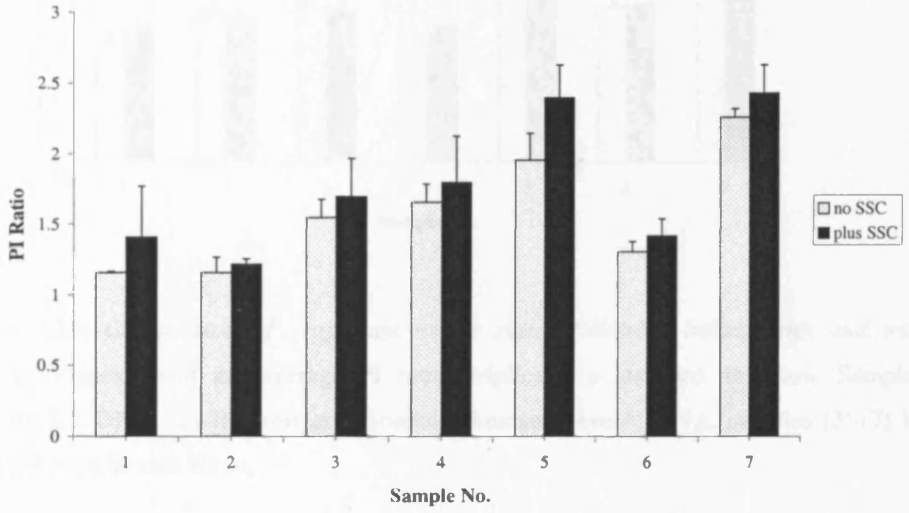

Figure 3.24: *Comparison of propidium iodide ratios following treatment with and without SSC buffer prior to baking.* Values given are average PI ratio (triplicate) ± standard deviation. Sample (1) ultrapure CT-DNA, (2) Boehringer Mannheim human genomic DNA, samples (3)-(7) DNA extracted from human blood.

Use of vacuum during baking increased the amount of DNA binding to NC filter BA79 quite dramatically and to a similar extent as SSC buffer. It was observed during repeated experiments that DNA binding to the membrane increased by about 70% when using a vacuum oven [$O.D._{PI,\ vacuum}$ 3543.8 versus $O.D._{PI,\ no\ vacuum}$ 2094.3 (Exp. I) and 1579.1 versus 910.6 (Exp. II)]. In contrast to above findings for SSC buffer, PI ratios obtained for human DNA samples remained similar or were slightly decreased when baking the NC filter in a vacuum oven (Figure 3.25). Standard deviations were similar in both cases. Furthermore, the possibility of adverse effects on M_1-dG appeared less likely as the method was more moderate.

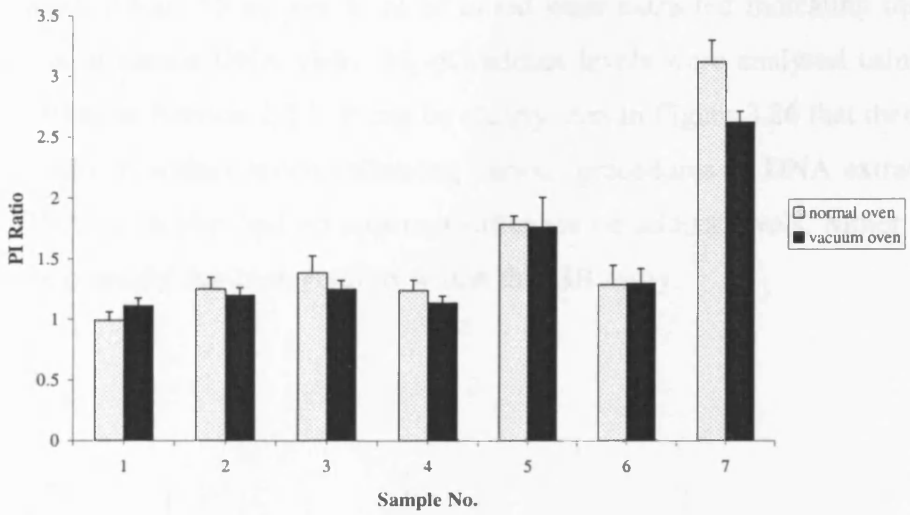

Figure 3.25: *Comparison of propidium iodide ratios following baking with and without vacuum.* Values given are average PI ratio (triplicate) ± standard deviation. Sample (1) ultrapure CT-DNA, (2) Boehringer Mannheim human genomic DNA, samples (3)-(7) DNA extracted from human blood.

3.2.4 Different Methods Used for DNA Extraction from Whole Blood

It was necessary with regard to the storage study to have a quick and reliable method for DNA extraction from whole blood that compared well with the routine procedure used in our laboratory. In order for one person to extract DNA from up to 36 blood samples in one day (as originally planned for the study on M_1-dG stability in stored whole blood), existing methods for DNA extraction, i.e. genomic tip protocol, had to be modified. The Qiagen QIAamp Blood Maxi Kit Protocol (spin columns) offered a quick, less laborious and less time-consuming way of extracting DNA from whole blood. No precipitation and subsequent washes of the DNA pellet were needed as the DNA was obtained ready in solution after the last step.

DNA was extracted from three different blood samples (T0413, T0793 and T0161) comparing the genomic tip procedure (detailed in Section 2.2.5.1 and 2.2.5.2) with the system described for the spin columns (see Section 2.2.5.3). Cell lysis was performed for the spin columns by incubating the blood samples at 70°C for 10 min. Age of the blood samples, i.e. time of storage at -80°C, varied between 6 months (T0793), 11 months (T0413) and approximately 15 months (T0161). DNA yield was similar for all samples despite the age differences. In general, extraction of fresh blood samples yields 15 to 20 μg

per ml of blood. About 55 μg per 3 ml of blood were extracted indicating that time of storage did not influence DNA yield. M_1-dG adduct levels were analysed using the ISB assay as described in Section 2.2.3. It can be clearly seen in Figure 3.26 that there were no major differences in adduct levels following various procedures of DNA extraction. The method of DNA extraction had no apparent influence on adduct levels. Minor variations observed were possibly due to deviations within the ISB assay.

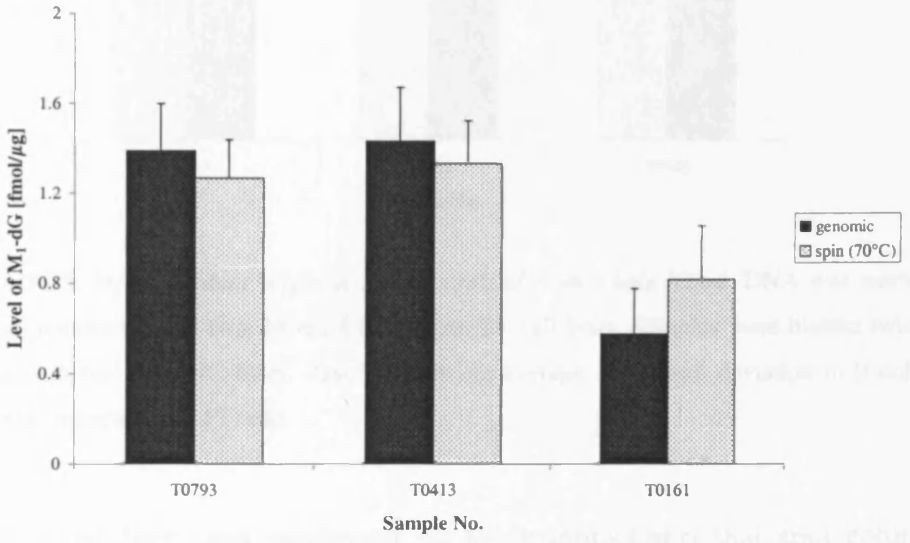

Figure 3.26: *M_1-dG adduct levels detected in DNA extracted from whole blood.* DNA was extracted using genomic tips (black bars) or spin columns (white bars). Cell lysis was performed for the spin columns by incubating the blood samples at 70°C for 10 min. Results acquired by ISB analysis and given above are average ± standard deviation in [fmol/μg] and were corrected with PI ratio.

Although no adverse effects were observed, the temperature applied for cell lysis using Qiagen QIAamp columns appeared quite high. Therefore, temperature was reduced to 50°C, time of incubation was extended from 10 min to 1 h, and both conditions compared. Again blood samples used for the comparative study varied quite considerably in age (T0653, 7 months; T0332, 12 months; T0145, 16 months). However, the results noted for the first dataset were confirmed; time of storage did not have any influence on DNA yield. With regard to the adduct, it can be seen in Figure 3.27 that the method of DNA extraction, to be precise temperature and time of cell lysis, had no adverse effect on M_1-dG levels. Adduct levels detected for all samples were independent of conditions used during cell lysis.

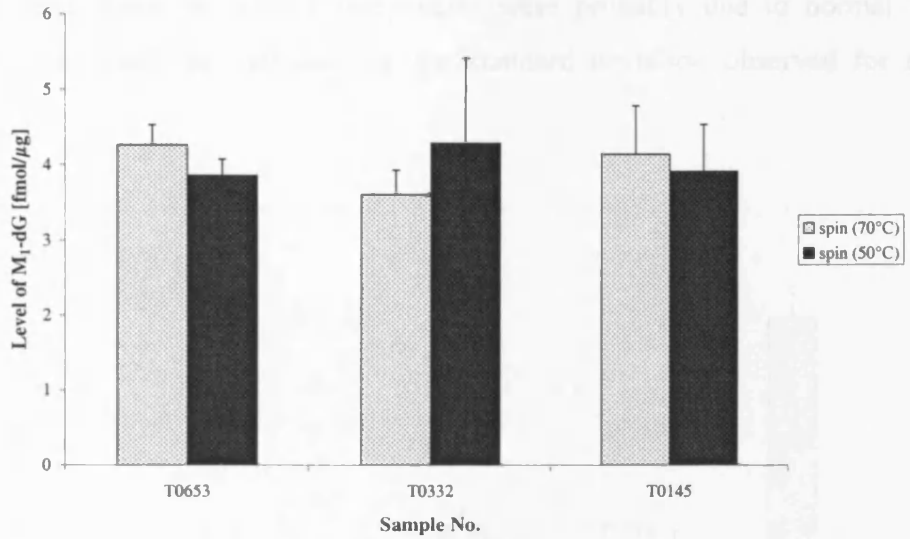

Figure 3.27: *M_1-dG adduct levels in DNA extracted from whole blood.* DNA was extracted using spin columns and two different conditions for cell lysis. Samples were blotted twice in triplicate on the same NC filter. Results given are average ± standard deviation in [fmol/µg] and were corrected with PI ratio.

It was discovered later (and confirmed by the manufacturer) that spin columns were designed for extraction of total DNA only and not genomic DNA. There was no step incorporated for the separation of genomic from mitochondrial DNA, i.e. separation of nuclei. Therefore, a combined approach was developed taking advantage of the less time consuming protocol described earlier for the spin columns but also including a step for the separation of nuclei.

Five different methods of DNA extraction were investigated by comparing M_1-dG adduct levels determined by ISB assay. Total DNA was extracted using the procedure described for Qiagen QIAamp columns (Section 2.2.5.3). Genomic DNA was extracted using either the standard protocol described for genomic tips (Section 2.2.5.1 and 2.2.5.2) or alternatively a combined approach as detailed in Sections 2.2.5.1 and 2.2.5.3. Results generated using the five different procedures are shown in Figure 3.28. Negative values as observed for sample (g+s/70°C) were due to relatively high background levels of M_1-dG in control CT-DNA i.e. in those cases the $O.D._{ISB}$ reading was below the intercept of the calibration line.

Results obtained did not allow any clear conclusion to whether M_1-dG adduct levels were dependent on the type of DNA extraction or not. Although correction using the PI ratio

diminished vast differences to some extent, variations between the five techniques were still observable. Some of these discrepancies were probably due to normal variations within the assay itself as indicated by the standard deviation observed for individual samples.

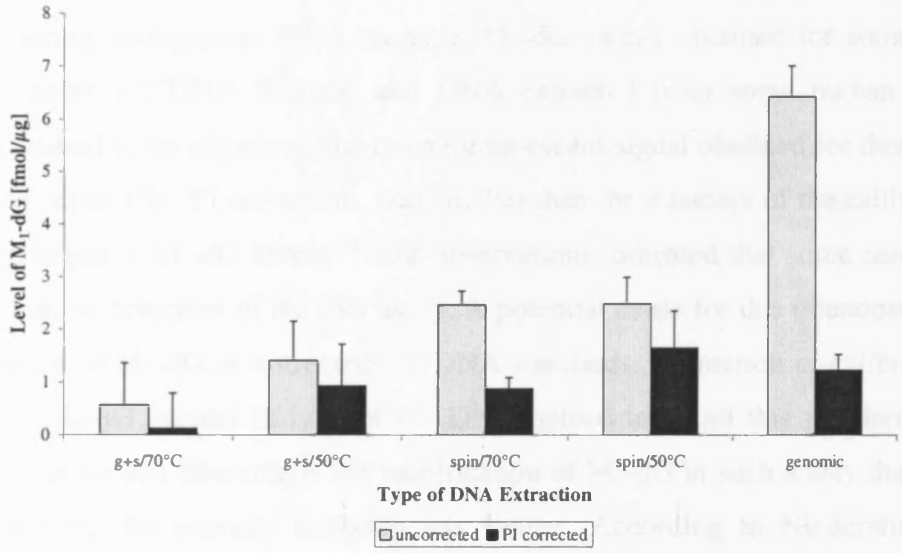

Figure 3.28: *M_1-dG adduct levels obtained for 5 different methods of DNA extraction.* The figure shows results obtained by ISB assay for one and the same blood sample using 5 different methods for DNA extraction. Values shown were either corrected with the PI ratio (black bars) or were left uncorrected (white bars). (g+s/70°C): extraction of genomic DNA using a combined method (incubation at 70°C for 10 min); (g+s/50°C): change of incubation time and temperature to 50°C for 1 h; (spin/70°C): extraction of total DNA using spin columns (lysis at 70°C, 10 min); (spin/50°C): spin column only (lysis at 50°C, 1 h); (genomic): extraction of genomic DNA using the genomic tip procedure.

Originally, it was expected that DNA extraction using spin columns [(spin/50°C) and (spin/70°C)] would yield the highest adduct levels as both, mitochondrial and genomic DNA were extracted. However, this was not the case, results did not differ greatly from those obtained using the genomic tip protocol (1.23 ± 0.3 fmol/µg). Results acquired using the combined technique (g+s/70°C) were lowest compared to the other methods. M_1-dG levels obtained for different, less extreme cell lysis conditions using the combined approach (g+s/50°C) were similar (0.93 ± 0.8 fmol/µg) when compared to the genomic tip procedure. Thus, it was decided to use the combined approach (cell lysis at 50°C for 1 h)

for the extraction of genomic DNA during blood and buffy coat storage experiments. The method was also relatively quick and less laborious.

3.2.5 Reduction of M_1-dG Levels Using Methoxyamine and Hydroxylamine

Background levels of adducts in untreated, control CT-DNA are one potential difficulty of assays measuring endogenous DNA damage. M_1-dG values obtained for some samples, such as ultrapure CT-DNA (Sigma) and DNA extracted from some human colorectal biopsies, appeared to be negative. The chemiluminescent signal obtained for these samples by ISB assay, even after PI correction, was smaller than the intercept of the calibration line i.e. yielding negative M_1-dG levels. These observations indicated that some samples were below the limit of detection of the ISB assay. A potential cause for this phenomenon could be the presence of M_1-dG in untreated CT-DNA standards. Correction of calibration lines for levels of M_1-dG present in control CT-DNA helped to avoid this problem. Another possibility to solve this dilemma is the modification of M_1-dG in such a way that it cannot be recognised by the primary antibody any longer. According to Niedernhofer et al. [Niedernhofer (1997)] M_1-dG is ring-opened to N^2-(3-oxo-propenyl)deoxyguanosine in the presence of base (pH > 8). In the following experiments this phenomenon was investigated and exploited, and ring closure inhibited by reaction of the aldehyde group with primary amines such as methoxyamine and hydroxylamine.

The method was first developed using highly MDA-modified CT-DNA enabling reaction monitoring by HPLC and optimisation of concentration and incubation time for the methoxyamine treatment.

Figure 3.29 shows the reduction in M_1-dGp levels following treatment with 5mM methoxyamine in 10mM K_2HPO_4 buffer at pH 8.0, 8.5 and 9.0 (treatment details see Section 2.2.10.1). Storage of samples overnight at -20°C already reduced M_1-dGp levels to about 42% of its original level. After 24 h incubation at 37°C only 12.1% of the adduct were present at pH 8.0, only slightly more (16.5%) at pH 9.0. No adverse influence was observed for normal nucleotides when methoxyamine was used. Furthermore the buffer system itself had no effect on M_1-dGp levels and normal nucleotides. Reduction in adduct levels appeared to be mostly independent of the pH although pH 9.0 appeared to be the least favourable. pH 8.0 yielded highest reduction in M_1-dGp levels and was therefore used in subsequent experiments.

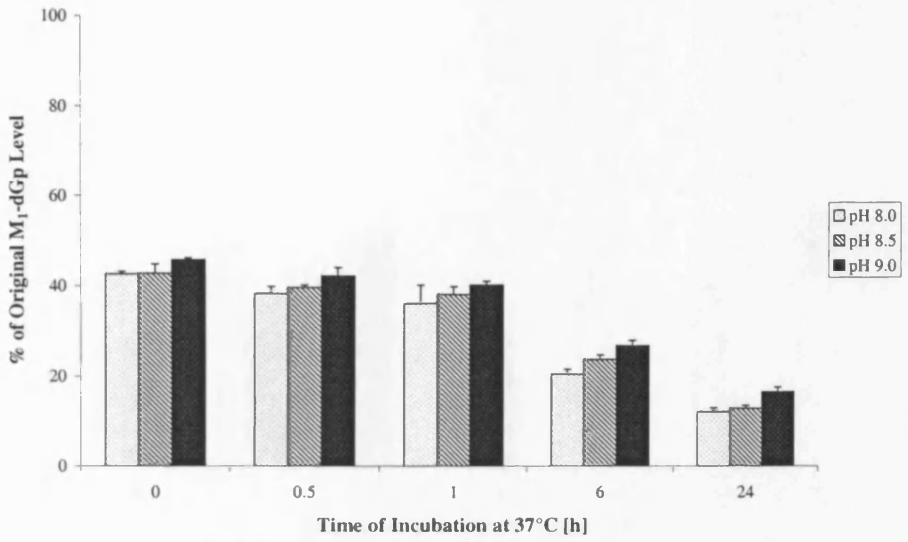

Figure 3.29: *Reduction of M_1-dGp levels following treatment with 5mM methoxyamine in 10mM K_2HPO_4 buffer (pH ranging from 8.0 to 9.0).* Samples were stored overnight at -20°C, incubated the next day at 37°C and analysed by enzymatic digestion and HPLC after 0, 0.5, 1, 6 and 24 h. Treatment details were described earlier in Section 2.2.10.1.

Highly modified DNA was treated in 10mM K_2HPO_4 (pH 8.0) with a range of methoxyamine concentrations (5, 20 and 50mM). All samples were stored for 66 h at -20°C, then incubated at 37°C and analysed after 0, 1, 6, 24, 48 and 72 h as described in more detail in Section 2.2.10.2. K_2HPO_4 buffer itself had no adverse effect on normal nucleotides and modified guanine bases. Incubation with 5mM methoxyamine yielded a 75% reduction after 66 h incubation in the freezer and a further reduction by only 5% following prolonged incubation at 37°C (Figure 3.30). Extended incubation at -20°C with methoxyamine appeared to have an effect on M_1-dGp levels. M_1-dGp levels were reduced by 58% and 75% following overnight and 66 h treatments at -20°C using 5mM methoxyamine respectively (Figure 3.29 versus Figure 3.30).

M_1-dGp values observed for 20mM and 50mM methoxyamine treatments were variable and not very reproducible. Moreover, normal nucleotides were also affected by these treatments (Figure 3.31).

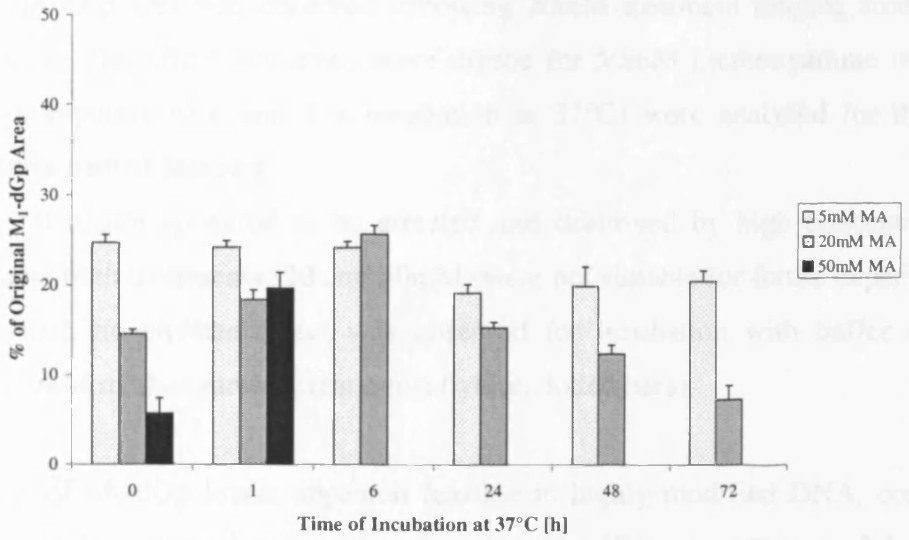

Figure 3.30: *Reduction of M_1-dGp levels using various concentrations of methoxyamine in phosphate buffer (pH 8.0).* MDA-treated CT-DNA was taken up in 10mM KP buffer (pH 8.0) and treated with 5, 20 or 50mM methoxyamine (MA). All samples were stored for 66 h at -20°C and then incubated at 37°C. Aliquots were analysed after 0, 1, 6, 24, 48 and 72 h of incubation and analysed by HPLC. Samples treated with 50mM methoxyamine were examined only after 0 and 1 h of incubation at 37°C. Treatment of DNA with KP only or water under above conditions served as negative controls for this experiment.

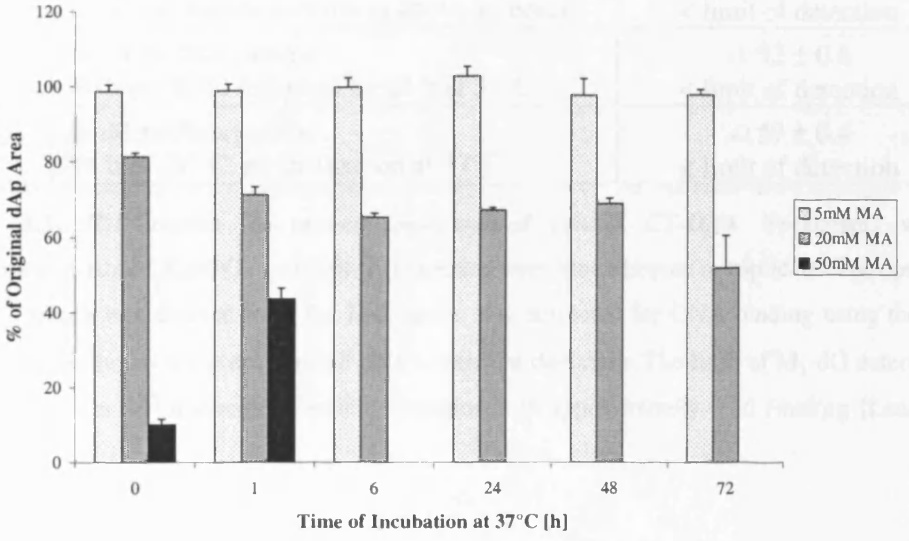

Figure 3.31: *Effect on dAp levels following various methoxyamine treatments in KP buffer at pH 8.0.* Highly modified CT-DNA was treated with 5, 20 or 50mM methoxyamine (MA). All samples were stored for 66 h at -20°C and then incubated at 37°C. Aliquots were analysed after 0, 1, 6, 24, 48 and 72 h of incubation and analysed by HPLC. Samples treated with 50mM methoxyamine were examined only after 0 and 1 h of incubation at 37°C.

A decrease in dAp area was observed following 20mM treatment ranging from 20% to 50% with time. The effect was even more drastic for 50mM methoxyamine treatments. Only two time-points (0 h and 1 h incubation at 37°C) were analysed for the 50mM methoxyamine-treated samples.

Since DNA structure appeared to be affected and destroyed by high concentrations of methoxyamine both treatments (20 and 50mM) were not suitable for future experiments. In contrast to that, no adverse effect was observed for incubation with buffer only (not shown) and 5mM methoxyamine treatments (white, dotted bars).

As reduction of M_1-dGp levels appeared feasible in highly modified DNA, control CT-DNA was treated using methoxyamine and analysed by IDB assay (Section 2.2.10.3). All samples appeared to yield negative results indicating that each was below the limit of detection of the assay (Table 3.2).

Sample	Treatment Conditions	Level of M_1-dG [fmol/μg]
(A)	2.5mM methoxyamine o/n (18 h) at -20°C followed by 24 h at 37°C	-0.36 ± 0.5 < limit of detection
(B)	5mM methoxyamine o/n at -20°C followed by 24 h 37°C	-0.57 ± 0.4 < limit of detection
(C)	10mM KP buffer (pH 8.0) only same incubation scheme as above samples	-0.30 ± 0.6 < limit of detection
(D)	5mM methoxyamine 70 h at -20°C followed by 24 h at 37°C	-1.52 ± 0.8 < limit of detection
(E)	5mM methoxyamine 94 h at -20°C, no incubation at 37°C	-0.59 ± 0.4 < limit of detection

Table 3.2: *IDB results for methoxyamine-treated control CT-DNA.* Treatments were performed in 10mM K_2HPO_4 (pH 8.0). All samples were blotted twice in triplicate. The optical density, which was derived from the IDB assay, was corrected for DNA binding using the PI ratio. Results shown are average of all dots ± standard deviation. The limit of M_1-dG detection is 5 adducts per 10^8 nucleosides which corresponds to approximately 0.16 fmol/μg [Leuratti (1999)].

The possibility of reducing M_1-dG levels in MDA-treated CT-DNA and generating a standard with reduced background seemed to be quick, feasible and reasonably reproducible. Although preliminary results looked quite promising, further development and improvement needed to be done. It has been shown recently by Daniels et al. [Daniels (1999)] that a stable acyclic adduct is formed from hydroxylamine addition to M_1-dG.

Therefore, the comparison between methoxyamine and hydroxylamine as well as using different buffer systems was investigated in further experiments. Methods were again optimised in the beginning using highly modified CT-DNA and HPLC analysis, and applied later to control CT-DNA and ISB analysis.

In the first of subsequent experiments 50mM buffer systems (MOPS and K_2HPO_4) were used along with hydroxylamine and methoxyamine. Experimental details are described in Section 2.2.10.4 and results shown in Figure 3.32.

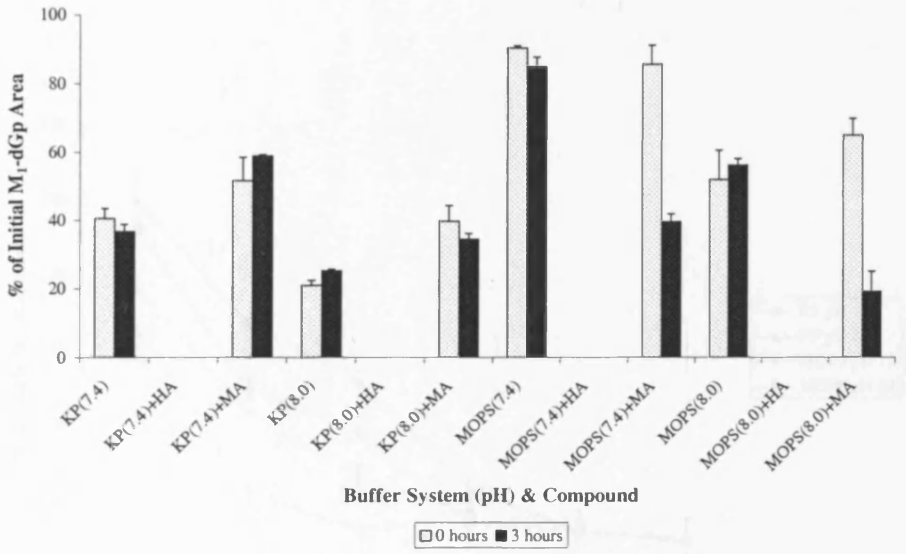

Figure 3.32: *Effect of 50mM buffer systems, hydroxylamine and methoxyamine on levels of M_1-dGp.* MDA-treated CT-DNA was reacted with 5mM hydroxylamine (HA) or methoxyamine (MA) at 37°C in 50mM buffer systems. Buffer systems used were 50mM K_2HPO_4 and MOPS with pH being either 7.4 or 8.0. Only samples taken after 0 h and 3 h were analysed by HPLC. Results are expressed as percentage of the original M_1-dGp area detected by HPLC and were also corrected for the amount of DNA (dAp) injected.

All reactions with hydroxylamine yielded the same result and were independent of the buffer system used and its pH. No M_1-dGp was detectable by HPLC fluorescence immediately and 3 h after addition of the amine. Buffer systems originally used as negative controls were also found to reduce adduct levels considerably. Values were compared to MDA-treated CT-DNA dissolved in water. Levels of M_1-dGp in phosphate buffer ranged from 21.1% (KP, pH 8.0) to 40.5% (KP, pH 7.4). Similar, albeit less severe, observations were made for 50mM MOPS. 90.4% of its initial adduct level were detectable at pH 7.4, and only 52.1% at pH 8.0 at the beginning of the experiment. Unexpectedly, an increase in

M_1-dGp levels was observed for samples incubated in phosphate buffer after addition of methoxyamine. Levels detected in these samples remained similar within the first three hours. In contrast to those observations, a decrease was observed over time when using methoxyamine in 50mM MOPS. Adduct levels were found to be reduced from 85.7% to 39.7% at pH 7.4, and from 65% down to 19.2% at pH 8.0.

The identical experimental set-up was repeated using 10mM buffer systems instead of 50mM ones (Section 2.2.10.4). Marked differences were observed when comparing the reactions between MDA-treated CT-DNA and the two amines, once again monitored by HPLC.

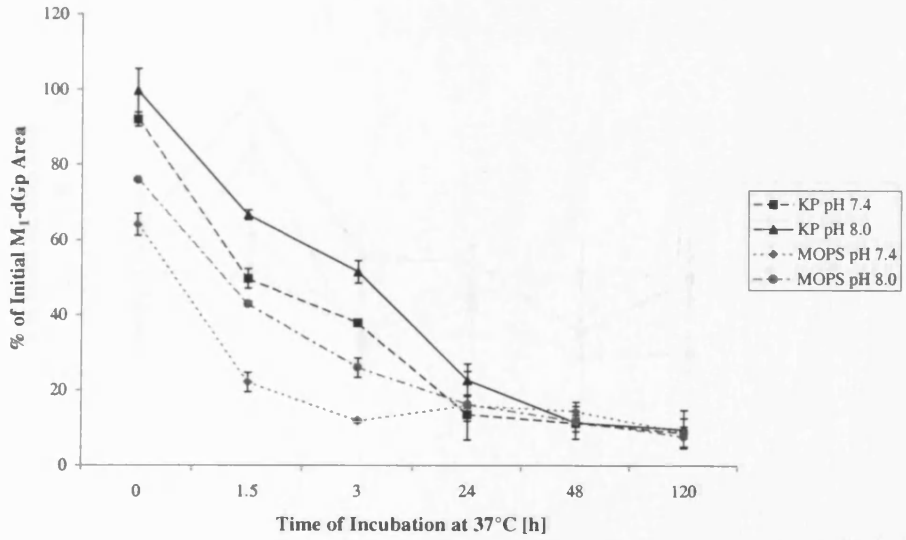

Figure 3.33: *Reduction of M_1-dGp levels using methoxyamine.* MDA-modified CT-DNA was treated at 37°C using 5mM methoxyamine in either 10mM MOPS or 10mM K_2HPO_4 (KP). pH of both buffer systems ranged from 7.4 to 8.0. Samples were taken at regular intervals, digested to dNp using MN and CSPDE and analysed by HPLC. Results (average ± standard deviation) are expressed as percentage of the original M_1-dGp area detected by HPLC.

The reaction using methoxyamine (Figure 3.33) followed a more gradual pattern, whereas an instantaneous reaction was taking place when using hydroxylamine (Figure 3.34). Highly modified CT-DNA was also incubated with each buffer system on its own as well as with water at 37°C. Neither water nor any 10mM buffer system used in the experiments had an effect on the level of modification (data not shown).

Evaluation of the buffer systems resulted in the observation that in general reactions with methoxyamine were more rapid in the beginning when taking place in MOPS (Figure

3.33). Similar observations were also made for pH of the buffer. pH 7.4 appeared favourable for the reaction of methoxyamine with highly modified CT-DNA especially in the first hours of the experiment. At the starting point 99.7% of the initial adduct level were detectable for samples incubated in phosphate buffer (pH 8.0). The lowest level observed was 64.1% in MOPS (pH 7.4). These variations appeared to level out after prolonged incubation at 37°C, resulting in a similar reduction of M_1-dGp levels being observed. Approximately 8-9% of the initial adduct level were detectable after 120 h of incubation with methoxyamine, this was relatively independent of pH and buffer system used.

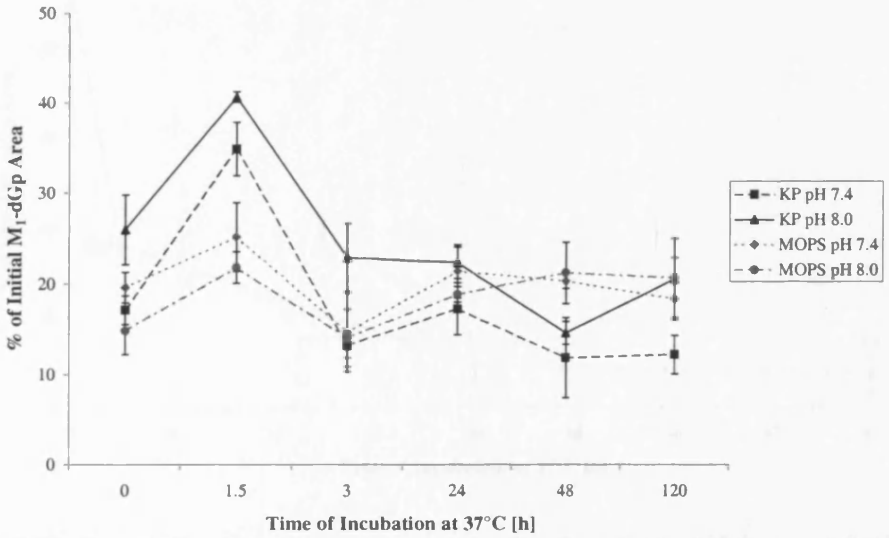

Figure 3.34: *Reduction of M_1-dGp levels using hydroxylamine.* MDA-modified CT-DNA was treated at 37°C using 5mM hydroxylamine in either 10mM MOPS or 10mM K_2HPO_4 (KP). pH of both buffer systems ranged from 7.4 to 8.0. Samples were taken at regular intervals, digested to dNp using MN and CSPDE and analysed by HPLC. Results (average ± standard deviation) are expressed as percentage of the original M_1-dGp area detected by HPLC.

On the contrary, hydroxylamine reacted immediately with the adduct in DNA (Figure 3.34). 14.9% of the original M_1-dGp level were detectable following 5mM treatment in 10mM MOPS (pH 8.0), 26.0% were measurable for the one in phosphate buffer at pH 8.0. Adduct levels appeared to increase somewhat as values detected by HPLC were generally higher after 1.5 h of incubation, ranging between 21.8% and 40.7%. The greatest reduction after 120 h of incubation was observed for 5mM hydroxylamine treatment in phosphate

buffer pH 7.4 with only 12.2% being detectable as M_1-dGp. Other incubation conditions yielded roughly an 80% decrease in adduct levels.

As reactions with methoxyamine appeared more consistent when compared to hydroxylamine, control CT-DNA was incubated using 5mM methoxyamine in 10mM phosphate buffer (pH 7.4) prior to ISB analysis. Treatment details are described in Section 2.2.10.5. The reaction was monitored through simultaneous incubation of highly modified MDA-treated CT-DNA using identical conditions and analysing aliquots at regular intervals by HPLC (detailed in Section 2.2.10.5).

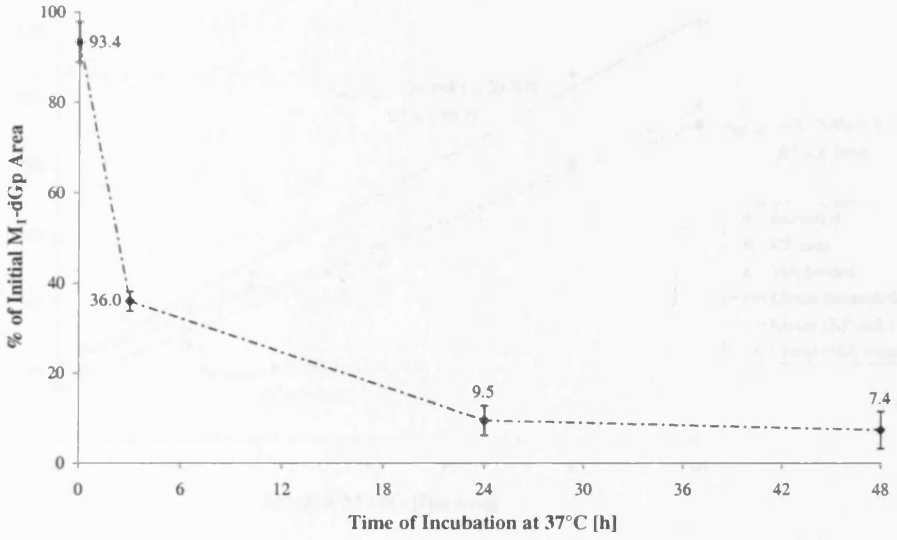

Figure 3.35: *Repeat of methoxyamine treatment in phosphate buffer.* MDA-treated CT-DNA was treated using 5mM methoxyamine in 10mM K_2HPO_4 buffer (pH 7.4) for up to 48 h at 37°C. Samples were treated as well as analysed in duplicate. Results (average ± standard deviation) are expressed as percentage of the original M_1-dGp area detected by HPLC. Methoxyamine treatments of MDA-treated and control CT-DNA (see Figure 3.36) were performed simultaneously.

Figure 3.35 shows the reduction in adduct levels in highly modified CT-DNA. Data correlates well with previously obtained results. Levels of adduct were reduced by 6.6% immediately after addition of methoxyamine. An exponential decrease in M_1-dGp levels was observed over time resulting in a 92.6% reduction after 48 h of incubation.

As mentioned earlier, untreated CT-DNA was incubated simultaneously to the monitoring reaction (Figure 3.35) in either the buffer system itself or with 5mM methoxyamine for 48 h at 37°C. Following precipitation, calibration lines for ISB analysis were generated as

usual. Effectively three calibration lines were prepared and compared to each other on the same filter using MDA-treated CT-DNA in all cases and either (i) standard, untreated control CT-DNA, (ii) phosphate buffer incubated control CT-DNA or (iii) methoxyamine-treated control CT-DNA for the preparation of appropriate dilutions. Results acquired by ISB assay were also corrected for DNA binding using the PI ratio. These PI corrected results obtained for calibration lines ranging from 0 to 10 fmol M_1-dG/μg using three different types of control CT-DNA are shown in Figure 3.36.

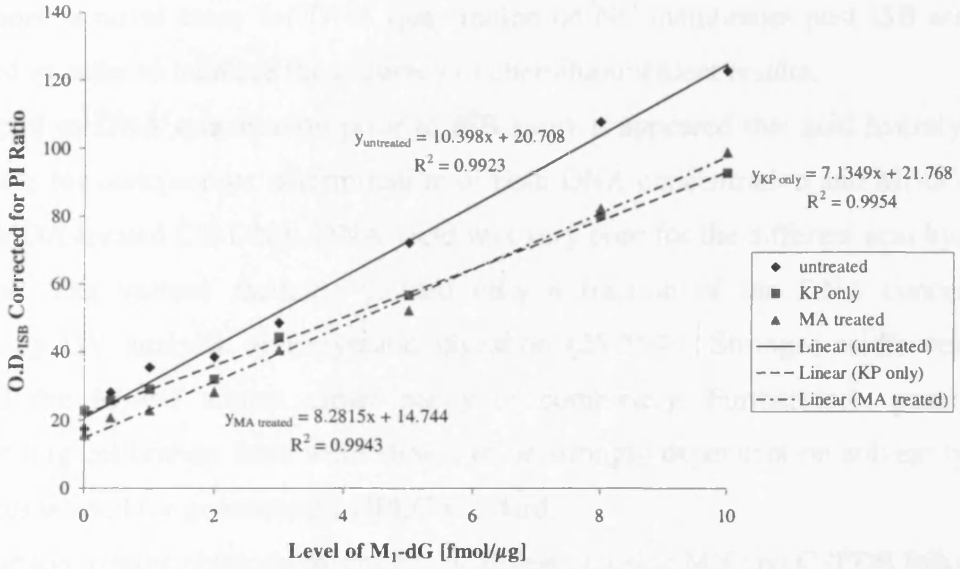

Figure 3.36: *Comparison of untreated, KP-incubated and methoxyamine-treated calibration lines by ISB assay.* Control CT-DNA was either treated with KP buffer pH 7.4 ('KP only') or 5mM methoxyamine ('MA treated') for 48 h at 37°C. Treated controls were then used for preparation of calibration lines ranging from 0 to 10 fmol M_1-dG/μg and compared to a normal calibration line ('untreated') using the ISB assay. Results shown are corrected for DNA binding using the PI ratio.

No major differences were detectable by ISB assay between the three calibration lines. However, using methoxyamine-treated control CT-DNA for preparation of the standard curve appeared to lower the intercept of the calibration line with the y-axis when compared to the normal calibration line (b = 14.7 versus 20.7). The intercept of the calibration line using control DNA which had been incubated in phosphate buffer only was comparable to the one obtained for the standard calibration line. The slope of the typical standard curve was slightly steeper when related to the one using methoxyamine-treated control CT-DNA (10.4 versus 8.3).

3.3 Discussion

One major aim of this project was the investigation of DNA adduct stability upon long-term storage which will be presented in Chapter 4. This study was focused on the M_1-dG adduct as this adduct was more likely to undergo changes. It was intended to use a very sensitive immunoslot blot assay in order to investigate (potential) changes in adduct levels in stored human samples. Although this method had already been developed by Leuratti et al. [Leuratti (1998)], several aspects such as DNA quantitation, fragmentation and binding as well as potential further improvements of the existing assay have been investigated. Furthermore, a novel assay for DNA quantitation on NC membranes post-ISB assay was developed in order to increase the accuracy of chemiluminescent results.

With regard to DNA quantitation prior to ISB assay it appeared that acid hydrolysis was not suitable for concomitant determination of both DNA concentration and M_1-dG adduct level in MDA-treated CT-DNA. DNA yield was very poor for the different acid hydrolysis conditions. The various methods yielded only a fraction of the DNA concentration obtained by UV analysis or enzymatic digestion (25-35%). Stronger acidic conditions destroyed the M_1-dG adduct either partly or completely. Furthermore, guanine and corresponding calibration lines were shown to be strongly dependent on solvent type and concentration used for generating a HPLC standard.

In comparison, results obtained by enzymatic digestion using MN and CSPDE followed by overnight incubation with NP1 correlated well with UV spectroscopic data. Simultaneous quantitation of DNA concentration and M_1-dG adduct level was feasible as well as reliable. G:C and A:T ratios in MDA-treated and control CT-DNA were established to approximately 1.0, thus validating this method and confirming its efficiency. Levels of adduct determined by enzymatic digestion were also confirmed by John Plastaras (Vanderbilt University, Nashville, USA) using LC-MS. The above approach also allowed routine analysis of DNA extracted from human leukocytes and tissues in order to check sample purity prior to ISB analysis. Furthermore, with regard to stability of long-term stored, highly modified CT-DNA, this technique allowed the possibility of observing multiple products of degradation (see Section 4.2.1). This would not have been feasible when using acid hydrolysis since DNA is hydrolysed to its most basic element i.e. DNA bases. The transition from nucleotide to nucleoside and/or base would not have been detectable. However when MN and CSPDE were applied to the digestion of DNA,

nucleotides were obtained allowing the observation of various products of degradation by HPLC.

A novel assay was developed in order to be able to quantitate the actual amount of DNA binding to NC filters after ISB and thereby allowing correction of chemiluminescent results. The propidium iodide stain proved to be very useful for correction of differences in DNA binding. It was shown that ISB values could be corrected effectively for amounts of DNA ranging from 0.5 to 2.5 μg/well. Correction using the PI ratio was not effective for very small amounts of DNA (0.25 μg) resulting in an underestimation of M_1-dG levels. Therefore, one would recommend that results obtained for samples with very little DNA binding to the membrane should be discounted. Instead, the amount of DNA blotted onto the ISB filter should be increased accordingly in subsequent experiments in order to obtain valid adduct data for this particular sample. With the intention of finding a confirmation of the PI assay several other dyes such as 33258 Hoechst (2-[2-(4-Hydroxyphenyl)-6-benzimidazole]-6-(1-methyl-4-piperazyl)-benzimidazole trihydrochloride), methylene blue (Sigma) and SYBR Green I (Molecular Probes) were investigated but none of them worked as well as propidium iodide on the nitrocellulose filter (data not shown). The dyes mentioned above produced very high levels of background fluorescence on NC membranes and the signal intensity appeared not to correlate well with the amount of DNA blotted. These dyes were therefore not suitable for correction of DNA binding. The use of nylon membranes instead of NC was briefly considered but abandoned. This would have possibly caused additional problems and made further adjustments of the ISB assay necessary.

Another problem associated with the ISB assay were differences in binding of human and CT-DNA to the NC membrane, these variations were identified by PI assay. To date the fundamental mechanism of absorption of nucleic acids to NC filters remains unclear, it is believed though to be non-covalent [Meinkoth (1984)]. Studies have shown that molecular weight, finite macromolecular conformation, ionic forces and weaker forces of attraction play a role [Gillam (1967), Kothari (1972)]. DNA is retained on nitrocellulose only when dissolved in buffers of high ionic strength [Phillips (1969)]. The latter might be explained as increasing salt concentrations correlate with decreasing electrostatic repulsion between the phosphate groups of the DNA backbone, resulting in more aggregated nucleic acid molecules that are more easily absorbed to the NC membrane. This observation might

explain the findings described earlier that bathing the NC filter in SSC buffer prior to baking increased DNA binding by 80%.

In general, it was noticed that less DNA was binding to the membrane for CT-DNA standards when compared to human samples. In some cases even up to 1.5 to 2.5 times more DNA was binding for human samples. This phenomenon could possibly be explained by differences in fragmentation of samples following sonication and heat denaturing. CT-DNA was shown to yield lower molecular weight fragments (100-600 bp) in comparison to human genomic DNA (> 600 bp). The underlying cause for this phenomenon might be poor quality of or trace amounts of ions in purchased CT-DNA (Sigma).

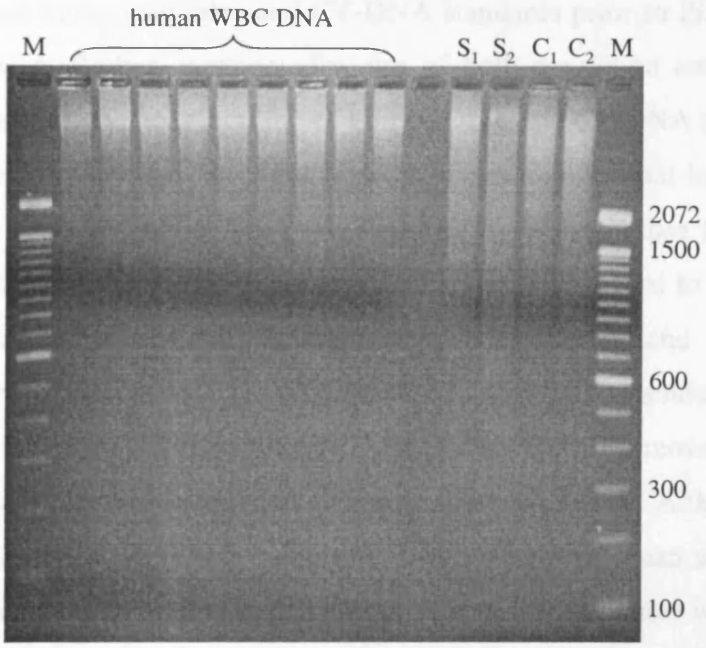

Figure 3.37: *Image of a 2% agarose gel of sonicated and heat-denatured human and cellular samples and CT-DNA standards.* All DNA samples shown above were sonicated for 20 min, heat-denatured for 5 min in a boiling water bath and then kept on ice for at least 10 min. (M) 100 bp DNA ladder (2072, 1500, 1400, ..., 200, 100 bp), (S_1) and (S_2) ISB CT-DNA standards (MDA-treated and untreated respectively), (C_1) and (C_2) cellular DNA (relatively recently extracted). Human WBC DNA samples originated from a long-term study and had been stored for approximately 2 years at different temperatures (-20°C, -80°C and liquid N_2).

However when the conditions of sample preparation were slightly altered, the pattern of fragmentation also changed (Figure 3.37). DNA obtained or extracted from different sources (human, cellular and CT-DNA) appeared to fragment more similarly following 20 min sonication using an ultrasonic bath (was 15 min) and heat-denaturing the samples

for only 5 min (was 10 min). These findings indicated that the fragmentation was mostly dependent on the length of time in the boiling water bath rather than the sonication step. In this instance CT-DNA gave rise to fragments > 600 bp with the majority still being high molecular weight. Nevertheless, the pattern of DNA binding was still immensely different when comparing the PI staining obtained for CT, human and cellular DNA samples with less DNA binding for CT-DNA standards.

Use of restriction endonucleases, specifically Eco RI and Sau 3A, was shown to standardise fragment size of DNA from various different sources. Digestion of samples independent of their origin yielded fragments greater or equal to 1500 bp when using Eco RI and between 100 bp and 2072 bp for Sau 3A. The idea was therefore to use one of these enzymes to digest human samples and CT-DNA standards prior to ISB analysis replacing the sonication step. Rather unexpectedly, use of both restriction endonucleases did not improve, i.e. standardise, DNA binding of human DNA and CT-DNA to the filter.

Comparison of sonicated and Eco RI digested samples showed that levels of M_1-dG were comparable. As expected more DNA was binding to nitrocellulose for Eco RI digested samples. Nevertheless, no improvement was achieved with regard to uniformity of DNA binding, differences were still apparent between human and CT-DNA. Similar observations were made when Sau 3A was used to replace the sonication step, PI ratios still varied between human samples and CT-DNA standards. Moreover, there appeared to be a problem with detection of the chemiluminescent signal. Although a signal was detectable for CT-DNA standards, none was measurable for human samples. The idea to replace the sonication step by one of these restriction endonucleases was abandoned since neither enzyme managed to homogenise DNA binding from different sources to NC membranes. A potential explanation but also an additional problem could be the presence of magnesium (Mg^{2+}) ions in the digestion buffer, which might interfere with DNA binding to NC membranes. Kube and Srivastava [Kube (1997)] reported that binding of viral DNA to nylon membranes was inhibited by Mg^{2+} ions, which are a crucial component of the DNase I digestion carried out prior to slot blot analysis. Furthermore, the authors noted that Mg^{2+} ions interfered with the absorption of plasmid DNA to nylon and nitrocellulose membranes.

Interference of Mg^{2+} might explain at least in part the problems observed for Sau 3A digested human samples. No chemiluminescent signal was detected for all human samples in accordance with very low DNA binding. Although EDTA was added to standards and samples after digestion at an equimolar concentration in order to chelate Mg^{2+} ions, its

concentration was possibly not sufficient to fully restore DNA binding of human samples. On the contrary, a strong adverse effect of Mg^{2+} ions on DNA binding could most likely be ruled out in the case of Eco RI as both chemiluminescent and fluorescent signals were detectable. In most cases, $O.D._{PI}$ was higher for digested samples compared to sonicated DNA.

Ideally, a source of DNA is required, preferably human, with low background levels of M_1-dG, which can then be used as a standard in the ISB assay. It is vital for accurate quantitation of DNA adducts by ISB analysis that a DNA standard with a similar macromolecular structure to that of unknown human, animal or cellular samples should be used. In theory, a standard generated from human DNA should yield fragments similar or even identical to human samples and therefore exhibit similar binding to NC membranes.

Prior to setting up the long-term storage experiments it was necessary to find a method for DNA extraction which made it feasible for one person to extract DNA from up to 36 blood samples in one day. Five different techniques were compared with each other using frozen blood and DNA samples were analysed using the ISB assay. Following the results presented in Section 3.2.4 it was decided to separate the nuclei according to the protocol described for the Qiagen genomic tips (Section 2.2.5.1) but to use the Qiagen QIAamp columns to extract the DNA following lysis at 50°C (Section 2.2.5.3). DNA was obtained ready in solution using this combined approach making DNA precipitation unnecessary. Results compared well with the method routinely used in our laboratory but offered a quicker way of DNA extraction. However, it was discovered when starting the storage experiments (see Chapter 4, Section 4.2.3) that the method although evaluated earlier using frozen blood samples was not suitable for fresh blood samples. DNA yield was very low and it was thus decided to use the standard procedure for Qiagen genomic tips (described in Section 2.2.5.1 and 2.2.5.2). This particular procedure had been used previously successfully to extract DNA from biopsies and blood samples (fresh and frozen). The only disadvantage was that the method was more time consuming and laborious making it difficult for one person to handle multiple samples.

Availability of a very sensitive assay is a prerequisite in order to detect and establish background levels of adducts in human samples. With its detection limit of 5 adducts per 10^8 normal nucleotides [Leuratti (1999)] the ISB assay offers this possibility for the detection of M_1-dG. Requirement of only small amounts of DNA makes it feasible to apply

this assay to a large number of samples and a wide variety of tissues. However, a particular problem of measuring endogenous DNA damage are naturally occurring background levels of the adduct of interest in control DNA. This usually results in levels of adduct being negative i.e. below the limit of detection of the assay.

Niedernhofer et al. [Niedernhofer (1997)] found that M_1-dG reacts with tris(hydroxymethyl)-aminomethane to form a conjugate with Tris, an enaminoimine. An increase in pH of Tris solution by one unit was reported on freezing relative to room temperature. Due to the unusual temperature coefficient it was proposed at that stage that Tris reacted with the ring-opened form of M_1-dG rather then the adduct itself.

Therefore in the case of M_1-dG, one option to address the problem of background levels was to ring-open the adduct to N^2-(3-oxo-1-propenyl)deoxyguanosine by raising the pH (pH > 8). The intention was to then react the aldehyde group with an amine in order to inhibit reoccurring ring formation and to stabilise the product, an oxime conjugate.

Preliminary experiments showed that M_1-dG levels in highly MDA-modified and untreated CT-DNA could be reduced quite dramatically using methoxyamine. It was demonstrated by HPLC that the level of M_1-dG in MDA-treated CT-DNA was reduced to approximately 12% of its original quantity subsequent to incubations at -20°C (o/n) and 37°C (24 h) using 5mM methoxyamine. It was also discovered that raising the pH of the phosphate buffer (10mM K_2HPO_4) from 8.0 to 9.0 did not improve the level of reduction. On the contrary, the reaction was slightly more efficient at pH 8.0. Higher concentrations of methoxyamine (20 and 50mM) were found to have adverse effects on normal nucleotides and were therefore not used in future experiments.

During the early experiments several methoxyamine-treated control CT-DNA samples were blotted on the NC filter. Reduction in M_1-dG levels following methoxyamine treatment was calculated as usual, relating samples to the calibration line and correcting them for PI staining. This was changed in subsequent experiments. Control CT-DNA was first treated using methoxyamine and then used to generate a calibration line. In order to be able to compare both data sets, the intercept (b = 14.744) of the methoxyamine-treated calibration line was converted using the standard calibration line (Figure 3.36; $y_{untreated}$ = 10.398x + 20.708). A level of approximately -0.57 fmol M_1-dG per μg of DNA was obtained for the methoxyamine-treated control CT-DNA. This value correlated quite well with results acquired earlier for control CT-DNA, which had been treated with 5mM methoxyamine and analysed by IDB assay (Table 3.2).

During the course of this work Daniels et al. [Daniels (1999)] published that the conversion of M_1-dG to its acyclic form is catalysed by primary amines and a stable acyclic adduct results from hydroxylamine addition to M_1-dG. It was therefore decided to compare reactions of MDA-treated CT-DNA with methoxyamine and hydroxylamine, alongside with a comparison of different buffer systems. Since increasing the pH from 8.0 to 9.0 did not improve the reduction of M_1-dG levels, it was decided to compare reactions also at a more physiological pH (pH 7.4).

It was discovered that even at physiological pH the reaction of M_1-dG with primary amines took place in highly modified CT-DNA. In general, pH 7.4 appeared favourable for the reaction with methoxyamine especially up to 24 h of incubation at 37°C. Comparison of methoxyamine and hydroxylamine showed that both reactions with M_1-dG in 10mM buffer systems followed a different pattern. Levels of M_1-dG decreased continuously over time for methoxyamine as opposed to an instant drop in adduct levels following hydroxylamine exposure. It also appeared that the reaction with methoxyamine was more consistent over time than the one with hydroxylamine. Especially towards the end of the incubation at 37°C, treatment with methoxyamine appeared slightly more efficient. The final level of M_1-dG was approximately 8% for methoxyamine and ranging from 12% to 20% for samples incubated with hydroxylamine.

In contrast to 10mM buffer systems, M_1-dGp was not detectable by HPLC fluorescence following incubation of MDA-treated CT-DNA with 5mM hydroxylamine in 50mM buffer systems (either K_2HPO_4 or MOPS). The reaction of M_1-dG in CT-DNA with the amine appeared to be instantaneous, complete, irreversible as well as independent of pH. It would thus be interesting with regard to future experiments to explore the effect of hydroxylamine on potential background levels in control CT-DNA using the ISB assay.

It would also be worth investigating the effect of methoxyamine or hydroxylamine on samples of known M_1-dG level (fmol range). It was shown that significant effects can be achieved and observed by HPLC for M_1-dG at high levels of modification (pmol range). Although a reduction in adduct levels was also observed using control CT-DNA, it might be easier and more accurate to detect changes in DNA samples with slightly higher M_1-dG levels using the ISB assay. For example, M_1-dG levels detected in cellular DNA were fairly high ranging around 10 fmol per μg of DNA. Therefore, a possible candidate for such future experiments could be DNA extracted from human cell lines.

Until recently, it was uncertain whether the adduct reacts directly with primary amines or hydrolyses under basic conditions. It is not fully conclusive from findings obtained during this project whether ring-opening is a prerequisite for the reaction of M_1-dG with primary amines or to whether the adduct reacts directly with hydroxylamine and methoxyamine. It appears though that ring-opening was not the limiting factor for the reaction between methoxyamine and M_1-dG in DNA since raising the pH of 10mM K_2HPO_4 did not improve overall reactivity and completion. The pyrimidopurinone was also shown to react fairly rapidly with both amines at neutral pH in intact DNA dissolved in 10mM buffer systems. Buffer systems (10mM K_2HPO_4, 10mM MOPS) used as negative controls did not influence the level of M_1-dG in modified CT-DNA. These findings were independent of pH. Levels of M_1-dG detected by HPLC were comparable in all cases with the one in water. If ring-opening of M_1-dG to N^2-(3-oxo-1-propenyl)deoxyguanosine was to take place it was not observable by HPLC and only occurred at a very low rate. It therefore looks as if alkaline pH is not necessary and that M_1-dG reacts directly with both amines and not its ring-opened form. A schematic diagram of the reaction between M_1-dG and both primary amines is shown in Figure 3.38.

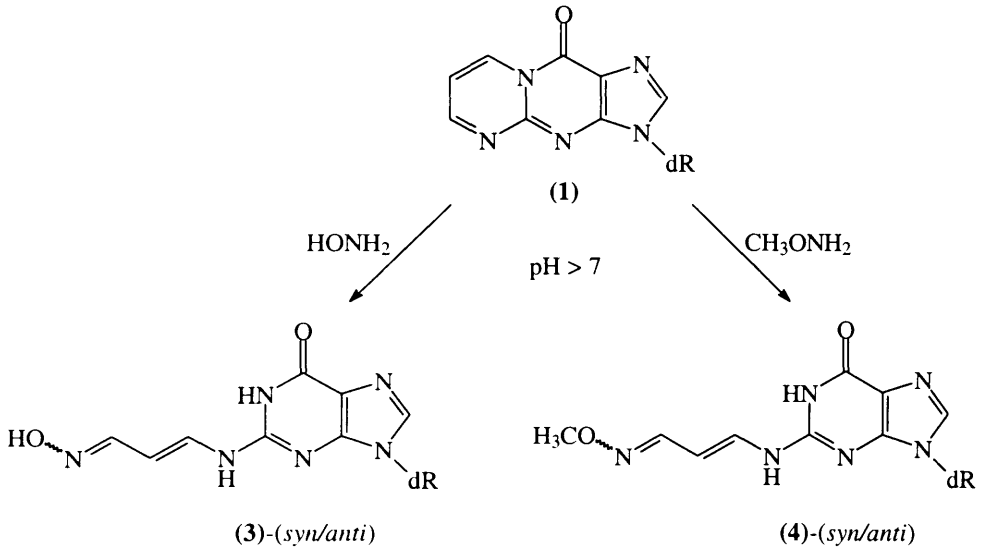

Figure 3.38: *Reaction of M_1-dG with hydroxylamine and methoxyamine.* M_1-dG in highly modified CT-DNA can react at physiological pH with hydroxylamine or methoxyamine forming oxime conjugates. Both *syn* and *anti* oxime isomers are possible in both reactions. Most likely M_1-dG reacts directly at physiological pH in 10mM buffered systems with the amines without forming the ring-opened structure as the reactive intermediate. (1) M_1-dG or pyrimido[1,2-α]purin-10(3H)-one; CH_3ONH_2 methoxyamine; $HONH_2$ hydroxylamine; (3) oxime conjugate; (4) methyloxime conjugate.

This hypothesis is supported by findings published recently by Schnetz-Boutaud et al. [Schnetz-Boutaud (2000)]. The M_1-dG adduct was shown to react at neutral pH with hydroxylamine to form oximes. The rate of reaction of M_1-dG with hydroxylamines at pH 7 was reported to be at least 150 times faster than the rate of hydrolysis of M_1-dG to its ring-opened form. Hydroxylamine addition was not only observed at the level of the nucleoside but also shown to take place in single- or double-stranded DNA (short oligonucleotides). Consequently, it was concluded that M_1-dG was directly reactive to nucleophiles.

Experiments carried out in buffer systems of higher molarity differed considerably from data obtained for treatments in a 10mM buffer. Even when the 50mM buffer systems were used as negative controls, i.e. without primary amine addition, a quite substantial reduction in M_1-dG levels was observed, particularly in phosphate buffered systems. At pH 7.4 only about 40% of its initial level were detectable, at pH 8.0 an even further decrease was observed. Only minor effects on the level of modification were noticed in MOPS at pH 7.4. At pH 8.0 approximately 50% of the original adduct level were still detectable by HPLC fluorescence. These findings suggest that M_1-dG is ring-opened almost instantaneously in 50mM buffer systems and that the degree of N^2-(3-oxo-1-propenyl)deoxyguanosine formation is also dependent on pH and buffer type. More alkaline conditions (pH 8.0 versus 7.4) appear to support and enhance ring-opening of M_1-dG to N^2-(3-oxo-1-propenyl)deoxyguanosine.

These observations might be explained by findings reported by Mao et al. [Mao (1999)]. Mao and co-workers described that M_1-dG hydrolyses rapidly and quantitatively at neutral pH to N^2-(3-oxo-1-propenyl)deoxyguanosine in duplex DNA when placed opposite to cytosine. Ring-opening was reported to be reversible on thermal denaturation and not to occur at neutral pH in single-stranded oligonucleotides or when M_1-dG was placed opposite thymine residues in a duplex (see also Figure 1.17). It was also discovered that the presence of a complementary cytosine was not necessary to stabilise the ring-opened form in duplex DNA at neutral pH. When N^2-(3-oxo-1-propenyl)deoxyguanosine was placed opposite to thymine in a duplex M_1-dG was not re-formed. They proposed that N^4 of the opposing cytosine residue was added to C8 of M_1-dG, forming a transient enaminoimine species that in return hydrolysed to N^2-(3-oxo-1-propenyl)deoxyguanosine (Figure 3.39). The isolation of a stable oxime from the reaction of M_1-dG with hydroxylamines at neutral pH supports the theory that an amine on the strand opposite to

the adduct in duplex DNA could add to C8 of the pyrimidopurinone [Schnetz-Boutaud (2000)].

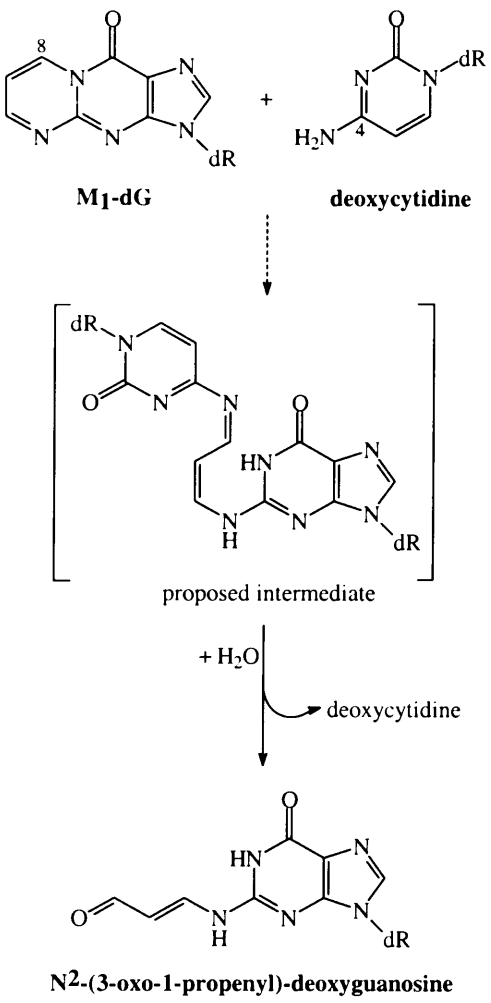

Figure 3.39: *Conversion of M_1-dG to its ring-opened form in duplex DNA.* The exocyclic amino group of the complementary cytosine (N^4) attacks the C8 position of the M_1-dG exocyclic ring and facilitates ring-opening via formation of a transient Schiff base. Addition of water to the Schiff base regenerates the catalytic cytosine and generates N^2-(3-oxo-1-propenyl)dG. M_1-dG is observed in single-stranded DNA at pH 6.8 whereas its ring-opened form is observed in duplex DNA when cytosine is the complementary base [Mao (1999)].

These findings suggest that M_1-dG itself as well as its ring-opened form are highly reactive electrophiles in DNA at neutral pH. This fact might have implications on the independent presence of the adduct and its ring-opened form in the human body. It could potentially result in significant consequences for mutagenesis and DNA repair or reaction with cellular protein nucleophiles leading to novel products and cross-links.

4 Stability of M_1-dG upon Storage

4.1 Introduction

In order to apply analytical methods, such as the immunoslot blot assay for the detection of M_1-dG, to large scale epidemiological prospective studies one has to be certain that adduct levels detected reflect true values in the samples examined. This is partly dependent on accurate method validation, including elimination of all possible sources of error, but also on sample collection, preparation and storage prior to analysis. It is also crucial to collect information linked to human samples in order to interpret the markers optimally. Date and time of collection, recent diet and dietary supplementation such as vitamins, smoking (recent or not), medication, medical history and illness etc. can be essential to the interpretation of biomarkers.

To date, most studies report freezing of tissue or blood samples shortly after collection followed by storage at -20°C or -80°C until further processing. However, the duration of storage is often not reported. Hypothetically, storage of tissue samples at -80°C should not affect DNA adduct levels, although ideally the DNA should be extracted as soon as possible after collection and under conditions which will not introduce artefactual DNA damage. As immediate DNA extraction may not always be feasible, an extensive knowledge of the stability of DNA adducts upon storage in general is crucial for future interpretation of such data.

Nevertheless, the influence of tissue storage on stability of DNA adducts has hardly been investigated and only few examples can be found in the literature. Binková et al. [Binková (1996)] examined whether tissue storage at -20°C and -80°C affects DNA adduct patterns and levels of benzo[α]pyrene-modified DNA in rats. It was reported that storage up to 10 months at either temperature did not significantly affect benzo[α]pyrene-derived DNA adducts levels and patterns analysed by ^{32}P-postlabelling. These findings indicate that biological samples can be used even after several months of storage for the analysis of benzo[α]pyrene adducts by ^{32}P-postlabelling.

Ma et al. [Ma (1995)] reported that application of two methods of sample preparation resulted in significantly different levels of platinum-DNA adducts. Total and unbound platinum and DNA adduct levels were analysed by atomic spectroscopy. Adduct levels in white blood cells (WBCs), which were collected after thawing frozen whole blood samples were higher than in freshly isolated WBCs. Simulation of the two methods *in vitro*

confirmed above findings. Especially after 0 h and 1 h of incubation levels differed by 494% and 110% respectively. After 4 h the variation was reduced to 19%, whereas after 24 h the difference was only 6% and no longer significant. Differences observed can be explained by the presence of unbound cisplatin in the blood sample tube, which can form DNA adducts *ex vivo*. However, the duration of storage did not have any effect on platinum adducts. DNA adduct levels in samples which were stored at -80°C for 20 min were not significantly different from the samples which were stored for 2 weeks at -80°C.

Different DNA adducts will have different stability over time depending on their chemical structure. Niedernhofer et al. [Niedernhofer (1997)] for example showed that the major malondialdehyde adduct M_1-dG is stable upon storage at 37°C in Tris solution (pH 7-8). However, freezing these solutions generates unstable species and results in the formation of a conjugate. Upon warming to room temperature the conjugation between Tris and M_1-dG is reversible. If organic solvents such as DMSO are present or added after freezing and thawing, the Tris-M_1-dG conjugate remains stable after 24 hours at room temperature. Investigations by Reddy and Marnett [Reddy (1995)] have also shown previously that M_1-dG is unstable at alkaline pH which causes ring opening. These are further considerations to be taken into account when working on malondialdehyde DNA adducts.

Another, often overlooked aspect is the stability of standards used for a specific assay. In order to obtain accurate, comparable and reproducible results, knowledge of the stability of standards used in a particular assay is significant. Checking standard stability should be part of routine quality control in order to avoid the phenomenon of laboratory drift. Validation of standards and methods is also essential to the comparison of results obtained at different times, by different people and/or in different laboratories. Recently, the stability of a methylated standard generated by treatment using N-methyl-N-nitrosourea has been investigated by Osborne and Phillips [Osborne (2000)]. It was reported that levels of O^6-methylguanine remained unchanged after storage for 5 years at -20°C. The methylated DNA also contained 7-methylguanine and 3-methyladenine, which were slowly cleaved from DNA on standing. The half-life for loss of 7-methylguanine at neutral pH was estimated to about 460 h at 22°C and 4 years at -20°C.

A detailed knowledge of the effect of long-term storage of samples on the stability of biomarkers of DNA damage is in view of prospective studies particularly important. Changes in adduct levels could occur due to instability of the adduct which will lead inevitably to a decrease in its level upon long-term storage. In the case of M_1-dG, adduct levels could increase due to artefactual adduct formation during sample storage, i.e. via

lipid peroxidation [Marnett (1999)] or direct oxidation of DNA bases [Dedon (1998)]. The third possible effect would be that no changes in M_1-dG levels occur upon storage.

Therefore, the following experiments were planned to investigate the stability of M_1-dG in standards and human samples upon storage.

- Stability of highly modified MDA-treated CT-DNA which is normally used as reference for sample quantitation in the ISB assay and as quality control. Standards were stored at RT, 4°C, -20°C and -80°C and stability assessed by HPLC following enzymatic digestion at regular intervals.
- As it is advisable to extract DNA from human samples immediately after collection, stability of the M_1-dG adduct was investigated in stored human DNA extracted from leukocytes and stored at -20°C, -80°C and liquid nitrogen. Stability assessment was performed using the ISB assay.
- Sometimes it is not feasible to extract DNA from human blood and tissues immediately after specimen collection. It is therefore extremely important to evaluate whether tissue storage affects DNA yield and adduct measurements. It was therefore intended to evaluate stability of M_1-dG in stored buffy coat (as it is put into practice in the EPIC study) and whole blood under the influence of antioxidants.
- Endogenous DNA damage, other than M_1-dG, caused by long-term storage was studied in CT-DNA standards and human DNA samples after approximately 2 years of storage by gel electrophoresis for the detection of single-strand breaks and SVPD-^{32}P-postlabelling assay for the detection of minor modifications including oxidative damage to DNA.

4.2 Results

4.2.1 Stability of M_1-dG in Highly Modified CT-DNA

In the immunoslot blot assay MDA-modified CT-DNA is usually diluted with unmodified DNA to obtain decreasing amounts of M_1-dG adduct (0-10 fmol) and used for generating standard curves.

In order to investigate the stability of highly modified DNA used in the ISB assay, calf thymus DNA (1 mg/ml) was treated with MDA (at a final concentration of 2mM) as described in Section 2.2.1. DNA pellets were taken up after treatment in HPLC grade water (pH 5.5) or KP buffer (10mM K_2HPO_4, pH 7.0). Final concentration of stored DNA

was approximately 0.5 μg/μl. The degree of modification following MDA treatment was established as approximately 18 pmol M_1-dG/μg. pH of the DNA solution in water was determined to pH 4.5, the one in KP buffer was pH 6.0. DNA solutions derived from the same treatment were stored at RT, 4°C, -20°C and -80°C for stability assessment of the standard. At interval time-points, a volume equivalent to 4 μg of DNA was taken out and digested to nucleotides using MN and CSPDE (digestion carried out in triplicate; Section 2.2.6.2). After digestion to dNp samples were taken up in 40 μl of H_2O, 10 μl were injected in triplicate onto the HPLC system described in Section 2.2.6.3, and final results for dAp and M_1-dGp areas were expressed as percentage compared to the starting values. A typical HPLC fluorescence trace obtained for M_1-dGp at the beginning of the study is shown in Figure 4.1.

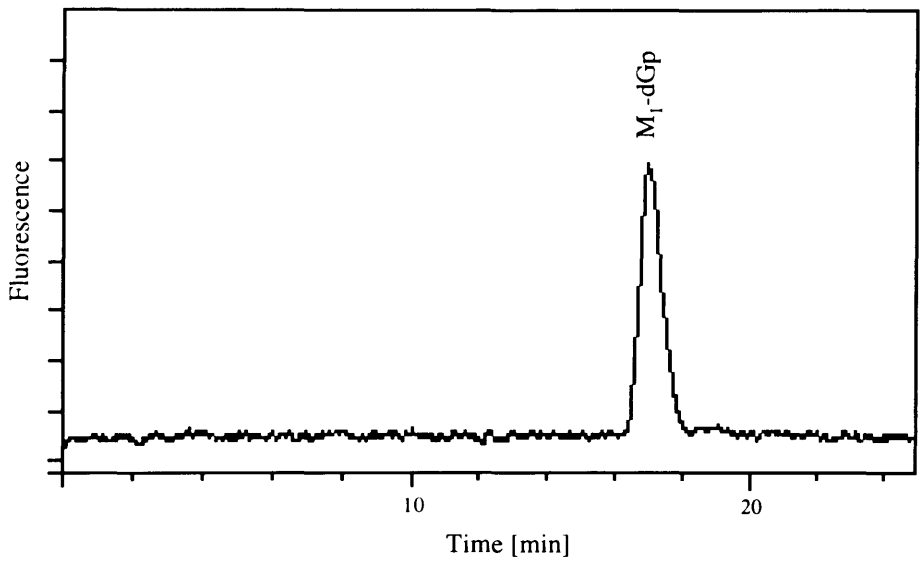

Figure 4.1: *Typical HPLC fluorescence separation of MDA-treated CT-DNA samples.* This figure shows a typical HPLC fluorescence separation of DNA samples prior to long-term storage for the determination of M_1-dGp after digestion with MN and CSPDE.

4.2.1.1 Long-Term Stability of MDA-Treated CT-DNA in Phosphate Buffer

Figure 4.2 illustrates the decomposition of MDA-modified DNA, which was dissolved after treatment in KP buffer and kept at RT. It can be clearly seen that DNA and adduct were stable at RT for about 3 weeks. Both the adduct M_1-dGp and normal nucleotides, in this case dAp, started to decompose after approximately 23 days of storage at RT and appeared to degrade at a similar rate for the entire duration of the study. The overall pattern

of degradation could be classified as of a first-order reaction i.e. exponential decrease with time. After approximately 49 days of storing the DNA at RT, 50% of the adducted DNA had decomposed.

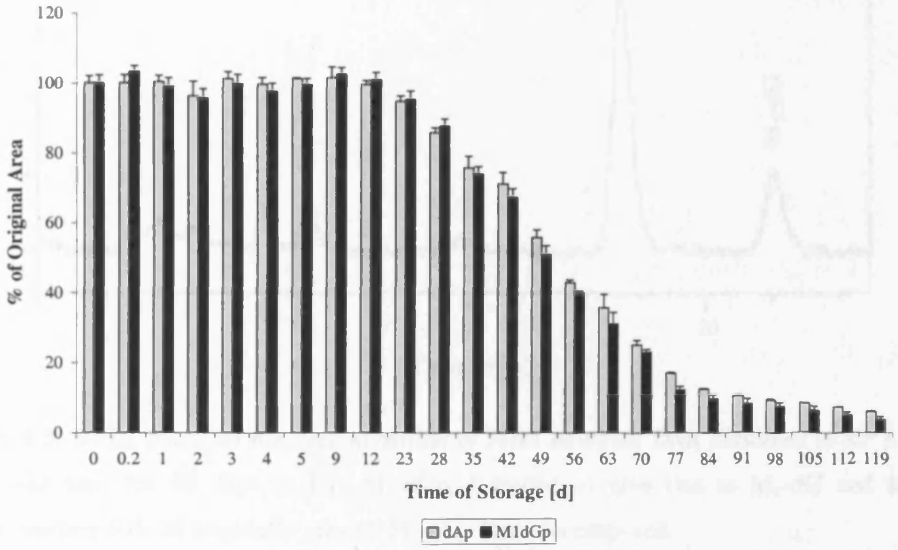

Figure 4.2: *Decomposition of highly modified CT-DNA, which was dissolved in KP buffer following MDA treatment and stored at RT.* Values shown are mean of percentage ± standard deviation.

Initially, M_1-dGp degraded to give rise to only M_1-dG. However, after approximately 40 days of storage multiple peaks were detectable by HPLC fluorescence (Figure 4.3), two of which were identified as M_1-G and M_1-dG by co-elution with standards. Normal nucleotides appeared to decompose to nucleosides, consequently multiple peaks were also detectable by UV. One peak was confirmed as 2'-dA. The study was stopped after 119 days, as accurate detection of M_1-dGp was no longer possible. Only 3.8% of its original value were measurable. Overall, MDA-modified DNA was found to be unexpectedly stable at RT.

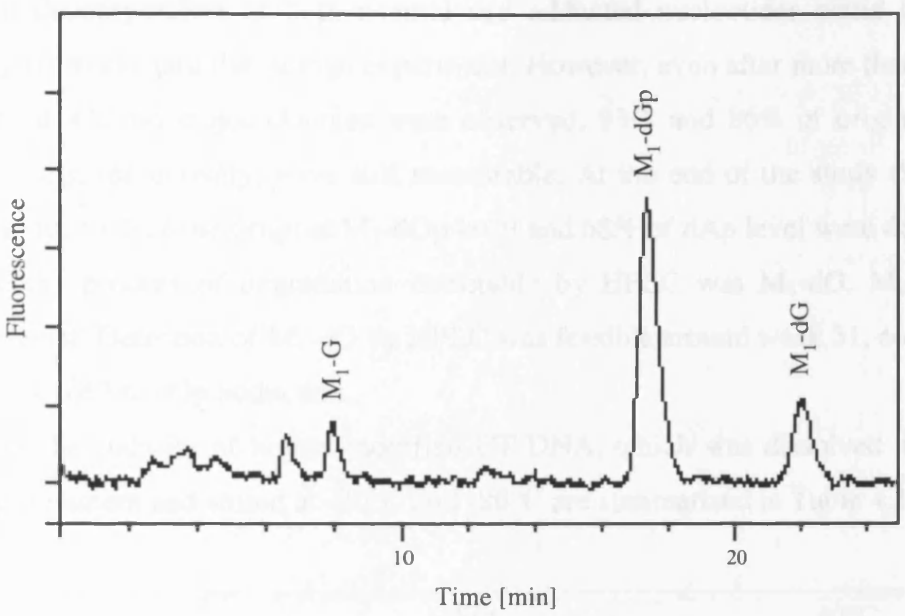

Figure 4.3: *HPLC trace for the decomposition of MDA-modified DNA dissolved in KP buffer.* DNA was kept for 49 days at RT, M_1-dGp degraded to give rise to M_1-dG and M_1-G. Approximately 50% of originally present M_1-dGp have decomposed.

Figure 4.4 shows the stability of MDA-treated CT-DNA in KP buffer, which was kept at 4°C following treatment.

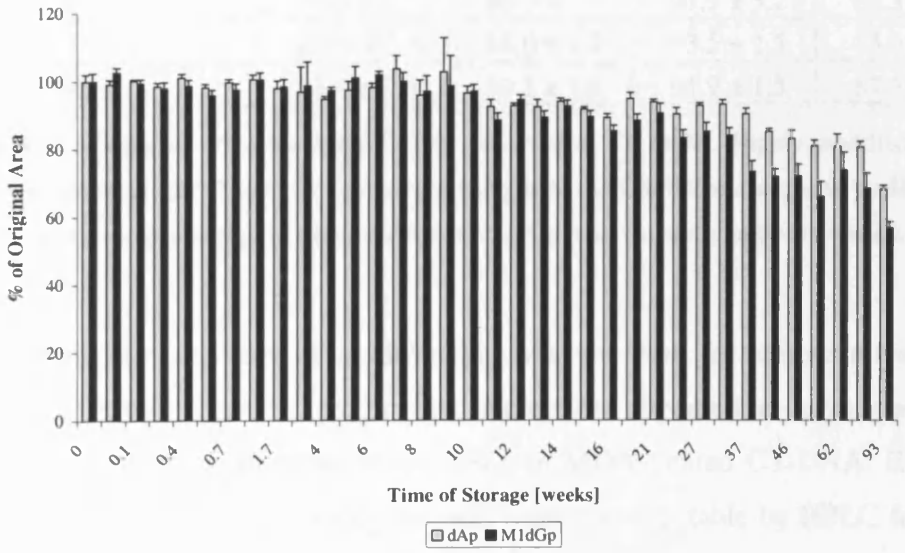

Figure 4.4: *Decomposition of highly modified CT-DNA, which was dissolved in KP buffer following MDA treatment and stored at 4°C.* Samples were analysed after 0, 0.03, 0.1, 0.3, 0.4, 0.6, 0.7, 1.3, 1.7, 3.3, 4, 5, 6, 7, 8, 9, 10, 11, 12, 13, 14, 15, 16, 19, 21, 24, 27, 31, 37, 42, 46, 52, 62, 74 and 93 weeks of storage. Values shown are mean of percentage ± standard deviation.

A gradual decomposition of both normal and adducted nucleotides could be observed beginning 10 weeks into the storage experiment. However, even after more than half a year of storage at 4°C no major changes were observed, 93% and 86% of original dAp and M_1-dGp levels, respectively, were still measurable. At the end of the study (93 weeks of storage) about 57% of the original M_1-dGp level and 68% of dAp level were detectable. At this stage the product of degradation detectable by HPLC was M_1-dG, M_1-G was not measurable yet. Detection of M_1-dG by HPLC was feasible around week 31, corresponding to a 15% loss of M_1-dGp adduction.

Results for the stability of highly modified CT-DNA, which was dissolved in KP buffer following treatment and stored at -20°C and -80°C are summarised in Table 4.1.

	-20°C		-80°C	
Time of Storage [weeks]	dAp [%]	M_1-dGp [%]	dAp [%]	M_1-dGp [%]
0	100.0 ± 2.1	100.0 ± 2.4	100.0 ± 2.1	100.0 ± 2.4
2	101.3 ± 3.8	103.4 ± 3.9	99.9 ± 1.9	101.4 ± 1.9
4	96.7 ± 2.1	101.1 ± 2.5	96.4 ± 5.4	100.5 ± 5.8
10	96.9 ± 1.9	99.9 ± 2.5	98.3 ± 3.5	102.1 ± 3.6
19	103.4 ± 2.0	100.2 ± 2.7	96.2 ± 2.9	92.7 ± 2.6
27	96.4 ± 3.5	90.7 ± 3.5	95.3 ± 2.8	88.8 ± 3.3
38	103.7 ± 3.0	86.3 ± 2.2	99.5 ± 2.1	83.3 ± 2.9
52	92.7 ± 1.7	81.6 ± 6.9	92.5 ± 1.5	80.5 ± 5.3
64	94.6 ± 2.7	86.0 ± 3.7	97.9 ± 3.2	88.5 ± 3.7
75	100.2 ± 1.6	88.6 ± 2.2	93.5 ± 2.5	83.6 ± 3.6
93	93.8 ± 1.6	89.1 ± 1.9	91.9 ± 1.5	87.6 ± 2.6

Table 4.1: *Storage of MDA-treated CT-DNA dissolved in KP buffer.* Highly modified CT-DNA was stored at -20°C and -80°C, digested using MN and CSPDE and analysed by HPLC. Results shown are percentage of original dAp or M_1-dGp area, mean ± standard deviation.

Only an approximate 10% loss of modification was observed for temperatures of -20°C and -80°C after 93 weeks of storage. Normal nucleotides appeared to degrade at a similar or slightly lower rate than adducted nucleotides in MDA-treated CT-DNA. Even at the final stage of the study products of degradation were not detectable by HPLC for samples kept at -20°C and -80°C.

4.2.1.2 Long-Term Stability of MDA-Treated CT-DNA in Water

Similar to experiments presented in the previous section, MDA-treated CT-DNA was also stored in water at RT, 4°C, -20°C and -80°C. Again, stability of modified and unmodified nucleotides was assessed by HPLC.

Figure 4.5 illustrates the decomposition of MDA-modified DNA, which was dissolved in water and kept at RT. Degradation of M_1-dGp started after 23 days similar to the experiment described earlier for CT-DNA stored in phosphate buffer (see Figure 4.2). However, decomposition was much slower and linear, normal nucleotides were not affected by it for the majority of the study. Interestingly the decay gave rise to one single product, namely M_1-G. Approximately 50% of its original M_1-dGp level were degraded after 18 weeks of storage at RT. At the end of this study, i.e. after 93 weeks, 12% of the original M_1-dGp level and 70% of normal nucleotides were still detectable by HPLC.

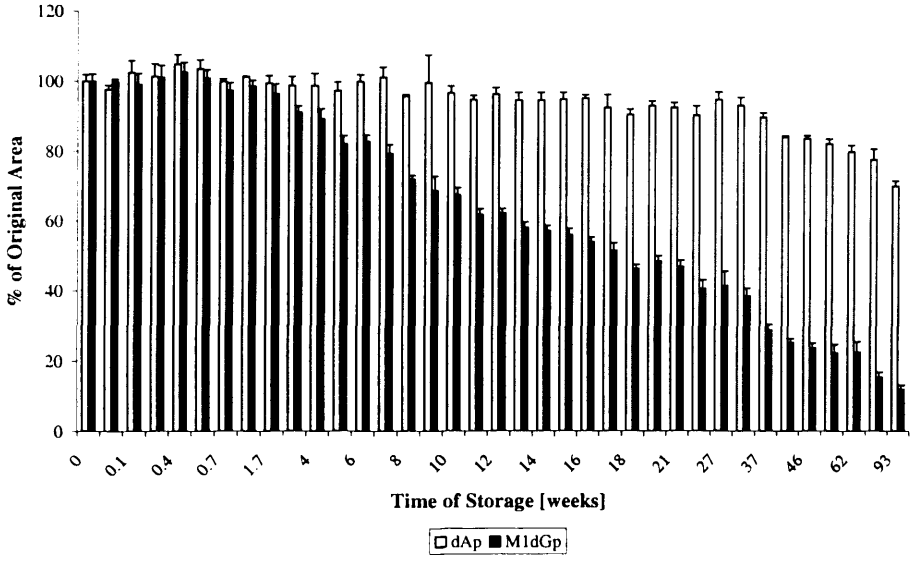

Figure 4.5: *Decomposition of highly modified CT-DNA, which was dissolved in water following MDA treatment and stored at RT.* Samples were analysed after 0, 0.03, 0.1, 0.3, 0.4, 0.6, 0.7, 1.3, 1.7, 3.3, 4, 5, 6, 7, 8, 9, 10, 11, 12, 13, 14, 15, 16, 19, 21, 24, 27, 31, 37, 42, 46, 52, 62, 74 and 93 weeks of storage. Results shown are percentage of original dAp or M_1-dGp area, mean ± standard deviation.

Figure 4.6 shows a typical HPLC fluorescence trace for the decomposition of MDA-modified CT-DNA, which was dissolved in water. In this case, approximately 50% of M_1-dGp were degraded to M_1-G after 18 weeks of storage at RT.

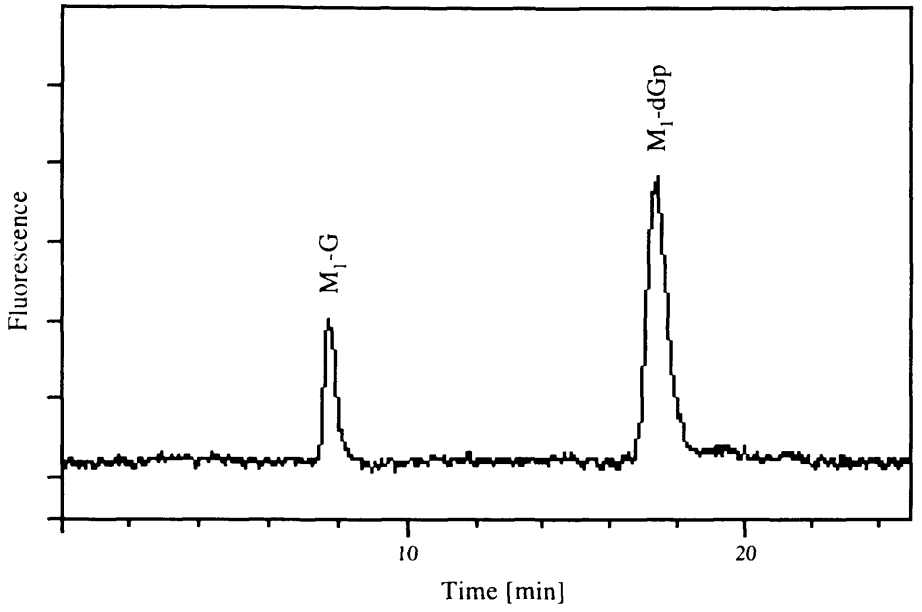

Figure 4.6: *HPLC trace for the decomposition of MDA-treated CT-DNA in water.* DNA was kept for 18 weeks at RT, M_1-dGp degraded to give rise to one single product namely M_1-G. Approximately 50% of the original compound have decomposed.

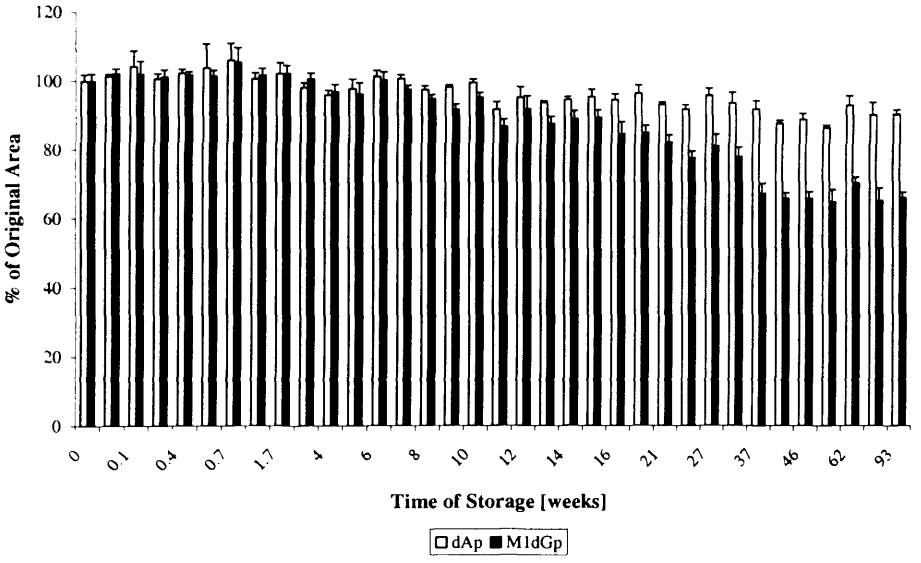

Figure 4.7: *Decomposition of highly modified CT-DNA, which was dissolved in water following MDA treatment and stored at 4°C.* Samples were analysed after 0, 0.03, 0.1, 0.3, 0.4, 0.6, 0.7, 1.3, 1.7, 3.3, 4, 5, 6, 7, 8, 9, 10, 11, 12, 13, 14, 15, 16, 19, 21, 24, 27, 31, 37, 42, 46, 52, 62, 74 and 93 weeks of storage. Results shown are percentage of original dAp or M_1-dGp area, mean ± standard deviation.

Figure 4.7 shows the stability of MDA-treated DNA in water kept at 4°C. Half a year into the study, about 20% of M_1-dGp were degraded. At the end of the storage experiment about 35% of adducted DNA had decomposed, whereas 90% of normal nucleotides remained unaffected.

Results for the stability of highly modified CT-DNA, which was dissolved in water following treatment and stored in freezers are summarised in Table 4.2. Following 93 weeks of storage approximately 20% and 15% loss of modification were observable in DNA samples kept at -20°C and -80°C, respectively.

	-20°C		-80°C	
Time of Storage [weeks]	dAp [%]	M_1-dGp [%]	dAp [%]	M_1-dGp [%]
0	100.0 ± 1.9	100.0 ± 2.1	100.0 ± 1.9	100.0 ± 2.1
2	103.4 ± 2.5	103.6 ± 2.8	100.4 ± 1.8	101.7 ± 1.7
4	101.6 ± 1.6	105.0 ± 2.2	95.4 ± 2.1	99.1 ± 2.1
10	98.4 ± 3.3	100.5 ± 4.3	98.6 ± 1.3	101.1 ± 1.2
19	99.4 ± 2.3	94.8 ± 1.9	98.0 ± 1.5	94.6 ± 1.5
27	101.7 ± 2.3	93.1 ± 3.6	99.2 ± 1.6	92.6 ± 2.7
38	101.9 ± 3.6	82.1 ± 2.4	99.2 ± 1.4	83.7 ± 1.8
52	86.5 ± 0.8	75.1 ± 5.1	93.7 ± 1.0	79.2 ± 2.2
64	85.9 ± 1.9	75.3 ± 4.1	97.6 ± 1.3	85.9 ± 2.1
75	93.1 ± 0.7	77.6 ± 2.0	95.0 ± 3.9	81.0 ± 4.1
93	83.6 ± 0.9	78.0 ± 1.5	93.2 ± 1.2	86.7 ± 1.5

Table 4.2: *Storage of MDA-treated CT-DNA dissolved in HPLC grade water.* Highly modified CT-DNA was stored at -20°C and -80°C, digested using MN and CSPDE and analysed by HPLC. Results shown are percentage of original dAp or M_1-dGp area, mean ± standard deviation.

Normal nucleotides appeared to degrade at a lower rate than adducted nucleotides in MDA-treated CT-DNA. Even at the final stage of the study products of degradation were not detectable by HPLC for samples stored at -20°C and -80°C.

4.2.2 DNA Damage Caused by Long-Term Storage in Highly Modified CT-DNA

In order to study the effect of long-term storage on DNA in more detail, MDA-treated CT-DNA was analysed by alkaline gel electrophoresis (described in Section 2.2.11.1) after approximately 27 months of storage. Alkaline agarose gels are most commonly used for

single-strand DNA electrophoresis. Many other lesions, such as abasic sites, are also labile under alkaline conditions. Therefore, the presence of these lesions contributes to the total number of single-strand breaks being detectable using this approach. An image of the alkaline gel is shown in Figure 4.8. It can be clearly seen that highly modified CT-DNA was extremely fragmented following long-term storage when compared to freshly prepared control DNA. The degree of fragmentation was dependent on both storage temperature and medium. The higher the temperature the more extensive the extent of DNA breakage was. Furthermore, samples dissolved in KP buffer exhibited an increased fragmentation rate following storage at RT and 4°C when compared to DNA stored in water.

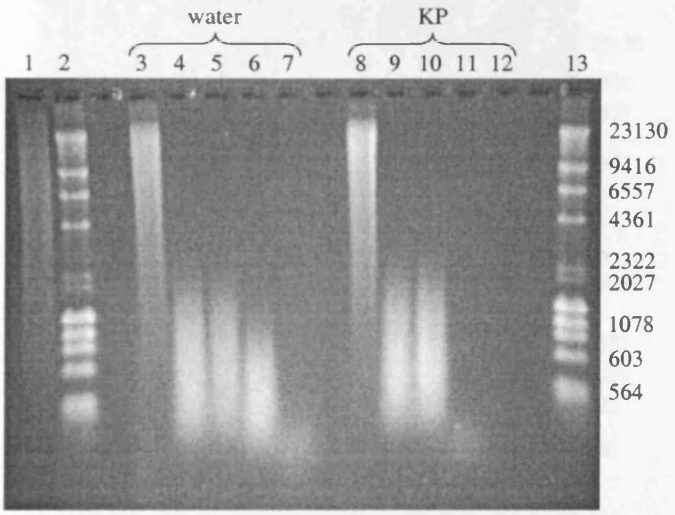

Figure 4.8: *Alkaline gel for MDA-treated CT-DNA stored at RT, 4°C, -20°C and -80°C for the duration of 27 months.* Lane (1) control (I) i.e. 5mM MDA-treated CT-DNA (1 h at 37°C; storage at -20°C for ca. 2 months), lanes (2) and (13) marker mix (λ DNA/*Hind* III and ΦX174 RF DNA/*Hae* III fragments), CT-DNA loaded in lane (3) to (7) and (8) to (12) was dissolved in water and KP buffer respectively prior to storage. Lane (3) freshly prepared untreated control CT-DNA, lane (4) -80°C, lane (5) -20°C, lane (6) 4°C, lane (7) RT, lane (8) freshly prepared untreated control CT-DNA, lane (9) -80°C, lane (10) -20°C, lane (11) 4°C, lane (12) RT (the original sample which had been stored in KP buffer at RT had long degraded thus a replacement sample was used instead; this substitute had been stored at 4°C for 18 months followed by 9 months of storage at RT). Temperatures given above indicate that MDA-treated CT-DNA had been stored at this particular temperature for the duration of approximately 2 years.

Long-term stored CT-DNA samples were analysed simultaneously by glyoxal agarose gel electrophoresis as described in Section 2.2.11.2. Glyoxal gel electrophoresis of single-

stranded DNA at neutral pH fractionates DNA according to size as in an alkali-agarose gel but while retaining alkali-labile sites intact. Comparison of results obtained for both gel types thus allows an estimation of the relative contribution of single-strand breaks and alkali-labile sites to the total number of breaks. In general, the pattern of fragmentation observed by glyoxal gel electrophoresis (Figure 4.9) was similar to the one described earlier for alkaline gels.

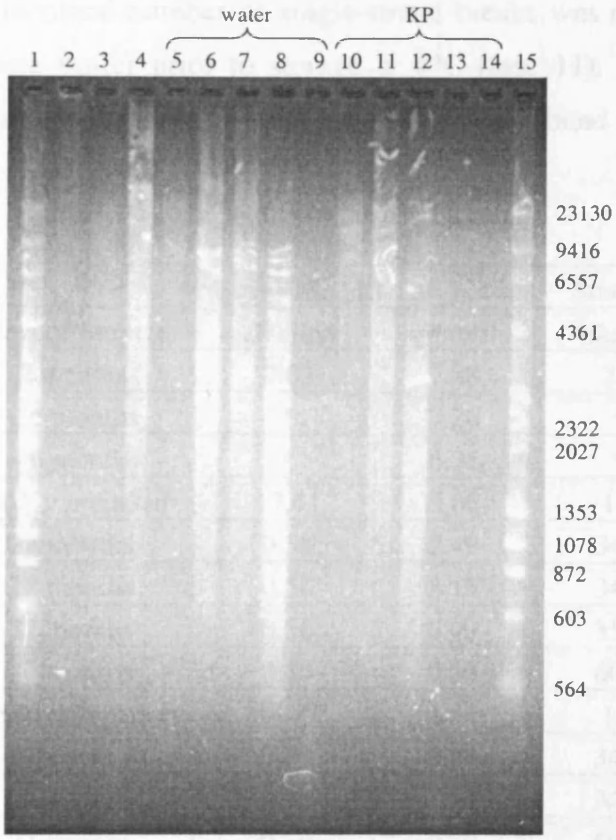

Figure 4.9: *Glyoxal gel for MDA-treated CT-DNA stored at RT, 4°C, -20°C and -80°C for the duration of 27 months.* Lanes (1) and (15) marker mix (λ DNA/*Hind* III and ΦX174 RF DNA/*Hae* III fragments), lane (2) control (I) 5mM MDA-treated CT-DNA (1 h at 37°C; storage at -20°C for ca. 2 months), lanes (3) control (II) 2mM MDA-treated CT-DNA (4 d at 37°C;10 fmol M_1-dG/μg), lane (4) control (III) 2mM MDA-treated CT-DNA (4 d at 37°C; 13.5 pmol M_1-dG/μg), CT-DNA loaded in lane (5) to (9) and (10) to (14) was dissolved in water and KP buffer respectively prior to storage. Lane (5) freshly prepared untreated control CT-DNA, lane (6) -80°C, lane (7) -20°C, lane (8) 4°C, lane (9) RT, lane (10) freshly prepared untreated control CT-DNA, lane (11) -80°C, lane (12) -20°C, lane (13) 4°C, lane (14) RT (comment made earlier in legend of Figure 4.8 for this particular sample applies again). Temperatures given above indicate that MDA-treated CT-DNA had been stored at this particular temperature for the duration of approximately 2 years.

Analysis of DNA fragment mobility distribution on agarose gels is a useful method for determining the frequency of strand breaks. The number of single-strand breaks per 10^4 bp was calculated for both gels according to the approach described in Section 2.2.11.1 and results are summarised in Table 4.3 alongside the average molecular weight M_w. The number of strand breaks obtained by alkaline gel electrophoresis was similar for most long-term stored samples (ca. 35 per 10^4 bp). One exception was CT-DNA dissolved in water, which displayed approximately 67 strand breaks per 10^4 bp after long-term storage at RT (lane 7). An identical number of single-strand breaks was observed for CT-DNA dissolved in phosphate buffer prior to storage at 4°C (lane 11). Short-term stored and freshly prepared controls (lanes 1, 3 and 8 respectively) exhibited as expected very little strand breaks (1-3 per 10^4 bp).

		M_w [10^4 bp]		Strand Breaks per 10^4 bp	
Sample Type	Time of Storage	alkaline	glyoxal	alkaline	glyoxal
control I	2 months	7.63	7.08	2.6	2.8
control II	~ 6 months	*	7.26	*	2.8
control III	~ 6 months	*	6.36	*	3.1
control/water	freshly prepared	17.41	5.66	1.1	3.5
-80°C/water	27 months	0.58	2.49	34.5	8.0
-20°C/water	27 months	0.58	2.15	34.5	9.3
4°C/water	27 months	0.56	0.90	35.7	22.2
RT/water	27 months	0.30	0.30	66.7	66.7
control/KP	freshly prepared	18.22	5.44	1.1	3.7
-80°C/KP	27 months	0.58	2.87	34.5	7.0
-20°C/KP	27 months	0.58	1.72	34.5	11.6
4°C/KP	27 months	0.30	0.30	66.7	66.7
RT/KP	27 months	n.d.	n.d.	n.d.	n.d.

Table 4.3: *Average molecular weight M_w and number of strand breaks per 10^4 bp of stored CT-DNA analysed by alkaline and glyoxal gel electrophoresis.* The number of strand breaks per 10^4 bp was calculated as described earlier in Section 2.2.11.1, with M_w being the average molecular weight. (X/Y) with X being the storage temperature and Y the medium utilised to dissolve CT-DNA in prior to storage. (*) samples were not analysed by alkaline gel electrophoresis; (n.d.) replacement sample not detectable; control (I) 5mM MDA-treated (1 h at 37°C) CT-DNA; control (II) 2mM MDA-treated (4 d at 37°C) CT-DNA, 10 fmol M_1-dG/μg; control (III) 2mM MDA-treated (4 d at 37°C) CT-DNA, 13.5 pmol M_1-dG/μg. Control/water and control/KP were untreated, freshly prepared DNA solutions.

A general increase in single-strand breaks was observed with increasing storage temperature when analysing the glyoxal agarose gel. Again a fairly low number of single-strand breaks was observed for freshly prepared CT-DNA controls (3-4 per 10^4 bp) and samples stored at -20°C and -80°C (7-12 per 10^4 bp). Highest number of strand breaks, 67 per 10^4 bp, was observed for samples dissolved in water stored at RT and those dissolved in phosphate buffer followed by long-term storage at 4°C. A third of that extent was observed for samples dissolved in water, which had also been stored at 4°C.

Instead of the original but too heavily degraded and thus discarded CT-DNA sample, which had been stored in KP buffer at RT, a replacement was used in above analyses. This substitute had been stored at 4°C for 18 months followed by 9 months of storage at RT. However, it was not feasible to determine the number of single-strand breaks in samples loaded in lanes 12 and 14 of the alkaline and glyoxal gel, respectively. These findings might not be surprising since the original sample was profoundly degraded after 119 days of storage i.e. approximately 4 months at RT (see Figure 4.2).

In order to obtain an estimate of the contribution of alkali-labile sites to the total number of strand breaks, one can subtract the number of breaks obtained by glyoxal gel electrophoresis from those by alkaline gel electrophoresis as the latter represents both single-strand breaks as well as alkali-labile lesions. Looking at relative proportions of alkali-labile sites as opposed to single-strand breaks, in general, more alkali-labile sites were detected in DNA stored long-term in freezers. About 3-fold more alkali-labile lesions than single-strand breaks were detected for samples dissolved in water and stored at -20°C and -80°C. About a third of the total number of strand breaks was caused by alkali-labile sites when looking at MDA-treated CT-DNA stored at 4°C which had been dissolved in water prior to long-term storage.

The contribution of alkali-labile lesions was approximately 2- and 4-fold higher in samples dissolved in phosphate buffer and stored at -20°C and -80°C, respectively. However, the analysis of samples by alkaline and glyoxal gel electrophoresis is a somewhat crude estimate. This makes the determination and comparison of absolute values shown in Table 4.3 very difficult if sometimes not feasible to obtain. This was the case for highly fragmented MDA-treated CT DNA samples such as RT/water and 4°C/KP. Relatively little intact DNA was left making the determination of M_w (and thereby the calculation of the number of single-strand breaks) fairly difficult and inaccurate. It appeared that in these cases some kind of threshold and upper limit of detection had been reached and that further distinction was not possible.

Samples were also analysed by SVPD-^{32}P-postlabelling assay enabling the detection of certain lesions such as abasic sites and oxidative thymine glycols and phosphoglycolates. The autoradiogram of the polyacrylamide gel obtained for long-term stored, highly modified CT-DNA is shown in Figure 4.10, corresponding results are presented in Figure 4.11.

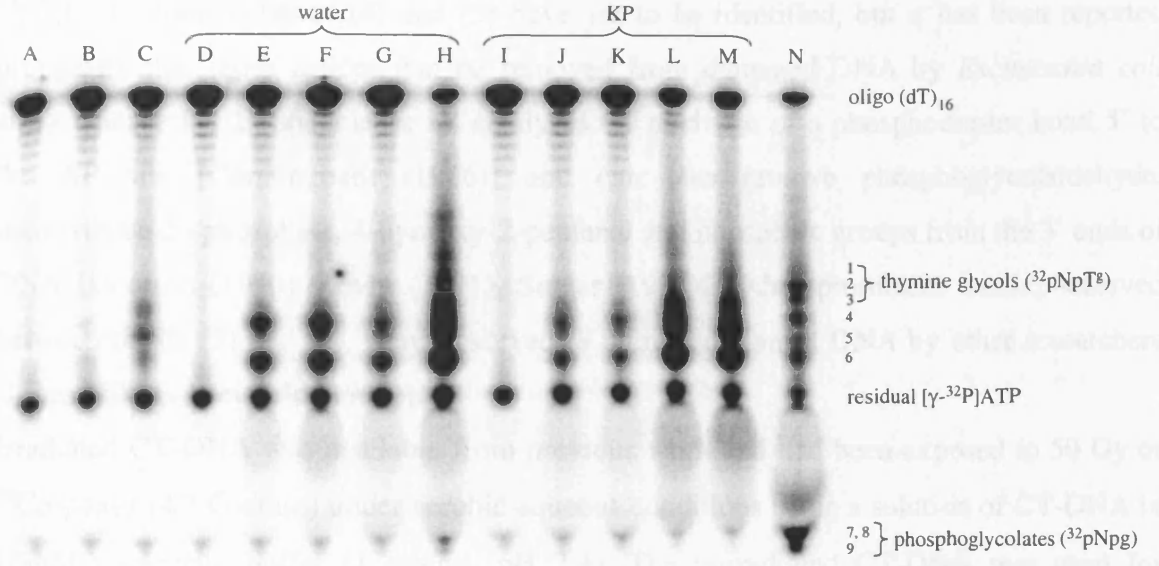

Figure 4.10: *Autoradiogram of polyacrylamide gel showing long-term stored, highly modified CT-DNA analysed by SVPD-^{32}P-postlabelling assay.* Samples shown above [lanes (E)-(H) and (J)-(M)] were stored at RT, 4°C, -20°C or -80°C for the duration of 27 months following MDA treatment. Lanes (A) to (C), i.e. controls (I), (II) and (III), are described in more detail in the legend of Table 4.3. Lanes (D) to (H) represent CT-DNA which had been dissolved in water prior to storage at -80°C (lane E), -20°C (lane F), 4°C (lane G) and RT (lane H). Samples shown in lane (D) and (I) represent untreated, freshly prepared control CT-DNA. Lanes (I) to (M) represent CT-DNA which had been dissolved in KP buffer prior to storage at -80°C (lane J), -20°C (lane K), 4°C (lane L) and RT (lane M). γ-irradiated CT-DNA (lane N) was used as a control in order to identify the type of damage caused by long-term storage.

The autoradiogram shows postlabelled products following long-term storage and oxidative damage generated by γ-irradiation as a positive control (Figure 4.10). Some of the detectable products in irradiated CT-DNA have been identified and described before [Jones (2000), Jones (1999)]. The labelled oligo(dT)$_{16}$ band can be seen at the top of the gel. Oligo (dT)$_{16}$ was used to consume the majority of the excess [γ-^{32}P]ATP, thereby reducing the background radioactivity in the vicinity of the small products. This band also reflects excess [γ-^{32}P]ATP remaining after labelling of the damage-containing dimer

species. Bands (1)-(3) represent the labelled thymine glycol-containing dinucleotides (^{32}pNpT^g). ^{32}pGpT^g is in band (1), ^{32}pApT^g and ^{32}pTpT^g are in band (2) and ^{32}pCpT^g is in band (3). Bands (7)-(9) are the labelled phosphoglycolate species (^{32}pNpg). This type of damage results from hydroxyl radical attack and oxidation at the C4'-carbon atom in deoxyribose. If separated sufficiently, band (7) contains the labelled deoxyguanosine 3'-phosphoglycolate (^{32}pGpg), band (8) contains ^{32}pApg and ^{32}pTpg and band (9) contains ^{32}pCpg. Lesions in bands (4) and (5) have yet to be identified, but it has been reported previously that those lesions can be removed from damaged DNA by *Escherichia coli* endonuclease IV. Endonuclease IV catalyses the cleavage of a phosphodiester bond 5' to the AP site [Cunningham (1986)] and can also remove phosphoglycolaldehyde, deoxyribose-5'-phosphate, 4-hydroxy-2-pentanal and phosphate groups from the 3' ends of DNA [Doetsch (1990), Levin (1991), Singer (1997)]. Other prominent bands, observed between bands (5) and (7), were observed in untreated control DNA by other researchers [Jones (2000), Weinfeld (1996)].

Irradiated CT-DNA was available from previous work and had been exposed to 50 Gy of ^{60}Co γ-rays (4.7 Gy/min) under aerobic aqueous conditions using a solution of CT-DNA in 10mM phosphate buffer (1 mg/ml, pH 7.4). The γ-irradiated CT-DNA was used for comparison and identification of the type of damage inflicted on highly MDA-modified CT-DNA by long-term storage. The pattern of damage in stored samples is clearly distinct from that of oxidative, radiation-induced damage. In particular no phosphoglycolates (telltale lesions of oxidative damage) and relatively low levels of activity in areas corresponding to thymine glycols were noted. Whilst the lesions present have not been identified they are possibly reminiscent of abasic sites [Weinfeld (1990)].

A clear increase in the amount of damage was observed for long-term stored CT-DNA samples with temperatures ranging from -80°C to RT. Relatively little damage was noticed for samples stored at -20°C and -80°C varying from about 1060 to 3400 fmol/μg. However when compared to various freshly prepared controls, the level of damage observed for these long-term stored samples was at least 10 times higher. CT-DNA which had been dissolved in water post MDA-treatment and stored at RT exhibited substantial damage of approximately 12200 fmol/μg. Samples stored in phosphate buffer at 4°C (4°C/KP) also displayed a high level of damage compared to controls (I)-(III) and samples stored in freezers, approximately 9400 fmol per μg of DNA were detectable.

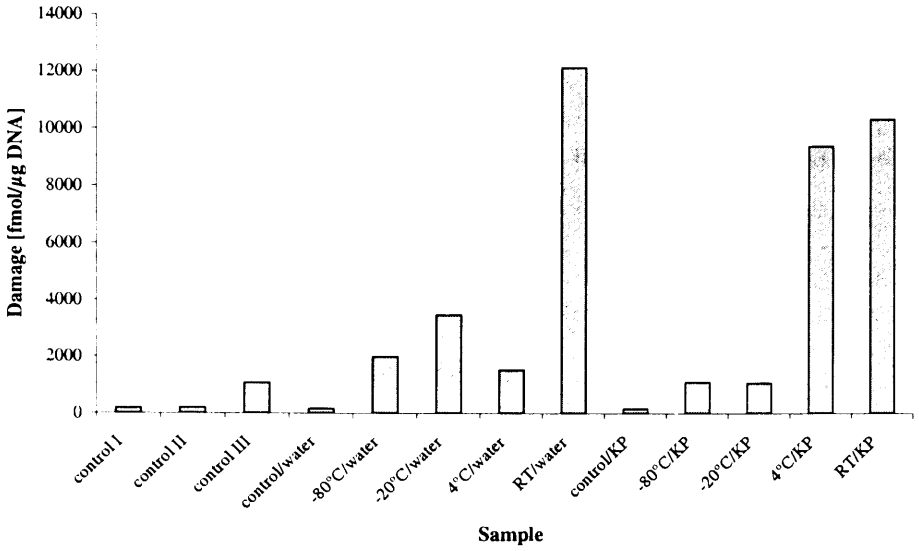

Figure 4.11: *Results obtained for stored, highly modified CT-DNA using the SVPD-^{32}P-postlabelling assay.* Samples shown above correspond to the autoradiogram shown in Figure 4.10 and were stored at RT, 4°C, -20°C or -80°C for the duration of just over 2 years. A more detailed explanation of abbreviations was given in legend of Table 4.3.

As mentioned earlier, no original sample was available for highly modified CT-DNA dissolved in KP buffer and stored at RT as the sample had long since decomposed and was therefore discarded. A replacement sample, which had been stored at 4°C for 18 months followed by 9 months of storage at RT, was used in above experiments. This particular sample, referred to as RT/KP, was not detectable by alkaline and glyoxal gel electrophoresis as it had decomposed excessively since its transferral to RT. Nevertheless, the level of damage was determined to approximately 10400 fmol/µg using the SVPD-^{32}P-postlabelling assay.

In order to allow a comparison of results obtained via alkaline gel electrophoresis and SVPD-^{32}P-postlabelling, the latter were converted from fmol damage per µg of DNA to lesions per 10^4 bp. There was a weak positive correlation between the two assays but absolute values per 10^4 bp did not correlate well, with the alkaline gel electrophoresis assay giving generally higher levels (data not shown).

4.2.3 Stability of M_1-dG in Human DNA Extracted from Leukocytes

The National Blood Service Centre in Sheffield supplied whole blood (supplemented with citrate phosphate dextrose anticoagulant) for usage in this storage experiment. Personal data of the three blood donors were as follows:

- donor (A) DOB 01.06.1966, male, blood group A^+
- donor (B) DOB 29.12.1960, male, blood group A^+
- donor (C) DOB 21.03.1959, male, blood group A^+

Unfortunately, no information about smoking status, diet, health and other important factors could be obtained.

DNA was extracted from 10 ml of blood (14x) per individual using the combined approach described in Chapter 2 (Section 2.2.5.1 and 2.2.5.3). It was then found that this method, although tested earlier during this project on frozen blood, was not suitable for fresh blood samples. DNA yield was only about 20% of the expected value. As the rest of the donated blood had been frozen for 6 days at -80°C, it was used for DNA extraction applying the standard protocol for the Qiagen QIAamp blood maxi kit (see Section 2.2.5.3). In this instance, it was irrelevant whether total or genomic DNA was extracted and stored. 10 ml of blood (16x) were used per donor. DNA concentration of the solution obtained was measured using a UV spectrophotometer. DNA purity was also checked by enzymatic digestion to dNp and HPLC analysis. Approximately 30 μg DNA aliquots were stored for each sample in triplicate at -20°C, -80°C and in liquid nitrogen for each time-point planned. At every time-point the appropriate 27 DNA samples were defrosted and analysed using the standard protocol for immunoslot blot (see Section 2.2.3) and PI staining (see Section 2.2.4).

The ISB assay was adapted to a 96-well dot blot apparatus in order to be able to analyse more samples on the same filter and to reduce the total number of filters needed for the analysis of stored samples. Figure 4.12 shows a typical immunodot blot (IDB) with constant amounts of DNA (1 μg/dot) but containing increasing amounts of M_1-dG (0-10 fmol/dot). Human samples extracted from whole blood were also present on the same filter. All samples and standards were blotted and analysed in triplicate on the same NC membrane.

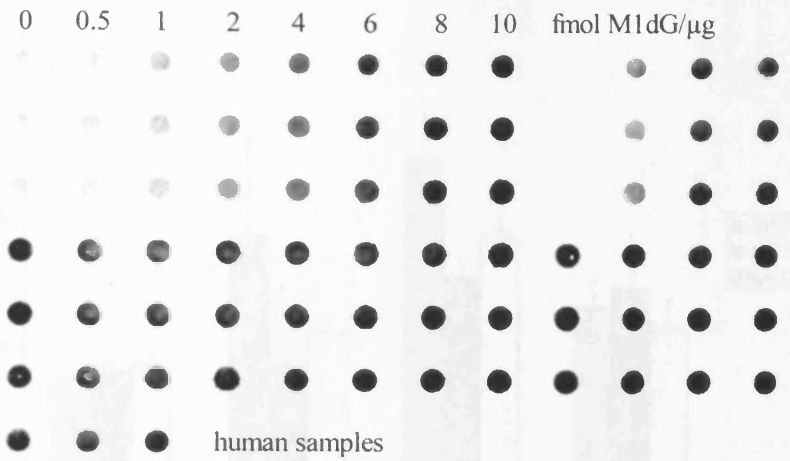

Figure 4.12: *IDB analysis of CT-DNA containing increasing amounts of M_1-dG [0-10 fmol/µg] and DNA from human blood samples.* Dots were visualised by chemiluminescent detection using SuperSignal Ultra (Pierce). The chemiluminescent signal was captured using Hyperfilm and the Biorad Fluor-S™ MultiImager.

The following figures (Figure 4.13, Figure 4.14 and Figure 4.15) illustrate PI corrected results obtained for M_1-dG in stored human DNA for donor (A), (B) and (C) respectively using the IDB assay. Calibration lines used for the analysis of samples were also corrected for background levels of M_1-dG present in control CT-DNA. Originally, it had been planned to analyse the human DNA samples after 0, 2 and 4 weeks of storage, following this initial period analysis was to be conducted at regular intervals every 6 to 12 months. However due to problems with the IDB assay (e.g. flat calibration lines, considerable day to day variations in signal intensity, low reproducibility of triplicates) this was not feasible and samples were analysed only after 0, 2, 4 and 100 weeks of storage.

Figure 4.13 shows M_1-dG results, expressed as adducts per 10^7 normal nucleotides, obtained for donor (A). Levels of M_1-dG adduct were 8.01 ± 1.0 per 10^7 normal nucleotides at the beginning of the storage experiment. However, after only 2 weeks of storage a small increase was noted for samples stored at -80°C and in liquid N_2. The rise in adducts was highest for samples stored at -20°C where levels increased by more than 2-fold.

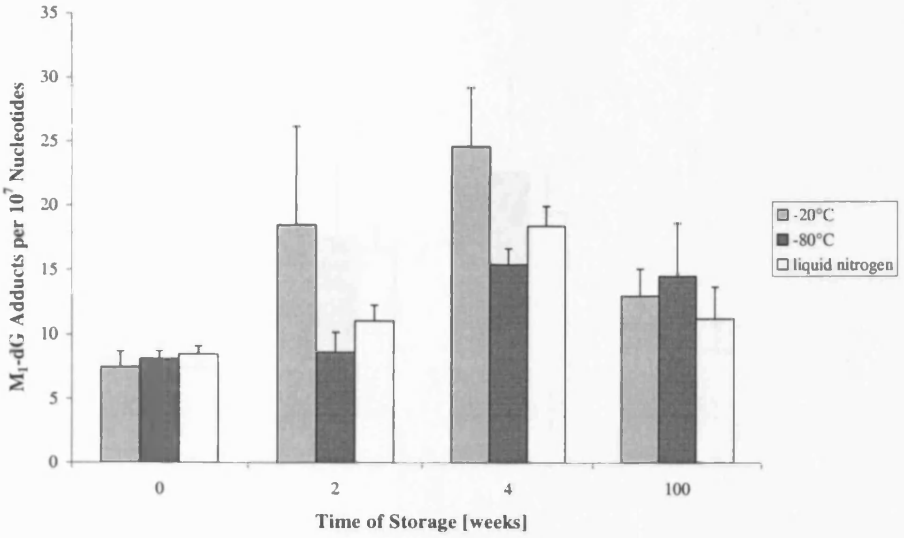

Figure 4.13: *Donor A - Changes in M_1-dG adduct levels in human DNA upon storage.* DNA was extracted from human leukocytes. DNA aliquots were then stored at -20°C, -80°C and in liquid nitrogen, and analysed by IDB assay after 0, 2, 4 and 100 weeks of storage. Results shown for each temperature and time-point are mean ± standard deviation of triplicate samples blotted in triplicate. Results presented above were corrected for PI staining. The calibration line was also corrected for M_1-dG levels detected in control CT-DNA.

After 4 weeks of storage a quite substantial increase in M_1-dG levels was observed for all samples independent of the storage temperature. In comparison to the initial value of M_1-dG, levels approximately doubled within 4 weeks of storage at -80°C and in liquid N_2. Adduct levels tripled for samples stored at -20°C within a month.

After approximately 2 years of storage, M_1-dG levels observed for samples stored at -80°C remained similar in comparison to results obtained for 4 weeks but were still higher than at the beginning. Samples stored at -20°C showed a sharp drop in adduct levels between 4 and 100 weeks of storage. However, M_1-dG levels were still higher when compared to the start of the experiment.

Adduct levels obtained after 100 weeks of storage for samples stored in liquid N_2 were similar to the ones analysed after 2 weeks and only slightly higher than in the beginning. Generally, adduct levels detected in donor (A) after 2 years were similar and independent of the storage temperature, however approximately 1.6 times higher than originally observed M_1-dG levels. At the end of the experiment levels observed for M_1-dG including all samples were 12.96 ± 3.2 adducts per10^7 normal nucleotides.

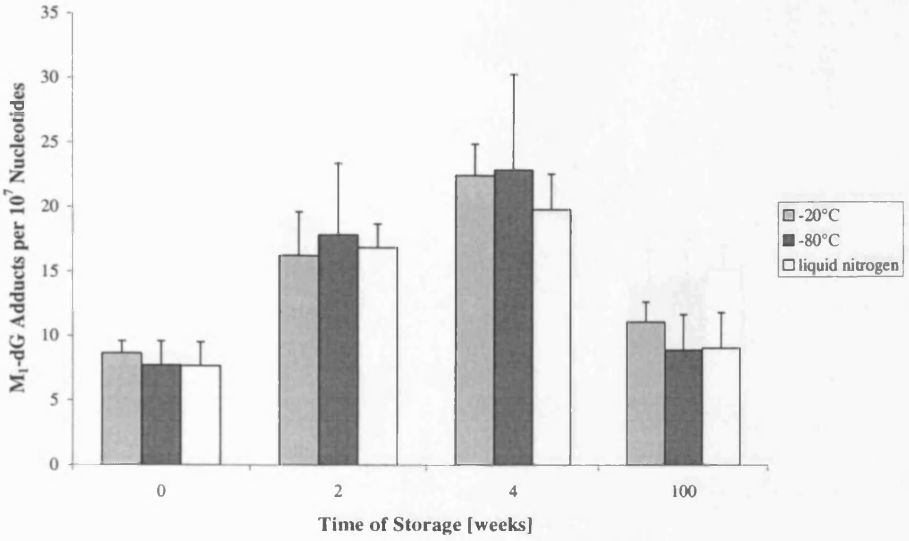

Figure 4.14: *Donor B - Changes in M_1-dG adduct levels in human DNA upon storage.* DNA was extracted from human leukocytes. DNA aliquots were then stored at -20°C, -80°C and in liquid nitrogen, and analysed by IDB assay after 0, 2, 4 and 100 weeks of storage. Results shown for each temperature and time-point are mean ± standard deviation of triplicate samples blotted in triplicate. Results presented above were corrected for PI staining. The calibration line was also corrected for M_1-dG levels detected in control CT-DNA.

The effect of long-term storage on M_1-dG levels, obtained for donor (B), is shown in Figure 4.14. Similar to donor (A), M_1-dG adduct levels were 8.02 ± 1.6 per 10^7 normal nucleotides prior to storage. Levels approximately doubled two weeks into the storage experiment independent of temperature. Number of M_1-dG adducts increased further after 4 weeks of storage, again independently of temperature. Levels of M_1-dG adduct detected were 16.97 ± 3.7 and 21.73 ± 4.6 per 10^7 nucleotides after two and four weeks respectively. After 100 weeks of storage, adduct levels detected in DNA extracted from whole blood donated by donor (B) decreased to almost its original level.

Only minor effects of storage temperature on adduct levels were observed. Levels detected in DNA samples stored at -20°C were slightly higher. Variations in adduction were well within the standard deviation though. Taken as a whole M_1-dG levels increased 1.2 times, yielding levels of 9.77 ± 2.5 adducts per 10^7 normal nucleotides at the end of the experiment.

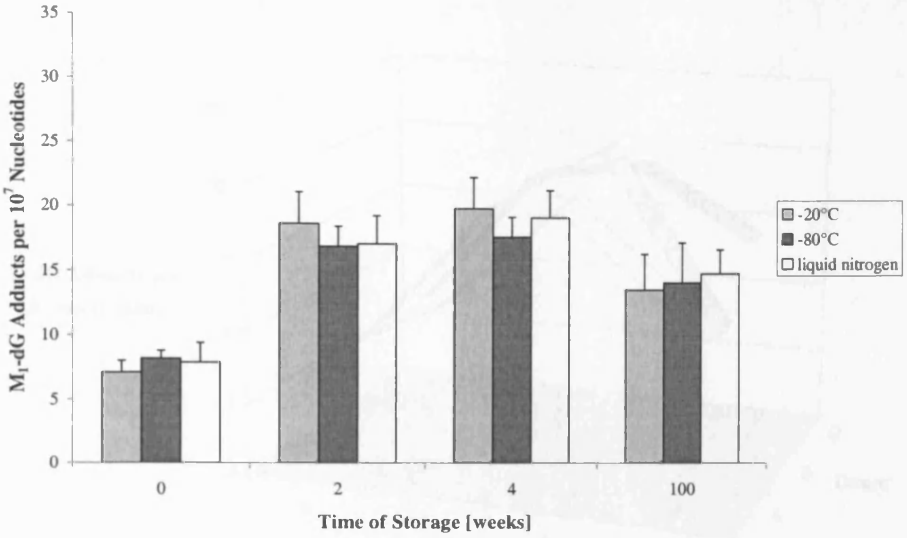

Figure 4.15: *Donor C - Changes in M_1-dG adduct levels in human DNA upon storage.* DNA was extracted from human leukocytes. DNA aliquots were then stored at -20°C, -80°C and in liquid nitrogen, and analysed by IDB assay after 0, 2, 4 and 100 weeks of storage. Results shown for each temperature and time-point are mean ± standard deviation of triplicate samples blotted in triplicate. Results presented above were corrected for PI staining. The calibration line was also corrected for M_1-dG levels detected in control CT-DNA.

Figure 4.15 shows M_1-dG results expressed as adducts per 10^7 normal nucleotides as obtained for donor (C). Levels of M_1-dG adducts were 7.72 ± 1.2 per 10^7 nucleotides at the beginning of the storage experiment, again very similar to donor (A) and (B). The figure shows a steep increase in the number of M_1-dG adducts following 2 and 4 weeks of storage. Similar to results observed for donor (B) adduct levels were fairly independent of temperature. The average adduct levels were 17.54 ± 2.1 and 18.85 ± 2.2 4 per 10^7 normal nucleotides after two and four weeks of storage, respectively. Both levels corresponded to an approximate 2.3-fold increase in adduct measurement.

Again, after almost 2 years of storage M_1-dG levels detected for donor (C) dropped slightly in comparison to the ones observed after 2 and 4 weeks. However, when compared to its original value, the number of M_1-dG adducts was still elevated. In general, levels were increased 1.8 times; 14.13 ± 2.6 adducts per 10^7 normal nucleotides were detected 100 weeks into the storage experiment.

Figure 4.16 summarises the findings obtained for M_1-dG levels in all donors over the time of 100 weeks. Results shown are the overall average per donor, not taking the possible influence of storage temperature into account.

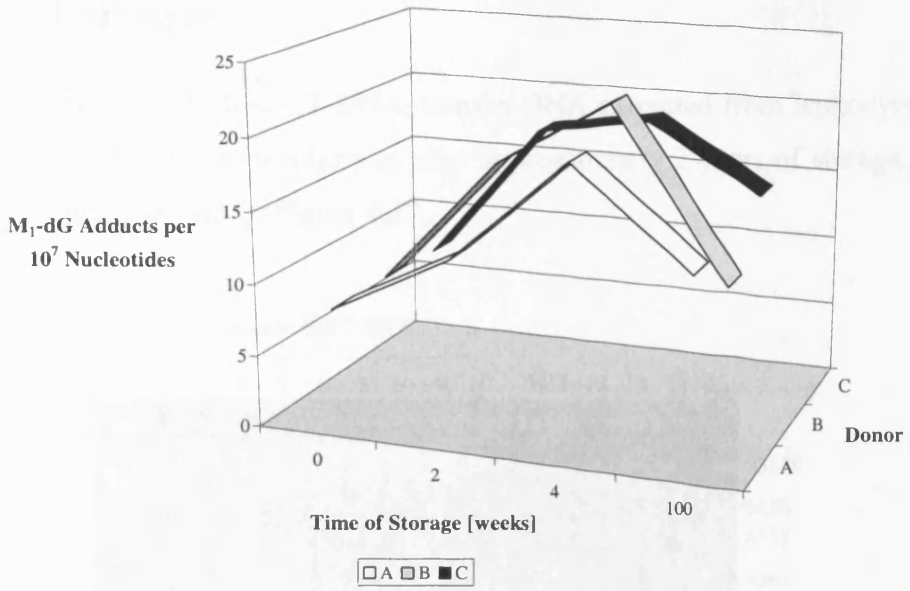

Figure 4.16: *Trend of M_1-dG levels during the course of 2 years.* M_1-dG levels are expressed as adducts per 10^7 nucleotides. All results obtained by IDB assay were PI corrected. Calibration lines were also corrected for background levels present in control CT-DNA. The overall average for each donor, time-point and temperature is shown in order to demonstrate the general trend of adduct levels over the years of storage.

Similar adduct levels were observed for donors (A), (B) and (C) at the beginning of the study. All samples showed an increase within the first two weeks and a further increase after one month into the study. Interestingly no further increase was observed between 4 and 100 weeks of storage for any sample. General trend after approximately 2 years of storage was a decrease in M_1-dG levels when compared to the result obtained after 4 weeks. However, when compared to the original adduct levels, levels observed after 100 weeks were still higher. Only in one sample [donor (B)] adduct levels observed at the beginning were comparable with those detected after 2 years. However, M_1-dG levels observed for donor (A) and (C) were 1.6 and 1.8 times higher at the end of the study when compared to the original levels.

4.2.4 DNA Damage Caused by Long-Term Storage in Human DNA Extracted from Leukocytes

Similar to the highly modified CT-DNA, human DNA extracted from leukocytes was also analysed by alkaline gel electrophoresis after approximately 2 years of storage. An image of the alkaline gel is shown in Figure 4.17.

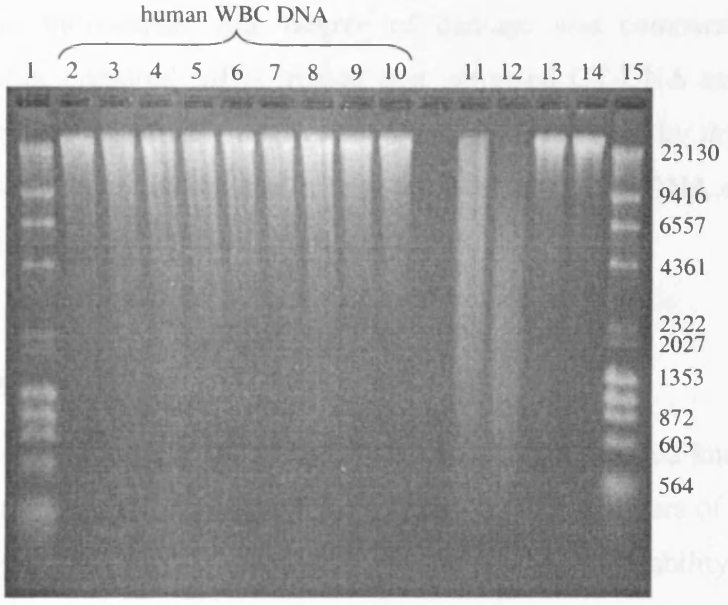

Figure 4.17: *Alkaline gel for human DNA following 2 years of storage at -20°C, -80°C and in liquid nitrogen.* Lanes (1) and (15) marker mix (λ DNA/*Hind* III and ΦX174 RF DNA/*Hae* III fragments), lane (2) A15/-20°C, lane (3) A16/-20°C, lane (4) A39/-80°C, lane (5) A40/-80°C, lane (6) A71/liqu N_2, lane (7) A72/liqu N_2, lane (8) B15/-20°C, lane (9) B39/-80°C, lane (10) B72/liqu N_2, lane (11) MDA-treated ISB standard, lane (12) untreated ISB standard, lane (13) control THP-1 cells, lane (14) MDA-treated THP-1 cells. Temperatures indicate that DNA from donor A or B had been stored at this particular temperature for approximately 2 years post DNA extraction from leukocytes.

It can be clearly seen from Figure 4.17, that most samples showed very little single-strand breaks. The average molecular weight M_w for all human samples (lanes 2 to 10) was greater than 23130 bp (top marker), which is equivalent to 0.86 single-strand breaks per 10^4 bp. Results obtained for cellular DNA samples (lanes 13 and 14) used as controls were similar following approximately 6 months of storage at -80°C. M_w for CT-DNA samples used for comparison was approximately 6557 bp and 3000 bp for treated (lane 11) and

untreated (lane 12) samples, respectively. These numbers correspond to about 3.1 single-strand breaks per 10^4 bp in the treated and 6.7 in the untreated ISB standard.

Samples were also analysed by SVPD-^{32}P-postlabelling assay, which enables the detection of abasic sites and oxidative lesions such thymine glycols and phosphoglycolates. The level of damage obtained for human samples ranged between 231.3 and 387.8 fmol per μg of DNA after approximately 2 years of storage (data not shown in more detail). No major differences in the level of damage were observed when comparing various storage temperatures and individuals. The degree of damage was comparable with the one observed in freshly prepared MDA-treated and untreated CT-DNA samples (see Figure 4.11) and is therefore essentially negligible. Damage represented by thymine glycols and phosphoglycolates was not detectable in long-term stored human DNA samples by SVPD-^{32}P-postlabelling analysis (autoradiogram also not shown).

4.3 Discussion

An important issue, especially for prospective studies, is a detailed knowledge about the effect of long-term storage of samples on the stability of biomarkers of DNA damage. As part of this project, stability of standards as well as M_1-dG stability in stored human samples was investigated.

One aspect of this study was to investigate the stability of MDA-modified CT-DNA upon storage. Temperatures ranging from RT to -80°C as well as two different buffer systems were chosen to carry out this study. Highly modified CT-DNA was found to be relatively stable at RT. Interestingly, differences in rate and pattern of decomposition were observable and dependent on whether KP buffer or water was used to dissolve the DNA post treatment. In water, only M_1-dGp appeared to undergo decomposition while the unmodified nucleotides seemed to be more stable over a longer period of time. Decomposition of the M_1-dGp adduct occurred at a much lower rate and yielded only a single product of degradation, M_1-G. In KP buffer, both modified and unmodified nucleotides degraded at a similar rate. This phenomenon was especially apparent for samples stored at RT. Marked differences were observed for samples stored at RT in water versus phosphate buffer. The study had to be stopped after 17 weeks of storage as detection of both adduct and unmodified nucleotides was no longer feasible for CT-DNA dissolved in KP buffer. For DNA dissolved in water and stored at RT, approximately 12% of initial M_1-dGp and 70% of dAp levels were still detectable by HPLC after 93 weeks of storage.

The comparison of degradation at lower temperatures, i.e. 4°C, showed that samples decomposed at a comparable rate and independently of the buffer system. Products of degradation, if detectable, remained the same as described for RT though. Differences in rate were less obvious, for example after 6 months of storage more than 80% of the original adduct level were still detectable for samples stored at 4°C independent of the solution. At the end of the storage experiment, 66.1% of M_1-dGp were detectable for DNA stored in water versus 56.9% in KP buffer at 4°C. In general, comparison of trends observed in water versus KP buffer showed that the rate of adduct decomposition was slightly slower with time for treated DNA dissolved in water. Differences in degradation of unmodified nucleotides were more marked. After 93 weeks of storage at 4°C, 90.3% of initial dAp level were detectable for samples dissolved in water whereas only 68.2% were detectable for those in KP buffer.

Similar observations regarding M_1-dGp levels were made for samples stored at -20°C and -80°C. The lowest adduct levels (78% of the initial value) were observed for MDA-treated CT-DNA which had been dissolved in water and stored for almost 2 years at -20°C. For the remaining samples, values for M_1-dGp compared well with each other, ranging from 86.7 ± 1.5% (water, -80°C) to 89.1 ± 1.9% (KP buffer, -20°C) and were within the standard deviations. Comparable observations were made for normal nucleotides. In contrast to observations made for samples stored at RT, KP buffer appeared more favourable for long-term storage of samples at -20°C or -80°C.

Highly MDA-modified DNA used as a standard in the ISB assay as well as human samples are routinely stored at -80°C in our laboratory. Nevertheless, it is useful to know that storing the standard at RT or in the fridge for a limited period of time will not have any negative, adverse effects on its quality.

In the beginning of the FORA (FOod Risk Assessment) project only stock solutions of both treated and untreated CT-DNA were stored as standards for the ISB assay. At a much later stage DNA standards were diluted in KP buffer to 0.1 μg/μl and 10 fmol M_1-dG/μg prior to storage. Unfortunately, this aspect was not included in the previously described study. It would therefore be interesting to investigate the effect of DNA concentration and level of modification on stability, rate and pattern of degradation in long-term stored samples. However, this would make checking the standards for stability, especially with respect to the adduct, much more difficult. HPLC of highly modified CT-DNA (pmol levels) is much more reliable, robust and accurate than the ISB assay, but not suitable for the detection of fmol levels. Too many different factors such as accuracy and reliability of

two assays (ISB assay and PI staining) and the equipment used, as well as antibodies utilised in the ISB technique can influence its outcome making the detection of low levels much more difficult and susceptible to variation.

As part of this work, stability of low levels of M_1-dG upon storage was assessed in human DNA extracted from leukocytes at -20°C, -80°C and in liquid nitrogen using the IDB assay. The standard protocol of the ISB assay was adapted to a 96-well dot blot apparatus which would allow a higher throughput and simultaneous analysis of more samples on the same blot. Almost identical adduct levels were observed for all three donors at the beginning of the study ranging from 7.72 to 8.02 adducts per 10^7 normal nucleotides. In contrast to the observations made for stored CT-DNA standards, all human samples showed an increase at least for the first month of storage. This initial increase was more or less independent of the storage temperature. Samples originating from donor (A), which were stored at -20°C exhibited a huge increase during the first month of the experiment. However, values obtained for triplicates varied quite dramatically, reflected in large standard deviations. No further increase was observed between 4 and 100 weeks of storage for any sample. The overall trend after approximately 2 years was a decrease in M_1-dG levels when compared to the level observed after 4 weeks. However, when compared to initial adduct levels, values observed after 100 weeks were still higher. Adduct levels observed at the beginning of the study were comparable in only one sample with those detected after 2 years. However, M_1-dG levels monitored for donor (A) and (C) were 1.6 and 1.8 times higher at the end of the study when compared to early levels.

This phenomenon can possibly be explained through two effects. The decrease between 4 and 100 weeks of storage corresponds to data observed by HPLC for CT-DNA standards where a continuous decrease in adduct levels was observed over time. However, the decrease observed for DNA extracted from human leukocytes was far greater than the one observed for CT-DNA stored at equivalent temperatures. Final levels ranged between approximately 45% (B), 66% (A) and 75% (C) when compared to M_1-dG values observed after 1 month. In contrast, final adduct levels observed for CT-DNA stored in water varied between 78% and approximately 87%.

However, the initial increase in adduct levels contradicts the observations made for MDA-treated CT-DNA. Probably M_1-dG was formed at the beginning of the experiment through direct oxidation of DNA bases as previously described by Dedon et al. [Dedon (1998)]. Dedon and co-workers explain a cascade of reactions that leads to the formation of base

propenals. This mechanism is initiated through direct oxidation of DNA by agents that abstract the C-4' hydrogen atom of the sugar backbone. Base propenals are oxopropenyl base derivatives that are structurally related to acroleins substituted at the β position with a good or moderate leaving group. These compounds, which also include M_1-dA and M_1-dC, transfer their oxopropenyl group to 2'-dG in order to form M_1-dG. This mechanism would offer a possible explanation of the increase in M_1-dG levels observed during the first month of the study. It would not have been possible to detect these minor changes (fmol levels) by HPLC as the method is not sensitive enough. HPLC enables only the detection of M_1-dG in highly modified DNA i.e. pmol levels of modification. The possibility to detect very low levels of M_1-dG levels is one of the most useful points of the ISB assay when compared to HPLC as it enables the detection of adducts in human samples. It should be noted, however, that such a highly sensitive assay is much more susceptible to variation and less robust when compared to HPLC. Therefore, one also has to consider differences in the ISB as the potential cause of changes observed for M_1-dG levels in stored human DNA. Concomitant analysis of M_1-dG levels using two different techniques would be the ideal way to approach a future investigation on adduct stability in human samples. One should thereby be able to rule out any uncertainty with respect to results obtained and methods used for the analysis. Long-term stability of M_1-dG in human DNA samples could have been evaluated in parallel to the ISB assay using for example ^{32}P-postlabelling. ^{32}P-post-labelling has been applied previously to the detection of M_1-dG adducts in human samples by various workers e.g. [Vaca (1995), Wang (1996), Fang (1996), Leuratti (1998)].

After approximately two years of storage, human leukocyte DNA and CT-DNA samples were also analysed by alkaline and glyoxal gel electrophoresis in order to assess any potential damage caused by long-term storage. Analysis of both agarose gels enabled the determination of the average molecular weight and thereby the number of single-strand breaks per 10^4 bp. Interestingly, major differences in the number of single-strand breaks were observed when comparing long-term stored human DNA with CT-DNA. It was apparent that highly modified CT-DNA showed a much higher extent of single-strand breaks when compared to human DNA extracted from leukocytes. Approximately 35 single-strand breaks per 10^4 bp were observed in CT-DNA stored in freezers by alkaline gel electrophoresis versus 0.9 per 10^4 bp for human DNA stored at equivalent temperatures. This almost 40-fold variation between human DNA and CT-DNA samples

could probably be caused by differences in the level of modification i.e. adduction (fmol versus pmol levels of M_1-dG respectively).

Another more likely explanation for this variation was the relatively poor starting quality of CT-DNA purchased from Sigma. This possibility was supported by findings that untreated freshly prepared control CT-DNA exhibited a much higher degree of single-strand breaks when compared to long-term stored human or short-term stored cellular DNA. One should thus consider for future experiments another company for the purchase of CT-DNA or its purification prior to use.

Type of damage detected in highly modified CT-DNA after 2 years of storage was identified to be non-oxidative using the SVPD-^{32}P-postlabelling assay. Thymine glycols and phosphoglycolates were not detectable in long-term stored DNA when compared to γ-irradiated CT-DNA. The combination of findings observed by alkaline gel electrophoresis and SVPD-^{32}P-postlabelling indicated that the damage detected in long-term stored CT-DNA most likely comprised of abasic site lesions. Further tests would be needed in order to classify and ascertain the type of damage. For example, long-term stored CT-DNA samples could be incubated with *Escherichia coli* endonuclease IV, which is known to remove abasic site lesions, prior to analysis by SVPD-^{32}P-postlabelling. Alternatively, the highly sensitive apurinic/apyrimidinic site assay described recently by Nakamura et al. [Nakamura (1998)] could also be used for the detection and quantitation of abasic sites in long-term stored DNA samples. The sensitivity of this slot-blot method enables the detection of 2.4 abasic sites per 10^7 bases.

Originally, it had also been planned to investigate the effect of long-term storage on M_1-dG levels in human whole blood and buffy coat. Especially the latter is very important with respect to the EPIC study where buffy coat is stored routinely over years in liquid nitrogen prior to analysis of samples. It was also intended to investigate the effect of antioxidants during storage of blood and buffy coat samples. Antioxidants would have been added prior to storage in order to avoid artefactual formation of M_1-dG, for example via peroxidation of lipids present in cellular membranes.

Unfortunately, this part of the study was abandoned after several unsuccessful, unsatisfactory attempts of starting the blood storage. Problems with the IDB assay such as flat calibration lines, massively varying signal intensity from day to day and poor reproducibility for duplicate/triplicate samples seemed to make it impossible to fulfil this aim. There also appeared to be an occasional problem with DNA extracted from whole

blood, as individually stored and extracted duplicates were not very reproducible with regard to M_1-dG quantitation by ISB. Although the DNA extraction technique (detailed in Section 2.2.5.1 and 2.2.5.2) is commonly used in our laboratory, variations in M_1-dG levels detected by ISB during the blood storage study might indicate a problem derived from this method making the analysis more problematic than originally anticipated. Usually DNA quality was determined by UV A_{260}/A_{280} ratio and HPLC using UV detection. Both methods confirmed that the technique used for DNA extraction yielded pure DNA. However, DNA purity and possible variations in M_1-dG are not necessarily linked. A comparison of multiple DNA extractions from one and the same blood sample might therefore prove beneficial. In order to make the detection of such variations more reliable and feasible by HPLC, highly modified CT-DNA could be added during the extraction procedure. The presence of antioxidants as a preventive measure during DNA extraction might also be worth a thorough investigation. Kvam and Tyrrell [Kvam (1997)] found that the amount of oxidative base damage measured in DNA extracted from human primary skin fibroblasts can be reduced to a stable lower level by adding increasing concentrations of the antioxidants desferrioxamine, histidine and reduced glutathione immediately before cell lysis. The level of 8-hydroxy-2'-deoxyguanosine (8-OHdG) without the use of antioxidants was determined to 220 adducts per 10^6 dG. The method of DNA extraction used in the work of Kvam and Tyrrell [Kvam (1997)], a kit from Qiagen, was basically identical to the protocol described earlier in Chapter 2 (Section 2.2.5.1 and 2.2.5.2) which is routinely used in our laboratory. A combination of 1mM desferrioxamine, 4mM histidine and 3mM reduced glutathione significantly reduced levels of oxidative damage and appeared to offer maximum protection. None of the antioxidants alone reduced the amount of DNA base damage as much as the combination. Furthermore, increasing the concentration of one of these antioxidants did not decrease the amount of 8-OHdG below 22 adducts per 10^6 dG. Inclusion of these antioxidants after cell lysis or at other steps of the procedure did not affect the level of DNA damage. Findings of this study lend considerable support to the necessity for an investigation whether antioxidants during DNA extraction from whole blood especially during cell lysis may affect M_1-dG levels.

In general, a prerequisite for the assessment of adduct stability in long-term stored human samples is the accurate and reproducible determination of absolute values. This task is relatively difficult to achieve due to the inherent limitations of the IDB assay discussed above. The experimental set-up could be improved by the use of a second technique in

parallel to the IDB assay for the detection of M_1-dG levels in stored human samples. Using a secondary technique would have allowed to determine the overall trend in adduct levels much more confidently and would have excluded measurement uncertainties to a significant extent even if absolute levels determined by both assays would not have been identical. Potential problems and variations in M_1-dG levels detected for stored duplicate samples, possibly due to the method used for DNA extraction, led to the final decision to abandon long-term storage of blood and buffy coat.

Although the study of the effect of long-term storage on M_1-dG levels in human samples was only partially completed, the evaluation of M_1-dG stability in highly modified standards resulted in some important pointers for future investigations. The completion of this work to human samples should nevertheless be attempted in the future, especially considering its impact on the evaluation of data collected in prospective studies such as EPIC.

5 Modulation of O^6-Alkylguanine Adduct Formation

5.1 Introduction

It has been shown in Chapter 1 that several nitrosated glycine derivatives react with DNA to form O^6-carboxymethylguanine and O^6-methylguanine adducts concurrently. The two pathways leading to the formation of both O^6-alkylguanine adducts are illustrated for diazoacetic acid in Figure 5.1. Relative proportions of these two adducts varied quite dramatically depending on which compound was used for modification. Ratios detected by immunoaffinity-RP-HPLC-fluorescence were 1:9.7 (APNG), 1:16.1 (KDA) and 1:38.5 (azaserine). In all three cases significantly more O^6-CMdG was formed when compared to O^6-MedG [Harrison (1999)].

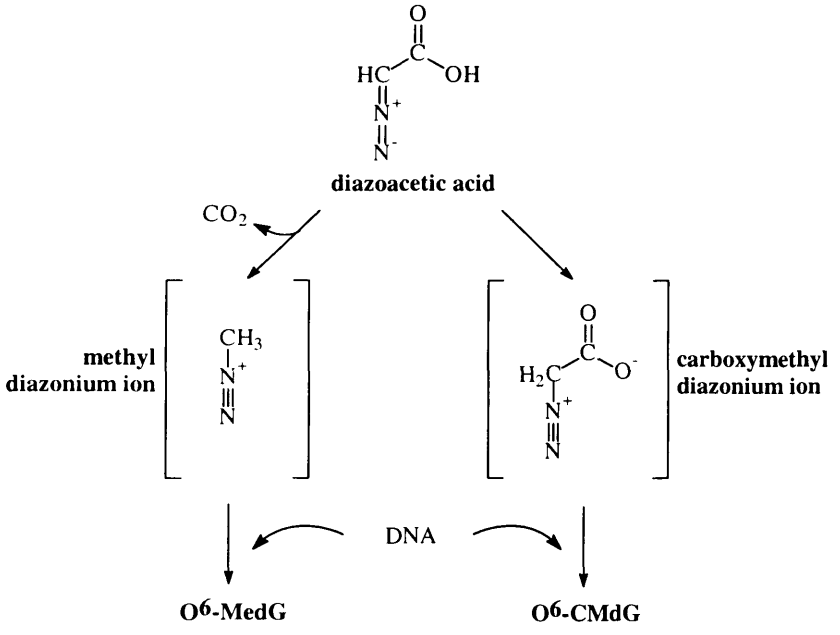

Figure 5.1: *Structure of diazoacetic acid and its reactive intermediates.* Diazoacetic acid can form an electrophilic carboxymethyldiazonium ion and via decarboxylation a methyldiazonium ion. Both highly reactive species can react with DNA and form O^6-CMdG and O^6-MedG DNA adducts respectively.

In general, the quantitation of low levels of O^6-alkylguanine adducts can pose a problem, because of the presence of much higher amounts of normal nucleosides. Therefore, it is necessary to incorporate an enrichment step prior to adduct detection. Immunoaffinity chromatography presents a means of performing highly selective purification of a

compound. The basic principles of this methodology are illustrated in Figure 5.2 and its specific application to the purification of O^6-MedG and O^6-CMdG DNA adducts is shown in Figure 5.3.

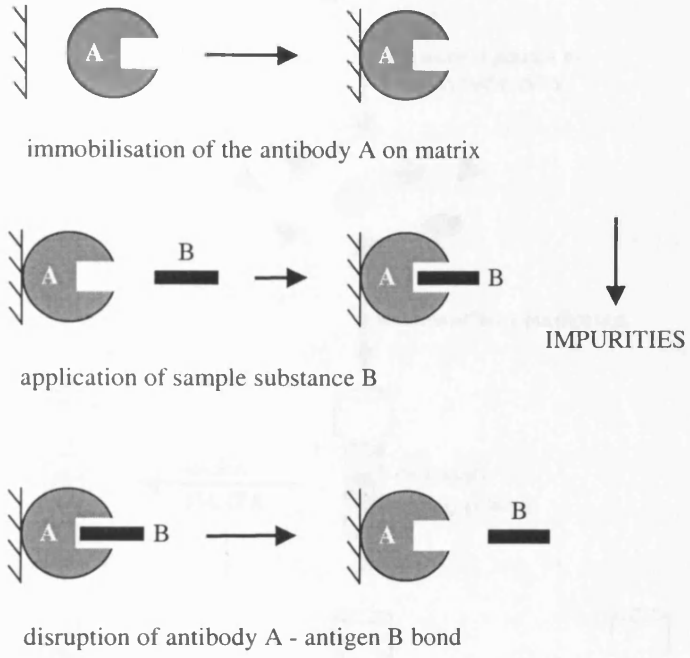

Figure 5.2: *Principle of immunoaffinity chromatography.* This method is based on the availability of a biospecific ligand, i.e. antibody (A), and the necessity that it can be covalently bound to a matrix. The soluble molecule of interest (antigen) exclusively interacts then with the insoluble antibody. The antigen (B) will thereby become temporarily insoluble and can be separated from soluble contaminants such as normal nucleosides.

This technique has been developed and applied previously for the purification of O^6-MedG and O^6-CMdG (Figure 5.3) by Harrison et al. [Harrison (1997), Harrison (1999)]. Following immunoaffinity purification, the samples are analysed by RP-HPLC as both O^6-alkylguanine adducts are naturally fluorescent.

Not only was the ratio of O^6-CMdG to O^6-MedG adducts influenced by the alkylating agent, but also the overall levels of DNA alkylation induced by the various nitrosated glycine derivatives were very different. Levels of DNA carboxymethylation were in the proportion of 1:11:134 following 5mM treatments using azaserine, APNG and KDA respectively [Harrison (1999)]. These results illustrate quite dramatically that the degree of carboxymethylation greatly depends on the compound, which is used for treatment.

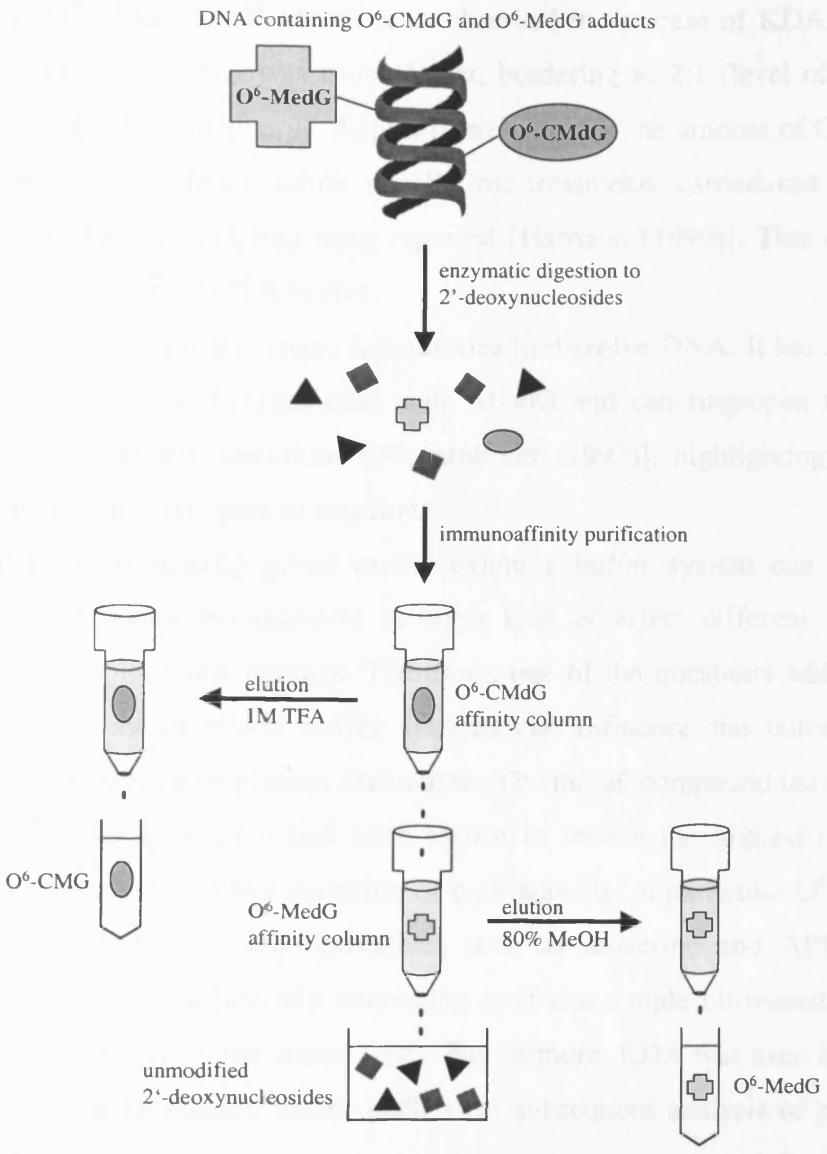

Figure 5.3: *Scheme for the immunoaffinity purification of O^6-CMdG and O^6-MedG adducts from DNA digests.* Briefly, DNA containing both O^6-alkylguanine adducts is digested to nucleosides and passed through the first column (O^6-CMdG), which elutes directly onto the second column (O^6-MedG). The immunoaffinity columns are then separately washed and the adduct of interest eluted using 80% MeOH and 1M TFA for O^6-MedG and O^6-CMdG respectively. Finally, the bases are quantitated using RP-HPLC as both adducts are naturally fluorescent.

It was found during studies on modification of CT-DNA with KDA under the same conditions as those needed to modify plasmid DNA that the ratio of O^6-CMdG to O^6-MedG did not correspond well to the one reported previously [Harrison (1999)]. Originally the plasmid had been dissolved in Tris-EDTA (pH 7.5), thus KDA treatments of CT-DNA were also carried out using this buffer system in order to reproduce the same

conditions. The O^6-CMdG to O^6-MedG ratio observed in the case of KDA treatments in Tris-EDTA buffer of CT-DNA was much lower, bordering to 2:1 (level of both adducts being uncorrected for IAC recovery). Approximately double the amount of O^6-CMdG was formed relatively to O^6-MedG, while usually for treatments carried out in phosphate buffered saline a ratio of 16:1 had been reported [Harrison (1999)]. This deviation was attributed to the use of Tris-EDTA buffer.

Tris-EDTA is frequently used in many laboratories to dissolve DNA. It has however been shown before that Tris forms cross-links with M_1-dG and can ring-open this particular DNA adduct under certain conditions [Niedernhofer (1997)], highlighting the fact that buffer components can participate in reactions.

Not much attention is usually given to the extent a buffer system can influence the outcome of certain reactions/treatments or what kind of effect different buffers might exhibit on, for example, DNA adducts. Therefore, one of the questions addressed in this chapter was the extent to which buffer systems can influence the outcome of DNA treatments based on nitrosated glycine derivatives. The model compound used in this study was potassium diazoacetate as it had been shown to induce the highest level of DNA modification, making the accurate detection of both adducts, in particular O^6-MedG, more feasible. Other nitrosated glycine derivatives such as azaserine and APNG were not considered here. KDA is particularly interesting as it is a simple nitrosated derivative of glycine, one of the most common amino acids. Furthermore, KDA was used for the *in vitro* modification of yeast expression vector pLS76 i.e. subsequent analysis of p53 mutations (see Chapter 6).

In subsequent sections several buffer systems and respective dilutions will be compared with each other with regard to DNA carboxymethylation and methylation at the O^6-position of guanine using KDA. Furthermore, various detection methods and HPLC systems will be compared with each other in order to find the most reliable and suitable method for this study. Another incentive was to find a method suitable for the detection of O^6-CMdG and O^6-MedG adducts in KDA-treated plasmid pLS76.

5.2 Results

5.2.1 Depurination of O^6-Alkylguanine Adducts

As explained in the introduction to this chapter, immunopurification followed by HPLC fluorescence detection has been applied previously to the detection of O^6-alkylguanine adducts in *in vitro* treated DNA samples.

Due to the very strong binding of O^6-CMdG to the immunoaffinity columns, fairly acidic conditions were required for its elution (1M TFA). Under these conditions O^6-CMdG was reported to extensively hydrolyse to the corresponding base, O^6-CMG. Therefore an O^6-CMG standard was essential for future HPLC analysis. Since a standard was not available commercially or from previous work, O^6-CMdG, which had been synthesised by R. Jukes, was treated with various acids in order to depurinate the compound to its base.

According to previously described work by Harrison et al. [Harrison (1999)] the eluates from the O^6-CMdG immunoaffinity columns required heating at 50°C for 60 min to completely hydrolyse O^6-CMdG to its corresponding base. These conditions were mimicked and samples analysed by HPLC using a 2 pmol/μl solution of O^6-CMdG as detailed in Section 2.3.3. O^6-CMdG was not detectable by HPLC immediately after dissolving the standard in 1M TFA (pH 0.34). Depurination to the base took place instantaneously and heating of the samples was not required. Similar findings, however less extreme, were observed when using 0.1M TFA (pH 1.1), approximately 26% depurinated to O^6-CMG instantly. Complete hydrolysis to O^6-CMG was observed for the next time point i.e. after 30 min of incubation at 45°C. Milder conditions were then applied to the hydrolysis, i.e. using 1M acetic acid (pH 2.3) followed by incubation at 50°C using a water bath. The kinetics of the depurination reaction of O^6-CMdG and consequent formation of O^6-CMG are shown in Figure 5.4. The reaction had gone to completion after 3 h of incubation at 50°C using 1M acetic acid.

As initially planned, a suitable O^6-CMG HPLC standard was prepared by hydrolysing O^6-CMdG to its corresponding base using 1M TFA at a large scale. Choosing the more drastic hydrolysis conditions ensured a quick and reliable way of generating O^6-CMG. Large scale depurination of O^6-CMdG to O^6-CMG and subsequent purification steps were carried out by R. Jukes.

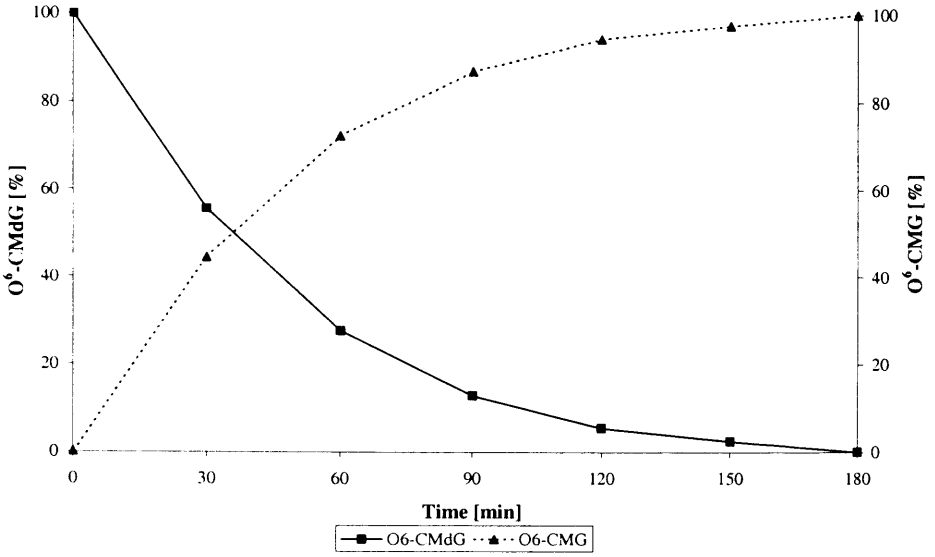

Figure 5.4: *Depurination of O^6-CMdG to O^6-CMG using 1M Acetic Acid at 50°C.* Samples were taken at defined time points i.e. every 30 min. 10 µl were injected directly onto the HPLC for simultaneous detection of O^6-CMdG and O^6-CMG. The original solution contained 2 pmol O^6-CMdG/µl. RP-HPLC was performed using an isocratic flow rate of 0.2 ml/min and 0.1% HFBA with 10% methanol (Section 2.3.1.2, system 2). Peaks were detected by fluorescence (λ_{Ex} 286 nm, λ_{Em} 378 nm).

The intention was to treat samples for example after immunoaffinity purification as mildly as possible and to avoid unnecessary high temperatures and severe acidic conditions over prolonged periods of time. Since a discrepancy was observed between previously published observations [Harrison (1998)] and results obtained during this work with regard to O^6-CMdG depurination, conditions of O^6-MedG hydrolysis were also re-evaluated. In general, O^6-MedG is eluted from IACs using 80% methanol. Samples are then dried down and hydrolysed to O^6-MeG at 50°C for 30 min using 0.1M HCl. Prior to evaporation of the liquid and HPLC analysis samples are neutralised using an equimolar solution of NaOH. Consequently, a stock solution of O^6-MedG was prepared (27.37 pmol/µl) and 10 µl of a 1:10 dilution in water injected directly onto the HPLC system. An appropriate volume was diluted accordingly using water and 1M HCl to obtain a 2.737 pmol/µl solution of O^6-MedG in 0.1M HCl. An aliquot of this solution (10 µl) was injected immediately onto the HPLC system. The remaining solution was incubated at 50°C and samples analysed by HPLC fluorescence at regular intervals (detailed in Section 2.3.4).

It can be clearly seen from Figure 5.5 that instantaneous depurination of O^6-MedG to O^6-MeG occurred. Even before incubation at 50°C levels of O^6-MedG were reduced by

about 32% and both nucleoside and base were detectable by HPLC. Even after only 15 min incubation at 50°C in 0.1M HCl the nucleoside form of the adduct was no longer detectable. Further increase in incubation time did not yield any major increase in O^6-MeG being detectable.

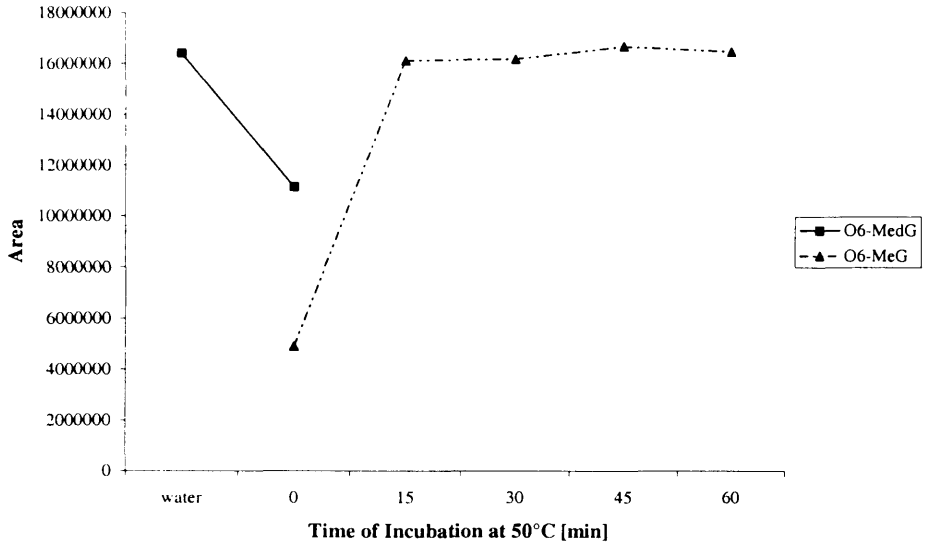

Figure 5.5: *Depurination of O^6-MedG to O^6-MeG using 0.1M HCl at 50°C.* Samples were taken at defined time points and 10 µl injected directly onto the HPLC for simultaneous detection of O^6-MedG and O^6-MeG. The original solution contained 2.737 pmol O^6-MedG/µl. RP-HPLC was performed using an isocratic flow rate of 0.2 ml/min and 0.1% HFBA with 15% methanol. Peaks were detected by fluorescence (λ_{Ex} 286 nm, λ_{Em} 378 nm).

5.2.2 Pattern of O^6-Alkylguanine Elution During Immunoaffinity Purification

Due to above findings, fractions obtained during immunoaffinity purification were also checked in order to see whether heating of the samples was required prior to HPLC analysis. The capacity of this particular set of O^6-CMdG immunoaffinity columns had been determined to 200 ng i.e. approximately 0.6 nmol [Harrison (1998)]. These columns were still available from previous work and were used for this specific experiment only. 50 ng i.e. 153.7 pmol O^6-CMdG were loaded on one immunoaffinity column and all five TFA fractions were collected, dried down overnight, taken up in water (100 µl) and analysed by RP-HPLC (10 µl). All TFA fractions showed one single peak for O^6-CMG confirming that O^6-CMdG was eluted as its corresponding base and that no residual O^6-CMdG was present after elution from IACs. The vast majority of O^6-CMG was detectable in fractions I and II

(63.2 and 34.3% respectively). As expected hardly any was detected in fractions III and IV (Figure 5.6). Heating of samples was not required prior to HPLC analysis, therefore this step was omitted in subsequent experiments.

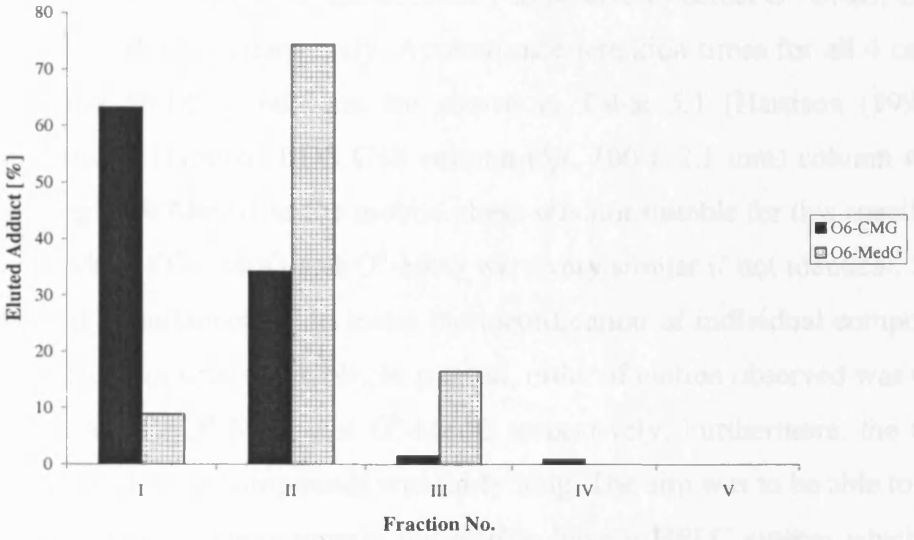

Figure 5.6: *Pattern of O^6-CMG and O^6-MedG elution.* RP-HPLC was performed using a Hypersil BDS C18 column (3μ, 100 x 2.1 mm) with an isocratic flow rate of 0.2 ml/min using 0.1% HFBA plus 15% methanol as mobile phase. Detection occurred by fluorescence (λ_{Ex} 286 nm, λ_{Em} 378 nm).

The pattern of elution was also investigated for O^6-MedG. Approximately 41.0 pmol O^6-MedG were loaded and purified using appropriate immunoaffinity columns as described in Section 2.3.9. The four 80% MeOH fractions were collected as 1 ml aliquots and evaporated to dryness. In order to be able to detect whether O^6-MedG was entirely eluted as the 2'-deoxynucleoside, samples were not hydrolysed, instead only taken up in 0.1% HFBA (16 μl) prior to HPLC analysis. It can be clearly seen from Figure 5.6 that the majority of O^6-MedG was detectable in the second methanol fraction, about 75% of the adduct were eluted in this particular aliquot. Approximately 8.9 and 16.5% O^6-MedG were observable in fractions I and III respectively. Furthermore, it was noted that the O^6-alkylguanine adduct was eluted entirely as O^6-MedG, no O^6-MeG was detectable upon elution and evaporation.

5.2.3 Development of a HPLC Method Enabling the Concomitant Detection of O^6-Alkylguanines and Corresponding 2'-Deoxynucleosides

In order to be able to detect possible decarboxylation of O^6-CMdG to O^6-MedG or the corresponding base to O^6-MeG, it was necessary to be able to detect O^6-CMG, O^6-CMdG, O^6-MeG and O^6-MedG simultaneously. Approximate retention times for all 4 compounds using the existing HPLC conditions are shown in Table 5.1 [Harrison (1999)]. It is apparent that using a Hypersil BDS C18 column (3μ, 100 x 2.1 mm) column with 0.1% HFBA containing 10% MeOH as the mobile phase was not suitable for this specific task as the retention times of O^6-CMdG and O^6-MeG were very similar if not identical. Standards were not injected simultaneously to make the identification of individual compounds and corresponding retention times feasible. In general, order of elution observed was O^6-CMG, O^6-CMdG followed by O^6-MeG and O^6-MedG respectively. Furthermore, the total time required to analyse all four compounds was fairly long. The aim was to be able to detect all O^6-alkylguanine adducts concomitantly but also to have a HPLC system which was not very time consuming, thus the existing HPLC conditions needed to be further developed and modified. Consequently, the amount of methanol in the mobile phase was changed. Table 5.1 shows the retention times for the four compounds using 0.1% HFBA and various amounts of methanol ranging from 10% to 15%. Good separation and simultaneous detection of all four standards was achieved using 0.1% HFBA with 15% MeOH (Figure 5.7). Additionally, the time needed for the detection of O^6-methyl- and O^6-carboxymethylguanine adducts was shortened. Approximately 13 min were required for the last compound (O^6-MedG) to be detected by HPLC fluorescence.

Mobile Phase	O^6-CMG	O^6-CMdG	O^6-MeG	O^6-MedG
0.1% HFBA, 10% MeOH	9.5 min	18.9 min	18.0 min	30.4 min
0.1% HFBA, 12.5% MeOH	7.6 min	13.3 min	13.8 min	21.2 min
0.1% HFBA, 15% MeOH	5.7 min	8.2 min	9.7 min	12.7 min

Table 5.1: *Influence of methanol content on the retention times of O^6-CMG, O^6-CMdG, O^6-MeG and O^6-MedG adducts.* Above table shows the dependence of O^6-CMG, O^6-CMdG, O^6-MeG and O^6-MedG retention times [min] on the methanol content of the mobile phase. RP-HPLC was performed using a Hypersil BDS C18 column (3μ, 100 x 2.1 mm) with an isocratic flow rate of 0.2 ml/min. Peaks were detected by fluorescence (λ_{Ex} 286 nm, λ_{Em} 378 nm).

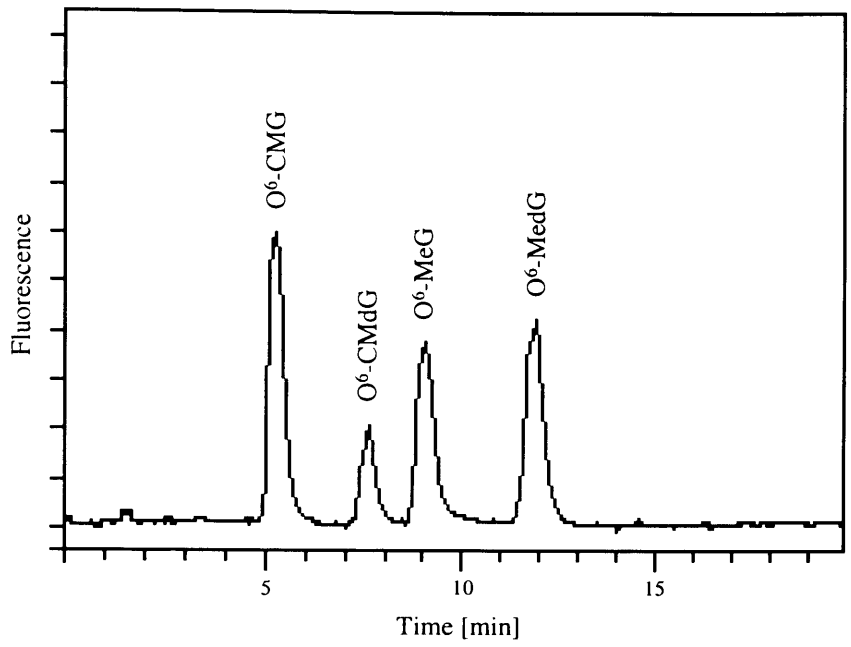

Figure 5.7: *HPLC trace for the simultaneous detection of O^6-CMG, O^6-CMdG, O^6-MeG and O^6-MedG adducts.* RP-HPLC was performed using a Hypersil BDS C18 column with an isocratic flow rate of 0.2 ml/min and 0.1% HFBA with 15% MeOH. Peaks were detected by fluorescence (λ_{Ex} 286 nm, λ_{Em} 378 nm).

5.2.4 Evaluation of O^6-Alkylguanine Adduct Detection

The aim of this part of the study was to compare previously applied methods (immunoaffinity purification of O^6-alkylguanine adducts) with the one currently used in the laboratory for the detection of O^6-CMdG in KDA-treated CT-DNA standards [Singh (2000)]. Various methods ranging from acid hydrolysis using hydrochloric or formic acid, and enzymatic digestion to dN with or without immunoaffinity purification were tested in order to determine the most reliable, suitable and least time-consuming method. These procedures are described in more detail in Section 2.3.10. CT-DNA was dissolved in PBS at a concentration of approximately 1 mg/ml and treated using 8mM KDA, also detailed in Section 2.3.10. Before starting the experiment, a new set of five immunoaffinity columns for the purification of O^6-CMdG was prepared according to the method described in Section 2.3.6. The pattern of O^6-CMG elution was essentially identical to the one presented in Figure 5.6. A complete set of O^6-MedG IACs was available from work previously conducted in this laboratory.

In this specific experiment, the HPLC method developed by R. Singh and B. Cupid was used in order to be able to inject unpurified, hydrolysed DNA samples onto the HPLC

column (see Section 2.3.1.1). Normally, a Hypersil BDS C18 column (3μ, 100 x 2.1 mm) is used for the detection of O^6-alkylguanine adducts, however this column is not suitable for the analysis of larger amounts of (unpurified) DNA since this would cause overloading the HPLC column. Therefore, RP-HPLC separations were carried out using a Shandon, Hypersil BDS C18 (5μ, 4.6 mm x 25 cm) column connected to a Hypersil BDS C18 guard cartridge. Analysis was performed using a flow rate of 1.0 ml/min, specifications and gradient are given in more detail in Section 2.3.1.1. Appropriate calibration lines were prepared using standards described in 2.3.5, charts of corresponding trendlines are not shown but equations as well as retention times obtained for O^6CMG, O^6-MeG and O^6-CMdG are given in Table 5.2.

Adduct of Interest	Equation	R^2	Range [pmol]	Retention Time
O^6-MeG	y = 158496x - 61533	0.9998	0.5 to 100	18.2 min
O^6-CMG	y = 150097x + 61938	0.9984	0.5 to 120	14.8 min
O^6-CMdG	y = 169288x - 198481	0.9863	0.5 to 100	15.3 min

Table 5.2: *Calibration lines generated for O^6-MeG, O^6-CMG and O^6-CMdG using a Hypersil BDS C18 (5μ, 4.6 mm x 25 cm) HPLC column.* A more detailed description of the HPLC system used for the generation of above calibration lines can be found in Section 2.3.1.1. 40 μl of each standard were injected in triplicate onto the HPLC column. R^2 is the correlation coefficient.

Comparison of all four techniques (Section 2.3.10) revealed that the detection of O^6-MeG was only feasible when enzymatic digestion to nucleosides followed by immunoaffinity purification was used (Figure 5.11). Although this method was far more time consuming then the others, immunopurification was necessary in order to detect and determine both O^6-alkylguanine adducts concurrently in an accurate and reproducible way.

It can be clearly seen in Figure 5.8 that due to the presence of adenine and guanine the concurrent detection of both adducts appeared fairly difficult and inaccurate following acid hydrolysis of KDA-treated CT-DNA. Similar HPLC traces to the one shown in Figure 5.8 were obtained when KDA-treated CT-DNA samples were digested to dN using MN, CSPDE and NP1 without immunoaffinity purification prior to HPLC analysis (HPLC fluorescence trace not shown). Again quantitation of low levels of adduct posed a problem because of the presence of normal nucleosides.

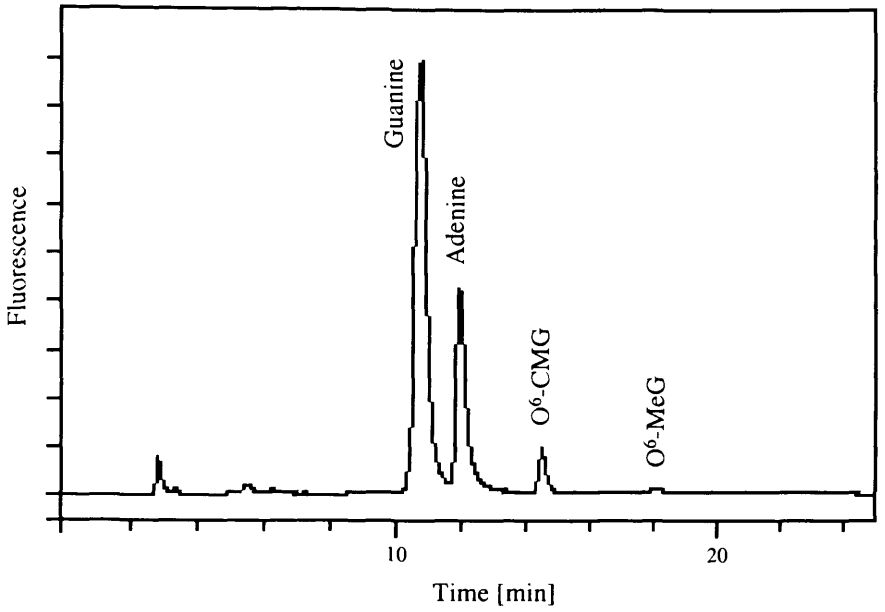

Figure 5.8: *HPLC chromatogram of an acid hydrolysed, 8mM KDA-treated CT-DNA sample.* RP-HPLC separation was carried out using a Shandon, Hypersil BDS C18 (5μ, 4.6 mm x 25 cm) column and a flow rate of 1.0 ml/min, specifications and gradient are given in more detail in Section 2.3.1.1. Peaks were detected by fluorescence (λ_{Ex} 286 nm, λ_{Em} 378 nm).

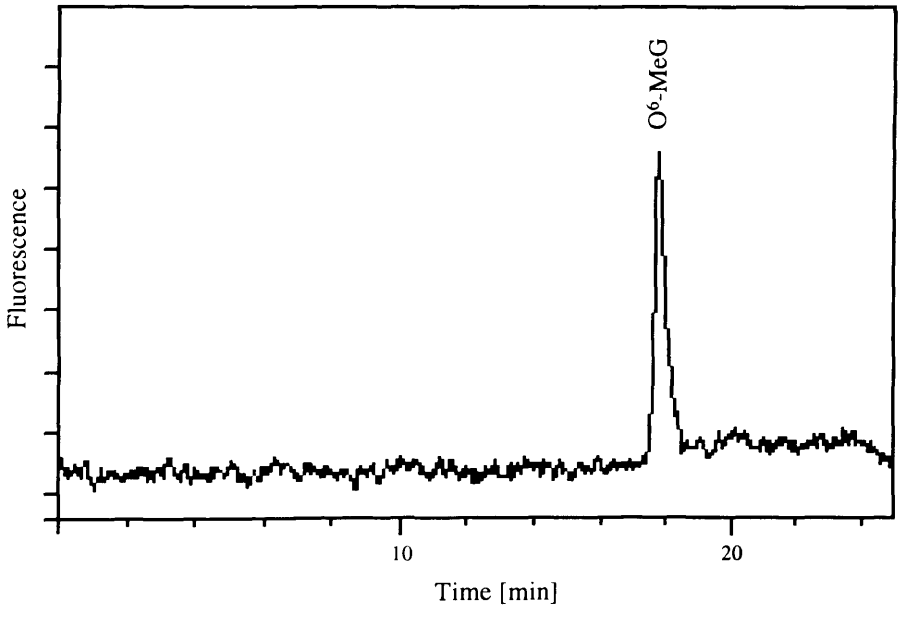

Figure 5.9: *HPLC chromatogram of O^6-MeG following enzymatic digestion and immunoaffinity purification of 8mM KDA-treated CT-DNA.* RP-HPLC separation was carried out following immunoaffinity purification using conditions outlined in legend of Figure 5.8.

In contrast to results acquired for the analysis of unpurified DNA samples as expected 'clean' HPLC traces were obtained for both O^6-alkylguanine adducts when using immunopurification prior to HPLC fluorescence analysis. The relevant HPLC traces are shown in Figure 5.9 and Figure 5.10 for O^6-MeG and O^6-CMG respectively. It can be clearly seen that both of the chromatograms were free of interfering peaks.

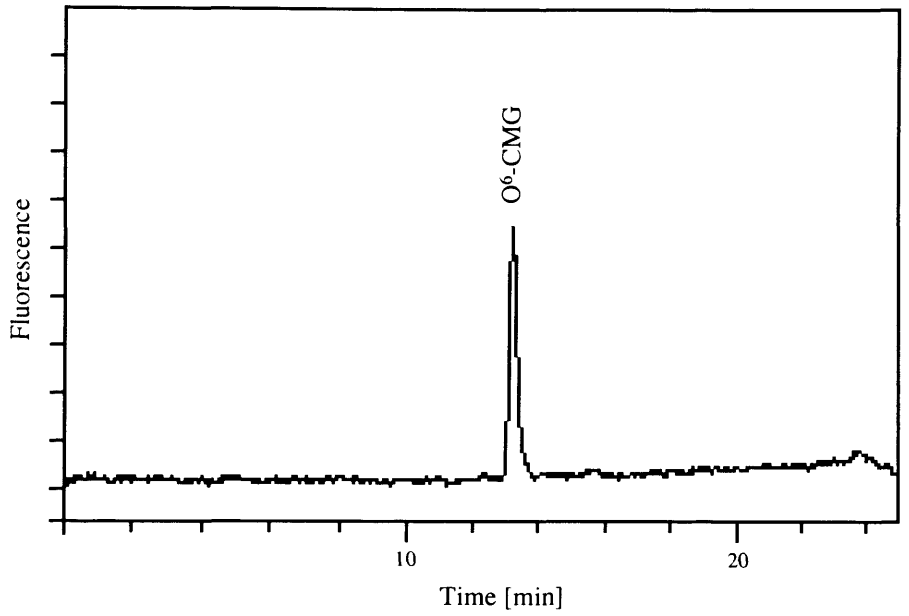

Figure 5.10: *HPLC chromatogram of O^6-CMG following enzymatic digestion and immunoaffinity purification of 8mM KDA-treated CT-DNA.* RP-HPLC separation was carried out using a Shandon, Hypersil BDS C18 (5μ, 4.6 mm x 25 cm) column and a flow rate of 1.0 ml/min, specifications and gradient are given in more detail in Section 2.3.1.1. Peaks were detected by fluorescence (λ_{Ex} 286 nm, λ_{Em} 378 nm).

Comparison of results acquired using all four techniques in a more quantitative manner showed that O^6-CMG levels seemed to vary depending on hydrolysis conditions (Figure 5.11). The most obvious observation, however, was that O^6-MeG was hardly detectable by three out of four techniques. As mentioned earlier, accurate detection of both O^6-alkylguanine adducts (O^6-MeG and O^6-CMG) appeared only feasible when DNA samples were purified using IACs (referred to as [ED-IAC] in Figure 5.11). With regard to the O^6-carboxymethyl adduct both methods using acid hydrolysis resulted in less O^6-CMG being detectable by HPLC fluorescence. Compared to enzymatic digestion followed by immunoaffinity purification, acid hydrolysis using formic acid [AH-FA] yielded 85% of the adduct. When HCl was used [AH-HCl] only 75% of the adduct were detectable by

HPLC fluorescence. Results acquired using enzymatic digestion and detection of O^6-alkyl-2'-deoxyguanosines [ED (no IAC)] correlated well with those obtained after immunoaffinity purification, though O^6-MedG was not detectable. Differences in O^6-CMG levels become more apparent as the recovery of both sets of IACs was assumed to be 100% at this stage and results presented in Figure 5.11 have not been corrected for it.

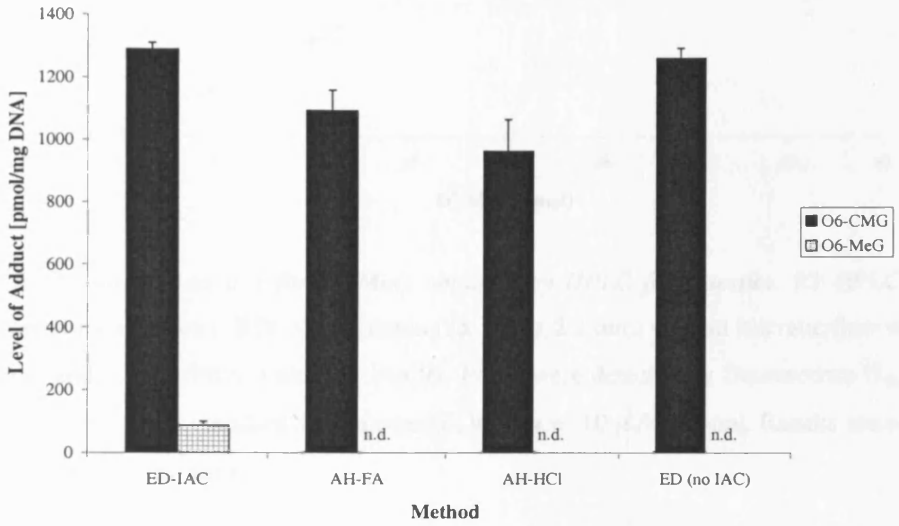

Figure 5.11: *Comparison of different methods for the detection of O^6-CMG and O^6-MeG.* CT-DNA was treated using 8mM KDA in PBS and analysed using the following methods: acid hydrolysis using 0.1M formic acid at 70°C for 1 h [AH-FA], acid hydrolysis using 0.1M HCl at 100°C for 30 min [AH-HCl], enzymatic digestion to dN [ED (no IAC)] or enzymatic digestion followed by IAC purification [ED-IAC].

5.2.5 Modulation of O^6-Alkylguanine Adduct Formation

Previously reported KDA treatments by Harrison et al. [Harrison (1999)] were usually performed in phosphate buffered saline (pH 7.3). In order to investigate whether methylation and carboxymethylation of DNA could be modulated using different buffer systems, CT-DNA was treated with 8mM KDA as described in Section 2.3.11. Aliquots of treated CT-DNA (24 μg) were digested to dN (Section 2.3.8) and purified using immunoaffinity columns as described in more detail in Section 2.3.9. Final analysis of both O^6-alkylguanine adducts was performed using HPLC fluorescence (Section 2.3.1.2, system 4). O^6-MedG samples, obtained after elution from the IAC, were hydrolysed to the base and compared to a calibration line ranging from 0.5 to 40 pmol O^6-MeG (Figure 5.12).

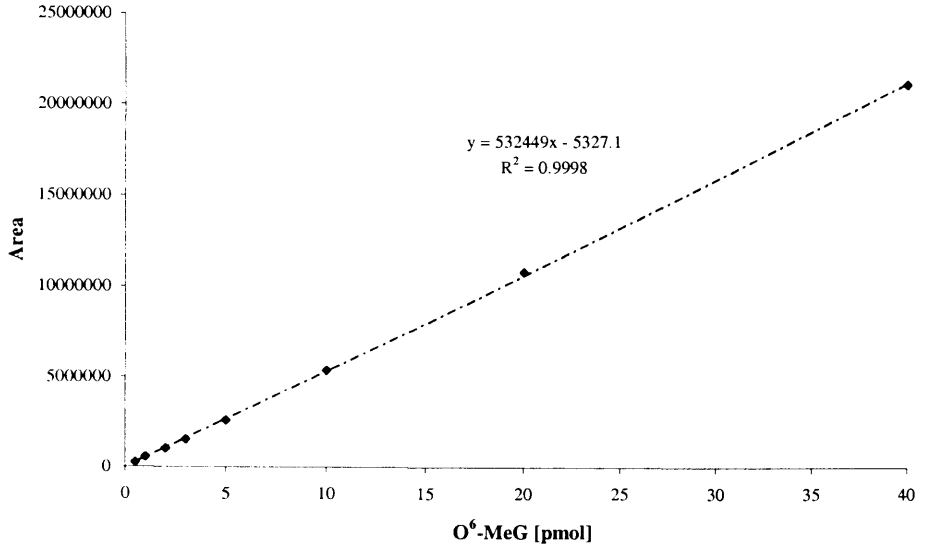

Figure 5.12: *Calibration line for O^6-MeG obtained by HPLC fluorescence.* RP-HPLC was performed using a Hypersil BDS C18 column (3μ, 100 x 2.1 mm) with an isocratic flow rate of 0.2 ml/min and 0.1% HFBA with 15% MeOH. Peaks were detected by fluorescence (λ_{Ex} 286 nm, λ_{Em} 378 nm). Each standard was injected in triplicate (10 μl/injection). Results shown are average ± standard deviation.

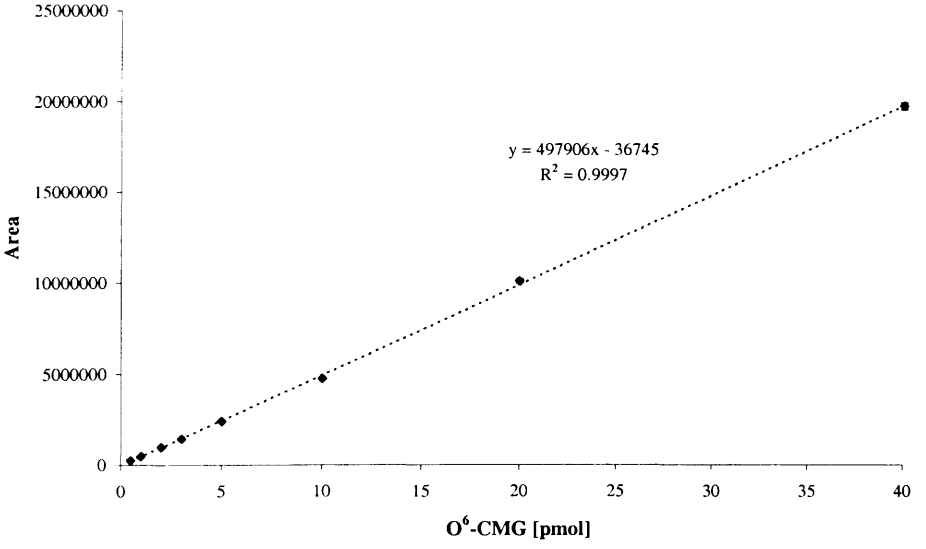

Figure 5.13: *Calibration line for O^6-CMG obtained by HPLC fluorescence.* RP-HPLC was performed using identical conditions described above for Figure 5.12.

As shown above, hydrolysis of the eluate obtained from IACs for O^6-CMdG was unnecessary as the base was acquired readily after fairly acidic elution conditions (1M

TFA). All samples were therefore compared to an appropriate calibration line ranging from 0.5 to 40 pmol O^6-CMG (Figure 5.13).

Since it had been discovered, while mimicking KDA treatments in plasmid, that relative proportions of O^6-CMG to O^6-MeG had been altered following incubations in Tris-EDTA (TE) buffer, the first comparison to be conducted was KDA treatments in either PBS or 1x TE buffer (10mM Tris, 1mM EDTA, pH 7.5). Results obtained after immunoaffinity purification and HPLC analysis are shown in Figure 5.14.

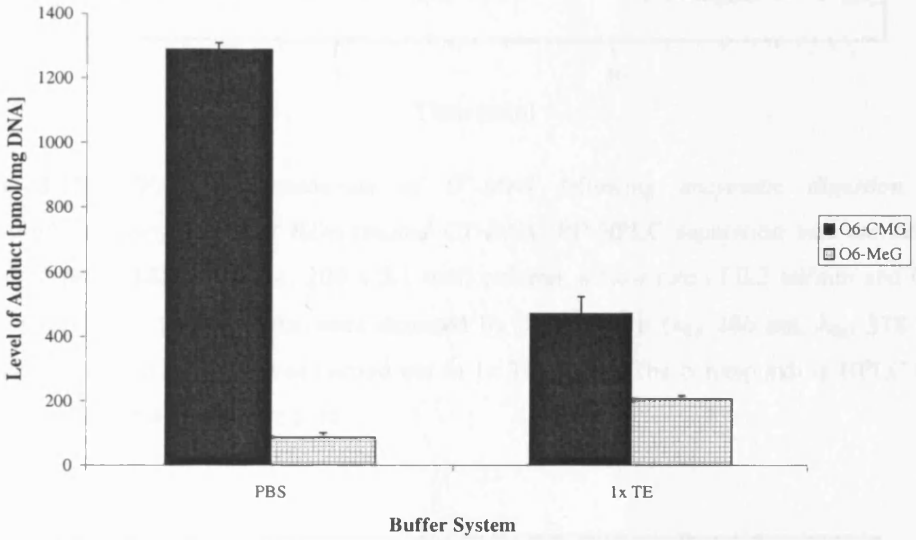

Figure 5.14: *O^6-CMG and O^6-MeG levels obtained after KDA treatment in PBS and 1x TE.* CT-DNA was treated overnight with 8mM KDA, the DNA was digested to nucleosides and purified using IACs. Both adducts were detected by HPLC fluorescence.

Major differences for O^6-alkylguanine adducts were observed following 8mM KDA treatment in PBS and 1x TE. Levels of O^6-MeG were increased following treatments in 1x TE buffer whereas O^6-CMG levels were decreased at the same time. The ratio of O^6-CMG to O^6-MeG was determined to approximately 14.7:1 in PBS, in 1x TE buffer the ratio was only 2.3:1. In PBS, 2.7 times more O^6-CMG was formed when compared to KDA treatments in TE buffer. In contrast to these findings, 2.4 times more O^6-MeG adduct was formed in 1x TE buffer as opposed to PBS. It appeared quite unlikely that the formation of both adducts was pH dependent as the pH of both buffer systems was very similar (pH_{PBS} 7.3 versus pH_{TE} 7.5).

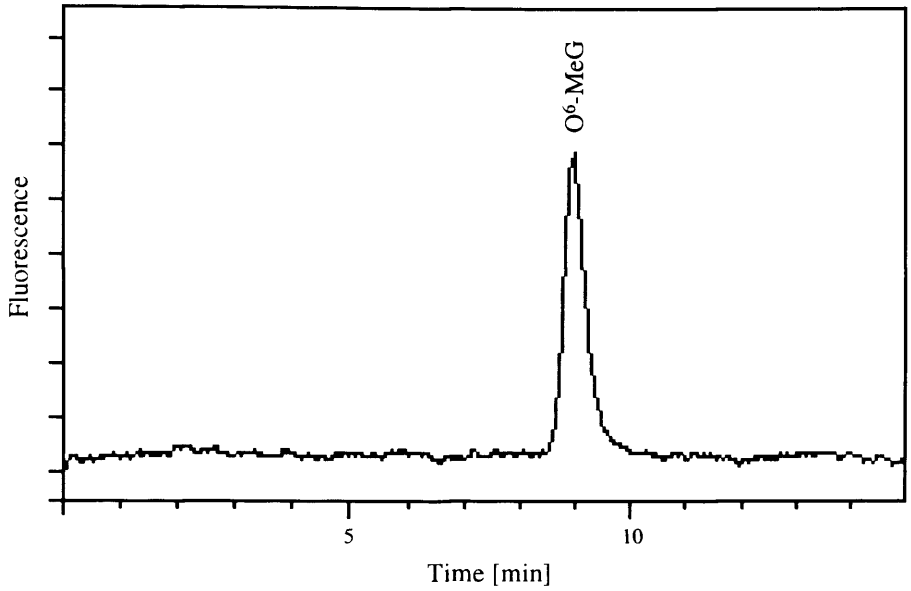

Figure 5.15: *HPLC chromatogram of O^6-MeG following enzymatic digestion and immunoaffinity purification of KDA-treated CT-DNA.* RP-HPLC separation was carried out using a Hypersil BDS C18 (3μ, 100 x 2.1 mm) column, a flow rate of 0.2 ml/min and 0.1% HFBA with 15% MeOH. Peaks were detected by fluorescence (λ_{Ex} 286 nm, λ_{Em} 378 nm). Treatment using 8mM KDA was carried out in 1x TE buffer. The corresponding HPLC trace for O^6-CMG is shown in Figure 5.16.

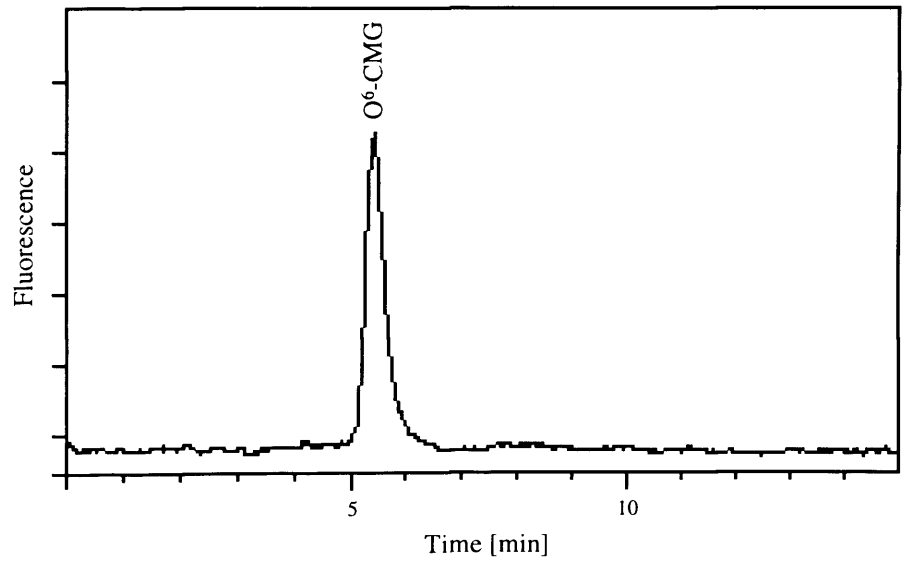

Figure 5.16: *HPLC chromatogram of O^6-CMG following enzymatic digestion and immunoaffinity purification of KDA-treated CT-DNA.* RP-HPLC separation was carried out as described in more detail in the above legend. The corresponding HPLC trace for O^6-MeG is shown in Figure 5.15.

HPLC chromatograms shown in Figure 5.15 and Figure 5.16 correspond to O^6-alkylguanine adducts formed after 8mM KDA treatment of CT-DNA. The treatment was carried out in 1x TE buffer overnight at 37°C. Peaks of O^6-CMG and O^6-MeG were detected by HPLC fluorescence following immunopurification of digested DNA.

In the following, modulation of O^6-CMG and O^6-MeG adduct formation was investigated using various different concentrations of Tris-EDTA. The pH remained the same (pH 7.5) and was corrected if necessary. The effect of 0.5x (5mM Tris, 0.5mM EDTA), 1x and 2x (20mM Tris, 2mM EDTA) TE buffer on carboxymethylation and methylation is shown in Figure 5.17.

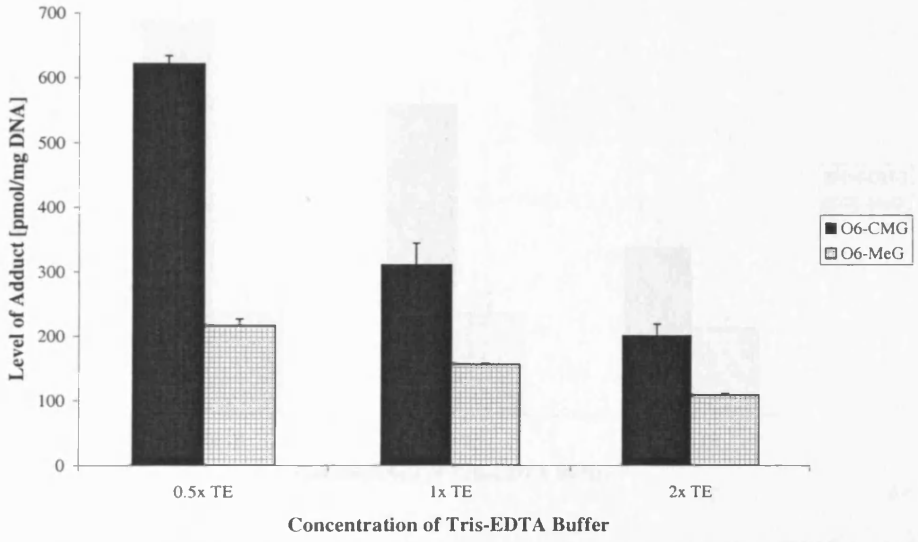

Figure 5.17: *Adduct levels obtained after KDA treatment in 0.5x, 1x and 2x TE.* CT-DNA was treated overnight with 8mM KDA, the DNA was digested to nucleosides and purified using IAC. Both adducts were detected by HPLC fluorescence.

Both carboxymethylation and methylation of DNA were highest in 0.5x TE buffer and lowest in 2x TE buffer. Ratio of O^6-CMG to O^6-MeG was 2.9:1, 2:1 and 1.8:1 for KDA treatments in 0.5x, 1x and 2x TE buffer respectively. When KDA treatments were performed using the least concentrated TE buffer, about three times more O^6-CMG was formed compared to 2x TE and approximately twice as much as in 1x TE buffer. Methylation showed a similar pattern, although to a lesser degree. Only twice as much O^6-MeG was formed in 0.5x TE buffer compared to the 4 times concentrated TE buffer, and just 38% more than in 1x TE buffer. The ratio of approximately 2:1 O^6-CMG to O^6-MeG adducts for 8mM KDA treatments in 1x TE buffer correlated relatively well with

findings observed for the previous experiment. However, absolute levels of both adducts were different.

Figure 5.18 shows the results obtained for 8mM KDA treatments in TE buffer with concentrations of the latter ranging from 0.05x (0.5mM Tris, 0.05mM EDTA) to 0.1x (1mM Tris, 0.1mM EDTA) and 0.5x Tris-EDTA buffer. The trend observed was similar to the one previously described i.e. the lower the TE concentration of the buffer system the higher the level of both O^6-alkylguanine adducts. However, the effect was less marked with regard to O^6-methylation.

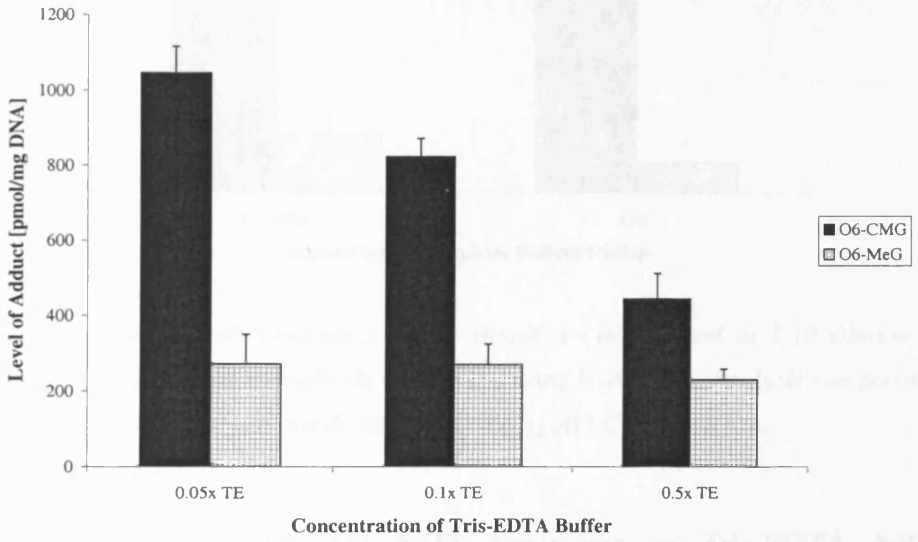

Figure 5.18: *Adduct levels obtained for KDA treatment in 0.05x, 0.1x and 0.5x TE buffer.* CT-DNA was treated overnight with 8mM KDA, the DNA was digested to nucleosides and purified using IAC. Both adducts were detected by HPLC fluorescence.

Both O^6-CMG and O^6-MeG levels were highest in 0.05x TE buffer and lowest in 0.5x TE buffer. Ratio of O^6-CMG to O^6-MeG was 3.8:1, 3:1 and 1.9:1 for treatments carried out in 0.05x, 0.1x and 0.5x TE buffer respectively. In 0.05x TE buffer, 2.3 times more O^6-CMG was formed compared to 0.5x TE and approximately 25% more than in 0.1x TE buffer. In contrast to that, almost identical amounts of O^6-MeG were formed in 0.05x and 0.1x TE buffer. The difference when compared to the KDA treatment in 0.5 TE buffer was approximately 18%. Standard deviations were relatively high especially for the methyl adduct when compared to previous data sets.

In the subsequent experiment the formation of O^6-CMG and O^6-MeG adducts was monitored for KDA treatments in PBS and its 1:10 dilution (Figure 5.19), pH of both buffer systems was identical.

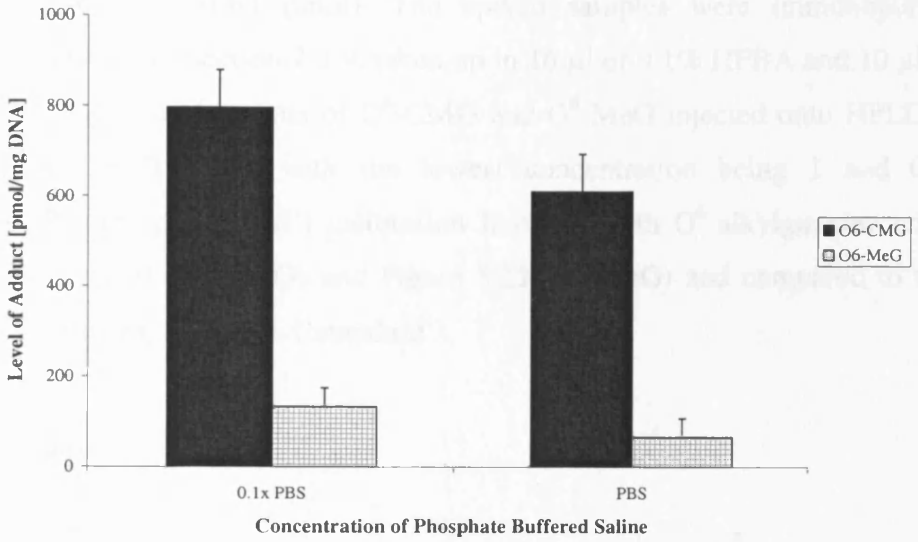

Figure 5.19: *Adduct levels obtained for KDA treatments in PBS and its 1:10 dilution.* CT-DNA samples were treated in duplicate o/n at 37°C using 8mM KDA. Analysis was performed also in duplicate using immunopurification followed by HPLC fluorescence.

Similar to observations made for KDA treatments in Tris-EDTA buffer, both carboxymethylation and methylation of the O^6-position of guanine were increased in the diluted PBS buffer system. The level of O^6-MeG almost doubled whereas the one for O^6-CMG increased by approximately 30% following 8mM KDA treatments in 0.1x PBS. Approximately 9 and 6 times more O^6-CMG adducts were formed when compared to O^6-MeG adducts for treatments in PBS and 0.1x PBS respectively.

5.2.6 Recovery of O^6-MedG and O^6-CMdG Immunoaffinity Columns

Results presented so far were not corrected for the recovery of immunoaffinity columns. New columns had been prepared for O^6-CMdG (as detailed in Section 2.3.6) prior to the analysis of results presented in Sections 5.2.4 and 5.2.5. These columns were tested prior to use. IACs for O^6-MedG were available from previous work described by Harrison et al. [Harrison (1998), Harrison (1999)]. The capacity of this set of columns had been determined to 500 ng (1.8 nmol) O^6-MedG, and the columns were shown to yield a linear

response for O^6-MeG between 0-15 pmol, with a recovery of approximately 79% [Harrison (1998)].

In order to determine the recovery of both sets of IACs 24 μg of CT-DNA were digested as usual using MN, CSPDE and NP1, and spiked with various amounts of O^6-MedG (0-32 pmol) and O^6-CMdG (0-64 pmol). The spiked samples were immunopurified and processed as detailed in Section 2.3.9, taken up in 16 μl of 0.1% HFBA and 10 μl analysed by HPLC fluorescence. Amounts of O^6-CMG and O^6-MeG injected onto HPLC equalled 0-40 pmol and 0-20 pmol, with the lowest concentration being 1 and 0.5 pmol, respectively. Resulting ('spiked') calibration lines for both O^6-alkylguanine adducts are shown in Figure 5.20 (O^6-CMG) and Figure 5.21 (O^6-MeG) and compared to respective calibration lines using standards ('standard').

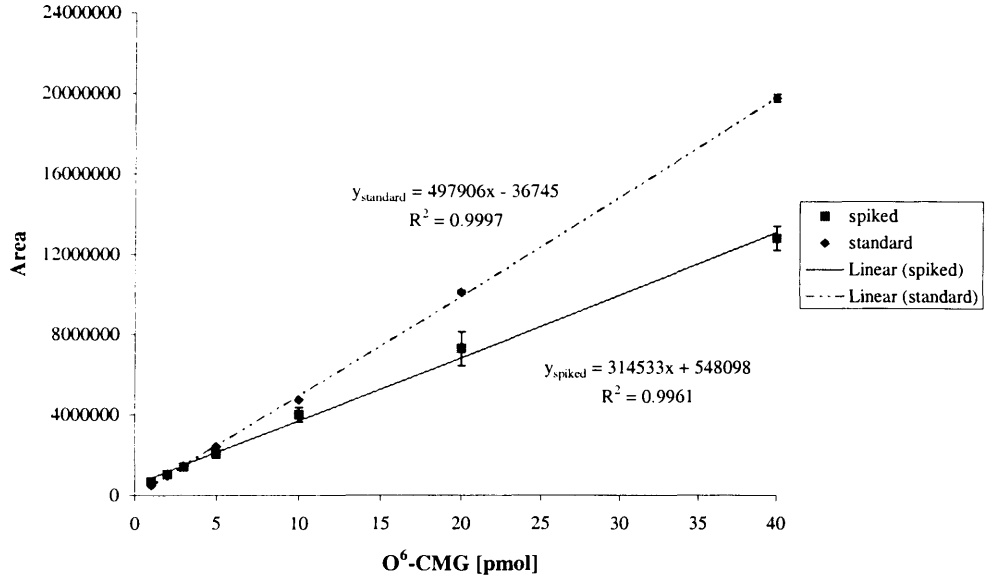

Figure 5.20: *O^6-CMG calibration lines generated using either O^6-CMdG spiked, digested CT-DNA samples or O^6-CMG standards.* 24 μg of CT-DNA were digested to dN, spiked with known amounts of O^6-CMdG, purified using immunoaffinity columns and analysed by HPLC fluorescence ('spiked'). Amounts given for O^6-CMG (x-axis) correlate to 15 μg of DNA being injected onto HPLC. The corresponding calibration line using O^6-CMG standards is also shown in above figure ('standard').

O^6-CMdG spiked DNA solutions yielded a linear response for the total range i.e. between 0-40 pmol O^6-CMG (per injection) and a recovery of approximately 75%. These findings correlated well with results obtained immediately after production of this set of O^6-CMdG columns (data not shown). O^6-CMG levels obtained for samples ranged from 3.4 to 28.9

response for O^6-MeG between 0-15 pmol, with a recovery of approximately 79% [Harrison (1998)].

In order to determine the recovery of both sets of IACs 24 μg of CT-DNA were digested as usual using MN, CSPDE and NP1, and spiked with various amounts of O^6-MedG (0-32 pmol) and O^6-CMdG (0-64 pmol). The spiked samples were immunopurified and processed as detailed in Section 2.3.9, taken up in 16 μl of 0.1% HFBA and 10 μl analysed by HPLC fluorescence. Amounts of O^6-CMG and O^6-MeG injected onto HPLC equalled 0-40 pmol and 0-20 pmol, with the lowest concentration being 1 and 0.5 pmol, respectively. Resulting ('spiked') calibration lines for both O^6-alkylguanine adducts are shown in Figure 5.20 (O^6-CMG) and Figure 5.21 (O^6-MeG) and compared to respective calibration lines using standards ('standard').

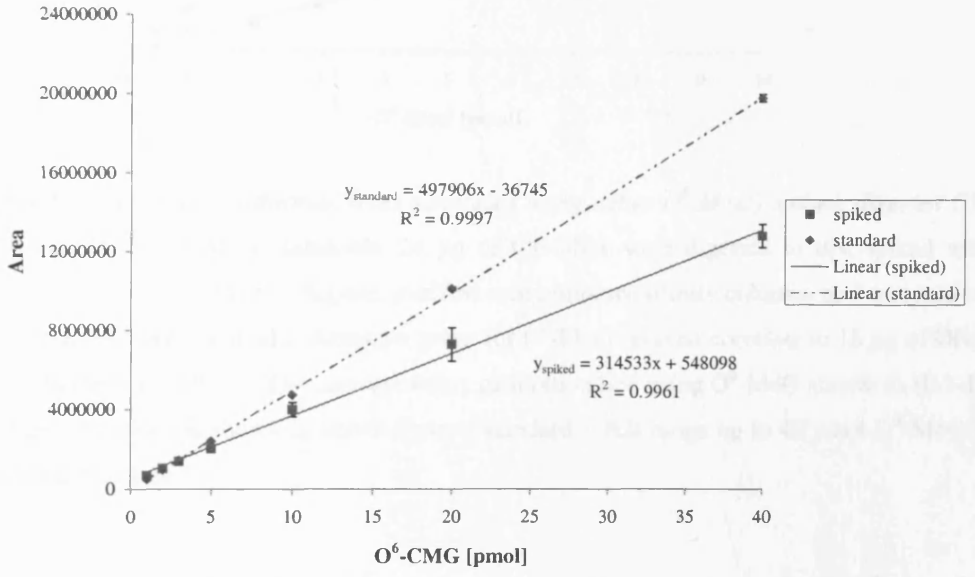

Figure 5.20: *O^6-CMG calibration lines generated using either O^6-CMdG spiked, digested CT-DNA samples or O^6-CMG standards.* 24 μg of CT-DNA were digested to dN, spiked with known amounts of O^6-CMdG, purified using immunoaffinity columns and analysed by HPLC fluorescence ('spiked'). Amounts given for O^6-CMG (x-axis) correlate to 15 μg of DNA being injected onto HPLC. The corresponding calibration line using O^6-CMG standards is also shown in above figure ('standard').

O^6-CMdG spiked DNA solutions yielded a linear response for the total range i.e. between 0-40 pmol O^6-CMG (per injection) and a recovery of approximately 75%. These findings correlated well with results obtained immediately after production of this set of O^6-CMdG columns (data not shown). O^6-CMG levels obtained for samples ranged from 3.4 to 28.9

pmol per injection when using the 'spiked' calibration line shown in Figure 5.20. Samples purified so far using these immunoaffinity columns were within the linear range and thus validated.

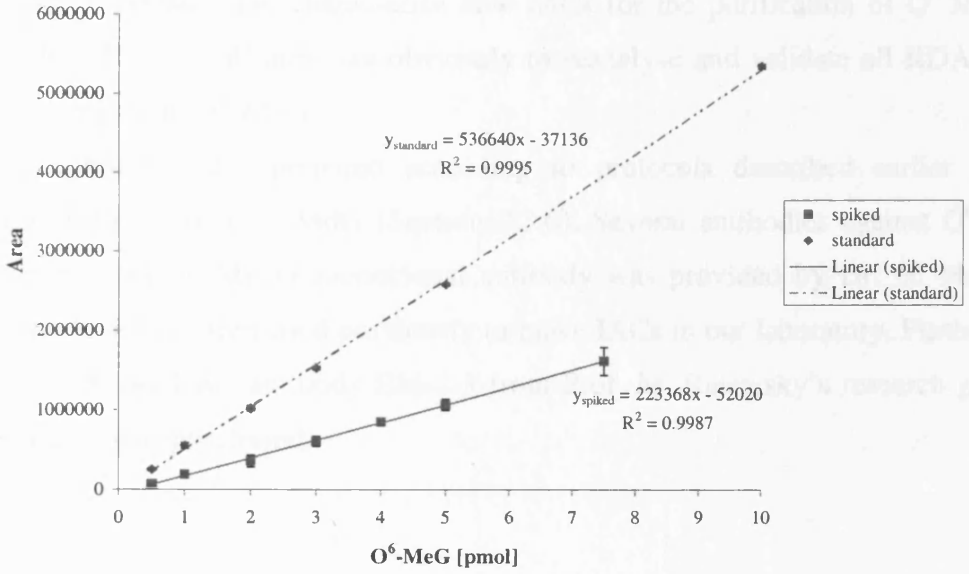

Figure 5.21: *O^6-MeG calibration lines generated using either O^6-MedG spiked, digested CT-DNA samples or O^6-MeG standards.* 24 μg of CT-DNA were digested to dN, spiked with known amounts of O^6-MedG (Sigma), purified using immunoaffinity columns and analysed by HPLC fluorescence ('spiked'). Amounts given for O^6-MeG (x-axis) correlate to 15 μg of DNA being injected onto HPLC. The corresponding calibration line using O^6-MeG standards (0.5-10 pmol per injection) is shown in above figure ('standard'), full range up to 40 pmol O^6-MeG is presented in Figure 5.12.

In contrast, linearity observed for O^6-MeG was limited in terms of range. O^6-MedG spiked DNA solutions resulted in a linear response only between 0 and 7.5 pmol O^6-MeG (per injection) and a recovery of approximately 40%. For concentrations of O^6-MedG higher than 12 pmol (i.e. 7.5 pmol O^6-MeG per injection), a similar area was detected by HPLC fluorescence as seen for 7.5 pmol O^6-MeG. These findings indicated a quite dramatic loss in recovery and linear range when compared to previously mentioned and published results [Harrison (1998)].

O^6-MeG levels obtained whilst using these immunoaffinity columns ranged from 1.5 to 9.9 pmol per injection using the 'spiked' calibration line shown in Figure 5.21 for calculations. Most data presented here were therefore still valid as only small amounts of DNA were injected onto HPLC (15 μg per sample). O^6-MeG levels could not be fully validated for

experiment No. III, i.e. KDA treatments in 0.05x, 0.1x and 0.5x TE buffer. O^6-MeG levels detected for these particular KDA treatments ranged between 8.4 and 9.9 pmol per injection and were thus outside the linear range.

It was therefore decided to leave results presented in Section 5.2.5 uncorrected for recovery and to prepare and characterise new IACs for the purification of O^6-MedG in DNA samples. The overall aim was obviously to reanalyse and validate all KDA-treated samples with regard to O^6-MeG.

Essentially columns were prepared according to protocols described earlier for the preparation of IACs for O^6-CMdG (Section 2.3.6). Several antibodies against O^6-MedG were evaluated. An O^6-MedG monoclonal antibody was provided by Dr. G. Margison, Manchester which had been used previously to make IACs in our laboratory. Furthermore, the O^6-MedG monoclonal antibody EM-2-3 from Prof. M. Rajewsky's research group in Essen, Germany was purchased.

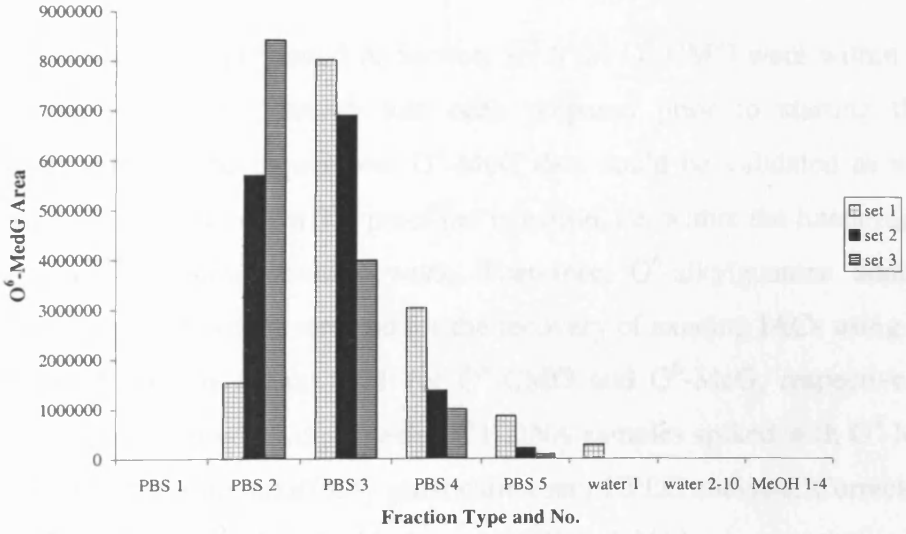

Figure 5.22: *Pattern of elution for three new sets of O^6-MedG immunoaffinity columns.* Columns were loaded with 40 pmol O^6-MedG, 1 ml fractions were collected, dried down and injected onto HPLC (no hydrolysis to O^6-MeG). Sum of areas obtained for individual fractions was approximately the same when comparing the three different sets shown above with each other. Fractions water 2-10 and MeOH 1-4 were only joined for demonstration purposes i.e. were collected and analysed individually.

Each set of columns was tested following preparation. O^6-MedG (40 pmol) was loaded onto the IAC and 1 ml fractions collected. Samples were normally dried down and

hydrolysed to O^6-MeG prior to HPLC analysis. However, for this experiment fractions were only dried down, and samples analysed immediately by HPLC. The sample, in this case the O^6-MedG standard, was applied in PBS/azide (PBS 1-5), followed by a water wash (water 1-10). Elution occurred using 80% MeOH (MeOH 1-4). Columns were then regenerated as usual using PBS/azide.

The elution pattern obtained for some of these columns is shown in Figure 5.22. In these particular cases the monoclonal antibody EM-2-3 had been used for the preparation. It can be clearly seen that all three sets of O^6-MedG IACs were not suitable for the analysis of KDA-treated DNA samples. O^6-MedG was not retained on any of the columns as shown. The majority of O^6-MedG was eluted almost immediately within the first five PBS fractions. The sum of O^6-MedG areas detected in all fractions, taking the injection volume into account, corresponded to 40 pmol indicating that no residual O^6-MedG remained bound to the IACs. After several unsuccessful attempts to generate new IACs for the purification of O^6-MedG in DNA this objective was abandoned.

As mentioned earlier, data presented in Section 5.2.5 for O^6-CMG were within the linear range (0-40 pmol) of IACs, which had been prepared prior to starting this work. Furthermore, except for one experiment O^6-MeG data could be validated as well. Most O^6-MeG adduct levels were below 7.5 pmol per injection, i.e. within the linear range, when using IACs available from previous work. Therefore, O^6-alkylguanine adduct levels presented in Section 5.2.5 were corrected for the recovery of existing IACs using equations shown in Figure 5.20 and Figure 5.21 for O^6-CMG and O^6-MeG, respectively. These equations had been generated using digested CT-DNA samples spiked with O^6-MedG and O^6-CMdG followed by immunoaffinity purification and HPLC analysis. Corrected results obtained for O^6-CMG and O^6-MeG adducts in [pmol/mg DNA] are presented in Table 5.3 and compared to previously obtained uncorrected levels.

Since the recovery of O^6-CMG and O^6-MeG IACs was not identical (75% and 40% respectively), taking the recovery for both columns into account obviously had quite a significant effect on absolute as well as relative adduct levels. In general, the correction did not have that great an impact on results obtained for O^6-CMG whereas the correction of O^6-MeG levels was quite substantial. A fairly pronounced effect was observed for the ratio of O^6-CMG to O^6-MeG adducts, with changes being influenced by the hugely different recoveries. Corrected as well as uncorrected ratios are presented in Table 5.4.

		Uncorrected Levels		Corrected Levels	
Exp. No.	Buffer	O^6-CMG	O^6-MeG	O^6-CMG	O^6-MeG
I	PBS	1289.6 ± 21.1	87.5 ± 13.7	1925.2 ± 33.4	221.6 ± 32.3
	1x TE	472.9 ± 53.2	207.0 ± 10.7	632.4 ± 84.3	506.7 ± 25.3
II	0.5x TE	622.8 ± 12.1	216.8 ± 10.4	893.0 ± 19.3	527.4 ± 24.9
	1x TE	311.5 ± 33.8	157.2 ± 1.6	399.9 ± 53.7	385.5 ± 3.8
	2x TE	201.3 ± 17.8	109.6 ± 3.4	225.7 ± 28.3	271.9 ± 8.6
III *	0.05x TE	1047.1 ± 70.5	272.0 ± 79.0	1564.7 ± 111.8	658.8 ± 188.8
	0.1x TE	825.7 ± 48.4	270.9 ± 54.8	1214.3 ± 76.8	656.0 ± 130.2
	0.5x TE	445.8 ± 67.6	230.0 ± 29.1	612.8 ± 107.1	558.7 ± 69.1
IV	PBS	612.4 ± 19.8	66.6 ± 3.0	881.6 ± 36.4	168.6 ± 9.0
	0.1x PBS	797.4 ± 83.1	134.0 ± 41.3	1135.4 ± 137.8	364.4 ± 85.5

Table 5.3: *Summary of all O^6-alkylguanine data, uncorrected and corrected for recovery of respective immunoaffinity columns.* Values for O^6-MeG and O^6-CMG above are given in [pmol/mg DNA]. Experiments marked with * could not be validated with regard to levels of O^6-MeG.

		Ratio O^6-CMG versus O^6-MeG	
Exp. No.	Buffer	Uncorrected	Corrected
I	PBS	14.7:1	8.7:1
	1x TE	2.3:1	1.2:1
II	0.5x TE	2.9:1	1.7:1
	1x TE	2.0:1	1.0:1
	2x TE	1.8:1	0.8:1
III *	0.05x TE	3.8:1	2.4:1
	0.1x TE	3.0:1	1.9:1
	0.5x TE	1.9:1	1.1:1
IV	PBS	9.2:1	5.2:1
	0.1x PBS	6.0:1	3.1:1

Table 5.4: *Relative proportion of O^6-CMG versus O^6-MeG adducts in KDA-treated CT-DNA, corrected and uncorrected for the recovery of respective IACs.* Ratios given in this table were calculated using O^6-alkylguanine adduct levels given in Table 5.3. Experiments marked with * could not be validated with regard to levels of O^6-MeG.

Relative proportions of O^6-CMG within individual treatments were not as dependent on correction for recovery, only minor changes were observed. Relative degree of O^6-methylation was also more or less independent of this correction.

For example, the following changes were observed for the first set of KDA treatments after correction of O^6-alkylguanine levels. The ratio of O^6-CMG to O^6-MeG (which had been 14.7 before correction) was determined to approximately 9:1 in PBS after correction. The extent of carboxymethylation and methylation was almost identical in 1x TE buffer post correction (1.2:1), whereas prior to correction the difference in O^6-alkylguanine adducts was greater than 2-fold. As expected, relative levels of individual adducts remained similar and virtually unaffected by the recovery of respective IACs. The extent of carboxymethylation was increased in PBS buffered conditions by 3 times when compared to 1x TE buffer post correction. Prior to correction, a 2.7-fold difference in the relative proportion of O^6-CMG levels had been observed. Similar observations were made for the degree of guanine methylation. Relative proportions changed from 2.4 prior to 2.3 after correction indicating that generally more O^6-MeG was formed in Tris-EDTA buffer.

5.3 Discussion

Several methods were re-evaluated for the detection of O^6-CMG and O^6-MeG, the main aim being initially the simultaneous detection of both adducts in KDA-treated plasmid pLS76 (see Chapter 6). It was confirmed that only immunopurification followed by HPLC fluorescence offered a selective and reliable method for the isolation of both O^6-alkylguanine adducts. Although more time consuming than acid hydrolysis or enzymatic digestion (without purification), immunopurification was necessary in order to be able to accurately detect O^6-MeG in particular. This was only feasible if the interfering unmodified bases or deoxynucleosides were eliminated prior to HPLC analysis.

Acid hydrolysis (using formic acid) was routinely applied by a colleague for the quantitation of O^6-CMG levels in KDA-treated CT-DNA. This CT-DNA was then used in the immunoslot blot assay for the detection of O^6-CMdG in gastric samples. In this particular study however, quantitation of O^6-MeG was not necessary. Furthermore, KDA concentrations for preparing the ISB standard ranged from 10 to 50mM making the detection of O^6-CMG by HPLC fluorescence using a Hypersil BDS C18 (5μ, 4.6 mm x 25 cm) column much more feasible and accurate [Singh (2000)].

Additionally, two different HPLC systems were evaluated. The application of a Hypersil BDS C18 (5μ, 4.6 mm x 25 cm) with a flow rate of 1.0 ml/min using a gradient of 0.1% HFBA and methanol offered the possibility of injecting increased amounts of digested

DNA without causing any overloading. The alternative HPLC system, which had been used as part of this study, consisted of a narrow bore Hypersil BDS C18 (3μ, 100 x 2.1 mm) column using an isocratic flow rate of 0.2 ml/min of 0.1% HFBA and MeOH (10-15%). In general, narrow bore columns improve chromatography by allowing the compound of interest to be concentrated in a relatively small volume of HPLC buffer, hence increasing the sensitivity. On detection the substance should be more concentrated in the flow cell of the respective detector and a narrower, sharper peak with increased height obtained. Another advantage of this system was that HPLC runs were less time consuming (15 min versus 25 min) i.e. samples were stored for less time in the autosampler thereby reducing the risk of sample degradation. Furthermore, columns with an internal diameter of 2.1 mm compared to 4.6 mm increase the sensitivity and use significantly less solvent.

The purification of both adducts from one sample was possible by allowing the eluate from the O^6-CMdG IAC to drip directly onto the IAC used for O^6-MedG purification (see Figure 5.3). Columns were then separated, as elution conditions used for O^6-CMdG were too severe for O^6-MedG. Elution of O^6-MedG using 1M TFA might cause demethylation of the more labile adduct. O^6-CMG was readily obtained following elution using TFA. The necessity of hydrolysis, i.e. depurination of O^6-CMdG, prior to HPLC analysis reported in the past [Harrison (1997)] could not be reproduced and was thus omitted. O^6-MedG was hydrolysed to its base prior to HPLC analysis using relatively mild acidic conditions.
New immunoaffinity columns were prepared successfully for the separation and purification of O^6-CMdG. O^6-CMdG spiked DNA solutions yielded a linear response for the total range i.e. between 0-40 pmol O^6-CMG (per injection) and a recovery of approximately 75%. Columns for the purification of O^6-MedG were still available from previous work. However, it was discovered after analysis of samples that the recovery was dramatically reduced. A linear response was observable within the range of 0, 0.5 to 7.5 pmol O^6-MeG (corresponding to 0, 0.8 to 12 pmol O^6-MedG spiked, digested DNA solutions). Recovery was approximately 40%. Higher concentrations up to 32 pmol O^6-MedG were also tested but yielded a similar fluorescence response as seen for 7.5 pmol O^6-MeG. These findings indicated a quite dramatic loss in recovery and linear range when compared to previously mentioned and published results. It was therefore decided to prepare new immunoaffinity columns for the purification of O^6-MedG in KDA-treated samples. Several different unsuccessful conditions and protocol modifications were tried in this endeavour. For example the separation of IgG from serum appeared unnecessary as no

precipitate was formed when using 40% ammonium sulphate solution. This step was thus omitted in subsequent attempts. Furthermore the cross-linker, dimethylpimelimidate, was purchased from different companies e.g. Pierce (usual supplier) and Sigma. As indicated before, two different monoclonal antibodies were also tested. The overall result was identical though with only the pattern of elution being slightly different. When using the monoclonal antibody kindly provided by Dr. G. Margison it appeared that at least some O^6-MedG was retained i.e. eluted in the first two MeOH fractions. The majority of O^6-MedG still remained unbound though indicating a very low binding capacity. Furthermore, columns initially looking very promising showed a sudden decrease in binding capacity after just a few runs.

Numerous ineffective attempts were undertaken and to date no satisfactory explanation has been found why the preparation of O^6-MedG IACs was not successful. This fact was even harder to comprehend as O^6-CMdG columns were prepared simultaneously to the first set of new O^6-MedG IACs (shown in Figure 5.22) using identical reagents and solutions. The linear range of this particular set of O^6-CMdG columns was identical to the ones previously used and characterised, and recovery almost identical. The elution pattern was also as expected (not shown), with the majority of O^6-CMdG eluting as O^6-CMG in TFA fraction 1 and 2. Although this new set had been prepared the columns were in fact never used for the purification of O^6-CMdG as the previous set was still working well.

Adduct levels detected in KDA-treated DNA samples were corrected for the recovery of O^6-CMdG and O^6-MedG columns, the latter being available from previous work. Columns used for the purification of O^6-CMdG had been prepared at the beginning of this project. After taking the recovery into account, 8mM KDA-treated CT-DNA samples exhibited values for O^6-CMG and O^6-MeG ranging from 3.4 to 28.9 and 1.5 to 9.9 pmol per injection (15 μg) respectively. Values obtained for the carboxymethyl adduct were fully validated as the linear range of corresponding IACs was 0-40 pmol O^6-CMG. With regard to the methyl adduct most data could be validated with the exception of levels obtained for KDA treatments carried out in 0.05x, 0.1x and 0.5x Tris-EDTA buffer. O^6-MeG levels detected for these treatments were relatively high in comparison to other conditions. Levels observed following 8mM KDA treatments in these particular buffer systems were 9.9 ± 2.8 (0.05x TE), 9.8 ± 2.0 (0.1x TE) and 8.4 ± 1.0 (0.5x TE) pmol O^6-MeG per 15 μg. Standard deviations determined for these particular samples were also unusually high. On average

standard deviations observed for other treatments were approximately ± 0.4 pmol per 15 μg injection. Nevertheless, standard deviations noticed for O^6-CMG using these particular dilutions of Tris-EDTA were also relatively high (Table 5.3) possibly indicating poor reproducibility of KDA treatments.

A question which cannot be answered retrospectively is why O^6-MeG levels higher than 7.5 pmol per injection could be measured in the first place despite them clearly exceeding the linear range. When the immunoaffinity columns were tested for recovery 7.5 pmol O^6-MeG was the highest level measurable. A possible explanation of this phenomenon could be that the capacity of O^6-MedG immunoaffinity columns decreased dramatically just prior to recovery determination. It is therefore vital to test immunoaffinity columns relatively frequently most certainly prior and post to usage in order to ensure comparability and full validity of results.

An approach for the detection of O^6-alkylguanine adducts which could avoid this necessity and/or the risk of changes in column capacity during experiments is to digest KDA-treated CT-DNA samples to 2'-deoxynucleosides. The technique would then incorporate two separate HPLC separations. In the first run, DNA digests could be analysed using for example a Hypersil BDS C18 (5μ, 4.6 mm x 25 cm) and conditions described previously. The appropriate adducts peaks could be collected during this separation. In a second HPLC separation both O^6-alkylguanine adducts could then be analysed and quantitated. This methodology could help to overcome the presence of much higher amounts of normal nucleosides but might also lead to some losses during sample collection and processing.

Comparison of several KDA treatments, which had been carried out using the same buffer system but at different times, showed that absolute levels of O^6-alkylguanine adducts were not reproducible (Table 5.3). Treatments carried out simultaneously were reproducible though as reflected in the relatively low standard deviations for both adducts.

In general, treatments carried out at a later stage exhibited lower adduct levels which might indicate a certain instability of the KDA stock upon storage at -80°C. Furthermore it was noted that the accurate determination of KDA concentrations was relatively difficult as the compound decomposed within seconds in neutral solutions (PBS). Experiments using a spectrophotometer (λ_{max} 249 nm, ε 10050) showed that the accurate determination of KDA was only feasible in alkaline solution (1M KOH, other alkaline dilutions were not tested). It was therefore essential for future treatments (of plasmid pLS76) that the KDA stock

solution was not only frozen in small aliquots but its concentration also confirmed frequently.

Ideally, KDA treatments in various buffer systems should have been carried out simultaneously for better and valid comparison of absolute levels. Unfortunately, as this was not the case in earlier presented experiments, only samples treated at the same time could be compared with each other. Comparison of O^6-CMG to O^6-MeG ratios showed that in some cases these could not be reproduced. The relative proportion of O^6-alkylguanine adducts observed for KDA treatments carried out in 1x TE buffer but at different times was very similar. However, the ratio differed quite dramatically when comparing KDA treatments in PBS. It appeared likely that the ratio of O^6-CMG to O^6-MeG was not only dependent on the buffer system but also on the absolute concentration of KDA and also possibly DNA. KDA degraded to some extent upon storage and determination of its concentration was only feasible in alkaline conditions. These points as well as the fact that the compound was very unstable in neutral solutions might explain differences observed between individual experiments.

Despite the drawbacks mentioned above, studies carried out on O^6-alkylation using KDA showed that it was possible to modulate carboxymethylation and methylation using different buffer systems. Tris-EDTA seemed to reduce the extent of carboxymethylation and increase methylation at the same time when compared to the reaction in PBS, via so far unknown mechanisms. O^6-CMG and O^6-MeG were formed to a similar extent when KDA treatments were carried out in 1x TE buffer (considering adduct levels obtained after correction for IAC recovery), whereas in PBS the reaction was in favour of O^6-CMG adducts.

Increasing TE concentrations tended to reduce the total amount of O^6-alkyl DNA damage. The lower the TE concentration, the more O^6-CMG and O^6-MeG was formed (when compared to higher concentrations of the same buffer). Furthermore the degree of damage was more extensive for treatments that had been carried out in PBS instead of 1x TE buffer. One possible explanation could be that Tris-EDTA buffer was likely to react with the alkylating agents generated from KDA in a similar way as DNA bases, Tris being a primary amine. Furthermore, the ratio of O^6-CMG to O^6-MeG changed with TE concentration suggesting that there was an additional effect on the pathway that led from carboxymethylating to methylating agent.

Additionally to these findings increasing PBS concentrations were shown to have a similar effect on DNA alkylation i.e. a reduction in total amount. Since no Tris was involved in this particular case there had to be another, additional explanation for this reduction of total O^6-alkyl DNA damage.

A factor which might play an important role in the modulation and formation of O^6-alkylguanine adducts is the ionic strength of the buffer system. Carboxymethylation and methylation were both shown to be increased in diluted buffer systems. Observations were made for various, diluted Tris-EDTA buffer systems as well as a 1:10 dilution of PBS. The ionic strength I of a buffer is defined as [Kunze (1990)]:

$$I = \frac{1}{2} (c_1 z_1^2 + c_2 z_2^2 + ... + c_n z_n^2) = \frac{1}{2} \Sigma c_i z_i^2$$

the summation being continued over all the different ionic species in the solution, where I is the ionic strength, z is the charge on the ionic species, and c is the molar concentration in [mol/l].

One approach to explore this theory would be to keep the ionic strength of buffer systems investigated constant e.g. through addition of neutral salts. For example in addition to PBS or Tris-EDTA sodium chloride could be added to the buffer system prior to KDA treatment thus standardising the ionic strength. If the ionic strength plays an important role in the modulation of O^6-alkylguanine adducts, levels observed for O^6-CMG and O^6-MeG should be identical or at least similar.

The quite dramatic manipulation of relative proportions of two mutagenic lesions arising from a common alkylating agent offered a rather unique situation and possibility especially with respect to KDA-induced p53 mutations. Therefore, KDA treatments were carried out in Tris-EDTA buffer as well as phosphate buffered saline in order to observe the effect of different proportions of O^6-alkylguanine adducts on the p53 mutational spectrum. In general, PBS favoured O^6-carboxymethylation whereas in Tris-EDTA equal amounts of O^6-CMG and O^6-MeG were formed. Adduct data as well as p53 mutational spectra obtained for KDA treatments of plasmid pLS76 in PBS and 1x TE buffer are presented in Chapter 6.

6 KDA- and MDA-Induced p53 Mutations

6.1 Introduction

One of the most frequently encountered genetic events in human malignancy is alteration of the p53 gene and its encoded protein [Friend (1994)]. The p53 gene has been implicated in many sporadic and inherited forms of human cancer. In normal cells, p53 protects DNA from insults as varied as drugs and radiation. This protection is achieved by co-ordinately blocking cell proliferation, stimulating DNA repair and promoting apoptotic cell death [King (1996)].

Interpretation of mutational spectra induced by carcinogens provides valuable information about the contribution of specific aetiologic factors in the development of human cancer. Sometimes epidemiological and experimental data link a causative factor to the development of a particular type of cancer. Specific mutational p53 spectra have been reported for skin tumours in individuals exposed to UV [Brash (1996)], liver tumours from people with exposure to dietary aflatoxin B_1 [Montesano (1997)] and for lung cancer in smokers [Hernandez-Boussard (1998)]. Usually however, there is a multitude of contributors to most types of cancer (including colon and gastric malignancies) making the identification of a link or (single) causal risk factor far more complicated if not impossible.

More than 80% of p53 mutations are missense mutations causing one amino acid to be substituted for another, usually altering protein conformation, and causing nuclear accumulation. Point mutations observed in p53 are exceptionally diverse in their localisation and nature. This led to a significant interest in the possibility that mutational spectra might offer information about the aetiology and molecular pathogenesis of human cancer. A database of point mutations was initiated in 1990 and has since been much further developed. To date the p53 mutation database at the International Agency for Research on Cancer (IARC) in Lyon, France, contains approximately 15121 somatic mutations, 196 germline mutations and a list of polymorphisms. This database offers the unique opportunity to identify and link mutations induced by a certain carcinogen *in vitro* to those observed in human cancer and thereby to possibly identify a causative factor.

The ability of the p53 protein to activate transcription is tightly linked with its tumour suppressor activity and is also its critical function. Mutations observed in tumours abolish this activity. In general, functional assays for p53 mutations test transcriptional competence.

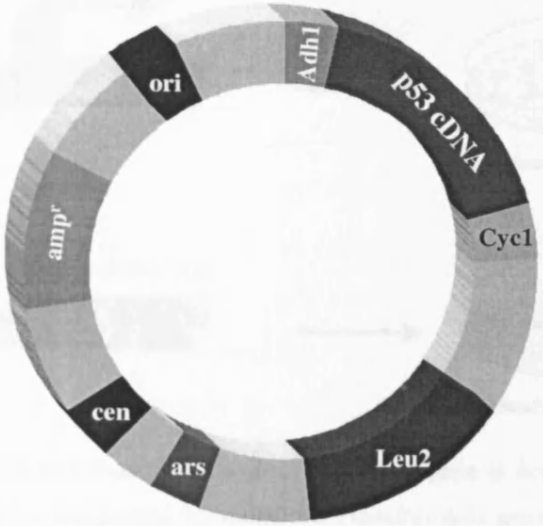

Figure 6.1: *pLS76 p53 yeast expression vector.* The p53 expression vector was first described and constructed by Ishioka et al. [Ishioka (1993)]. The vector harbours human wild-type p53 cDNA under the control of an ADH1 promotor and the LEU2 gene as a selectable marker (picture courtesy of P. Burns).

The yeast expression vector pLS76 illustrated in Figure 6.1 was first described and constructed by Ishioka et al. [Ishioka (1993)]. Plasmid pLS76 contains the human p53 cDNA coding sequences expressed from the ADH1 constitutive promoter and the LEU2 gene as a selectable marker. The vector also contains the CYC1 terminator downstream of the p53 cDNA, CEN6 and ARSH4 for stable low copy number replication.

Flaman et al. [Flaman (1995)] developed a functional assay for the detection of p53 mutations in which human p53 expressed in the haploid *Saccharomyces cerevisiae* strain yIG397 activates/controls transcription of the ADE2 gene as illustrated in Figure 6.2 and Figure 6.3. Yeast cells containing wild-type p53 express ADE2, and form white and normal sized colonies on plates containing limited adenine. On the contrary, cells containing mutant p53 fail to express the ADE2 gene. As a consequence of adenine being limiting for growth, relatively small, red colonies are formed. The red colouring observed in these colonies originates from a build-up of an intermediate metabolite of adenine metabolism.

The yeast-based p53 functional assay was used to select mutants based on a key function of the p53 protein. A defect in transactivation ability validated the method for its use for mutagenesis studies [Pietenpol (1994), Ory (1994)].

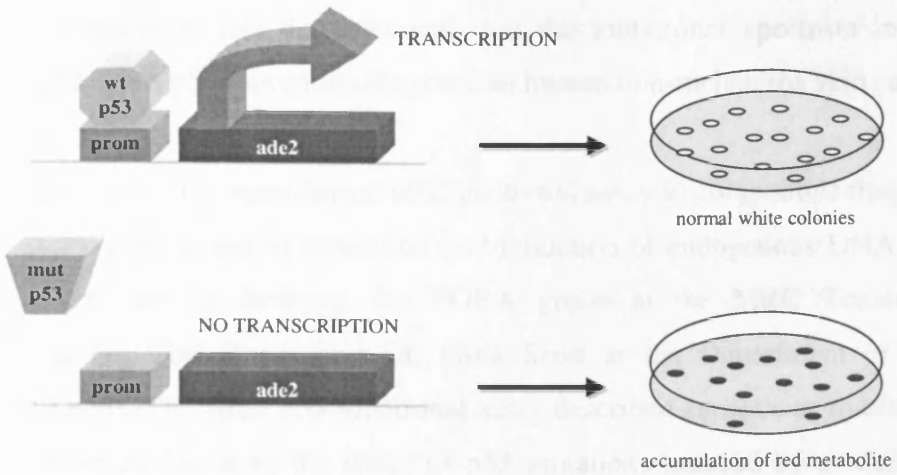

Figure 6.2: *Yeast-based p53 Functional Assay.* The ADE2 gene is not expressed if the p53 transactivation function is inactivated by mutation. Transformants are selected on plates that lack leucine but contain sufficient adenine for adenine auxotrophs to grow and turn red due to build-up of an intermediate metabolite. Mutant clones appear as small red colonies against the background of white adenine prototrophs (picture courtesy of P. Burns).

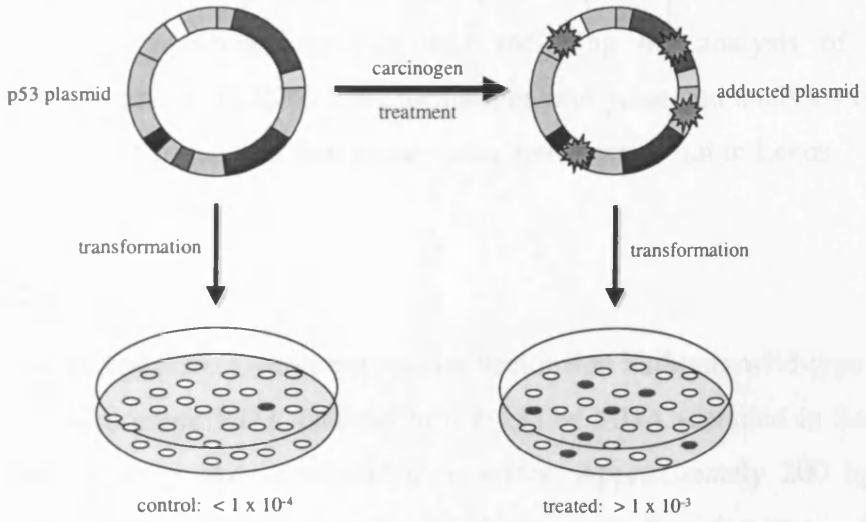

Figure 6.3: *p53 mutation induction.* The yeast expression vector that harbours wild-type p53 cDNA is treated *in vitro* with carcinogens e.g. KDA or MDA and transfected into the *Saccharomyces cerevisiae* yeast strain yIG397 containing the ADE2 gene regulated by a p53-responsive promotor (picture courtesy of P. Burns).

This assay was applied recently to the analysis of p53 mutational spectra induced by the antineoplastic drug chloroethyl-cyclohexyl-nitroso-urea (CCNU) [Inga (1997), Inga (1995)]. Another mutagenesis study [Inga (1998)] using the same assay investigated the

effect of UV irradiation and demonstrated that the mutational spectrum in yeast was indistinguishable from p53 mutations observed in human non-melanoma skin cancer.

It was decided to apply the yeast-based p53 functional assay to compounds frequently used in our laboratory with regard to formation and induction of endogenous DNA adducts. A collaboration was set up between the FORA group at the MRC Toxicology Unit (Leicester) and Dr. Phil Burns and Dr. Gina Scott at the Department of Pathology, University of Leeds. The yeast p53 functional assay described earlier was routinely applied in their laboratory in Leeds to the study of p53 mutations induced by a wide variety of mutagens. The aim of the collaborative project was to investigate KDA- and MDA-induced p53 mutational spectra and to compare them with the IARC p53 mutation database (version R5, June 2001) [Hernandez-Boussard (1999)]. It was hoped to establish a link between *in vitro* data and certain types of human cancer. Additionally, the effect of KDA treatment conditions i.e. buffer systems (PBS versus Tris-EDTA) was investigated on p53 mutational spectra. *In vitro* treatments of the yeast expression vector containing human wild-type p53 were performed in Leicester including the analysis of M_1-dG and O^6-alkylguanine adducts in pLS76. Transformations into yeast and analyses of mutational spectra using the yeast-based p53 functional assay were carried out in Leeds.

6.2 Results

Aliquots of plasmid pLS76, a yeast expression vector that harbours wild-type p53 cDNA, were treated *in vitro* using KDA (see Section 2.4.1) or MDA (detailed in Section 2.4.2), purified by precipitation and resuspended in water. Approximately 200 ng of treated plasmid were transformed into yeast cells (*Saccharomyces cerevisiae*, strain yIG397) by a lithium acetate procedure (described in Section 2.4.4). The transformants were incubated at 35°C on minimal medium agar plates supplemented with a limiting concentration of adenine (MM+ade5) for 3 to 5 days. On minimal medium containing limiting amounts of adenine but lacking leucine, colonies expressing wild-type p53 were white but colonies lacking functional p53 were red due to build-up of a metabolite of adenine biosynthesis. Mutant red colonies were picked from these primary transformation plates and sub-cultured on supplemented minimal medium to confirm their mutant phenotype. Single colonies were picked from these plates and grown overnight in minimal medium containing excess adenine (MM+ade200). Plasmid was rescued from these cultures using a

phenol-chloroform based DNA extraction procedure (see Section 2.4.5) and the p53 cDNA was PCR amplified with one of the primers having biotin attached at the 5' end (Section 2.4.6).

Consequently, single-stranded DNA could be separated using uniform, superparamagnetic, polystyrene beads with streptavidin attached covalently to the bead surface as described in Section 2.4.7. Codons 90 to 290 of the PCR products were sequenced on solid phase (Dynabeads) using an ABI prism dRhodamine dye terminator cycle sequencing kit and an ABI 377 DNA sequencer (see Section 2.4.8). The resulting sequences were analysed using ABI Prism Sequence Navigator software. The KDA- or MDA-induced mutations that were identified were then compared to the IARC p53 mutation database [Hernandez-Boussard (1999)]. Only mutations between codons 90 and 290 in the IARC database were considered for analyses and comparison to the *in vitro* induced spectra. In general, GC→AT transitions at CpG sites were not taken into account unless stated otherwise as these base pair substitutions are believed to originate from spontaneous deamination of 5-methylcytosine [Ehrlich (1981)].

6.2.1 KDA-Induced p53 Mutations in Plasmid pLS76

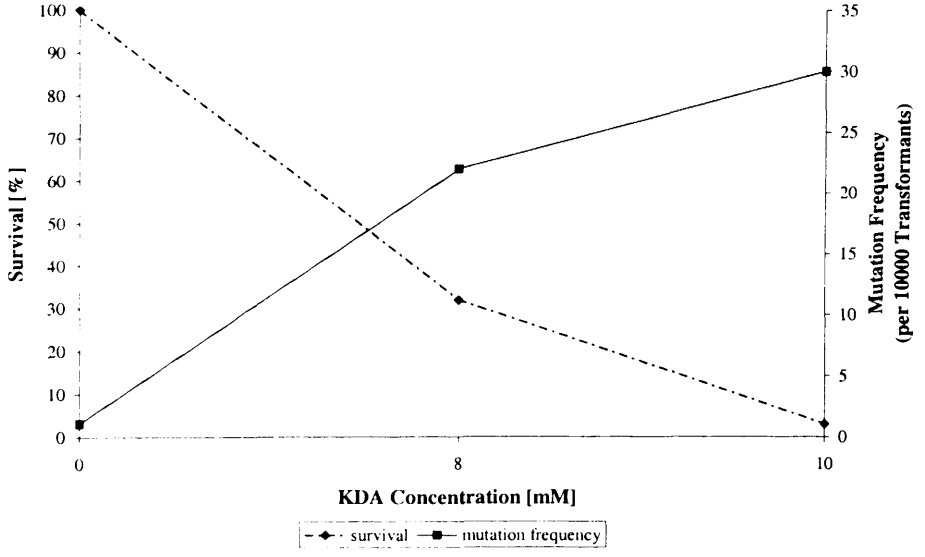

Figure 6.4: *Mutation frequency and survival rate in undamaged and damaged pLS76 after KDA treatment in 1x TE buffer.* Plasmid pLS76 was treated using 8 and 10mM KDA overnight at 37°C. Survival represents the total number of colonies obtained for treated samples divided by the number of colonies on control plates. Mutation frequency indicates the number of red colonies compared to the number of total colonies.

Since it had been shown earlier that adduct levels of O^6-CMdG and O^6-MedG could be modulated quite dramatically using different buffer systems, *in vitro* KDA treatments of plasmid pLS76 were carried out in 1x TE buffer and PBS.

Survival and mutation frequency obtained for controls and KDA treatments in 1x TE buffer are displayed in Figure 6.4. Survival represents the total number of colonies obtained for treated samples divided by the number of colonies on control plates. The mutation frequency indicates the number of red colonies compared to the number of total colonies. A dose-dependent decrease in survival and increase in mutation frequency were observed. For 8mM KDA treatment in 1x TE buffer a survival rate of 32% was observed whereas the survival was only about 3% for 10mM KDA indicating a steep decline of survival. The mutation frequency was increased 20-fold following incubation with 8mM KDA and 27-fold above background level after 10mM KDA treatment in 1x TE buffer.

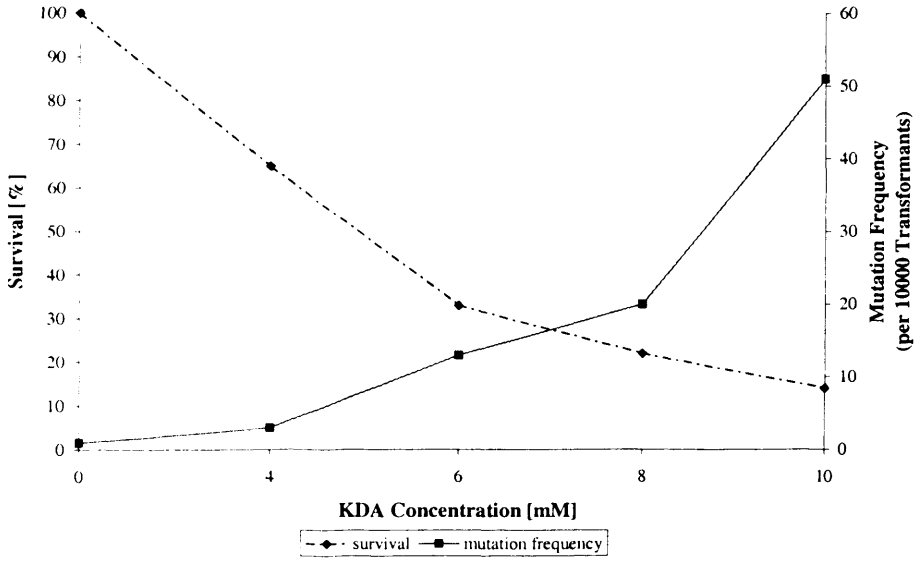

Figure 6.5: *Mutation frequency and survival rate in undamaged and damaged pLS76 after KDA treatment in PBS.* Plasmid pLS76 was treated using 4, 6, 8 and 10mM KDA overnight at 37°C.

Similar to above described observations, a dose-dependent decrease in survival and increase in mutation frequency were observed for KDA treatments of pLS76 in PBS (Figure 6.5). The survival rate decreased to 65% for 4mM KDA treatment and down to 14% for the highest concentration of KDA (10mM). The mutation frequency was increased 22-fold following incubation with 8mM KDA and 55-fold above background level after 10mM KDA treatments in PBS.

Differences between the two treatment buffers were mainly observed when comparing the survival rate and mutation frequency obtained for the highest concentration of KDA. Higher survival and mutant frequency ratio were observed for 10mM KDA treatments in PBS when compared to TE buffer. In PBS the mutation frequency was approximately twice as high as the one observed for KDA treatments at an equimolar concentration in 1x TE buffer. Simultaneously, the survival was increased by almost 5-fold, 14% versus 3% observed in PBS and 1x TE respectively. In contrast to these observations, the increase in mutation frequency was similar when comparing 8mM treatments, survival differed slightly though. In fact a 1.5-fold higher survival rate was observed for KDA treatments carried out in 1x TE.

Subsequent 8mM KDA treatments of plasmid pLS76 were carried out several times in parallel in order to obtain enough mutants for p53 analysis. Some of the KDA-treated aliquots and appropriate controls were kept for the determination of O^6-alkylguanine adducts. Samples were digested and immunopurified as described earlier (Section 2.3.9) and analysed by HPLC using a Hypersil BDS C18 column (3μ, 100 x 2.1 mm), 0.1% HFBA containing 15% MeOH as the mobile phase and an isocratic flow rate of 0.2 ml/min. Results shown in Figure 6.6 are corrected (post) and uncorrected (prior) for the recovery of appropriate IACs.

Taking the recovery into account, levels of O^6-alkylguanine adducts (O^6-CMdG and O^6-MedG) were almost identical for 8mM KDA treatments carried out in 1x TE buffer. In contrast to this, O^6-CMdG levels were approximately 13 times higher when compared to O^6-MedG levels obtained for treatments carried out in PBS. A 4-fold increase was observed for methylation at the O^6-position of guanine following KDA treatments in 1x TE whereas the extent of carboxymethylation was decreased. Approximately 4 times more O^6-CMdG was formed subsequently to treatments in PBS when compared to carboxymethyl adduct levels obtained for TE buffer.

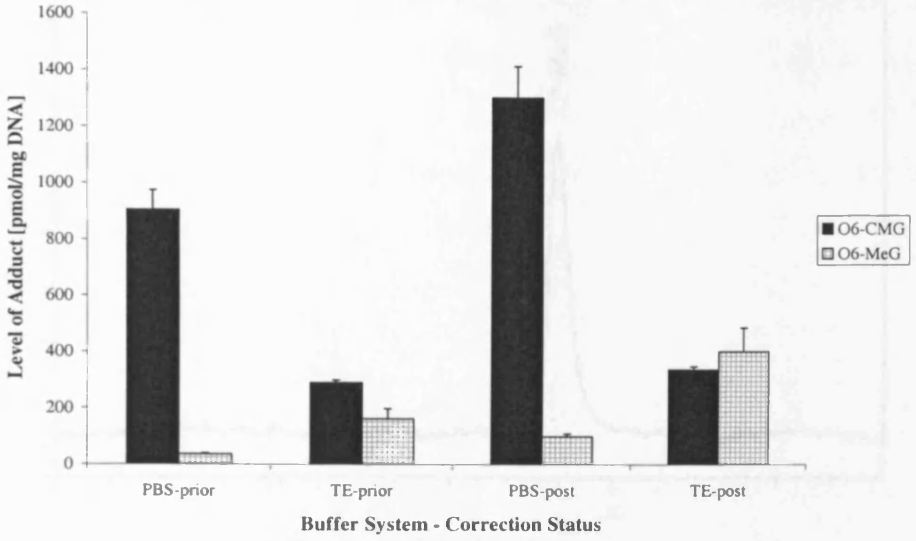

Figure 6.6: *Level of O^6-alkylguanine adducts in plasmid pLS76 following 8mM KDA treatment.* Samples (24 μg; duplicate treatments/controls were analysed at least in duplicate) were purified after digestion to dN using IACs. RP-HPLC was performed using a Hypersil BDS C18 column (3μ, 100 x 2.1 mm), 0.1% HFBA containing 15% MeOH as the mobile phase and an isocratic flow rate of 0.2 ml/min. An equivalent of 15 μg pLS76 in 10 μl 0.1% HFBA was injected onto the HPLC system. Peaks were detected by fluorescence (λ_{Ex} 286 nm, λ_{Em} 378 nm). Levels shown for both adducts are uncorrected (prior) and corrected (post) for recovery of respective IACs.

Typical HPLC traces obtained for KDA-treated plasmid pLS76 are shown in Figure 6.7 and Figure 6.8 for O^6-MeG and O^6-CMG respectively. In this particular case, 8mM KDA treatments had been carried out overnight at 37°C in 1x TE buffer. An equivalent of 15 μg plasmid was injected onto the HPLC system. Adduct peaks were detected by HPLC fluorescence and corresponded to O^6-alkylguanine adduct levels of approximately 336.8 pmol O^6-CMG and 402.1 pmol O^6-MeG per mg of plasmid (corrected for recovery of IACs). Levels in [pmol/mg] correlate to about 104 O^6-CMG and 124 O^6-MeG adducts per 10^6 normal nucleotides. Retention times of O^6-alkylguanine adducts were observed to approximately 5.5 min and 9.2 min for O^6-CMG and O^6-MeG respectively.

The level of O^6-alkylguanine modification based on the length of the p53 coding sequence (393 amino acids i.e. 1179 bases in length) was calculated to approximately 0.12 O^6-CMG and 0.15 O^6-MeG adducts for KDA treatments in 1x TE buffer and 0.48 O^6-CMG and 0.04 O^6-MeG adducts for the *in vitro* treatments carried out in PBS.

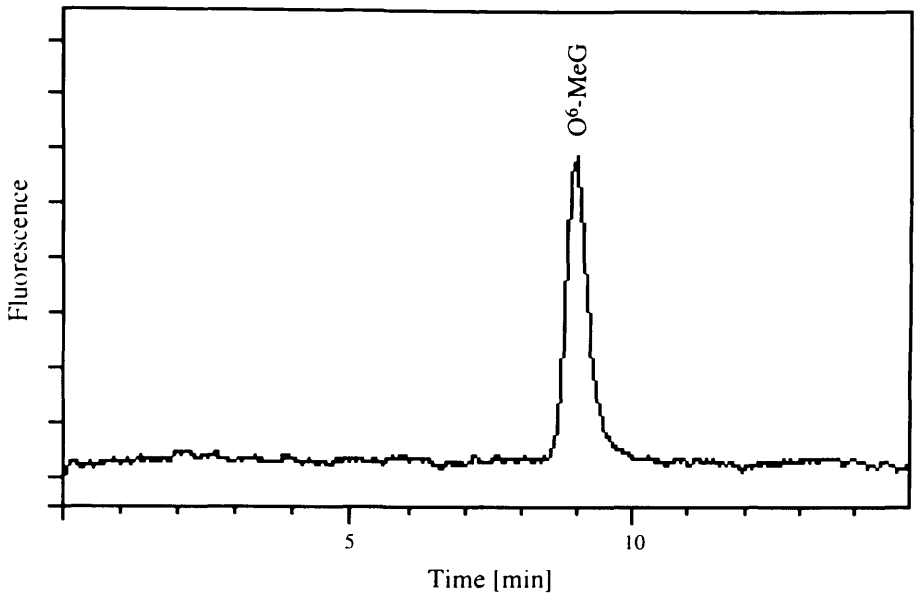

Figure 6.7: *Typical HPLC chromatogram of O^6-MeG following enzymatic digestion and immunoaffinity purification of KDA-treated plasmid pLS76.* Treatment of plasmid pLS76 was carried out in 1x TE buffer using 8mM KDA. RP-HPLC separation using fluorescence detection was performed as described earlier in legend of Figure 6.6.

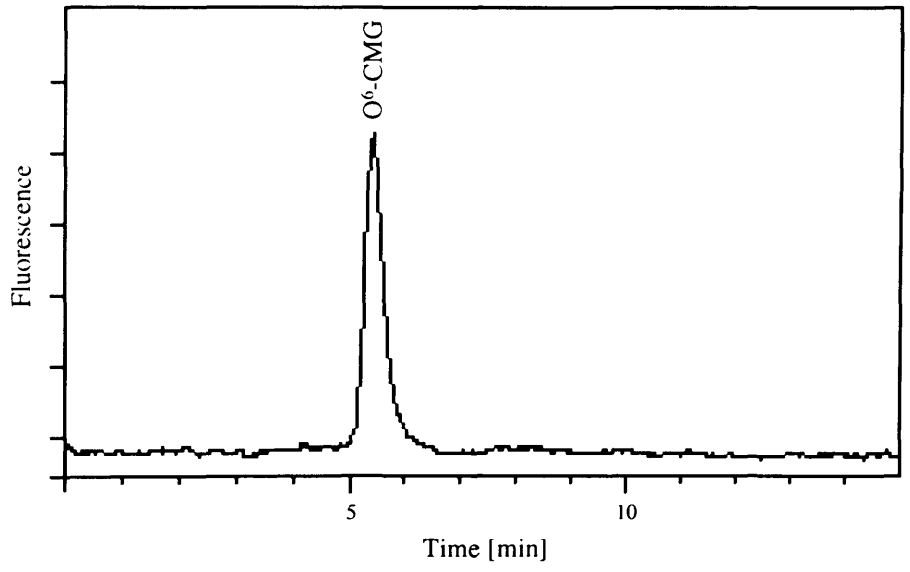

Figure 6.8: *Typical HPLC chromatogram of O^6-CMG following enzymatic digestion and immunoaffinity purification of KDA-treated plasmid pLS76.* Treatment of plasmid pLS76 was carried out in 1x TE buffer using 8mM KDA. RP-HPLC separation using fluorescence detection was performed as described previously in legend of Figure 6.6.

Figure 6.9 illustrates the region of plasmid pLS76 from bases 701 (codon 234) to 710 (codon 237) sequenced with the dRhodamine dye terminator cycle sequencing kit. In this

particular case a p53 mutation which was induced by 6mM KDA treatment in PBS is shown. The sequence given corresponds to the anti-sense or transcribed strand, here displayed in 5'→3' direction with the top sequence representing wild-type and the bottom mutant p53. Comparison of both sequences exemplifies an A→G transition (shown T→C) of nucleotide 707 i.e. AT→GC mutation. In this case, codon 236 mutated from TAC to TGC corresponding to an amino acid change from tyrosine to cysteine.

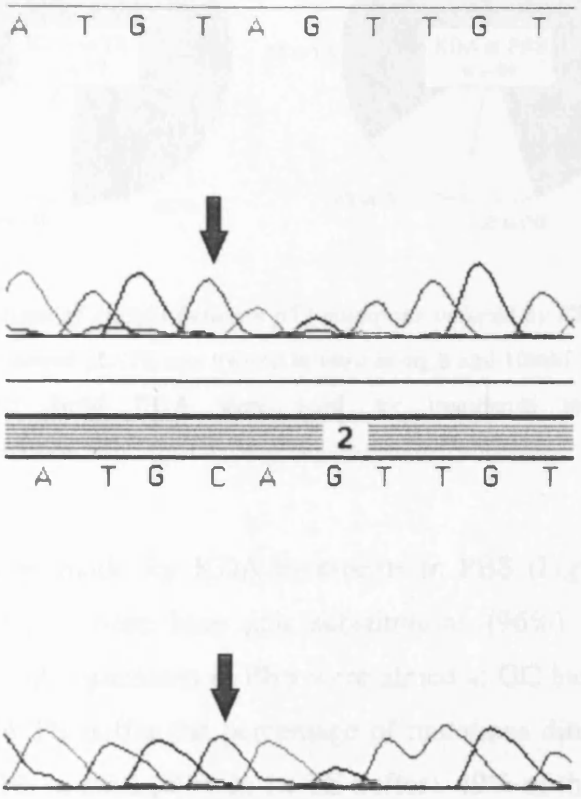

Figure 6.9: *Region of pLS76 from bases 701 to 710 sequenced with the dRhodamine dye terminator cycle sequencing kit.* Top sequence represents wild-type p53, the bottom one mutant p53. Comparison of both sequences illustrates a T→C transition i.e. AT→GC mutation. In this particular case, codon 236 has mutated from TAC to TGC. This corresponds to an amino acid change from tyrosine to cysteine. This particular mutation was induced by 6mM KDA treatment of plasmid pLS76 in PBS and was not observed for KDA treatments in 1x TE buffer.

In general, the most common mutations induced by KDA were base pair substitutions (Figure 6.10). Approximately 57% of all mutations induced by KDA treatment in 1x TE buffer were targeted at GC base pairs, whereas 29% were directed against AT base pairs. Of these substitutions, 53% were transitions, most of which were GC→AT (74%) base

pairs. Transversions accounted for 47% of the base pair substitutions and were comprised largely of GC→TA (42%) and AT→TA (32%). The remaining mutations (14%) were identified to be mainly base pair deletions (9/11).

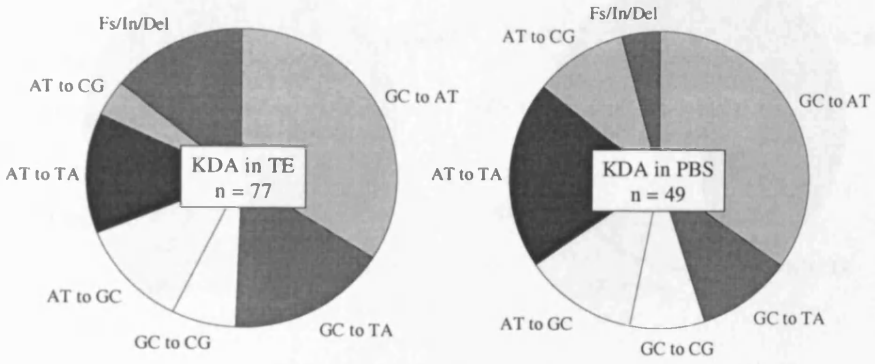

Figure 6.10: *Comparison of classes between p53 mutations induced by KDA treatments in 1x TE buffer and PBS.* Plasmid pLS76 was treated *in vitro* using 8 and 10mM KDA for treatments in 1x TE. 6 and 8mM KDA were used for treatments in PBS. Fs/In/Del frameshift/insertion/deletion.

Similar observations were made for KDA treatments in PBS (Figure 6.10), again most common mutations induced were base pair substitutions (96%). Roughly 53% of all mutations induced by KDA treatments in PBS were aimed at GC base pairs. In contrast to treatments carried out in TE buffer the percentage of mutations directed against AT base pairs was elevated to 43% in PBS (29% in 1x TE buffer). 49% of these substitutions were transitions, most of which were GC→AT (74%) base pairs. Transversions accounted for 51% of the base pair substitutions and encompassed mainly AT→TA (42%), other transversions were essentially represented by equal percentages. The remaining mutations (4%) were identified to be base pair deletions (2/2).

Comparison of the types of mutation within the p53 spectra of human colon and stomach tumours (excluding CpG sites) showed that the characteristics i.e. proportion of transitions, transversions and frameshifts were very similar (Figure 6.11). This resemblance could imply that the same agents may contribute to both types of cancer. However a mutational spectrum is not only characterised by the type of base pair substitution and mutation but

also the location where the mutation occurs and how many times these alterations have been independently observed.

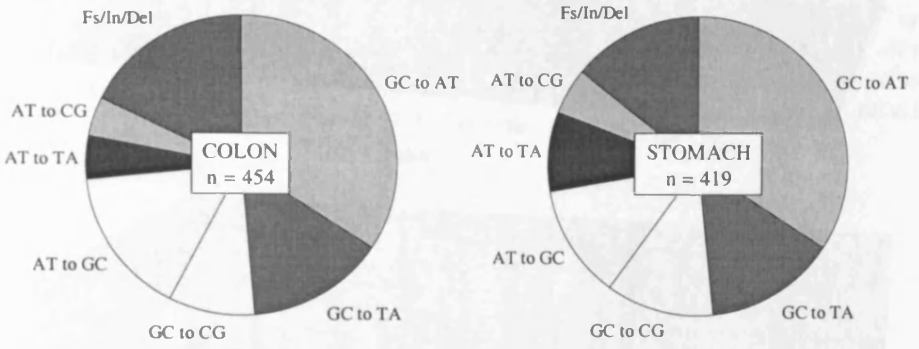

Figure 6.11: *Comparison of p53 mutations observed in human colon and stomach tumours.* Data presented in above figure were adapted from the IARC p53 database. GC→AT transitions at CpG sites were not included.

To illustrate the importance of this, the type of base pair substitution (GC→AT, AT→GC, GC and AT transversions) observed in colon and stomach tumours were plotted versus the location and number of mutations. p53 mutations observed between codon 125 and 200 are illustrated in Figure 6.12 whereas base substitutions detected within codons 200 and 290 are shown in Figure 6.13. Since the total number of mutations listed in the p53 database are 454 and 419 for colon and stomach tumours respectively, base substitutions that occurred at least 4 times were highlighted in a darker colour.

Comparison of both spectra exemplifies the importance of taking the location of the mutation into account and not only its type. Although the types of mutation observed in both human cancers resembled each other to a large extent, one of the most prominent single base substitutions observed in the mutational spectrum of colon cancer, a GC to AT transition at codon 241, was not detected in gastric tumours. On the other hand the p53 spectrum observed for stomach cancer showed mutational hotspots at codons 138, 159, 266, 275 and 289. All of these single base substitutions were GC→AT transitions which were not observed to this extent in colon cancer. Only three of the most common mutations coincided in both p53 mutational spectra (codons 173, 179 and 220).

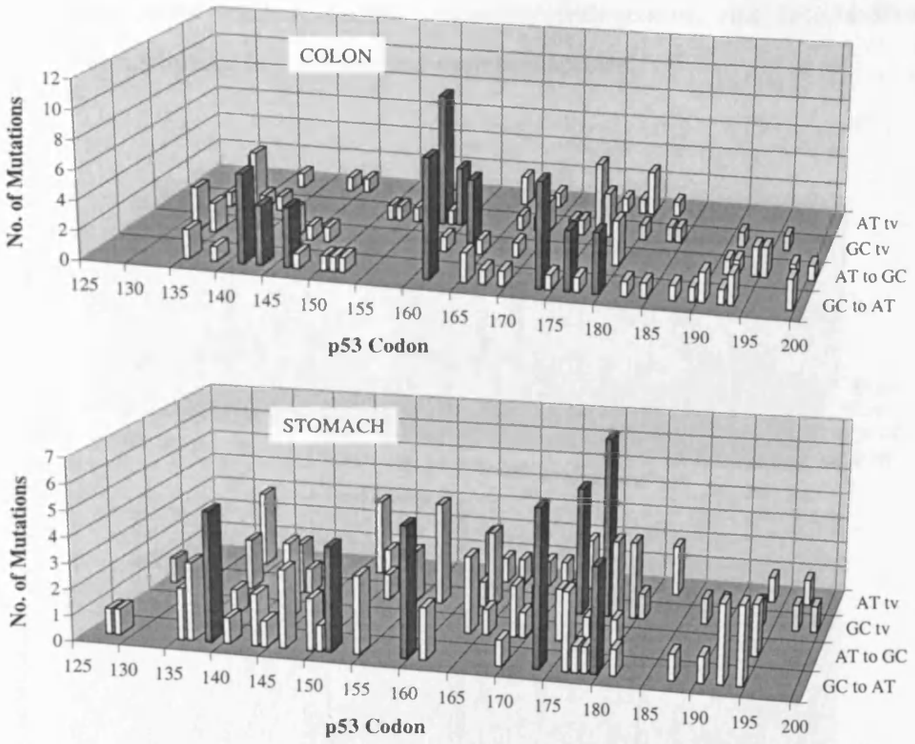

Figure 6.12: *Comparison of mutational p53 hotspots observed in human colon and stomach cancer (codon 125 to 200).* The total number of mutations listed in the database is 454 and 412 for colon and gastric p53 mutations respectively. Therefore codons with at least 4 identical colon or stomach mutations were highlighted in darker colouring. Displayed in this figure are mutations between codon 125 and 200, base substitutions occurring at codons 200 to 290 are displayed in Figure 6.13. GC→CG and GC→TA tranversions were summarised as GC tv, AT tv refers to AT→TA and AT→CG transversions. Transversions were only marked if at least 4 single base substitutions were identical.

These differences might not only emphasise the importance that not just types of mutations are compared, but might also indicate the varying contribution of causative factors, mutagenic processes as well as differences in repair occurring within the two different organs.

Lutz et al. [Lutz (1998)] applied a novel approach to analyse the p53 mutation database of the European Molecular Biology Laboratory. This method was aimed at investigating organ specificity of causative factors and potential organ-to-organ relationships in cancer pathogenesis. Resulting values of this approach could range from 0 (full concordance) to 2 (full discordance). Lutz et al. reported a minimum organ-to-organ discordance value of 0.95 for stomach versus colon [Lutz (1998)]. It was therefore postulated that for organs

with small discordance values common, possibly endogenous, risk factors should be considered for contributing to the observed mutation spectra.

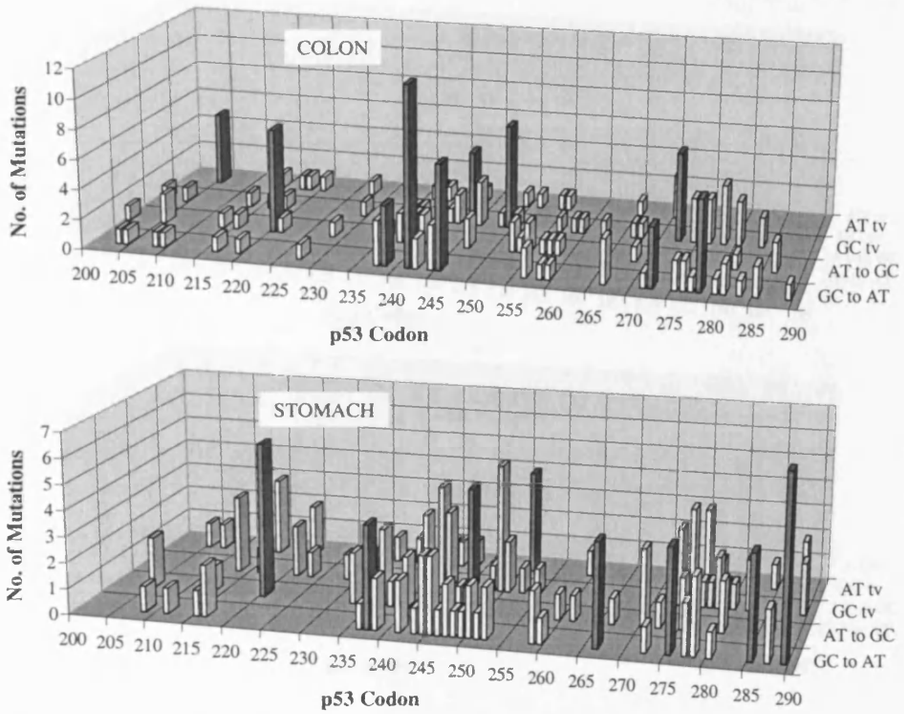

Figure 6.13: *Comparison of mutational p53 hotspots observed in human colon and stomach cancer (codon 200 to 290).* The total number of mutations listed in the database is 454 and 412 for colon and gastric p53 mutations respectively. Therefore codons with at least 4 identical colon or stomach mutations were highlighted in darker colouring. Displayed in this figure are mutations between codon 125 and 200, base substitutions occurring at codons 200 to 290 are displayed in Figure 6.12. GC→CG and GC→TA tranversions were summarised as GC tv, AT tv refers to AT→TA and AT→CG transversions. Transversions were only marked if at least 4 single base substitutions were identical.

Figure 6.14 shows base pair substitutions obtained for KDA treatments in 1x TE buffer (white bars) and PBS (medium coloured bars) together with their location and number within the p53 gene. Mutations common to both spectra were characterised by darker colouring. Again types of substitutions were plotted versus the number and location along the p53 sequence analysed. Mutual transitions were observed at codons 146, 192 and 249 (GC→AT) and at codon 232 (AT→GC). Common AT transversions were discovered at

codons 139, 164, 256 and 280 whereas only one GC transversion was detectable in both spectra (codon 279).

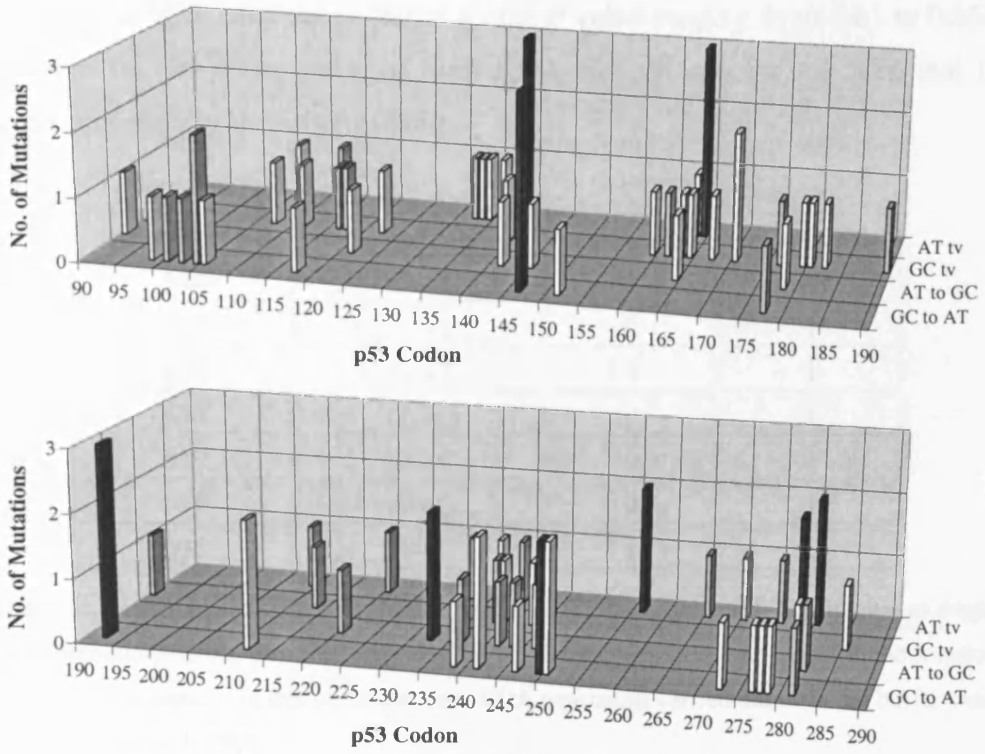

Figure 6.14: *Mutational Spectra obtained for KDA.* This chart shows base pair substitutions obtained for KDA treatments in 1x TE buffer (white bars) and PBS (medium coloured bars). Mutations common to both treatments are highlighted in the darker colour.

Another method for the comparison of mutational spectra at the same locus has been developed and published by Cariello et al. [Cariello (1994a), Cariello (1994b)]. This program was applied to the comparison of KDA-induced spectra. The algorithm performs a statistical test to provide an exact measure of the relatedness of two spectra. The input for the program is a text file containing the number and type of mutations observed in two spectra (example given in Table 6.1). The output is a probability or P value indicating the relatedness of the two spectra, a P value of < or = 0.05 means that the spectra are different. The use of this program demonstrated for example that p53 mutations observed in hepatocellular carcinomas from groups of low and high aflatoxin exposure were indeed different ($P < 0.003$) [Cariello (1994a)].

In Table 6.1 an example is given in order to illustrate the data layout necessary for carrying out Cariello statistics. The table shows only a fraction of the mutations induced by KDA

treatments in PBS and TE buffer. A file containing the two columns of numbers was submitted to the program. Application of this statistical tool to the comparison of KDA-induced spectra, i.e. TE buffer versus PBS gave a P value of 0.64 following 10000 iterations with the 95% confidence limits on the P value ranging from 0.63 to 0.65. The P value obtained for the comparison of both KDA-induced spectra indicated that the two spectra were statistically indistinguishable.

Nucleotide No.	Type of Mutation	KDA in TE	KDA in PBS
574	C→T	1	2
625	A→T	0	1
632	C→T	2	1
638	G→C	0	1
659	A→C	0	1
659	A→G	0	1
695	T→C	1	1

Table 6.1: *Example to illustrate the format needed for Cariello statistics.* The number of single base substitutions in the p53 gene obtained for KDA treatments is given based on the location and nature of mutation. In this particular case KDA treatments carried out in 1x TE buffer were compared to those in PBS.

Therefore both datasets were combined for future analyses and treated as one spectrum. The resulting classes of mutations are displayed in Figure 6.15 and compared to the ones observed for N-methyl-N-nitrosourea (MNU), a monofunctional methylating agent [Beranek (1990)]. The MNU spectrum presented in Figure 6.15 was generated in Leeds using identical techniques for mutation analysis and was presented earlier elsewhere [Fronza (2000), Scott (2000)].

The vast majority of mutations induced by 2mM MNU treatments were GC→AT transitions (83.5%). Transversions of GC→CG and AT→CG were not observed. Frameshifts accounted for approximately 4% of all mutations. Roughly 86% of all mutations were directed against GC base pairs, whereas those aimed at AT base pairs only accounted for 10%. AT→GC transitions accounted for the majority of mutations at AT base pairs (70%), approximately 98% of all mutations at GC base pairs were GC→AT transitions clearly dominating the MNU-induced spectrum.

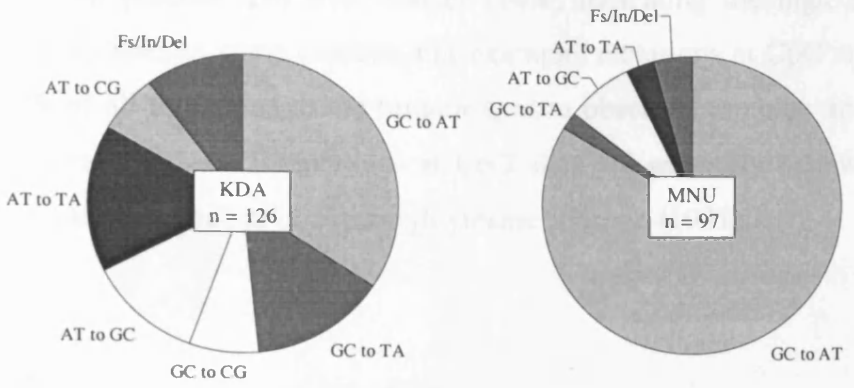

Figure 6.15: *Comparison of classes between p53 mutations induced by KDA and MNU.* Plasmid pLS76 had been treated previously in Leeds using 2mM MNU [Fronza (2000), Scott (2000)], MNU data presented here were adapted from these publications. KDA treatments in 1x TE and PBS shown before were combined since they were shown to be statistically indistinguishable (P value > 0.6) using Cariello's software program.

In contrast to the spectrum induced by MNU 56% of all KDA mutations were aimed at GC base pairs, whereas about a third was directed at AT base pairs. Of all base substitutions 49% were accounted for by transversions and 51% by transitions. Transitions mainly comprised of GC→AT mutations (74%), AT→GC mutations accounted for 26%. Transversions were mainly GC→TA mutations (33%) and AT→TA mutations (36%). Frameshifts accounted for 10% of all KDA-induced mutations and comprised largely of deletions (85%).

Comparison of mutations induced by MNU and KDA to mutations seen in colon and gastric cancer (Figure 6.11) showed that the types of mutation observed in human cancers matched closest with those obtained for the nitrosated glycine derivative. The nature of mutations as well as percentages were almost identical to the one observed for KDA and vastly different to the one obtained for MNU. These findings might support the hypothesis that the presence of O^6-CMdG might play an important role in the aetiology of GI tract cancer.

Looking at the relative proportion of KDA-induced mutations in various tumour spectra within codons 90 to 290 (Figure 6.16) values ranging from 10% for liver (Lv) and prostate (Ps) up to 30% for esophageal (Es) cancer were observed (excluding CpG sites). Including GC→AT mutations at CpG sites values increased up to 44% for colon cancer (Co) but

remained low for prostate and liver cancer (14%) indicating the high contribution of mutations at CpG sites in some cancers. For example, mutations at CpG sites contributed 44% and 36% of all mutations to the tumour spectra observed in colon and stomach (St) cancer respectively. GC→AT mutations at CpG sites are generally believed to originate from spontaneous deamination of 5-methylcytosine [Ehrlich (1981)].

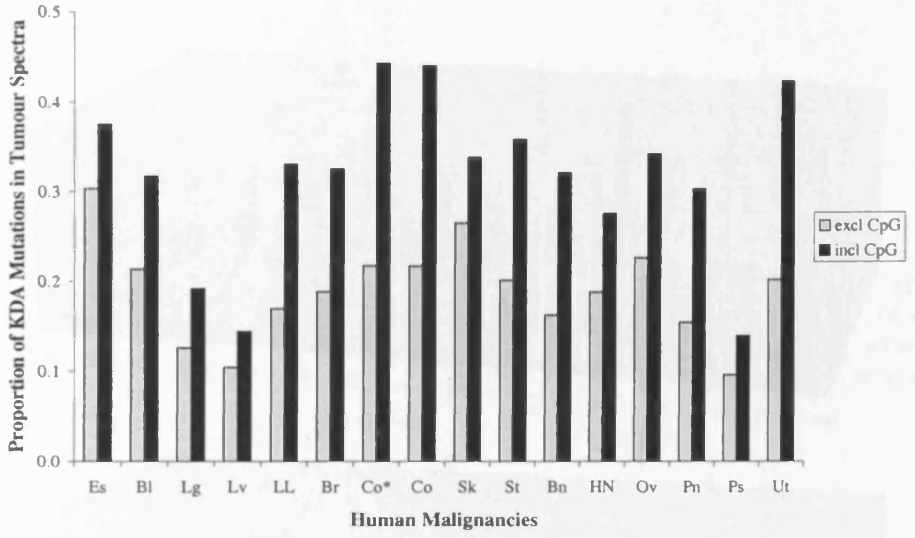

Figure 6.16: *Relative proportion of KDA-induced mutations in spectra of various human malignancies.* The number of cancers that could be attributed to KDA were compared to/divided by the total number of xyz cancer type as given in the IARC p53 database between codons 90 and 290. Darker bars include GC→AT mutations at CpG sites whereas the lighter ones exclude them. (Es) esophagus, (Bl) bladder, (Lg) lung, (Lv) liver, (LL) leukaemia and lymphoma, (Br) breast, (Co*) colon, colorectum and rectum, (Co) colon, (Sk) skin, (St) stomach, (Bn) brain, (HN) head and neck, (Ov) ovarian, (Pn) pancreas, (Ps) prostate, (Ut) uterine.

Figure 6.17 illustrates the p53 mutations observed in gastric tumours that can also be induced by the nitrosated glycine derivative KDA in the yeast-based p53 functional assay (dark bars). One of the most common base pair substitutions in stomach cancer is the AT→GC transition at codon 220. KDA was shown to be able to induce the identical mutation *in vitro*. One of the gastric mutational hotspots, a GC transversion at codon 176 was also seen in the KDA-induced p53 spectrum. GC→AT mutations at codons 146, 151, 192, 277 and 278 were observed in the yeast based assay as well as in the p53 database.

However other hotspots in the gastric tumour spectrum such as GC→AT transitions at codons 138, 159, 173 and 289 were not observed *in vitro*.

The KDA-induced *in vitro* spectrum was compared to the mutational p53 spectrum for stomach cancer using the statistical tool introduced earlier [Cariello (1994a), Cariello (1994b)]. Application of Cariello's software package to the comparison of both spectra resulted in a probability value of $P < 0.001$ indicating that the two spectra were different.

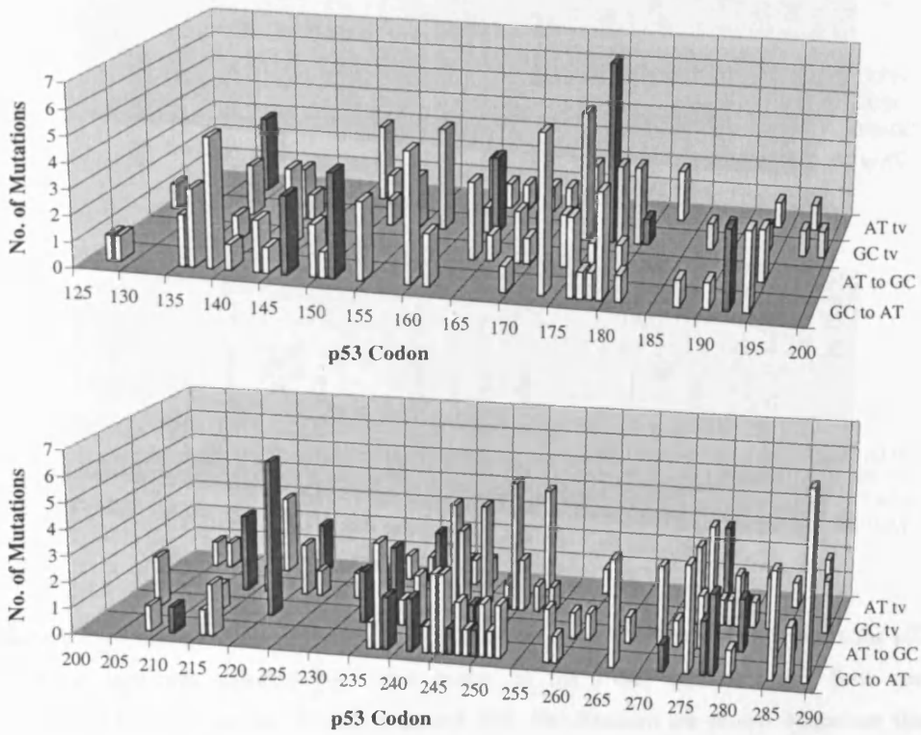

Figure 6.17: *Gastric p53 mutations induced by KDA in vitro.* The figure above shows the p53 mutational spectrum reported for gastric cancer in the IARC p53 database. Base pair substitutions between codon 125-200 (top) and 200- 290 (bottom) are shown. Mutations that were induced by KDA *in vitro* and detectable using the yeast-based p53 functional assay but were also common to the spectrum of gastric cancer were highlighted (dark bars).

Figure 6.18 exemplifies the p53 mutations observed in colon tumours that were also induced by KDA *in vitro* (dark bars). The most abundant hotspot in colon cancer is the GC→AT transition at codon 241. KDA was able to cause the identical mutation at codon 241 in the yeast-based p53 functional assay. The AT→GC transition at codon 220 was also common to both spectra and constitutes one of the major hotspots in the p53 spectrum of colon cancer. Similar observations were made for GC→AT mutations at codons 146, 238,

272 and 278. Other hotspots in the mutational spectrum of colon cancer such as GC→AT transitions at codons 141, 161, 173 and 245 as well as the AT→GC mutation at codon 163 were not detectable *in vitro*.

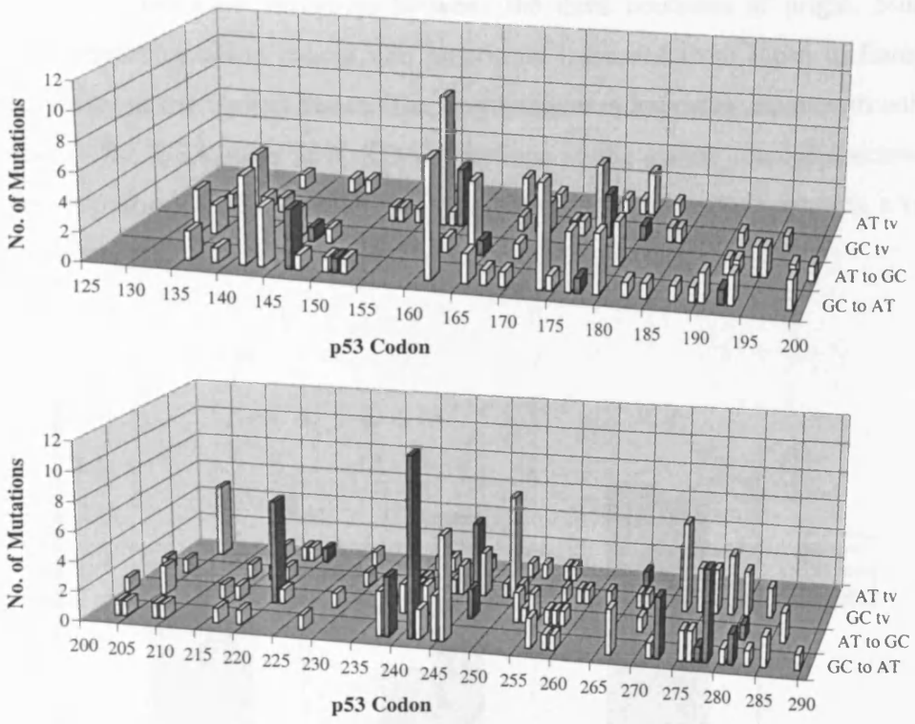

Figure 6.18: *Colon p53 mutations induced by KDA in vitro.* The figure above shows the p53 mutational spectrum reported for colon cancer in the IARC p53 database. Base pair substitutions between codon 125-200 (top) and 200- 290 (bottom) are shown. Mutations that were induced by KDA *in vitro* and detectable using the yeast-based p53 functional assay but were also common to the spectrum of colon cancer were highlighted (dark bars).

Figure 6.19 shows the proportion of KDA mutations in colon, stomach and esophageal cancer per country of origin. Countries chosen for the analysis were Japan, Europe and USA. Proportions were calculated by dividing the number of KDA-induced e.g. gastric p53 mutations per country by the total number of stomach mutations observed in this particular country. Only base pair substitutions between codon 90 and 290 were considered for the analysis, again CpG sites were excluded.

No major differences were observed between the three different countries with regard to the proportion of KDA mutations in the esophageal tumour spectrum. Average proportion of mutations that could potentially be attributed to KDA was 28% of the p53 spectrum. For

colon tumours the proportion of KDA mutations varied slightly, an increase from 17% in Japan to 22% in the United States was noticeable. The fraction obtained for Europe was in the middle of those observed for Japan and USA. Interestingly, comparison of the proportion of KDA mutations that could be found in the p53 mutational spectrum of gastric tumours revealed dramatic variations between the three countries of origin. Similar to observations made for colon cancer, the proportion increased from Japan to Europe and was even greater in the United States. The percentage was lowest in Japan with only 11% and highest in the USA with 36% KDA mutations in the gastric tumour spectrum. For Europe the proportion of KDA mutations lay in between the other two countries, a value of 26% was determined.

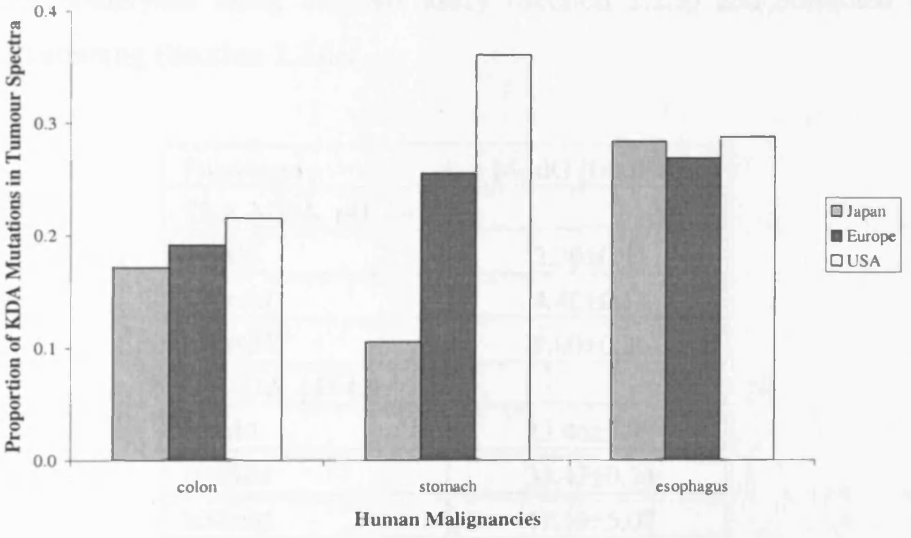

Figure 6.19: *Proportion of KDA mutations in stomach, colon and esophagus p53 mutational spectra in different countries of origin.* The number of e.g. colon cancers that could be attributed to KDA in one particular country were compared to/divided by the total number of mutations listed for colon cancer in this specific country. Only base pair substitutions between codon 90 and 290 were compared excluding mutations at CpG sites.

6.2.2 MDA-Induced p53 Mutations in Plasmid pLS76

Originally it had been planned to treat plasmid pLS76 using sodium malondialdehyde (NaMDA) in order to generate p53 mutations *in vitro*. NaMDA was used since it was reported in earlier studies that during generation of MDA via TMP hydrolysis impurities were generated, which were nearly 30-fold more mutagenic than MDA [Marnett (1980)].

Therefore utilisation of NaMDA appeared advantageous when compared to MDA for the induction and analysis of p53 mutations.

NaMDA was synthesised as outlined in Section 2.2.2. Preliminary treatments of plasmid pLS76 (4 days at 37°C, pH 7.4) showed that even doses as high as 40mM NaMDA did not result in an increase in mutation frequency or a decrease in survival.

Therefore several altered conditions were tried and mimicked using CT-DNA (0.3 mg/ml), for example the pH of the incubation/treatment buffer was changed and concentrations of NaMDA were further increased (Table 6.2). DNA solutions were also treated using the commercially available malondialdehyde tetrabutylammonium salt (TBA-MDA; Fluka No. 63287). Following precipitation using isopropanol, samples were analysed by HPLC fluorescence. M_1-dG levels were too low and thus not detectable using this approach. The samples were reanalysed using the ISB assay (Section 2.2.3) and corrected for DNA binding by PI staining (Section 2.2.4).

Treatment	M_1-dG [fmol/μg]
TBA-MDA, pH 7.4	
50mM	2.30±0.11
100mM	4.40±0.11
200mM	9.00±0.36
NaMDA, pH 4.5	
20mM	23.46±1.79
100mM	33.47±0.74
200mM	47.59±5.07
NaMDA, pH 7.4	
20mM	4.84±0.45
100mM	8.18±0.42
200mM	10.19±0.77

Table 6.2: *pH dependence of M_1-dG formation.* CT-DNA (0.3 mg/ml) was incubated with NaMDA and TBA-MDA (concentrations given in table above). Reaction mixtures were incubated for 4 days at 37°C in 100mM phosphate buffer with pH varying between 4.5 and 7.4 (NaMDA). Incubations with TBA-MDA were carried out at pH 7.4 only. DNA was precipitated using isopropanol and analysed by ISB assay. Values given above are average ± standard deviation, measured in fmol M_1-dG per μg of DNA.

Some of the samples exceeded the highest ISB standard (10 fmol/μg) thus making an accurate determination of M_1-dG levels not always feasible. The values obtained gave at

least an indication about the efficiency of the treatment. It was discovered that changes in pH from 7.4 to 4.5 had a considerable effect on the level of modification (Table 6.2).

In general, levels of M_1-dG were about 4 to 5 times higher for incubations carried out at pH 4.5. The level of modification obtained for 20mM NaMDA treatments at pH 7.4 and 4.5 corresponded to approximately 14 and 72 adducts per 10^7 normal nucleotides respectively. Adduct levels obtained for TBA-MDA treatments were slightly lower than those observed for NaMDA treatments at equivalent, neutral pH. Observations with regard to pH dependence of M_1-dG formation correlated well with findings published recently by Plastaras et al. [Plastaras (2000b)]. Plastaras and co-workers reported approximately 62 and 770 adducts per 10^8 nucleotides for 20mM NaMDA treatments at pH 7.4 and 4.5, respectively.

Overall the level of modification using NaMDA or TBA-MDA was low compared to MDA treatments. The latter usually generated M_1-dG levels of about 18 pmol per μg DNA following 2mM treatments. Fairly high adduct levels were needed in plasmid pLS76 in order to obtain a response in transformed yeast cells. It was therefore decided to use MDA generated by TMP hydrolysis for *in vitro* treatments of the yeast expression vector.

Usually DNA was incubated for 4 days at 37°C using MDA at concentrations of 1 or 2mM (pH 4.5). Transferral of these conditions to plasmid however caused unforeseen complications, even samples which had been incubated with the phosphate buffer only showed an increase in mutation frequency.

It was therefore decided to shorten the incubation time considerably and to increase the concentration of MDA at the same time. Final treatment conditions are detailed in Section 2.4.2. Concentrations of MDA ranged from 1, 5, 10 to 15mM, 10mM treatments were repeated multiple times in order to generate enough mutants for mutation analysis. Survival rate and mutation frequency observed following MDA treatments using this dose-range are shown in Figure 6.20.

A dose-dependent decrease in survival and increase in mutation frequency were observed for *in vitro* MDA treatments. A survival rate of 83% was observed for the lowest MDA concentration whereas the survival was only about 1.6% for 15mM MDA indicating a steep decline of survival. Approximately 74% and 35% survival were observed for 5 and 10mM MDA treatments respectively. The mutation frequency was slightly increased by 1.4-fold following incubation with 1mM MDA and approximately 9-fold above background level after 10mM MDA treatment. The highest concentration of MDA yielded an extensive increase in mutation frequency. Compared to background levels observed on

control plates the 15mM MDA treatment generated a 196-fold increase in mutation frequency.

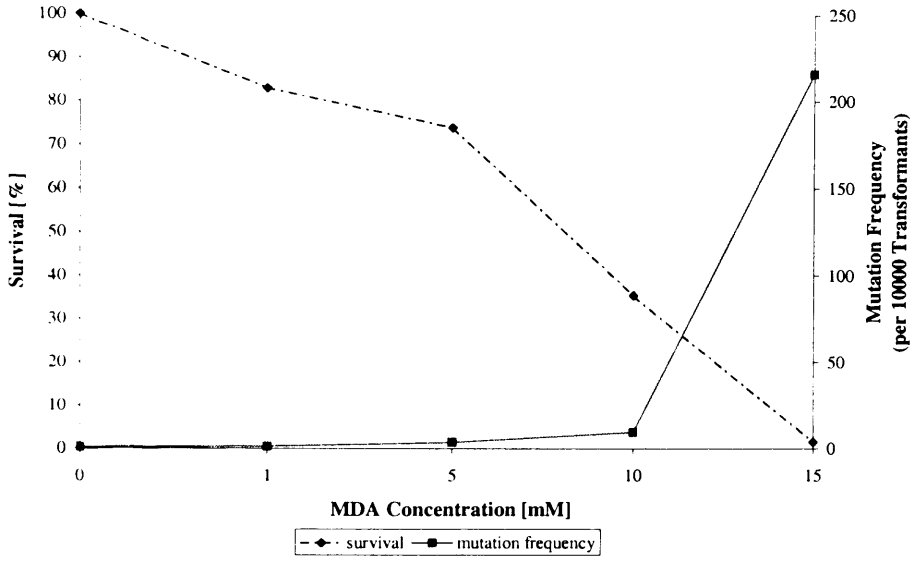

Figure 6.20: *Survival rate and mutation frequency following 1, 5, 10 and 15mM MDA treatments of plasmid pLS76.* Plasmid pLS76 was treated in phosphate buffer (100mM, pH 4.5) using several MDA concentrations (1 to 15mM) for 1 h at 37°C. Survival represents the total number of colonies obtained for treated samples divided by the number of colonies on control plates. Mutation frequency indicates the number of red colonies compared to the number of total colonies.

Multiple 10mM MDA treatments (n = 8) were carried out in order to generate enough mutants for subsequent analysis of p53 mutations as well as determination of M_1-dG adduct levels. Survival rate observed for these treatments was 24.6 ± 5.1%, the corresponding mutation frequency per 10000 transformants was 14.6 ± 3.4 (n = 72 plates) i.e. 5.8-fold above background. From these treatments a total of 154 MDA-induced mutants was isolated and PCR amplified. Approximately 60% of these mutants resulted in a PCR product following amplification. It was planned originally to try a different method for the preparation of plasmid from yeast in order to obtain PCR products from all MDA-induced mutants however time did not permit this. A total number of only 18 mutations was identified after all available PCR products had been sequenced and analysed using the ABI Prism Sequence Navigator software. Alternative mutations on plasmid pLS76 outside the p53 gene interfering with expression of p53 could be a potential explanation for this low number apart from possible technical problems. The mutation frequency observed for

multiple 10mM MDA treatments was lower than the originally observed one (5.8- versus 9-fold above background). Ideally a mutation frequency of 10 and higher is aimed for in order to have a clear distinction to spontaneous mutations. Spontaneous mutants on control plates are routinely analysed but very rarely result in a mutation being detectable following sequencing. To date no distinct pattern of spontaneous mutations has been identified. Results obtained for *in vitro* treatments of plasmid pLS76 using MDA are presented in Figure 6.21.

The MDA-induced p53 mutational spectrum was dominated by two main features. Firstly, about 56% of all mutations observed *in vitro* were deletions, secondly single base substitutions occurred exclusively at GC base pairs. Approximately 38% of mutations at GC base pairs were transitions. GC→TA and GC→CG transversions accounted for 50% and 12.5% of all single base substitutions respectively.

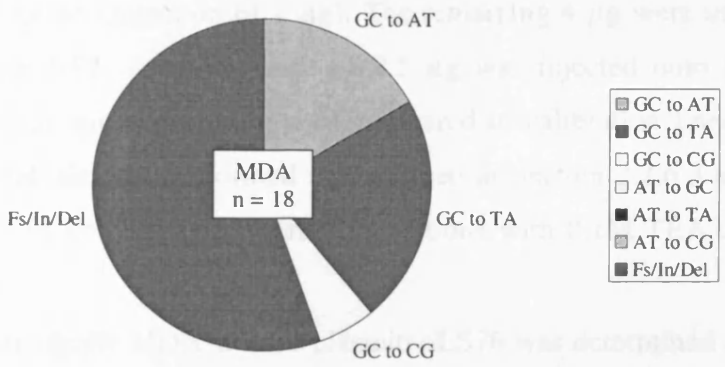

Figure 6.21: *Classes of MDA-induced p53 mutations.* The yeast expression vector pLS76 was treated *in vitro* using 10mM MDA (1 h at 37°C, 100mM phosphate buffer pH 4.5) and transformed into yeast cells.

A list of all MDA-induced p53 deletions that were detected using the yeast-based p53 functional assay is shown in Table 6.3. Single base deletions were observed exclusively at sites of multiple repeats of guanine or cytosine. Two thirds of single base frameshifts occurred at cytosine residues.

As the total number of mutations for *in vitro* MDA treatments of the yeast expression vector pLS76 was relatively low no further analyses and comparison with the IARC p53 database were undertaken.

Codon	p53 Sequence	Base Change
104-105	CAG GGC	1 bp del
152-174		large del
153	CCC	1 bp del
153	CCC	1 bp del
155-156	ACC CGC	1 bp del
176-178	TGC CCC CAC	1 bp del
176-178	TGC CCC CAC	1 bp del
176-178	TGC CCC CAC	1 bp del
217-218	GTG GTG	1 bp del
243-244	ATG GGC	1 bp del

Table 6.3: *List of all MDA-induced deletions in the p53 sequence of plasmid pLS76.*

Several of the 10mM MDA-treated plasmid samples including negative controls had been kept for the analysis of M_1-dG levels. 6 μg of treated and control plasmid were digested to dNp as detailed in Section 2.4.2 using MN and CSPDE. 2 μg of the digested DNA were used for DNA quantitation (injection of 1 μg). The remaining 4 μg were used for further digestion to dN using NP1. An equivalent of 2.5 μg was injected onto the RP-HPLC system (Section 2.2.6.3) and samples (n = 8) compared to calibration lines for dAp and M_1-dG. RP-HPLC analysis was performed as described in Section 2.2.6.3 using a narrow bore Hypersil BDS C18 column and isocratic conditions with 0.1M TEA containing 4% MeOH as the eluent.

The level of adduct in 10mM MDA-treated plasmid pLS76 was determined to 3.95 ± 0.19 pmol M_1-dG/μg which is equivalent to approximately 122 M_1-dG adducts per 10^5 normal nucleotides. This degree of modification corresponds to 1.44 M_1-dG adducts when based on the length of the p53 coding sequence. Figure 6.22 illustrates a HPLC fluorescence trace obtained for 10mM MDA-treated plasmid, the amount of DNA injected onto the system corresponded to 2.5 μg. The corresponding UV (260 nm) HPLC trace is not shown since an almost identical separation was shown earlier for MN and CSPDE digested CT-DNA (Figure 3.7).

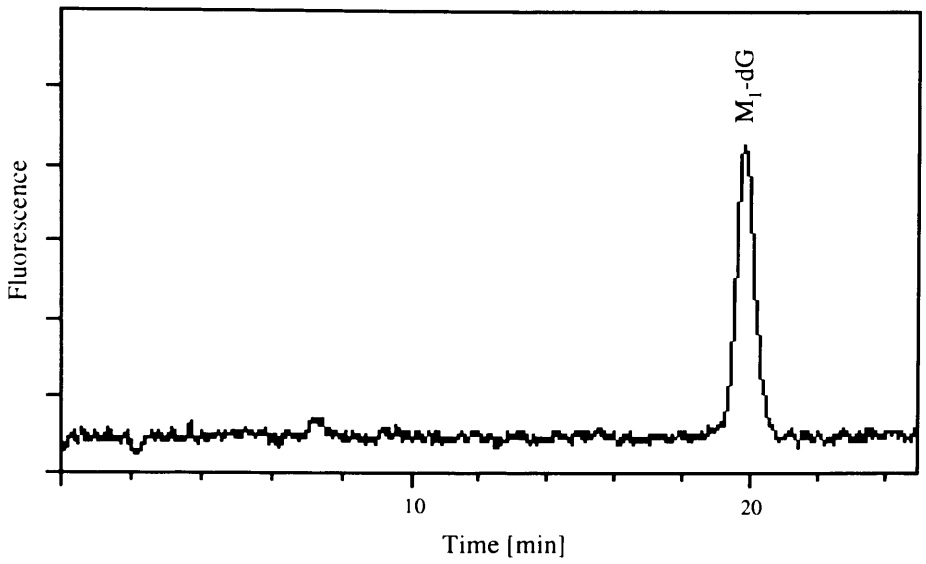

Figure 6.22: *HPLC fluorescence trace for MDA-treated pLS76.* RP-HPLC analysis was performed as described in Section 2.2.6.3 using a narrow bore Hypersil BDS C18 column (100 x 2.1 mm; including a prefilter) and isocratic conditions with 0.1M TEA containing 4% MeOH as the eluent (flow 0.2 ml/min). M_1-dG peak was detected by fluorescence (λ_{Ex} 360 nm, λ_{Em} 500 nm). Amount injected corresponded to 2.5 μg of 10mM MDA-treated plasmid pLS76.

6.3 Discussion

The quite dramatic manipulation of relative proportions of two mutagenic lesions offered a rather unique situation and possibility with regard to KDA-induced p53 mutations. As part of a collaborative project the yeast expression vector pLS76 that harbours wild-type p53 cDNA was treated *in vitro* using KDA in PBS or 1x TE buffer and transfected into a yeast strain containing the ADE2 gene regulated by a p53-responsive promotor.

O^6-alkylguanine adduct levels were determined in 8mM KDA-treated plasmid using immunopurification followed by HPLC fluorescence. It was discovered that in Tris-EDTA buffer carboxymethylation and methylation at the O^6-position of guanine occurred to a similar extent, confirming results presented earlier (Chapter 5). In contrast, O^6-CMdG was predominantly formed in PBS with a ratio of 13:1 O^6-CMdG to O^6-MedG adducts being determined (Figure 6.6).

Despite the quite substantial, buffer-modulated differences in O^6-alkylguanine adduct formation, proportion and types of KDA-induced mutations were very similar (Figure 6.10). Analysis using a software package developed by Cariello [Cariello (1994a)] showed that spectra obtained via KDA treatments in Tris-EDTA and PBS buffer were statistically

indistinguishable (P value > 0.6). As a consequence of these findings the question to be addressed was: why were the classes of mutation observed for KDA treatments in both buffer systems almost identical, despite vastly different adduct levels. One possible and quite likely explanation of this phenomenon could be the efficient repair of O^6-MedG by O^6-alkylguanine-DNA alkyltransferases suggesting that the spectra observed for KDA were mainly due to the carboxymethylation product. In contrast to the O^6-methylation product of guanine, O^6-CMdG is known not to be repaired by O^6-alkylguanine-DNA alkyltransferases [Shuker (1997)].

This hypothesis found considerable support when comparing the p53 mutational spectra induced by KDA and MNU (Figure 6.15). Both spectra varied quite dramatically with GC→AT transitions clearly dominating the MNU-induced p53 spectrum (83.5%). On the contrary this type of base pair substitution only comprised 34% of the spectrum induced by the nitrosated glycine derivative. These findings suggest that O^6-alkylguanine-DNA alkyltransferases were able to repair KDA-induced O^6-MedG efficiently in yeast cells and independently of the buffer system i.e. level of modification.

The prevalence of GC→AT transitions in the MNU-induced p53 spectrum is considered to be due to the miscoding properties of O^6-MedG. In general, it has been assumed that O^6-alkylguanine miscodes as a consequence of its stable mispair with thymine. This mispairing of O^6-methylguanine with thymine during DNA replication has been reported to result exclusively in GC→AT transitions [Loechler (1984)]. Another premutagenic lesion originating from DNA alkylation, O^4-alkylthymine, has been shown to mispair with guanine, resulting in AT→GC transitions [Preston (1986)]. In contrast, bulky carcinogen adducts potentially cause the DNA bases to be unreadable and stall replication. These non-instructive sites will then be preferentially filled with adenine by DNA polymerases. Formation of bulky guanine adducts for example will thereby cause a GC→TA transversion [Strauss (1991)].

No such information is available on the O^6-carboxymethylation product of guanine. O^6-CMdG might act in a similar way as O^6-MedG and O^4-alkylthymine i.e. as a miscoding lesion altering the hydrogen bonding properties of the base and thereby causing DNA polymerase to misread the base pairing. Alternatively, the adduct could function like bulky DNA adducts as a non-coding lesion. Further work is needed in order to establish the distinct mutational feature caused by O^6-CMdG.

A general problem of alkylating agents is that adducts are formed at many sites in DNA, making the determination which type of adduct causes which particular mutation and why immensely difficult if not impossible. The fact that KDA not only generates the carboxymethyldiazonium but also a methyldiazonium ion complicates this matter further. Additionally, mutations induced by a particular compound can be influenced by the DNA sequence, its dose, efficiency/deficiency in repair and other factors.

As KDA concomitantly carboxymethylates and methylates DNA it is possibly not the most suitable compound in order to establish a link between O^6-carboxymethylation, p53 mutations and certain types of cancer. In order to be able to link p53 mutations to O^6-CMdG specifically one would need to develop an approach or a substance to only carboxymethylate DNA without concurrently occurring methylation. Adduct site-specific mutagenesis studies, in which a single adduct is built into a vector, can be used to overcome this problem. Another potential approach might be the treatment of plasmid using MNU at a concentration that generates the equivalent level of O^6-MedG adducts seen in KDA treatments, and in the next step to compare and 'subtract' one spectrum from the other. It would have been therefore valuable to analyse levels of O^6-MedG in previously MNU-treated plasmid in order to be able to correlate and compare obtained mutational spectra in a more efficient way. Unfortunately MNU samples were no longer available in Leeds to conduct this comparison and analysis.

Alternatively, KDA-modified plasmid could be treated using O^6-alkylguanine-DNA alkyltransferases known to repair O^6-MedG efficiently but not O^6-CMdG [Shuker (1997)]. Treatment using this repair enzyme would need to be carried out post KDA treatment and prior to transformation into yeast cells in order to determine a p53 spectrum characteristic of carboxymethylated bases.

Comparison of KDA- and MNU-induced p53 spectra with those published for colon and stomach cancer (Figure 6.11) showed that types of mutations generated by KDA resembled the human spectra closest. Some of the p53 mutational hotspots found in colon and stomach cancer were also detectable in the *in vitro* spectrum generated by KDA (Figure 6.17 and Figure 6.18). These findings might suggest a potential role of nitrosated glycine derivatives in the aetiology of GI tract cancer. However, comparison of KDA-induced and gastric p53 mutational spectra using the Cariello algorithm did not further support this hypothesis. A P value < 0.001 was obtained clearly indicating that there was no statistical evidence of the two spectra being related. In general, a P value < 0.05 signifies that two spectra are different.

Interestingly when taking the country of origin into account quite substantial differences in the proportion of KDA mutations in the gastric tumour spectrum became apparent. These variations were also observable for colon cancer although to a lesser extent, but were not evident for esophageal cancer (Figure 6.19). The contribution of KDA mutations in the gastric tumour spectrum was lowest in Japan (11%) and highest in the USA with 36%.

The mechanisms leading to the formation of N-nitroso compounds (NOC) and subsequent decomposition to DNA alkylating agents is complex. A model of the aetiology of gastric cancer has been proposed by Correa [Correa (1992)]. Several mechanisms leading to the formation of NOC intermediates have been outlined: acid or bacterially catalysed nitrosation, and nitrosation from nitric oxide (NO).

The increased risk of developing gastric cancer has also been linked with high intake of smoked, salted and nitrated foods, high intake of carbohydrates and low intake of fruits, vegetables and milk. Another important link has been proposed between gastric cancer and *Helicobacter pylori* infection which is believed to play a role in about 60% of all cases [Stadtländer (1999)].

Endogenous nitrosation of dietary amino acids and peptides has been suggested as a major route of exposure to genotoxic agents in the gastrointestinal tract [Shephard (1989), Challis (1989)]. Nitrosation of glycine, one of the most abundant amino acids, results in the formation of diazoacetic acid and thereby in the creation of carboxymethyl- and methyldiazonium ions. It would therefore seem likely that nitrosation products of glycine would constitute a major source of alkylating agents in the gastric contents.

Recent *in vitro* studies in our laboratory using conditions similar to those found in the GI tract *in vivo* showed that treatment of glycine with NO results in the formation of diazoacetate. Furthermore, incubation of the reaction mixture with 2'-dG and DNA formed O^6-CMdG and O^6-MedG DNA adducts. These findings suggested that diazoacetate was a key alkylating agent formed from the nitrosation of glycine under physiological conditions [Cupid (2001)].

Variations in the proportion of KDA mutations in the gastric p53 spectrum might possibly be explained by the highly variable protein intake in different countries, peaking in the USA with its high red meat diet. Bingham et al. [Bingham (1996)] established a link between high intake in red meat and increased endogenous intestinal production of NOC and nitrite. This association could not be made for white meat and fish.

In contrast to KDA-induced p53 mutations which comprised of 90% base substitutions, the majority of mutations caused by MDA (Figure 6.21), one of the major products of lipid peroxidation, was accounted for by deletions (56%). Two thirds of all single base deletions occurred at sites of multiple cytosine repeats, 33% at a polyguanine tract (Table 6.3). Base substitutions (44%) occurred exclusively at GC base pairs. This prevalence of substitutions at GC base pairs most likely results from the fact that M_1-dG is the major DNA adduct formed upon reaction with malondialdehyde [Marnett (1994b)].

The predominance of deletions was inconsistent with earlier mutagenicity studies using MDA [Benamira (1995)]. Benamira and co-workers reacted single-stranded M13MB102 DNA with MDA at neutral pH prior to transformation into strains of *E. coli*. The authors reported that MDA induced mainly base pair substitutions (76%) in the *lacZ*$_\alpha$ forward mutation assay using a recombinant M13 bacteriophage. C→T and A→G transitions accounted for 32% and 25% respectively, whereas G→T mutations comprised of 35%. Frameshift mutations were identified in 16% of the induced mutants and comprised of mainly single base insertions.

The spectrum of mutations induced by M_1-dG has been studied by site-specific approaches using M13 vectors replicated in *E. coli* [Fink (1997)]. Fink et al. reported that genomes containing a cytosine opposite M_1-dG resulted in roughly equal numbers of M_1-dG→A and M_1-dG→T mutations with few M_1-dG→C mutations. However, frameshifts were not induced in this system. The authors indicated that M_1-dG was also a strong block to replication. Single base substitutions reported by Fink et al. correlated well with MDA-induced mutations detected via the yeast-based p53 functional assay. Using the latter system, 37.5% of all mutations at GC base pairs were transitions (GC→AT), approximately 50% were GC→TA transversions. 12.5% of base substitutions were accounted for by GC→CG transversions.

Interestingly, alterations in a polycytidine tract were detected by Habano et al. in mitochondrial DNA (mtDNA) [Habano (1998)]. These modifications within the D-loop, a non-coding displacement loop region of mtDNA, accounted for 44% of 45 sporadic colorectal carcinomas. Three of the colorectal carcinomas also exhibited frameshift mutations in a polyadenosine or polycytidine tract within NADH dehydrogenase genes. Other structural changes within mtDNA reported in the literature are large-scale deletions (> 50 bp) in gastric [Burgart (1995)] and renal cell carcinomas [Horton (1996)].

Furthermore about 42% of all mutations within the D-loop of mtDNA in primary breast cancers were deletions and insertions in a homopolymeric C-stretch [Parrella (2001)].

Mitochondrial DNA has been believed to suffer greater endogenous oxidative damage than nuclear DNA. The main reasons for this greater susceptibility to oxidative damage are (i) the lack of protective histones, (ii) the close proximity of the mitochondrial electron transport chain, a site of superoxide anion generation and (iii) the lack/deficiency in some repair mechanisms [Beckman (1999)].

p53 mutations generated by MDA *in vitro* and their similarity to mitochondrial mutations found in human cancers might support the hypothesis that mtDNA is more susceptible to endogenous oxidative damage. Other studies have indicated that mtDNA when compared to nuclear DNA contains an elevated level of base damage such as 8-oxoguanine [Richter (1988)]. The findings presented above might also suggest a role of lipid peroxidation in oxidative damage of mtDNA. A comparison of M_1-dG levels, the major malondialdehyde DNA adduct, in mitochondrial and nuclear DNA would therefore be interesting and would possibly offer further clarification with regard to type and extent of oxidative damage occurring in mtDNA.

Nevertheless, one has to keep in mind that the total number of MDA-induced p53 mutations was very small, hence no comparison with p53 mutations in the IARC database was conducted. An expansion of the number of MDA mutants and p53 mutations would therefore be one of the main aims for future work. Furthermore, method development for mtDNA extraction and detection of M_1-dG adducts in mtDNA would also constitute a key part in an upcoming project.

7 Conclusions and Future Work

Several different aspects of various DNA adducts have been investigated as part of this project. Areas of research included stability upon long-term storage as well as the detection and modulation of adducts. The promutagenic potential of O^6-alkylguanine and M_1-dG adducts was also investigated as part of a collaboration using a yeast-based p53 functional assay. The main findings and conclusions are summarised in the following section, along with some indication of future directions for various aspects of the work.

Stability of M_1-dG in Highly Modified CT-DNA Standards and Stored Human DNA Extracted from Leukocytes

Possibly one of the least studied questions in biomonitoring is the stability of DNA adducts. This particular issue is of great concern in the context of sample collection, processing and storage. Very little information can be found in the literature on this topic in general and long-term stability of DNA adducts in particular. M_1-dG, the major adduct formed by the reaction of malondialdehyde with DNA, is frequently used as a biomarker in diet-related studies in our laboratory. Immediate sample processing such as DNA extraction and analysis is not always feasible. The stability of biomarkers in human, animal and cellular samples and also that of standards needed to be studied. Analysis and validation of standards used for the determination of samples should therefore be part of a frequent quality control in order to avoid any assay drift. Hence as part of this project stability of M_1-dG upon storage was not only assessed in human samples but also in highly modified CT-DNA standards used in the ISB assay.

MDA-treated CT-DNA was dissolved in 10mM phosphate buffer (pH 7.0) or water and stored at temperatures ranging from -80°C to RT. Stability of M_1-dGp was assessed by HPLC fluorescence after enzymatic digestion to dNp. It was discovered that standards stored at RT in phosphate buffer degraded quickest. Initially no changes were detectable. After approximately three weeks of storage an exponential decrease in M_1-dGp levels was observed and within 119 days the sample was fully decomposed. Detection of M_1-dGp was no longer feasible by HPLC fluorescence. Products of degradation in DNA samples stored in phosphate buffer were M_1-dG and M_1-G. Normal nucleotides, as assessed by determining dAp and analysed by HPLC UV detection, degraded at a similar rate as MDA-modified guanines.

In contrast to these findings, degradation of the standard was much slower in water. Normal nucleotides remained relatively unaffected and only one product of degradation was formed, namely M_1-G. At the start, degradation was similar to samples stored in phosphate buffer i.e. beginning after three weeks of storage at RT. After 93 weeks of storage at ambient laboratory temperature 12% of the original M_1-dGp level and 70% of normal nucleotides were still detectable by HPLC. It is apparent from these proportions that degradation of normal nucleotides was much slower than that of modified bases. The rate of degradation after approximately three weeks was more or less linear for both, modified and unmodified, nucleotides.

Degradation at 4°C and lower temperatures was much slower. Differences between samples dissolved in water and phosphate buffer were not as marked as for RT. Overall, highly MDA-modified CT-DNA proved relatively stable even at RT and 4°C. Even after 93 weeks of storage at -20°C and -80°C comparatively little degradation was detectable by HPLC. It is general practice in our laboratory to store standards at -80°C, thus results obtained should not be affected by any deterioration. It is useful to know that MDA-treated DNA samples can be stored at RT or 4°C for a short period of time without having any adverse effects on standard quality and the level of modification.

Stability of low levels of M_1-dG was investigated in stored human DNA extracted from leukocytes. Samples were stored at -20°C, -80°C and in liquid nitrogen and analysed after 0, 2, 4 and 100 weeks of storage using the IDB assay. Adduct levels obtained were corrected via PI ratio. In contrast to highly modified CT-DNA, an overall increase was observed during the first month of storage which was independent of storage temperature. Analysis of subsequent samples, i.e. after 100 weeks of storage, showed that levels of M_1-dG had decreased again. Levels were still elevated though when compared to the initial adduct level at the start of the experiment. The preliminary increase could possibly be explained by formation of M_1-dG through direct oxidation of DNA bases as previously described by Dedon et al. [Dedon (1998)]. The subsequent decrease might have then been based on the overall degradation of M_1-dG levels similar to the one detected for MDA-treated CT-DNA by HPLC. It could be possible that an initial increase also took place in ISB standards but was too low to be detectable by HPLC. Enzymatic digestion followed by HPLC analysis used for the detection of pmol levels of adduct is a much more robust method and should therefore produce more reliable results than the ISB assay. It would therefore be useful for future studies in which low levels of adduct need to be determined

accurately over a long time span that two methods are used simultaneously. For example, low levels of M_1-dG in human samples could also be detected by ^{32}P-postlabelling e.g. [Vaca (1995)]. This comparative approach of two techniques would allow a higher accuracy of results as well as certainty and reliability of observed trends. Although observations with regard to the stability of low levels of M_1-dG in stored human samples were not fully conclusive, it is apparent that stability of DNA adducts and biomarkers in general is an important issue that needed addressing. One has to be certain that markers used for the analysis of samples are reliable and stable over a certain period of time. In conclusion to findings obtained during this work, it appears advisable to analyse M_1-dG levels in human samples immediately after collection and DNA extraction. Storage does not appear suitable as adduct levels seem to increase initially. More time-points would be needed to fully validate and further observe the behaviour of M_1-dG levels over extended periods of time.

It was interesting to note that long-term stored human and CT-DNA samples exhibited vastly different numbers of strand breaks at equivalent storage temperatures. About 0.9 and 35 single-strand breaks per 10^4 bp were detectable by alkaline gel electrophoresis in human and CT-DNA, respectively. These variations might have originated in the different levels of modification (fmol versus pmol) or the poor starting quality of CT-DNA purchased from Sigma. As freshly dissolved control CT-DNA already showed a much higher extent of single-strand breaks when compared to long-term stored human DNA the latter explanation appears more likely. In general, the number of strand breaks observed in MDA-treated CT-DNA increased with increasing storage temperature and was overall higher for samples which had been dissolved in phosphate buffer rather than water.

Long-term stored highly modified CT-DNA samples were also subjected to the SVPD-^{32}P-postlabelling assay. The pattern of damage was clearly distinct from that of oxidative, radiation-induced damage. No indicative lesions of oxidative damage represented by thymine glycols and phosphoglycolates were observed in long-term stored samples. Further identification of the type of damage induced by long-term storage of MDA-treated CT-DNA is necessary. To date, results obtained via alkaline gel electrophoresis and SVPD-^{32}P-postlabelling indicate that abasic sites might be formed in long-term stored, highly modified CT-DNA samples. In order to ascertain the type of damage further experiments need to be carried out. Samples could be incubated with *E. coli* endonuclease IV prior to analysis, which has been reported to remove abasic site lesions. Alternatively, the presence of abasic sites could be detected and quantitated using a slot blot assay for the

detection of apurinic/apyrimidinic sites in DNA developed by Nakamura et al. [Nakamura (1998)]. Lesions are detected by reaction of the aldehydic group of ring-opened abasic sites with a novel aldehyde reactive probe. For example, the rate of spontaneous depurination of CT-DNA can be determined using this technique. It also allows the detection of endogenous levels of abasic sites in genomic DNA as well as the determination of lesions in a human cell line following methyl methanesulphonate treatment.

Further Development of the ISB Assay and Reduction of M_1-dG Levels Using Primary Amines

One of the main problems of the ISB assay, which had been set up previously in our laboratory [Leuratti (1998)], was differences in fragmentation and DNA binding between CT-DNA standards and human or cell culture-derived DNA samples. In general, CT-DNA yielded lower molecular weight fragments following sonication and heat-denaturing, while human samples produced larger fragments. This was thought initially to be the explanation for differences in binding behaviour to nitrocellulose. Usually more DNA bound to the NC membrane for human samples and less for CT-DNA standards. An assay was therefore developed in order to correct for these differences. The PI assay was shown to correct M_1-dG adduct levels efficiently over a wide range of DNA concentrations (0.5 to 2.5 μg/well). For less DNA (0.25 μg/well) correction of ISB results using the PI ratio did not work. Efforts to standardise DNA fragmentation were successful using restriction endonucleases as well as different duration in the ultrasonic and boiling water bath. Nonetheless, variable binding of DNA to NC membranes was still observed. These findings suggested other underlying mechanisms for the variations in DNA binding rather than differences in fragmentation. Reports can be found in the literature that Mg^{2+} ions can inhibit DNA binding to membranes [Kube (1997)]. It is therefore assumed that differences in DNA quality and purity, presence of salt impurities were the underlying cause for different DNA binding patterns. Differences in fragmentation upon sonication might also indicate a generally poor starting material used for ISB standards (CT-DNA from Sigma). Ideally, DNA from the same source, e.g. human, should be used for the analysis of samples in future studies. For this purpose its quality and binding properties need to be tested and if necessary the purchased DNA needs to be re-purified prior to use.

Very low background levels of M_1-dG are essential for using DNA as a standard in the ISB assay. It is fairly difficult to find an appropriate source of DNA, which exhibits very low,

ideally no background levels of M_1-G in control DNA. A method was therefore developed in order to reduce levels of M_1-dG in control DNA samples. Recently, it was reported that M_1-dG would ring-open to N^2-(3-oxo-1-propenyl)deoxyguanosine at alkaline pH [Niedernhofer (1997)]. It was therefore assumed that ring-opening of the adduct at alkaline pH was a prerequisite for the reaction of M_1-dG with primary amines. Primary amines would then react with the aldehyde group of the ring-opened form of M_1-dG, thereby inhibiting ring formation and consequently recognition by the primary antibody. However, it was shown using HPLC detection that M_1-dG levels in highly MDA-modified CT-DNA can be effectively reduced not only at pH > 8 but also at neutral pH using primary amines such as methoxyamine or hydroxylamine. These experiments suggested that M_1-dG itself was a reactive lesion at physiological conditions and that alkaline pH was unnecessary for the reaction with primary amines. In general, treatments using 5mM methoxyamine in various buffer systems (10mM, pH 7.4 and 8.0) were slightly more efficient when compared to hydroxylamine. Interestingly, the pattern of reaction differed also with time. Methoxyamine seemed to react relatively slowly, forming what appeared to be a more stable oxime conjugate with M_1-dG. Original levels of modification were shown to be reduced to approximately 8% after 120 h incubation at 37°C using 5mM methoxyamine. These findings were relatively independent of the buffer system (MOPS or phosphate buffer, 10mM) and pH (7.4 or 8.0) used. In contrast, differences were observed when comparing the two primary amines with each other. Hydroxylamine reacted instantaneously although less effectively with the adduct. The conjugate appeared less stable however, as variations in the extent of M_1-dGp reduction were noticeable by HPLC. The above findings are supported by the work of Schnetz-Boutaud et al. [Schnetz-Boutaud (2000)] who reported that the M_1-dG adduct can react at neutral pH with hydroxylamine to form oximes. The rate of reaction between M_1-dG and the primary amine at pH 7 was reported to be at least 150 times faster than the rate of hydrolysis of M_1-dG to N^2-(3-oxo-1-propenyl)deoxyguanosine.

Mechanisms of reaction appeared to depend on the molarity of the buffer system though. Experiments using 50mM buffer systems suggested that M_1-dG was ring-opened to N^2-(3-oxo-1-propenyl)deoxyguanosine. A significant reduction in M_1-dG levels was observable by HPLC without primary amines being present in the reaction mixture i.e. incubation with buffer only. The reduction appeared to depend on the pH and the buffer system. In general, an increase in pH from 7.4 to 8.0 resulted in less adduct being detectable. Furthermore, the reduction was more efficient in phosphate buffered systems than MOPS buffer.

It was also shown using the ISB assay that methoxyamine treatment of control CT-DNA reduced slightly its background level of M_1-dG. Use of methoxyamine-treated control CT-DNA resulted in a smaller intercept when compared to the usual calibration line. Treatments were carried out in 10mM buffer systems and might thus be further improved by an increase in buffer molarity combined with hydroxylamine treatment. M_1-dG present in highly modified CT-DNA was shown to react most efficiently with the primary amine using these particular conditions. No adduct was detected by HPLC fluorescence.

It was reported by Mao et al. [Mao (1999)] only recently that M_1-dG hydrolyses rapidly and quantitatively at neutral pH to N^2-(3-oxo-1-propenyl)deoxyguanosine in duplex DNA when placed opposite to cytosine but not thymine residues. These findings might explain observations made for negative controls in buffer systems with higher molarity where a substantial decrease in adduct levels was observed. However, no decrease in M_1-dG levels was detectable by HPLC in 10mM buffer systems in the absence of primary amines.

The findings confirmed that M_1-dG can react at neutral pH with primary amines resulting in a significant decrease in adduct level. The mode of action however appeared to be dependent on the molarity of the buffer system. Higher molarity appeared to support ring-opening of M_1-dG to N^2-(3-oxo-1-propenyl)deoxyguanosine whereas in 10mM buffer systems the adduct appeared to react directly with primary amines. The reactivity of M_1-dG and its ring-opened form at physiological pH might have serious implications on mutagenesis, DNA repair and reaction with cellular proteins in the human body.

MDA-induced p53 Mutations

The promutagenic potential of malondialdehyde and corresponding DNA adducts was studied as part of a collaborative project with Dr. Phil Burns and Dr. Gina Scott in Leeds. The yeast expression vector pLS76 that harbours wild-type p53 cDNA was treated with malondialdehyde and transformed into yeast cells. The aim of this collaboration was to compare *in vitro* mutational spectra with the p53 mutation database at IARC and to possibly identify MDA (and KDA, see later) as risk factors in certain types of human malignancies. The p53 mutational spectrum obtained for MDA treatments of plasmid pLS76 was dominated by single base deletions. The high incidence of MDA-induced deletions at polycytosine (6/9) and polyguanine (3/9) sites and the similarity to mutations found in mitochondria of human cancers might suggest a potential role of malondialdehyde and its main adduct formed with DNA, M_1-dG, in endogenous oxidative damage of

mtDNA. However the total number of mutations (n = 18) obtained for MDA treatments *in vitro* was too low to draw any significant conclusions.

In the yeast-based p53 functional assay MDA not only caused deletions but also initiated mutations at GC but not AT base pairs. Comparison with site-specific mutagenicity studies of M_1-dG [Fink (1997)] showed that data correlated well with each other. GC→AT and GC→TA mutations contributed the majority of all substitutions, while GC→CG transversions only accounted for a relatively small percentage. The fairly low number of MDA-induced p53 mutations did not permit any comparison with the p53 database at IARC. Expansion of the MDA-induced p53 mutational spectrum would therefore be very valuable with regard to future comparisons.

As mentioned earlier, several authors have reported the occurrence of frameshifts in mitochondrial DNA, e.g. [Habano (1998)]. These frameshift mutations occurred most commonly in a polycytidine tract. It has been suggested previously that mitochondrial DNA is exposed to greater oxidative damage than nuclear DNA. The comparison of M_1-dG levels in both types of DNA might thus prove very interesting. This would incorporate the development of a method for the extraction of mtDNA as well as a technique for the detection of M_1-dG adducts present in mtDNA. The latter objective would be feasible using the ISB assay.

Modulation of O^6-Alkylguanine Adducts and KDA-induced p53 Mutations

Also in teamwork with Leeds, the promutagenic potential of potassium diazoacetate, a model compound for nitrosated glycine derivatives, was investigated. It was discovered during the course of this work that levels of O^6-alkylguanine adducts could be modulated considerably using different buffer systems during DNA treatment with potassium diazoacetate. For example in KDA-treated plasmid pLS76, levels of both adducts were similar in Tris-EDTA buffer (10mM Tris, 1mM EDTA, pH 7.5) but differed greatly following incubations in phosphate buffered saline. Levels of O^6-CMdG were approximately 13 times higher than O^6-MedG in PBS. Furthermore, about 4 times greater levels of O^6-CMdG were detected for treatments in PBS whereas levels of O^6-MedG were higher in Tris-EDTA (also 4x). To date the underlying mechanisms are unknown. The ionic strength of the buffer system might play an important role in these modulations as levels of both adducts were shown to decrease with increasing concentrations of TE and PBS. Furthermore, Tris being a primary amine could potentially influence the formation of

O^6-alkyguanine adducts via reaction with one or both alkylating agents. Assuming that this hypothesis was plausible, it would appear that Tris suppressed the formation and/or reactivity of the carboxymethyldiazonium ion while at the same time enhancing these properties for the methyldiazonium ion.

This remarkable modulation of relative proportions of O^6-alkylguanine adducts, two promutagenic lesions, offered a rather unique opportunity when looking at KDA-induced p53 mutations. As part of the collaboration with Leeds, the yeast expression vector pLS76 was treated *in vitro* using KDA in PBS or 1x TE buffer and transfected into the *S. cerevisiae* yeast strain yIG397. The presumption that p53 mutational spectra would differ due to dissimilar proportions and possibly different contributions of two O^6-alkylguanine adducts could not be shown. In fact, p53 mutation spectra obtained for KDA treatments in PBS and 1x TE buffer were statistically indistinguishable (P value > 0.6). However, comparison of types of mutation reported for MNU [Fronza (2000), Scott (2000)] with those obtained for KDA revealed substantial differences. The MNU spectrum was dominated by GC→AT transitions whereas this particular class of mutation only contributed about 34% to all KDA mutations. GC→AT transitions are generally believed to be caused by the miscoding properties of O^6-MedG, the latter forming a stable mispair with thymine. Differences between the two spectra suggested therefore that mutations induced by KDA were mainly caused by the carboxymethylation product. In all likelihood, levels of O^6-MedG were efficiently repaired by O^6-alkylguanine-DNA alkyltransferases in yeast cells.

KDA was shown to induce some p53 mutations found in colon and stomach cancer. Hotspots such as the AT→GC transition at codon 220 were found in both human spectra and the *in vitro* spectrum. One of the major hotspots found in colon cancer, a GC→AT transition at codon 241 was also common to the KDA-induced p53 spectrum. Classes of mutation induced by the nitrosated glycine derivative resembled those observed for GI tract cancer. However, there was no statistical evidence that the p53 spectrum of stomach cancer and the *in vitro* KDA spectrum were similar. On the contrary, a P value of < 0.001 indicated that the two spectra were different.

Interestingly, significantly different proportions of KDA mutations in gastric tumour spectra were observed when taking the country of origin into account. The contribution was lowest in Japan (11%) and highest in the USA (36%), while the proportion obtained for Europe was in between with 26%. A similar trend was observed for colon cancer. The

differences were not so marked and ranged from 17% to 22% only, with the lowest proportion of KDA mutations in Japan and the highest in the States. No such variations were found in esophageal cancer.

Endogenous nitrosation of dietary amino acids and peptides has been proposed as a major route of exposure to genotoxic agents in the gastrointestinal tract [Shephard (1989), Challis (1989)]. Cupid et al. [Cupid (2001)] showed that diazoacetate was formed upon treatment of glycine with NO at conditions similar to those found in the GI tract *in vivo*. Moreover, incubation of the reaction mixture with 2'-dG and DNA resulted in the formation of O^6-CMdG and O^6-MedG DNA adducts. These findings suggested that diazoacetate was a key alkylating agent formed from the nitrosation of glycine under simulated physiological conditions. It had also been shown that increased consumption of red meat, but not white meat and fish, led to elevated levels of NOC [Bingham (1996)]. Differences observed for the proportion of KDA mutations in gastric p53 spectra might therefore originate from different dietary habits in Europe, USA and Japan. In general, fish is more commonly eaten in Asian countries, USA on the other hand is well known for its high consumption of red meat.

Although O^6-CMdG has been detected in human gastric biopsies [Singh (2000)] it is highly unlikely to be the only contributor to these types of human malignancies. Other candidates, such as reactive oxygen species (e.g. hydroxy radicals), nitroso compounds and other causative factors, also need to be considered as cancer of the GI tract is most likely caused by a multitude of compounds and not one single agent.

The general difficulty with alkylating agents is that multiple sites of DNA get alkylated. This makes the determination of individual and lesion-specific contributions to the mutational spectrum fairly difficult and unpredictable. In order to study mutations specifically induced by O^6-CMdG one would need to develop a method to incorporate the adduct into specific DNA sequences. The study of adduct site-specific mutagenesis would allow the determination of the coding properties of O^6-CMdG. In contrast to O^6-MedG, O^4-alkylthymine and bulky adducts, no such information is available for O^6-CMdG to date. Alternatively, incubation of KDA-treated yeast expression vector pLS76 using O^6-alkyl-guanine-DNA alkyltransferases prior to transformation into yeast cells might allow the study of O^6-CMdG specific mutagenesis. As this adduct was shown to be not repaired by O^6-alkylguanine-DNA alkyltransferases [Shuker (1997)] it might not only be an important and possibly persistent biomarker but also a contributor to some types of human malignancies.

Overall Conclusions

The main objectives set out at the beginning of this project could be achieved in the majority of cases. The assessment of M_1-dG stability in CT-DNA standards was successfully completed. However, the influence of long-term storage in human samples was not fully conclusive and only one part of the study was conducted. Stability of M_1-dG in stored human tissues, i.e. whole blood and buffy coat, was not carried out due to too many problems arising during the course of the experiment. In general, the limited reproducibility of the ISB assay over time made the study of the effect of long-term storage on M_1-dG in human samples not feasible. The assay allows an allocation of a ranking order to individual samples but not the determination of absolute levels. However, detection and quantitation of absolute levels is essential for the stability assessment of M_1-dG in human samples. Other sensitive assays have been used previously to analyse the M_1-dG adduct in human tissue, such as ^{32}P-postlabelling and GC/EC NCI/MS. Thus, future studies need to focus not only on the long-term stability of M_1-dG in stored human samples but also on the development and application of alternative approaches.

Many other important aspects surrounding the ISB assay have been investigated and led to the development of a significantly improved assay. The novel propidium iodide stain allows the correction for differences in DNA binding to nitrocellulose. Without this correction, results obtained by ISB assay would not reflect true adduct levels. This might ultimately lead to misinterpretation of data sets.

Results on the promutagenic potential of O^6-alkylguanine and M_1-dG adducts presented above raise the possibility that nitrosated glycine derivatives might play an important role in gastric carcinogenesis. Preliminary data also suggested that exposure to the major product of lipid peroxidation appeared as a likely candidate for mutations observed in mitochondrial DNA.

Overall, the results presented in this thesis highlight some important aspects of DNA damage and its significance for cancer risk. Firstly, the interpretation of quantitative DNA adduct measurements must be based upon secure knowledge about the stability of the adducts, as well as factors influencing their formation. Secondly, there are only a few examples of mutational patterns in key genes in tumours being informative about the aetiology of the disease. The results on O^6-CMdG in the human p53 gene suggest that this adduct may be a useful marker in future epidemiological studies on diet and cancer.

8 Bibliography

Anderson, D. and Blowers, S.D. (1994) Limited Cancer Bioassay to Test a Potential Food Chemical. *The Lancet*, **344**, 343-344.

Anderson, D., Hambly, R.J., Yu, T.W., Thomasino, F. and Shuker, D.E.G. (1999) The Effect of Potassium Diazoacetate on Human Peripheral Lymphocytes, Human Adenocarcinoma Colon Caco-2 Cells, and Rat Primary Colon Cells in the Comet Assay. *Teratogenesis, Carcinogenesis and Mutagenesis*, **19**, 137-146.

Bartholomew, B. and Hill, M.J. (1984) The Pharmacology of Dietary Nitrate and the Origin of Urinary Nitrate. *Food Chem. Toxicol.*, **22**, 789-795.

Bartsch, H., Nair, J. and Owen, R.W. (1999) Dietary Polyunsaturated Fatty Acids and Cancer of the Breast and Colorectum: Emerging Evidence for Their Role as Risk Modifiers. *Carcinogenesis*, **20**, 2209-2218.

Bartsch, H., Ohshima, H., Pignatelli, B. and Calmels, S. (1992) Endogenously Formed N-Nitroso Compounds and Nitrosating Agents in Human Cancer Etiology. *Pharmacogenetics*, **2**, 272-277.

Basu, A.K. and Marnett, L.J. (1983) Unequivocal Demonstration that Malondialdehyde is a Mutagen. *Carcinogenesis*, **4**, 331-333.

Basu, A.K., Marnett, L.J. and Romano, L.J. (1984) Dissociation of Malondialdehyde Mutagenicity in *Salmonella typhimurium* from its Ability to Induce Interstrand DNA Cross-links. *Mutation Research*, **129**, 39-46.

Beach, A.C. and Gupta, R.C. (1992) Human Biomonitoring and the ^{32}P-Postlabelling Assay. *Carcinogenesis*, **13**, 1053-1074.

Beckman, K.B. and Ames, B.N. (1999) Endogenous Oxidative Damage of mtDNA. *Mutation Research*, **424**, 51-58.

Benamira, M., Johnson, K., Chaudhary, A., Bruner, K., Tibbetts, C. and Marnett, L.J. (1995) Induction of Mutations by Replication of Malondialdehyde-modified M13 DNA in *Escherichia coli*: Determination of the Extent of DNA Modification, Genetic Requirements for Mutagenesis, and Types of Mutations Induced. *Carcinogenesis*, **16**, 93-99.

Beranek, D.T. (1990) Distribution of Methyl and Ethyl Adducts Following Alkylation with Monofunctional Alkylating Agents. *Mutation Research*, **231**, 11-30.

Bingham, S.A., Pignatelli, B., Pollock, J.R.A., Ellul, A., Malaveille, C., Gross, G., Runswick, S., Cummings, J.H. and Neill, I.K.O. (1996) Does Increased Endogenous Formation of N-Nitroso Compounds in the Human Colon Explain the Association Between Red Meat and Colon Cancer? *Carcinogenesis*, **17**, 515-523.

Binková, B., Hubálek, F. and Srám, R. (1996) Stability of Benzo[α]pyrene DNA Adducts in Rat Tissues During Their Long-term Storage at -20°C or -80°C. *Mutation Research*, **371**, 229-235.

Bos, J.L. (1989) ras Oncogenes in Human Cancer: A Review. *Cancer Research*, **49**, 4682-4689.

Brambilla, G., Cavanna, M., Parodi, S. and Baldini, L. (1972) Induction of Tumours in Newborn and Adult Swiss Mice by N-Diazoacetylglycine Amide. *European Journal of Cancer*, **8**, 127-129.

Brash, D.E., Ziegler, A., Jonason, A.S., Simon, J.A., Kunala, S. and Leffell, D.J. (1996) Sunlight and Sunburn in Human Skin Cancer: p53, Apoptosis, and Tumor Promotion. *J. Invest. Dermatol. Symp. Proc.*, **1**, 136-142.

Bressac, B., Kew, M., Wands, J. and Ozturk, M. (1991) Selective G to T Mutations of p53 Gene in Hepatocellular Carcinoma from Southern Africa. *Nature*, **350**, 429-431.

Burgart, L.J., Zheng, J., Shu, Q., Strickler, J.G. and Shibata, D. (1995) Somatic Mitochondrial Mutation in Gastric Cancer. *American Journal of Pathology*, **147**, 1105-1111.

Burns, P.A., Gordon, A.J.E. and Glickman, B.W. (1987) Influence of Neighbouring Base Sequence on N-Methyl-N'-nitro-N-nitrosoguanidine Mutagenesis in the lacI Gene of *Escherichia coli*. *J. Mol. Biol.*, **194**, 385-390.

Burns, P.A., Gordon, A.J.E., Kunsmann, K. and Glickman, B.W. (1988) Influence of Neighboring Base Sequence on the Distribution and Repair of N-Ethyl-N-nitrosourea-induced Lesions in *Escherichia coli*. *Cancer Research*, **48**, 4455-4458.

Busby, W.F., Shuker, D.E.G., Charnley, G., Newberne, P.M., Tannenbaum, S.R. and Wogan, G.N. (1985) Carcinogenicity in Rats of the Nitrosated Bile Acid Conjugates N-Nitrosoglycocholic Acid and N-Nitrosotaurocholic Acid. *Cancer Research*, **45**, 1367-1371.

Cariello, N.F., Piegorsch, W.W., Adams, W.T. and Skopek, T.R. (1994a) Computer Program for the Analysis of Mutational Spectra: Application to p53 Mutations. *Carcinogenesis*, **15**, 2281-2285.

Cariello, N.F., Beroud, C. and Soussi, T. (1994b) Database and Software for the Analysis of Mutations at the Human p53 Gene. *Nucleic Acids Research*, **22**, 3549-3550.

Challis, B.C. (1989) Chemistry and Biology of Nitrosated Peptides. *Cancer Surveys*, **8**, 363-384.

Challis, B.C., Glover, B.R. and Pollock, J.R.A. (1987). Peptide Nitrosation in Dilute Acid. In H. Bartsch, I. O'Neill and R. Schulte-Hermann (Ed.), *The Relevance of N-Nitroso Compounds in Human Cancer* (pp. 345-350). Lyon, France: International Agency for Research on Cancer.

Chaudhary, A., Nakubo, M., Reddy, G., Yeola, S., Morrow, J., Blair, I. and Marnett, L.J. (1994) Detection of Endogenous Malondialdehyde-Deoxyguanosine Adducts in Human Liver. *Science*, **265**, 1580-1582.

Cho, Y., Gorina, S., Jeffrey, P.D. and Pavletich, N.P. (1994) Crystal Structure of a p53 Tumour Suppressor-DNA Complex. *Science*, **265**, 346-355.

Correa, P. (1988) A Human Model of Gastric Carcinogenesis. *Cancer Research*, **48**, 3554-3560.

Correa, P. (1992) Human Gastric Carcinogenesis: A Multistep and Multifactorial Process - First American Cancer Society Award Lecture on Cancer Epidemiology and Prevention. *Cancer Research*, **52**, 6735-6740.

Cunningham, R.P., Saporito, S.M., Spitzer, S.G., Weiss, B. (1986) Endonuclease IV (nfo) Mutant of *Escherichia coli*. *Journal of Bacteriology*, **168**, 1120-1127.

Cupid, B.C., Singh, R. and Shuker, D.E.G. (2001) DNA-Alkylating Intermediates Are Formed by the Reaction of Nitric Oxide with Glycine Under Simulated Physiological Conditions. *manuscript in preparation.*

Daniels, J.S., Nguyen, V., Schnetz-Boutaud, N. and Marnett, L.J. (1999). Development of a Template-directed Primer Extension Assay to Probe the Formation of the Malondialdehyde Adduct Pyrimido[1,2-α]purin-10(3H)-one (M_1G) in DNA. Proceedings of the 20th Annual AACR Meeting, Philadelphia, USA.

Decaprio, A.P. (1997) Biomarkers: Coming of Age for Environmental Health and Risk Assessment. *Environmental Science and Technology*, **31**, 1837-1848.

Dedon, P.C., Plastaras, J.P., Rouzer, C.A. and Marnett, L.J. (1998) Indirect Mutagenesis by Oxidative DNA Damage: Formation of the Pyrimidopurinone Adduct of Deoxyguanosine by Base Propenal. *Proc. Natl. Acad. Sci. USA*, **95**, 11113-11116.

De Groot, A.J.L., Jansen, J.G., van Valkenburg, C.F.M. and van Zeeland, A.A. (1994) Molecular Dosimetry of 7-Alkyl- and O^6-Alkylguanine in DNA by Electrochemical Detection. *Mutation Research*, **307**, 61-66.

Denissenko, M.F., Pao, A., Tang, M.S. and Pfeifer, G.P. (1996) Preferential Formation of Benzo[α]pyrene Adducts in Lung Cancer Mutational Hotspots in p53. *Science*, **274**, 430-432.

Doetsch, P.W. and Cunningham, R.P. (1990) The Enzymology of Apurinic/Apyrimidinic Endonucleases. *Mutation Research*, **236**, 173-201.

Dolan, M.E., Oplinger, M. and Pegg, A.E. (1988) Sequence Specificity of Guanine Alkylation and Repair. *Carcinogenesis*, **9**, 2139-2143.

Drouin, R., Gao, S. and Holmquist, G.P. (1996a). Agarose Gel Electrophoresis for DNA Damage Analysis. In G.P. Pfeifer (Ed.), *Technologies for Detection of DNA Damage and Mutations* (pp. 37-43). New York: Plenum Press.

Drouin, R., Rodriguez, H., Gao, S.W., Gebreyes, Z., O'Connor, T.R., Holmquist, G.P. and Akman, S.A. (1996b) Cupric Ion/Ascorbate/Hydrogen Peroxide-Induced DNA Damage: DNA-Bound Copper Ion Primarily Induces Base Modifications. *Free Radical Biology and Medicine*, **21**, 261-273.

Ehrenberg, S.L. and Osterman-Golkar, S. (1980) Alkylation of Macromolecules for Detecting Mutagenic Agents. *Teratogenesis, Carcinogenesis, and Mutagenesis*, **1**, 105-127.

Ehrlich, M. and Wang, R.Y.H. (1981) 5-Methylcytosine in Eukaryotic DNA. *Science*, **212**, 1350-1357.

Everett, S.M., Singh, R., Leuratti, C., White, K.L.M., Neville, P., Greenwood, D., Marnett, L.J., Schorah, C.J., Forman, D., Shuker, D.E.G. and Axon, A.T.R. (2001) Levels of Malondialdehyde-Deoxyguanosine in the Gastric Mucosa: Relationship with Lipid Peroxidation, Ascorbic Acid, and *Helicobacter pylori*. *Cancer Epidemiology, Biomarkers and Prevention*, **10**, 369-376.

Fang, J., Vaca, C., Valsta, L. and Mutanen, M. (1996) Determination of DNA Adducts of Malonaldehyde in Humans: Effects of Dietary Fatty Acid Composition. *Carcinogenesis*, **17**, 1035-1040.

Farmer, P.B. (1994) Carcinogen Adducts: Use in Diagnosis and Risk Assessment. *Clinical Chemistry*, **40**, 1438-1443.

Fink, S.P., Reddy, G.R. and Marnett, L.J. (1997) Mutagenicity in *Escherichia coli* of the Major DNA Adduct Derived from the Endogenous Mutagen Malondialdehyde. *Proceedings of the National Academy of Sciences of the USA*, **94**, 8652-8657.

Flaman, J.M., Frebourg, T., Moreau, V., Charbonnier, F., Martin, C., Chappuis, P., Sappino A.P., Limacher, J.M., Bron, L., Benhattar, J., Tada, M., van Meir, E.G., Estreicher, A. and Iggo, R.D. (1995) A Simple p53 Functional Assay for Screening Cell Lines, Blood, and Tumors. *Proc. Natl. Acad. Sci. USA*, **92**, 3963-3967.

Frei, J.V., Swenson, D.H., Warren, W. and Lawley, P.D. (1978) Alkylation of Deoxyribonucleic Acid *in vivo* in Various Organs of C57BL Mice by the Carcinogens N-Methyl-N-Nitrosourea, N-Ethyl-N-Nitrosourea and Ethyl Methansulphonate in Relation to Induction of Thymic Lymphoma. *Biochem. J.*, **174**, 1031-1044.

Friend, S. (1994) p53: A Glimpse at the Puppet Behind the Shadow Play. *Science*, **265**, 334-335.

Friesen, M.D., Garren, L., Prevost, V. and Shuker, D.E.G. (1991) Isolation of Urinary 3-Methyladenine Using Immunoaffinity Columns prior to Determination by Low-Resolution Gas Chromatography-Mass Spectrometry. *Chemical Research in Toxicology*, **4**, 102-106.

Fronza, G., Inga, A., Monti, P., Scott, G., Campomenosi, P., Menichini, P., Ottaggio, L., Viaggi, S., Burns, P.A., Gold, B. and Abbondandolo, A. (2000) The Yeast p53 Functional Assay: A New Tool for Molecular Epidemiology. Hopes and Facts. *Mutation Research*, **462**, 293-301.

Gillam, I., Millward, S., Blew, D., von Tigerstrom, M., Wimmer, E. and Tener, G.M. (1967) The Separation of Soluble Ribonucleic Acids on Benzoylated Diethylaminomethylcellulose. *Biochemistry*, **6**, 3043-3056.

Glickman, B.W., Horsfall, M.J., Gordon, A.J.E. and Burns, P.A. (1987) Nearest Neighbor Affects G:C to A:T Transitions Induced by Alkylating Agents. *Environmental Health Perspectives*, **76**, 29-32.

Goda, Y. and Marnett, L. (1991) High-Performance Liquid Chromatography with Electrochemical Detection for Determination of the Major Malondialdehyde-Guanine Adduct. *Chemical Research in Toxicology*, **4**, 520-524.

Gómez-Sánchez, A., Hermosín, I., Lassaletta, J.M. and Maya, I. (1993) Cleavage and Oligomerization of Malondialdehyde. *Tetrahedron*, **49**, 1237-1250.

Goth, R. and Rajewsky, M.F. (1974) Persistence of O^6-Ethylguanine in Rat Brain DNA: Correlation with Nervous System Specific Carcinogenesis by Ethylnitrosourea. *Proc. Natl. Acad. Sci. USA*, **71**, 639-643.

Greenblatt, M.S., Bennett, W.P., Hollstein, M. and Harris, C.C. (1994) Mutations in the p53 Tumor Suppressor Gene: Clues to Cancer Etiology and Molecular Pathogenesis. *Cancer Research*, **54**, 4855-4878.

Guthrie, C. and Fink, G.R. (1991). *Guide to Yeast Genetics and Molecular Biology*. San Diego, California: Academic Press Inc.

Habano, W., Nakamura, S. and Sugai, T. (1998) Microsatellite Instability in the Mitochondrial DNA of Colorectal Carcinomas: Evidence of Mismatch Repair Systems in Mitochondrial Genome. *Oncogene*, **17**, 1931-1937.

Hainaut, P. (1995) The Tumour Suppressor Protein p53: A Receptor to Genotoxic Stress that Controls Cell Growth and Survival. *Current Opinion in Oncology*, **7**, 76-82.

Hainaut, P. and Hollstein, M. (2000) p53 and Human Cancer: The First Ten Thousand Mutations. *Advances in Cancer Research*, **77**, 81-137.

Hall, C.N., Badawi, A.F., O'Connor, P.J. and Saffhill, R. (1991) The Detection of Alkylation Damage in the DNA of Human Gastrointestinal Tissues. *British Journal of Cancer*, **64**, 59-63.

Harrison, K.L. (1998) PhD Thesis on 'Biomarkers of Exposure to Nitrosation Products of Amino Acids and Peptides'. University of Leicester.

Harrison, K.L., Fairhurst, N., Challis, B.C. and Shuker, D.E.G. (1997) Synthesis, Characterisation, and Immunochemical Detection of O^6-(Carboxymethyl)-2'-deoxyguanosine: A DNA Adduct Formed by Nitrosated Glycine Derivatives. *Chemical Research in Toxicology*, **10**, 652-659.

Harrison, K.L., Jukes, R., Cooper, D.P. and Shuker, D.E.G. (1999) Detection of Concomitant Formation of O^6-Carboxymethyl- and O^6-Methyl-2'-deoxyguanosine in DNA Exposed to Nitrosated Glycine Derivatives Using a Combined Immunoaffinity/HPLC Method. *Chemical Research in Toxicology*, **12**, 106-111.

Hazen, S.L., Hsu, F.F. and Heinecke, J.W. (1996) p-Hydroxyphenylacetaldehyde Is the Major Product of L-Tyrosine Oxidation by Activated Human Phagocytes. *J. Biol. Chem.*, **271**, 1861-1867.

Hazen, S.L., Hsu, F.F., D'Avignon, A. and Heinecke, J.W. (1998) Human Neutrophils Employ Myeloperoxidases to Convert a-Amino Acids to a Battery of Reactive Aldehydes: A Pathway for Aldehyde Generation at Sites of Inflammation. *Biochemistry*, **37**, 6864-6873.

Hernandez-Boussard, T., Rodriguez-Tome, P., Montesano, R. and Hainaut, P. (1999) IARC p53 Mutation Database: A Relational Database to Compile and Analyse p53 Mutations in Human Tumors and Cell Lines. *Human Mutation*, **14**, 1-8.

Hernandez-Boussard, T.M. and Hainaut, P. (1998) A Specific Spectrum of p53 Mutations in Lung Cancer from Smokers: Review of Mutations Compiled in the IARC p53 Database. *Environ. Health Perspect.*, **106**, 385-391.

Hill, M.J. (1996) Endogenous N-Nitrosation. *European Journal of Cancer Prevention*, **5**, 47-50.

Hill, M.J. (1996a) Factors Controlling Endogenous N-Nitrosation. *European Journal of Cancer Prevention*, **5**, 71-74.

Hill, M.J. (1996b) N-Nitrosation at Non-Gastric Sites. *European Journal of Cancer Prevention*, **5**, 105-108.

Hollstein, M., Moeckel, G., Hergenhahn, M., Spiegelhalder, B., Keil, M., Werle-Schneider, G., Bartsch, H. and Brickmann, J. (1998) On the Origins of Tumor Mutations in Cancer Genes: Insights from the p53 Gene. *Mutation Research*, **405**, 145-154.

Horsfall, M.J., Gordon, A.J.E., Burns, P.A., Zielenska, M., van der Vliet, G.M.E. and Glickman, B.W. (1990) Mutational Specificity of Alkylating Agents and the Influence of DNA Repair. *Environmental & Molecular Mutagenesis*, **15**, 107-122.

Horton, T.M., Petros, J.A., Heddi, A., Shoffner, J., Kaufman, A.E., Graham, S.D., Gramlich, T. and Wallace, (1996) Novel Mitochondrial DNA Deletion Found in a Renal Cell Carcinoma. *Genes, Chromosomes and Cancer*, **15**, 95-101.

Hsu, I.C., Metcalf, R.A., Sun, T., Welsh, J.A., Wang, N.J. and Harris, C.C. (1991) Mutational Hotspot in the p53 Gene in Human Hepatocellular Carcinomas. *Nature*, **350**, 427-428.

Hussain, S.P. and Harris, C.C. (1998) Molecular Epidemiology of Human Cancer: Contribution of Mutation Spectra Studies of Tumor Suppressor Genes. *Cancer Research*, **58**, 4023-4037.

Hussain, S.P. and Harris, C.C. (1999) p53 Mutation Spectrum and Load: The Generation of Hypotheses Linking the Exposure of Endogenous or Exogenous Carcinogens to Human Cancer. *Mutation Research*, **428**, 23-32.

Inga, A., Iannone, R., Campomenosi, P., Molina, F., Menichini, P., Abbondandolo, A. and Fronza, G. (1995) Mutational Fingerprint Induced by the Antineoplastic Drug Chloroethyl-cyclohexyl-nitrosourea in Mammalian Cells. *Cancer Research*, **55**, 4658-4663.

Inga, A., Iannone, R., Monti, P., Molina, F., Bolognesi, M., Abbondandolo, A., Iggo, R. and Fronza, G. (1997) Determining Mutational Fingerprints at the Human p53 Locus with a Yeast Functional Assay: A New Tool for Molecular Epidemiology. *Oncogene*, **14**, 1307-1313.

Inga, A., Scott, G., Monti, P., Aprile, A., Abbondandolo, A., Burns, P.A. and Fronza, G. (1998) Ultraviolet-light Induced p53 Mutational Spectrum in Yeast is Indistinguishable from p53 Mutations in Human Skin Cancer. *Carcinogenesis*, **19**, 741-746.

Ishioka, C., Frebourg, T., Yan, Y.X., Vidall, M., Friend, S.H., Schmidt, S. and Iggo, R. (1993) Screening Patients for Heterozygous p53 Mutations Using a Functional Assay in Yeast. *Nature Genetics*, **5**, 124-129.

Jackson, P.E., Hall, C.N., Badawi, A.F., O'Connor, P.J., Cooper, D.P. and Povey, A.C. (1996) Frequency of Ki-ras Mutations and DNA Alkylation in Colorectal Tissue from Individuals Living in Manchester. *Molecular Carcinogenesis*, **16**, 12-19.

Janero, D. (1990) Malondialdehyde and Thiobarbituric Acid-Reactivity as Diagnostic Indices of Lipid Peroxidation and Peroxidative Tissue Injury. *Free Radical Biology and Medicine*, **9**, 515-540.

Johnson, K.A., Fink, S.P. and Marnett, L.J. (1997) Repair of Propanodeoxyguanosine by Nucleotide Excision Repair *in vivo* and *in vitro*. *J. Biol. Chem.*, **272**, 11434-11438.

Johnson, K.A., Mierzwa, M.L., Fink, S.P. and Marnett, L.J. (1999) MutS Recognition of Exocyclic DNA Adducts That Are Endogenous Products of Lipid Peroxidation. *The Journal of Biological Chemistry*, **274**, 27112-27118.

Jones, G.D.D. and Weinfeld, M. (2000). A ^{32}P-Postlabelling Protocol to Measure Oxidative DNA Damage. In J. Lunec and H.R. Griffiths (Ed.), *Measuring in vivo Oxidative Damage: A Practical Approach* (pp. 107-124). John Wiley & Sons, Ltd.

Jones, G.D.D., Dickinson, L., Lunec, J. and Routledge, M.N. (1999) SVPD-Post-Labeling Detection of Oxidative Damage Negates the Problem of Adventitious Oxidative Effects During ^{32}P-Labeling. *Carcinogenesis*, **20**, 503-507.

Karran, P. and Lindahl, T. (1985) Cellular Defence Mechanisms Against Alkylating Agents. *Cancer Surveys*, **4**, 583-599.

King, R.J.B. (1996). *Cancer Biology*. Essex: Addison Wesley Longman Limited.

Kothari, R.M. and Taylor, M.W. (1972) RNA Fractionation on Modified Celluloses. I. Ecteola-, Ectham-, Amino-Ethyl-, Nucleic Acid-, and Nitro-Cellulose. *Journal of Chromatography*, **73**, 449-462.

Kube, D.M. and Srivastava, A. (1997) Quantitative DNA Slot Blot Analysis: Inhibition of DNA Binding to Membranes by Magnesium Ions. *Nucleic Acid Research*, **25**, 3375-3376.

Kunze, U.R. (1990). *Grundlagen der quantitativen Analyse*. Stuttgart: Georg Thieme Verlag.

Kvam, E. and Tyrrell, R.M. (1997) Artificial Background and Induced Levels of Oxidative Base Damage in DNA from Human Cells. *Carcinogenesis*, **18**, 2281-2283.

Kyrtopoulos, S.A. (1989) N-Nitroso Compound Formation in Human Gastric Juice. *Cancer Surveys*, **8**, 423-442.

Kyrtopoulos, S.A. (1998) O^6-Alkylguanine-DNA Alkyltransferase: Influence on Susceptibility to the Genetic Effect of Alkylating Agents. *Toxicology Letters*, **102-103**, 53-57.

Kyrtopoulos, S.A., Vrotsou, B., Golematis, B., Bonatsos, M. and Lakiotis, G. (1984) O^6-Methylguanine-DNA Transmethylase Activity in Extracts of Human Gastric Mucosa. *Carcinogenesis*, **5**, 943-947.

La, D.K. and Swenberg, J.A. (1996) DNA Adducts: Biological Markers of Exposure and Potential Applications to Risk Assessment. *Mutation Research*, **365**, 129-146.

Leaf, C.D., Wishnok, J.S. and Tannenbaum, S.R. (1989) Mechanisms of Endogenous Nitrosation. *Cancer Surveys*, **8**, 323-334.

Leuratti, C., Singh, R., Deag, E.J., Griech, E., Hughes, R., Bingham, S.A., Plastaras, J.P., Marnett, L.J. and Shuker, D.E.G. (1999). A Sensitive Immunoslot-Blot Assay for the Detection of Malondialdehyde in Human DNA. In B. Singer and H. Bartsch (Ed.), *Exocyclic DNA Adducts in Mutagenesis and Carcinogenesis* (pp. 197-203). Lyon, France: International Agency for Research on Cancer.

Leuratti, C., Singh, R., Lagneau, C., Farmer, P., Plastaras, J., Marnett, L. and Shuker, D. (1998) Determination of Malondialdehyde-induced DNA Damage in Human Tissue Using an Immunoslot Blot Assay. *Carcinogenesis*, **19**, 1919-1924.

Leuratti, C., Watson, M.A., Deag, E.J., Welch, A., Singh, R., Gottschalg, E., Marnett, L.J., Atkin, W., Day, N.E., Shuker, D.E.G. and Bingham, S.A. (2002) Detection of Malondialdehyde-DNA Adducts in Human Colorectal Mucosa: Relationship with Diet and the Presence of Adenomas. *Cancer Epidemiology, Biomarkers and Prevention*, **11**, 267-273.

Levin, J.D., Shapiro, R. and Demple, B. (1991) Metalloenzymes in DNA-Repair - *Escherichia coli* Endonuclease IV and *Saccharomyces cerevisiae* APN1. *J. Biol. Chem.*, **266**, 22893-22898.

Lindahl, T. (1982) DNA Repair Enzymes. *Ann. Rev. Biochem.*, **51**, 61-87.

Liu, R.H. and Hotchkiss, J.H. (1995) Potential Genotoxicity of Chronically Elevated Nitric Oxide: A Review. *Mutation Research*, **339**, 73-89.

Loeb, L.A.P.B.D. (1986) Mutagenesis by Apurinic/Apyrimidinic Sites. *Annu. Rev. Genet.*, **20**, 201-230.

Loechler, E.L. (1994) A Violation of the Swain-Scott Principle, and not S_N1 versus S_N2 Reaction-Mechanisms, Explains Why Carcinogenic Alkylating-Agents Can Form Different Proportions of Adducts at Oxygen Versus Nitrogen in DNA. *Chemical Research in Toxicology*, **7**, 277-280.

Loechler, E.L., Green, C.L. and Essigmann, J.M. (1984) *In vivo* Mutagenesis by O^6-Methylguanine Built Into a Unique Site in a Viral Genome. *Proc. Natl. Acad. Sci. USA*, **81**, 6271-6275.

Longnecker, D.S. and Curphey, T.J. (1975) Adenocarcinoma of the Pancreas in Azaserine-treated Rats. *Cancer Research*, **35**, 2249-2258.

Loveless, A. (1969) Possible Relevance of O-6 Alkylation of Deoxyguanosine to the Mutagenicity and Carcinogenicity of Nitrosamines and Nitrosamides. *Nature*, **223**, 206-207.

Ludeke, B.I. and Kleihues, P. (1988) Formation and Persistence of O^6-(2-hydroxyethyl)-2'-deoxyguanosine in DNA of Various Rat Tissues Following a Single Dose of N-Nitroso-N-(2-hydroxyethyl)urea. An Immuno-slot-blot Study. *Carcinogenesis*, **9**, 147-151.

Lutz, W.K., Fekete, T. and Vamvakas, S. (1998) Position- and Base Pair-Specific Comparison of p53 Mutation Spectra in Human Tumors: Elucidation of Relationships Between Organs for Cancer Etiology. *Environmental Health Perspectives*, **106**, 207-211.

Ma, J., Verweij, J., Planting, A.S.T., de Boer-Dennert, M., van Ingen, H.E., van der Burg, M.E.L., Stoter, G. and Schellens, J.H.M. (1995) Current Sample Handling Methods for Measurements of Platinum-DNA Adducts in Leukocytes in Man Lead to Discrepant Results in DNA Adduct Levels and DNA Repair. *British Journal of Cancer*, **71**, 512-517.

Malkin, D. (1994) Germline p53 Mutations and Heritable Cancer. *Annu. Rev. Genet.*, **28**, 443-465.

Mao, H., Schnetz-Boutaud, N.C., Weisenseel, J.P., Marnett, L.J. and Stone, M.P. (1999) Duplex DNA Catalyzes the Chemical Rearrangement of a Malondialdehyde Deoxyguanosine Adduct. *Proc. Natl. Acad. Sci. USA*, **96**, 6615-6620.

Marnett, L. (1994a) Generation of Mutagens During Arachidonic Acid Metabolism. *Cancer and Metastasis Reviews*, **13**, 303-308.

Marnett, L. (1994b). DNA Adducts of α,β-unsaturated Aldehydes and Dicarbonyl Compounds. In K. Hemminki, A. Dipple, D. Shuker, F. Kadlubar, D. Segerbäck and H. Bartsch (Ed.), *DNA Adducts: Identification and Biological Significance* (pp. 151-163). Lyon, France: International Agency for Research on Cancer.

Marnett, L.J. (1999) Lipid Peroxidation - DNA Damage by Malondialdehyde. *Mutation Research*, **424**, 83-95.

Marnett, L.J. and Tuttle, M.A. (1980) Comparison of the Mutagenicities of Malondialdehyde and the Side Products Formed during Its Chemical Synthesis. *Cancer Research*, **40**, 276-282.

Marnett, L.J., Basu, A.K., O'Hara, S.M., Weller, P.E., Rahman, A.F.M.M. and Oliver, J.P. (1986) Reaction of Malondialdehyde with Guanine Nucleosides: Formation of Adducts Containing Oxadiazabicyclononene Residues in the Base-Pairing Region. *J. Am. Chem. Soc.*, **108**, 1348-1350.

May, P. and May, E. (1999) Twenty Years of p53 Research: Structural and Functional Aspects of the p53 Protein. *Oncogene*, **18**, 7621-7636.

Meinkoth, J. and Wahl, G. (1984) Review - Hybridization of Nucleic Acids Immobilized on Solid Supports. *Analytical Biochemistry*, **138**, 267-284.

Mientjes, E.J., Hochleitner, K., Luiten-Schuite, A., van Delft, J.H.M., Thomale, J., Berends, F., Rajewsky, M.F., Lohman, P.H.M. and Baan, R.A. (1996) Formation and Persistence of O^6-

Ethylguanine in Genomic and Transgene DNA in Liver and Brain of lambda-lacZ Transgenic Mice Treated with N-Ethyl-N-nitrosourea. *Carcinogenesis*, **17**, 2449-2454.

Miller, E.C. (1978) Some Current Perspectives on Chemical Carcinogenesis in Humans and Experimental Animals. *Cancer Research*, **38**, 1479-1496.

Mirvish, S.S. (1995) Role of N-Nitroso Compounds (NOC) and N-Nitrosation in Etiology of Gastric, Esophageal, Nasopharyngeal and Bladder Cancer and Contribution to Cancer of Known Exposures to NOC. *Cancer Letters*, **93**, 17-48.

Mirvish, S.S. (1996) Inhibition by Vitamins C and E of *in vivo* Nitrosation and Vitamin C Occurrence in the Stomach. *European Journal of Cancer Prevention*, **5**, 131-136.

Moll, U.M. and Schramm, L.M. (1998) p53 - An Acrobat in Tumorigenesis. *Crit. Rev. Oral Biol. Med.*, **9**, 23-37.

Montesano, R., Hainaut, P. and Wild, C.P. (1997) Hepatocellular Carcinoma: From Gene to Public Health. *J. Natl. Cancer Inst.*, **89**, 1844-1851.

Mukai, F. and Goldstein, B. (1976) Mutagenicity of Malonaldehyde, a Decomposition Product of Peroxidized Polyunsaturated Fatty Acids. *Science*, **191**, 868-869.

Musarrat, J. and Wani, A.A. (1994) Quantitative Immunoanalysis of Promutagenic 8-Hydroxy-2'-deoxyguanosine in Oxidized DNA. *Carcinogenesis*, **15**, 2037-2043.

Müller, E. (1908) Über Pseudodiazoessigsäure. *Chemische Berichte*, **41**, 3116-3139.

Nakamura, J., Walker, V.E., Upton, P.B., Chiang, S.Y., Kow, Y.W. and Swenberg, J.A. (1998) Highly Sensitive Apurinic/Apyrimidinic Site Assay Can Detect Spontaneous and Chemically Induced Depurination under Physiological Conditions. *Cancer Research*, **58**, 222-225.

Nehls, P., Adamkiewicz, J. and Rajewsky, M. (1984) Immuno-Slot-Blot: A Highly Sensitive Immunoassay for the Quantitation of Carcinogen-modified Nucleosides in DNA. *Journal of Cancer Research and Clinical Oncology*, **108**, 23-29.

Niedernhofer, L., Riley, M., Schnetz-Boutaud, N., Sanduwaran, G., Chaudhary, A., Reddy, G. and Marnett, L. (1997) Temperature-Dependent Formation of a Conjugate between Tris(hydroxy-methyl)aminomethane Buffer and the Malondialdehyde-DNA Adduct Pyrimidopurinone. *Chemical Research in Toxicology*, **10**, 556-561.

O'Driscoll, M., Macpherson, P., Xu, Y.Z. and Karran, P. (1999) The Cytotoxicity of DNA Carboxymethylation and Methylation by the Model Carboxymethylating Agent Azaserine in Human Cells. *Carcinogenesis*, **20**, 1855-1862.

Ohshima, H. and Bartsch, H. (1981) Quantitative Estimation of Endogenous Nitrosation in Humans by Monitoring N-Nitrosoproline Excretion in Urine. *Cancer Research*, **41**, 3658-3662.

Ohshima, H.B.H. (1994) Chronic Infection and Inflammatory Processes as Cancer Risk Factors: Possible Role of Nitric Oxide in Carcinogenesis. *Mutation Research*, **305**, 253-264.

Ory, K., Legros, Y., Auguin, C. and Soussi, T. (1994) Analysis of the Most Representative Tumour-derived p53 Mutants Reveals that Changes in Protein Conformation are not Correlated with Loss of Transactivation or Inhibition of Cell Proliferation. *The EMBO Journal*, **13**, 3496-3504.

Osborne, M.R. and Phillips, D.H. (2000) Preparation of a Methylated DNA Standard, and Its Stability on Storage. *Chemical Research in Toxicology*, **13**, 257-261.

Parrella, P., Xiao, Y., Fliss, M., Sanchez-Cespedes, M., Mazzarelli, P., Rinaldi, M., Nicol, T., Gabrielson, E., Cuomo, C., Cohen, D., Pandit, S., Spencer, M., Rabitti, C., Fazio, V.M. and Sidransky, D. (2001) Detection of Mitochondrial DNA Mutations in Primary Breast Cancer and Fine-Needle Aspirates. *Cancer Research*, **61**, 7623-7626.

Pegg, A.E. (1984) Methylation of the O^6 Position of Guanine in DNA is the Most Likely Initiating Event in Carcinogenesis by Methylating Agents. *Cancer Investigation*, **2**, 223-231.

Pegg, A.E. (2000) Repair of O^6-Alkylguanine by Alkyltransferases. *Mutation Research*, **462**, 83-100.

Pegg, A.E. and Byers, T.L. (1992) Repair of DNA Containing O^6-Alkylguanine. *The FASEB Journal*, **6**, 2302-2310.

Pfeifer, G.P. and Denissenko, M.F. (1998) Formation and Repair of DNA Lesions in the p53 Gene: Relation to Cancer Mutations? *Environmental & Molecular Mutagenesis*, **31**, 197-205.

Phillips, A.P. (1969) A Study of Factors Influencing the Retention of DNA by Membrane Filters. *Biochimica et Biophysica Acta*, **195**, 186-196.

Phillips, D. (1996) DNA Adducts in Human Tissues: Biomarkers of Exposure to Carcinogens in Cigarette Smoke. *Environmental Health Perspectives*, **104**, 453-458.

Pieper, R.O. (1998). Cellular Response to Methylation Damage. In J.A. Nickoloff and M.F. Hoekstra (Ed.), *DNA Damage and Repair, Vol. 2: DNA Repair in Higher Eukaryotes*. Totowa, NJ: Humana Press Inc.

Pietenpol, J.A., Tokino, T., Thiagalingam, S., El-Deiry, W.S., Kinzler, K.W. and Vogelstein, B. (1994) Sequence-specific Transcriptional Activation is Essential for Growth Suppression by p53. *Proc. Natl. Acad. Sci. USA*, **91**, 1998-2002.

Plastaras, J.P., Guengerich, F.P., Nebert, D.W. and Marnett, L.J. (2000a) Xenobiotic-metabolizing Cytochromes P450 Convert Prostaglandin Endoperoxide to Hydroxyheptadecatrienoic Acid and the Mutagen, Malondialdehyde. *The Journal of Biological Chemistry*, **275**, 11784-11790.

Plastaras, J.P., Riggins, J.N., Otteneder, M. and Marnett, L.J. (2000b) Reactivity and Mutagenicity of Endogenous DNA Oxopropenylating Agents: Base Propenals, Malondialdehyde, and N^{ε}-Oxopropenyllysine. *Chemical Research in Toxicology*, **13**, 1235-1242.

Podmore, K., Farmer, P.B., Herbert, K.E., Jones, G.D.D. and Martin, E.A. (1997) ^{32}P-Postlabelling Approaches for the Detection of 8-Oxo-2'deoxyguanosine-3'-monophosphate in DNA. *Mutation Research*, **178**, 139-149.

Preston, B.D., Singer, B. and Loeb, L. (1986) Mutagenic Potential of O^4-Methylthymine *in vivo* Determined by an Enzymatic Approach to Site-Specific Mutagenesis. *Proc. Natl. Acad. Sci. USA*, **83**, 8501-8505.

Puju, S., Shuker, D.E.G., Bishop, W.W., Falchuk, K.R., Tannenbaum, S.R. and Thilly, W.G. (1982) Mutagenicity of N-Nitroso Bile Acid Conjugates in *Salmonella typhimurium* and Diploid Human Lymphoblasts. *Cancer Research*, **42**, 2601-2604.

Reddy, G.R. and Marnett, L.J. (1995) Synthesis of an Oligodeoxynucleotide Containing the Alkaline Labile Malondialdehyde-Deoxyguanosine Adduct Pyrimido[1,2-α]purin-10(3H)-one. *J. Am. Chem. Soc.*, **117**, 5007-5008.

Richardson, F.C. and Richardson, K.K. (1990) Sequence-dependent Formation of Alkyl DNA Adducts: A Review of Methods, Results and Biological Correlates. *Mutation Research*, **233**, 127-138.

Richardson, K.K., Richardson, F.C., Crosby, R.M., Swenberg, J.A. and Skopek, T.R. (1987) DNA Base Changes and Alkylation Following *in vivo* Exposure of *Escherichia coli* to N-Methyl-N-Nitrosourea and N-Ethyl-N-Nitrosourea. *Proc. Natl. Acad. Sci. USA*, **84**, 344-348.

Richter, C., Park, J.W. and Ames, B.N. (1988) Normal Oxidative Damage to Mitochondrial and Nuclear DNA is Extensive. *Proc. Natl. Acad. Sci. USA*, **85**, 6465-6467.

Rouzer, C., Chaudhary, A., Nokubo, M., Ferguson, D., Reddy, G., Blair, I. and Marnett, L. (1997) Analysis of the Malondialdehyde-2'-Deoxyguanosine Adduct Pyrimidopurinone in Human

Leukocyte DNA by Gas Chromatography/Electron Capture/Negative Chemical Ionisation/Mass Spectrometry. *Chemical Research in Toxicology*, **10**, 181-188.

Saffhill, R., Margison, G.P. and O'Connor, P.J. (1985) Mechanisms of Carcinogenesis Induced by Alkylating Agents. *Biochimica et Biophysica Acta*, **823**, 111-145.

Samson, L. and Cairns, J. (1977) A New Pathway for DNA Repair in *Escherichia coli*. *Nature*, **267**, 281-283.

Schnetz-Boutaud, N., Daniels, J.S., Hashim, M.F., Scholl, P., Burrus, T. and Marnett, L.J. (2000) Pyrimido[1,2-α]purin-10(3H)-one: A Reactive Electrophile in the Genome. *Chemical Research in Toxicology*, **13**, 967-970.

Scott, G.B., Griech, E. and Burns, P.A. (2000). Mutational Mechanisms and Biomarkers in Gastrointestinal Carcinogenesis. Keystone Symposium 'Molecular epidemiology: a new tool in cancer prevention', Taos, New Mexico, 10-15 February 2000.

Seto, H., Okuda, T., Takesue, T. and Ikemura, T. (1983) Reaction of Malonaldehyde with Nucleic Acid. I. Formation of Fluorescent Pyrimido[1,2-α]purin-10(3H)-one Nucleoside. *Bull. Chem. Soc. Jpn.*, **56**, 1799-1802.

Sevilla, C., Mahle, N., Eliezer, N., Uzieblo, A., O'Hara, S., Nokubo, M., Miller, R., Rouzer, C. and Marnett, L. (1997) Development of Monoclonal Antibodies to the Malondialdehyde-Deoxyguanosine Adduct, Pyrimidopurinone. *Chemical Research in Toxicology*, **10**, 172-180.

Shephard, S.E. and Lutz, W.K. (1989) Nitrosation of Dietary Precursors. *Cancer Surveys*, **8**, 401-421.

Shuker, D.E.G. and Margison, G.P. (1997) Nitrosated Glycine Derivatives as a Potential Source of O^6-Methylguanine in DNA. *Cancer Research*, **57**, 366-369.

Shuker, D.E.G., Tannenbaum, S.R. and Wishnok, J.S. (1981) N-Nitroso Bile Acid Conjugates. 1. Synthesis, Chemical Reactivity, and Mutagenic Activity. *Journal of Organic Chemistry*, **46**, 2092-2096.

Sidransky, D. and Hollstein, M. (1996) Clinical Implications of the p53 Gene. *Annu. Rev. Med.*, **47**, 285-301.

Singer, B. (1985) *In vivo* Formation and Persistence of Modified Nucleosides Resulting from Alkylating Agents. *Environmental Health Perspectives*, **62**, 41-48.

Singer, B. (1986) O-Alkyl Pyrimidines in Mutagenesis and Carcinogenesis: Occurrence and Significance. *Cancer Research*, **46**, 4879-4885.

Singer, B. and Essigmann, J.M. (1991) Site-Specific Mutagenesis: Retrospective and Prospective. *Carcinogenesis*, **12**, 949-955.

Singer, B. and Hang, B. (1997) What Structural Features Determine Repair Enzyme Specificity and Mechanism in Chemically Modified DNA. *Chemical Research in Toxicology*, **10**, 713-731.

Singh, R., Leuratti, C., Griech, E., Parente, V., Axon, A.T.R., Everett, S., Forman, D. and Shuker, D.E.G. (2000). The Role of *Helicobacter pylori* Infection on the Modulation of O^6-Carboxymethylguanine DNA Adducts in Gastric Tissue Arising from the Nitrosation of Amino Acids and Peptides. Proceedings of the 21st Annual AACR Meeting, San Francisco, USA, 1-5 April 2000.

Singh, R., Leuratti, C., Josyula, S., Sipowicz, M.A., Diwan, B.A., Kasprzak, K.S., Schut, H.A.J., Marnett, L.J., Anderson, L.M. and Shuker, D.E.G. (2001) Lobe-specific Increases in Malondialdehyde DNA Adduct Formation in the Livers of Mice Following Infection with *Helicobacter hepaticus*. *Carcinogenesis*, **22**, 1281-1287.

Spalding, J.W. (1988) Toxicology and Carcinogenesis Studies of Malonaldehyde Sodium Salt (3-Hydroxy-2-propenal, Sodium Salt) in F344/N Rats and B6C3F1 Mice. *NTP Technical Report*, **331**, 5-13.

Stadtländer, C.T.K.H. and Waterbor, J.W. (1999) Molecular Epidemiology, Pathogenesis and Prevention of Gastric Cancer. *Carcinogenesis*, **20**, 2195-2207.

Stone, K., Ksebati, M. and Marnett, L. (1990a) Investigation of the Adducts Formed by Reaction of Malondialdehyde with Adenosine. *Chemical Research in Toxicology*, **3**, 33-38.

Stone, K., Uzieblo, A. and Marnett, L. (1990b) Studies of the Reaction of Malondialdehyde with Cytosine Nucleosides. *Chemical Research in Toxicology*, **3**, 467-472.

Strauss, B. (1991) The 'A Rule' of Mutagen Specificity: A Consequence of DNA Polymerase Bypass of Non-instructional Lesions? *BioEssays*, **13**, 79-84.

Swain, C.G. and Scott, C.B. (1953) Quantitative Correlation of Relative Rates: Comparison of Hydroxide Ion with other Nucleophilic Reagents Towards Alkyl Halides, Esters, Epoxides and Acyl Halides. *J. Am. Chem. Soc.*, **75**, 141.

Swann, P.F. and Magee, P.N. (1968) Nitrosamine-Induced Carcinogenesis: The Alkylation of Nucleic Acids of the Rat by N-Methyl-N-nitrosourea, Dimethylnitrosamine, Dimethyl Sulphate and Methyl Methanesulphonate. *Biochem. J.*, **110**, 39-47.

Tenovuo, J. (1986) The Biochemistry of Nitrates, Nitrites, Nitrosamines and other Potential Carcinogens in Human Saliva. *J. Oral Pathology & Medicine*, **15**, 303-307.

The EUROGAST Study Group (1994) O^6-Methylguanine in Blood Leukocyte DNA: An Association with the Geographic Prevalence of Gastric Cancer and with Low Levels of Serum Pepsinogen A, a Marker of Severe Chronic Atrophic Gastritis. *Carcinogenesis*, **15**, 1815-1820.

Vaca, C., Fang, J., Mutanen, M. and Valsta, L. (1995) ^{32}P-Postlabelling Determination of DNA Adducts of Malonaldehyde in Humans: Total White Blood Cells and Breast Tissue. *Carcinogenesis*, **16**, 1847-1851.

Vaca, C., Wilhelm, J. and Harms-Ringdahl, M. (1988) Interaction of Lipid Peroxidation Products with DNA. A Review. *Mutation Research*, **195**, 137-149.

Van Delft, J.H.M., van Winden, M.J.M., Luiten-Schuite, A., Ribeiro, L.R. and Baan, R.A. (1994) Comparison of Various Immunochemical Assays for the Detection of Ethylene Oxide-DNA Adducts with Monoclonal Antibodies Against Imidazole Ring-opened N7-(2-hydroxyethyl)guanosine: Application in a Biological Monitoring Study. *Carcinogenesis*, **15**, 1867-1873.

Vogel, E.W. and Nivard, M.J.M. (1994) The Subtlety of Alkylating Agents in Reactions with Biological Macromolecules. *Mutation Research*, **305**, 13-32.

Wang, M., Dhingra, K., Hittelman, W., Liehr, J., de-Andrade, M. and Li, D. (1996) Lipid Peroxidation-induced Putative Malondialdehyde-DNA Adducts in Human Breast Tissues. *Cancer Epidemiology, Biomarkers and Prevention*, **5**, 705-710.

Ward, J.B. and Henderson, R.E. (1996) Identification of Needs in Biomarker Research. *Environmental Health Perspectives*, **104** (suppl. 5), 895-900.

Weinfeld, M., Liuzzi, M. and Jones, G.D.D. (1996). A Postlabeling Assay for Oxidative Damage. In G.P. Pfeifer (Ed.), *Technologies for Detection of DNA Damage and Mutations* (pp. 63-71). New York: Plenum Press.

Weinfeld, M., Liuzzi, M. and Paterson, M.C. (1990) Response of Phage T4 Polynucleotide Kinase toward Dinucleotides Containing Apurinic Sites: Design of a ^{32}P-Postlabelling Assay for Apurinic Sites in DNA. *Biochemistry*, **29**, 1737-1743.

Wild, C.P., Smart, G., Saffhill, R., Boyle, J.M. (1983) Radioimmunoassay of O^6-Methyldeoxy-guanosine in DNA of Cells Alkylated *in vitro* and *in vivo*. *Carcinogenesis*, **4**, 1605-1609.

Wild, C.P. and Pisani, P. (1998) Carcinogen DNA and Protein Adducts as Biomarkers of Human Exposure in Environmental Cancer Epidemiology. *Cancer Detection and Prevention*, **22**, 273-283.

Woutersen, R.A., Appel, M.J., van Garderen-Hoetmer, A. and Wijnands, M.V.W. (1999) Dietary Fat and Carcinogenesis. *Mutation Research*, **443**, 11-127.

Xu, G.P. and Reed, P.I. (1993) N-Nitroso Compounds in Fresh Gastric Juice and Their Relation to Intragastric pH and Nitrite by Employing an Improved Analytical Method. *Carcinogenesis*, **14**, 2547-2551.

Yau, T.M. (1979) Mutagenicity and Cytotoxicity of Malondialdehyde in Mammalian Cells. *Mech. Ageing Dev.*, **11**, 137-144.

Yi, P., Sun, X., Doerge, D.R. and Fu, P.P. (1998) An Improved ^{32}P-Postlabeling/High-Performance Liquid Chromatography Method for the Analysis of the Malondialdehyde-Derived 1,N^2-Propanodeoxyguanosine DNA Adduct in Animal and Human Tissues. *Chemical Research in Toxicology*, **11**, 1032-1041.

Zarbl, H., Sukumar, S., Arthur, A.V., Martin-Zanca, D. and Barbacid, M. (1985) Direct Mutagenesis of Ha-ras-1 Oncogenes by N-Nitroso-N-Methylurea During Initiation of Mammary Carcinogenesis in Rats. *Nature*, **315**, 382-385.

Zurlo, J., Curphey, T.J., Hiley, R. and Longnecker, D.S. (1982) Identification of 7-Carboxymethylguanine in DNA from Pancreatic Acinar Cells Exposed to Azaserine. *Cancer Research*, **42**, 1286-1288.

9 Thesis Associated Publications

9.1 Journal/Book Publications

Gottschalg, E., Scott, G., Singh, R., Leuratti, C., Burns, P.A. and Shuker, D.E.G. Endogenous Nitrosation of Glycine in the Aetiology of Human Gastric Cancer: DNA Adduct Detection and p53 Mutation Spectra. (manuscript in preparation).

Leuratti, C., Watson, M.A., Deag, E.J., Welch, A., Singh, R., **Gottschalg, E.**, Marnett, L.J., Atkin, W., Day, N.E., Shuker, D.E.G. and Bingham, S.A. (2002) Detection of Malondialdehyde-DNA Adducts in Human Colorectal Mucosa: Relationship with Diet and the Presence of Adenomas. *Cancer Epidemiology, Biomarkers and Prevention*, **11(3)**, 267-273.

Leuratti, C., Singh, R., Deag, E.J., **Griech, E.**, Hughes, R., Bingham, S.A., Plastaras, J.P., Marnett, L.J. and Shuker, D.E.G. (1999). A Sensitive Immunoslot-Blot Assay for the Detection of Malondialdehyde in Human DNA. In B. Singer and H. Bartsch (Ed.), *Exocyclic DNA Adducts in Mutagenesis and Carcinogenesis* (pp. 197-203). Lyon, France: International Agency for Research on Cancer.

9.2 Conference Abstracts

Griech, E., Leuratti, C. and Shuker, D.E.G. Stability of malondialdehyde-deoxyguanosine in highly modified CT-DNA upon storage and its modulation using methoxyamine. Proceedings of the BACR/MEG-UKEMS meeting on 'Applicability and Relevance of Methods used for Molecular Cancer Epidemiology', Ambleside, Cumbria, UK, 21-23 September 2000.

Griech, E., Scott, G.B., Singh, R., Leuratti, C., Burns, P.A. and Shuker, D.E.G. Buffer-mediated modulation of DNA carboxymethylation and methylation induced by diazoacetate and its significance. Proceedings of the EEMS 2000 meeting on 'Challenges of Mutation Research for the XXIst Century', Budapest, Hungary, 22-26 August 2000.

Singh, R., Leuratti, C., **Griech, E.**, Parente, V., Axon, A.T.R., Everett, S., Forman, D. and Shuker, D.E.G. The role of *Helicobacter pylori* infection on the modulation of O^6carboxymethyl-guanine DNA adducts in gastric tissue arising from the nitrosation of amino acids and peptides. Proceedings of the 21st Annual AACR Meeting, San Francisco, USA, 1-5 April 2000.

Scott, G.B., **Griech, E.** and Burns, P.A. Mutational mechanisms and biomarkers in gastrointestinal carcinogenesis. Keystone Symposium 'Molecular epidemiology: a new tool in cancer prevention', Taos, New Mexico, 10-15 February 2000.

Leuratti, C., Singh, R., Deag, E., **Griech, E.**, Hughes, R., Bingham, S., Plastaras, J.P., Marnett, L.J. and Shuker, D.E.G. Development and application of an immunoslot-blot assay for the detection of malondialdehyde-dG in human tissues. Proceedings of the 4th Winter Research Conference on 'Biological markers of oxidative stress', Valloire, France, 21-26 March 1999.

Leuratti, C., Singh, R., Deag, E., Hughes, R., Bingham, S., **Griech, E.**, Marnett, L.J. and Shuker, D.E.G. Detection of malondialdehyde-deoxyguanosine in white blood cells of volunteers on standardised diets. BACR/Royal Society of Medicine Joint Special Conference on 'Carcinogenesis and Chemo-prevention', London, UK, 7-8 December 1998.

Leuratti, C., Singh, R., Deag, E., Hughes, R., Bingham, S., **Griech, E.**, Marnett, L.J. and Shuker, D.E.G. Detection of malondialdehyde-deoxyguanosine in human tissues in relation to diet. MEG meeting on 'Meat and Cancer - is there a link?', London, UK, 20 November 1998.